Resistance Mechanisms in Cancer Immunotherapy

Inauguraldissertation

zur
Erlangung der Würde eines Doktors der Philosophie
vorgelegt der
Philosophisch-Naturwissenschaftlichen Fakultät
der Universität Basel

von
Marcel Philipp Trefny

Basel, 2021

Genehmigt von der Philosophisch-Naturwissenschaftlichen Fakultät auf Antrag von

Prof. Dr. Alfred Zippelius, Prof. Dr. Christoph Hess und Prof. Dr. Pedro Romero

Basel, den 17.12.2019

Prof. Dr. Martin Spiess
Dekan

Resistance Mechanisms to Cancer Immunotherapy

Dissertation of Marcel Philipp Trefny, MSc. Life Sciences, of Zürich, Switzerland

Under the supervision of Prof. Alfred Zippelius at the Laboratory of Cancer Immunology, Department of Biomedicine, University of Basel and University Hospital of Basel, Switzerland

Submitted to the Faculty of Sciences of the University of Basel and the thesis committee,
Prof. Dr. Alfred Zippelius, Prof. Dr. Christoph Hess and Prof. Dr. Pedro Romero
on 18th November 2019, in Basel, Switzerland

Preamble

In accordance with paragraph 16 of the „Promotionsordnung der Philosophisch-Naturwissenschaftlichen Fakultät der Universität Basel" of 15th September 2015, this thesis contains previously published, unpublished but submitted, and unpublished work. I will first introduce the field of cancer immunology, then focus on mechanisms of resistance towards cancer immunotherapy. This is followed by a study on a genetic polymorphism associated with resistance to cancer immunotherapy, which we published in Clinical Cancer Research. Followingly, I will present an unpublished continuation of this work on natural killer cells, which was recently submitted to a scientific journal. In the last section, I will elaborate on my unpublished and ongoing work on T cell dysfunction, a central feature in resistance to immunotherapy. This work is presented with an extended discussion and will be significantly modified and shortened before the submission to a peer-reviewed scientific journal. In each chapter, I will summarize and discuss the possible future directions for this work.

Table of Contents

1. Introduction

In the following chapter, I will introduce the field of cancer immunology and immunotherapy, which should give the reader an overview of the state-of-the-art. First, I will summarize the current views on how the immune system influences cancer development and treatment. Then, I will describe the most prominent approaches in cancer immunotherapy and how resistance against these therapies can occur. Each subchapter of the presented work then contains its own introduction and discussion specific to each topic.

1.1. Cancer Immunology

1.1.1.   The Immune System

The main functions of the immune system are to protect the organism from foreign and dangerous insults. For example, the immune system shields and protects the body from infections by pathogens such as bacteria, viruses, and parasites. The immune system achieves this goal through concerted actions of a multitude of different cell types, most prominently cells of hematopoietic origin and epithelial barriers. Immune cells must be able to distinguish "self" from "non-self" to fulfill their functions. A complex system of cytokines, chemokines, and pattern recognition receptors such as toll-like and phagocytosis receptors, but also T, B, and NK cell receptors, are required to mediate protective immunity. In addition, a multitude of inhibitory receptors such as sialoglycan receptors, killer immunoglobulin-like receptors, and co-inhibitory receptors help to maintain tissue homeostasis while avoiding overt immune-mediated toxicity. Decades of research into immunology and infections led to highly successful worldwide vaccination campaigns in the 20th century. New technologies, epidemics such as the human immunodeficiency virus (HIV), and the advent of cancer immunology spurred new waves of innovation and continue to drive substantial efforts to understand the human immune system. (Abbas, Lichtman, Pillai, & Preceded by Abbas, n.d.)

1.1.2.   The Origins of Cancer Immunology

Cancers of non-viral origin are inherent "self" and therefore are more challenging to detect and eliminate than infections. For this reason, it was long debated whether the immune system even plays a role in tumor control. However, already in the 19th century, Dr. William B. Coley successfully initiated treatments of soft tissue sarcomas with Staphylococcus pyogenes, effectively the first immunotherapy of modern history. For some time, however, these results were not understood and appreciated by the field (Decker et al., 2017). Since the second half of the 20th century, numerous essential discoveries such as T cells (J. F. A. P. Miller, Mitchell, & Weiss, 1967), dendritic cells (Steinman & Cohn, 1973), and mammalian histocompatibility complex (MHC) restriction (Zinkernagel & Doherty, 1974) permitted a more systematic approach to cancer immunology.

1.1.3. Cancer Immunoediting

A defining feature of cancers is their altered genome and epigenome. These aberrations can be detected by the immune system. The importance of the immune system in cancer development has been exemplified in seminal work by Robert Schreiber and colleagues, in which they discovered that an absence of lymphocytes or IFNγ led to increased tumor incidence in mouse models (Dighe, Richards, Old, & Schreiber, 1994; Schreiber, Old, & Smyth, 2011; Shankaran et al., 2001). The dominating concept termed "Elimination, Editing, Equilibrium, and Escape" describes, how upon cancer cell transformation, the immune system can react and "eliminate" cancer cells because of their alterations. However, cancer cells can evolve under immune pressure and acquire new alterations - so-called "editing" occurs. Immune pressure and the constant evolution of cancer cells may then lead to an "equilibrium" state, during which cancer cells are kept in check but are not eliminated. In some cases, these cells then "escape" immune cell recognition or elimination (Schreiber et al., 2011). These stages have later been described in multiple models and human patients, and as of today, scientists keep discovering new layers of complexity and modifications to the concept of immunoediting.

1.1.4. The Cancer Immunity Cycle

Chen and Mellman integrated some of the most critical aspects of cancer immunology into an intuitive representation called the "cancer immunity cycle" (Figure 1).
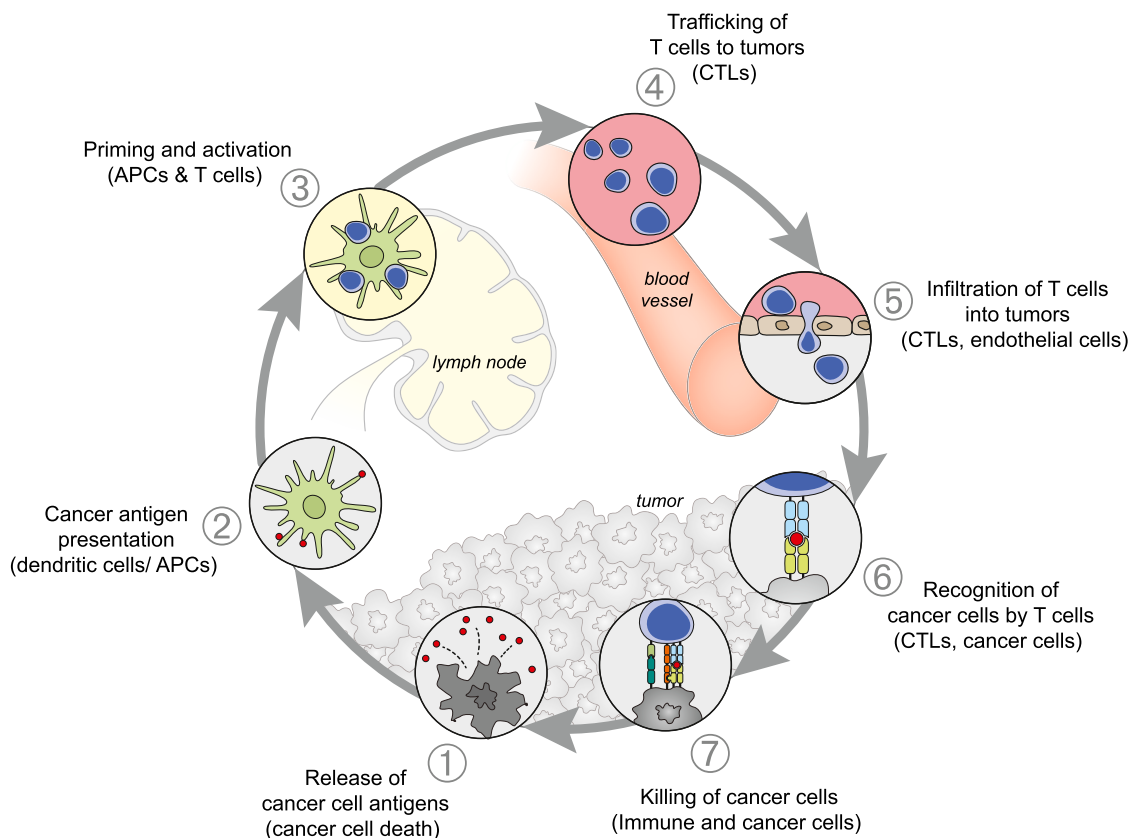

Figure 1 The Cancer Immunity Cycle by Chen and Mellman
The self-propagating 'cancer immunity cycle' focusing on T cell-mediated immunity (D. S. Chen & Mellman, 2013).

According to their T cell-focused model, the cycle starts with the release of cancer antigens from dying tumor cells. These antigens can be presented by antigen-presenting cells, which in turn prime T cell presumably in the lymph node. These activated T cells then undergo differentiation into cytotoxic effector cells, migrate out of lymphatic organs into the bloodstream, and infiltrate into the tumor. T cells then recognize tumor cells by the presentation of the same specific peptide on its major histocompatibility complex I (MHC-I) molecules. This leads to the killing of cancer cells by the T cells and the release of more antigen. (D. S. Chen & Mellman, 2013) The next section will introduce some of the critical features of this cycle.

Cancer Cell Death

Cell death classically occurs through apoptosis. Apoptosis is a central mechanism in organ development, and even in adults, billions of cells die through apoptosis every day. This means that in the vast majority of cases, the immune system should not induce an immune response against apoptotic cells. Indeed, multiple studies demonstrated that the injection of apoptotic cancer cells into mice generally induces peripheral tolerance (Ferguson, Choi, & Green, 2011). This process involves myeloid cells that are recruited to the site of cell death, which recognize apoptotic cells through "eat-me" signals such as phosphatidyl-serine (Pitt, Kroemer, & Zitvogel, 2017). These macrophages are then polarized into tolerogenic 'M2' macrophages, which inhibit immune responses, for example, through interleukin (IL) 10 and transforming growth factor (TGF) β secretion (Mantovani, Sozzani, Locati, Allavena, & Sica, 2002; Weigert et al., 2007). Additionally, apoptotic cells often do not release molecules that elicit dendritic-cell activation through so-called danger-associated molecular patterns (DAMPs) (Matzinger, 1994). The absence of stimulation to dendritic cells causes a lack of cross-presentation in dendritic cells and the absence of cluster of differentiation 40 ligand (CD40L) stimulation by CD4 T cells. In the absence of co-stimulation, CD8 T cells are sub-optimally primed and become highly susceptible to TRAIL-mediated activation-induced cell death, a pathway required for peripheral tolerance (Ferguson et al., 2011).

On the other hand, many forms of immunogenic cell death have been described. Interestingly, even accidental necrosis, for example, induced by freezing and thawing, was not able to prime protective immune responses. Many studies have shown that successful priming with tumor cells requires exposure of immunogenic molecules on their surface, including ATP, calreticulin, high mobility group protein B1 (HMGB1), and others (Galluzzi, Buqué, Kepp, Zitvogel, & Kroemer, 2017).

Cancer Antigens and Neoantigens

Evidence that cancer cells express specific antigens was provided through a series of experiments involving tumor transplants. Often, these transplanted tumors were rejected even from syngeneic mice, and this protection could be transferred by the adoptive transfer of T cells (Kepp, Zitvogel, & Kroemer, 2019). The most obvious class of tumor antigens are viral antigens, which are inherently immunogenic. Although tumors of viral origin are a minority, these antigens remain an essential class of antigens, for example, in human papillomavirus-associated genital cancers (Kenter et al., 2009). In addition to viral antigens, a variety of other tumor antigen classes exist. These include so-called 'cancer-testis' antigens, which are non-mutated proteins that escape tolerance because of expression restricted to immunologically-privileged organs such as the testes. The prime example is the first human tumor-specific antigen to be identified called melanoma-associated antigen 1 (MAGEA1) (van der Bruggen et

6

al., 1991). Another class of tumor antigen is derived from proteins overexpressed but not exclusively expressed by tumor cells. These include tyrosinase, envelope glycoprotein M (GP100), and melanoma antigen recognized by T cells 1 (MART1), which are highly expressed by melanoma cells but can also be found on melanocytes (Coulie, Van Den Eynde, Van Der Bruggen, & Boon, 2014). Then there are so-called neoantigens, which include non-synonymous mutations in coding regions, frameshifts, splice variants, fusion genes and translation of non-coding regions (Smith et al., 2019). An enormous number of neoantigens in oncogenic driver and non-driver genes has been described, and these are rarely shared among patients (Smith et al., 2019). Alternatively, even alterations in the glycosylation profile can lead to tumor antigens, for example, the sialyl-Lewis antigen or sialyl-Tn antigen (Stowell, Ju, & Cummings, 2015). Today, significant research efforts are undertaken to identify and employ tumor antigens, for example, through vaccinations.

T Cell Priming and Recruitment

Multiple lines of evidence indicated the importance of CD103+ dendritic cells (DCs) in CD8 T cell priming and recruitment to the tumor (Broz et al., 2014; Seng-Ryong Woo et al., 2014). These dendritic cells are recruited via CCL4 produced by tumor cells, acquire tumor antigens, and effectively prime CD8 T cells. These primed T cells are then recruited to the tumor via CXCL9 and CXCL10 (Spranger & Gajewski, 2018). Related dendritic cells in humans correlate with overall survival in human melanoma (Barry et al., 2018), but it remains unclear whether they are superior in cross-presentation compared to other subsets also in humans (Sánchez-Paulete et al., 2017). There is considerable evidence that CD103+ cross-presenting DCs (also termed cDC1s) take up tumor antigens and migrate to lymph nodes, whereas their potential to prime T cells in the tumor microenvironment itself remains unclear. The presence of specific cDC1 subsets in the tumor was essential for the continuous priming of transferred T cells, which had already been primed (Broz et al., 2014). Additionally, blockade of lymphocyte recirculation did not completely ablate *in situ* activation of T cells (Tauriello et al., 2018). In addition, the site of priming during a successful checkpoint blockade response remains debated.

Importantly, primed and differentiated tumor-antigen specific T cells can be found in the tumor at elevated levels compared to the periphery (Romero et al., 1998; Zippelius et al., 2004). Novel barcoding technologies have enabled the identification of many populations of cancer antigen-specific T cells, including neoantigen-specific T cells in human tumor samples (Bentzen et al., 2016). In addition, next-generation sequencing technologies allowed the confirmation of immunoediting in murine models (Matsushita et al., 2012) and human cancer tissue (Angelova et al., 2018). The same study in human colorectal cancer provided evidence for an association between immune activity and immunoediting. Metastases with low immunoediting and low immune activity were more prone to recur. They also found a group of metastases where the absence of immunoediting was associated with regulatory T cells, PD-L1, and low T cell diversity (Angelova et al., 2018). These studies confirm that tumor-specific T cells are primed and recruited to tumors; however, this apparently does not lead to tumor rejection in most cases of macroscopic tumors.

Tumor Cell Recognition and Killing

If all preceding steps led to the generation of tumor-specific activated T cells that reached the tumor, these cells finally need to kill tumor cells and complete the cycle. T cells can kill tumor cells with several effector mechanisms. Probably the most directed and productive is the degranulation pathway. Molecules, including perforin and granzyme, are stored in intracellular granules and are released by cytotoxic T and NK cells into the synaptic cleft towards tumor cells. Granzymes are potent inducers of cell-intrinsic apoptosis in the target cells by cleaving caspases or BH3-interacting domain death agonist. Perforin perforates the cell membranes and is required for the delivery of granzymes into the cytosol of target cells. In addition, the expression of FasL can induce apoptosis on target cells through Fas, which triggers caspase-8 initiated cell death. (Golstein & Griffiths, 2018) Additionally, T (and NK) cells kill tumor cells through the release of cytokines, most prominently IFNγ and TNFα (Kearney et al., 2018).

As these pathways seem to trigger apoptosis, it remains unclear if this represents an immunogenic cell death and propagates the cancer immunity cycle. Nevertheless, a broadening of the tumor-antigen specific T cell repertoire has been observed after peptide vaccinations (Gulley et al., 2017), also in human patients vaccinated with HER2/neu peptides (Ljunggren & Malmberg, 2007). It remains to be elucidated, in which pathways and cells are essential to propagate the cancer immunity cycle to widen therapeutic responses against tumors.

1.1.5.   NK Cells in Cancer

Natural killer cells are a subset of innate lymphoid cells and control cancers directly by the rapid killing of tumor cells through perforin, granzymes, and the ligation of death receptor-mediated pathways (Guillerey & Smyth, 2016). NK cells also secrete a wide variety of cytokines, most prominently IFNγ (Morvan & Lanier, 2016). NK cells have an essential role in cancer immunosurveillance through their ability to recognize stressed or aberrant cells. For example, they are able to react to cells with a lack of MHC-I molecules ("lack of self"). This makes NK cells important partners to T cells, most of which rely entirely on peptides presented on MHC molecules. Additionally, they are able to sense cellular stress, for example, DNA damage by the recognition of NKG2-D type II integral membrane protein (NKG2D) ligands (Vivier et al., 2011). This function is potentially important to limit tumor escape by continuous mutation of T cell epitopes. Unlike with T cells, the expression of activating and inhibitory receptors is not clearly linked to altered functionality (Vivier et al., 2011). In addition, NK cells are scarce in tumors, and their presence does not correlate well with clinical outcomes in chemotherapy or radiotherapy (Carrega et al., 2008; Platonova et al., 2011). This might explain why NK cells were less studied in the context of cancer immunotherapy. Nevertheless, recent data suggest that NK cells are critical for recruiting dendritic cells in human melanoma, and this correlated with response to programmed death 1 (PD-1) blockade (Barry et al., 2018). Therefore, NK cells clearly deserve more attention in the field of cancer immunology. In chapters 2.1 and 2.2 of this thesis, I will report on the role of inhibitory receptor PD-1 on NK cells in human lung cancers.

1.2. Cancer Immunotherapy

1.2.1. Checkpoint Inhibition Immunotherapy

Immune checkpoint inhibition and cellular therapies show impressive clinical results in immuno-oncology. (June et al., 2018; Ribas & Wolchok, 2018; Wei, Duffy, & Allison, 2018). Importantly, patients that respond to immunotherapy often benefit from long-lasting remissions, which in some patients could even be curative (McDermott et al., 2014). The most widely and successfully used immunotherapies are based on the inhibition of PD-1 and cytotoxic T lymphocyte antigen 4 (CTLA-4). Both targets are upregulated receptors on activated and dysfunctional T cells. Upon ligand binding, they inhibited T cell activation and were therefore termed "checkpoints". Checkpoint inhibitors are now approved, among other cancer entities, in melanoma (Robert, Long, et al., 2015; Robert, Schachter, et al., 2015), non-small cell lung cancer (NSCLC) (Borghaei et al., 2015b; Brahmer et al., 2015; Reck, Rodríguez-Abreu, et al., 2016), renal cell cancer (Motzer et al., 2015, 2019), urothelial cancer (Balar et al., 2017), skin squamous cell cancer (Migden et al., 2018) and Hodgkin's Lymphoma (Ansell, 2017). Moreover, PD-1 blockade with pembrolizumab has been approved for any tumor with high microsatellite-instability or mismatch repair deficiency irrespective of tumor origin, which is the first tissue-agnostic approval in oncology (Federal Drug Administration, 2017).

PD-1 and CTLA-4 seem to fulfill non-redundant functions (Wei et al., 2019, 2017), and PD-1 blockade can act synergistically with CTLA-4 blockade, for example in PD-L1 negative melanoma (Larkin et al., 2015) and NSCLC with high tumor mutational burden (Hellmann et al., 2018). Moreover, several combinations of two distinct immune checkpoint pathways (PD-1 and CTLA-4) or in combination with chemotherapy/targeted therapies have been successfully applied to treat patients with metastatic melanoma, head and neck cancer, lung cancer and kidney cancer (Blank et al., 2018; Hellmann et al., 2018; Motzer et al., 2018; Postow et al., 2015). While combination therapies of PD-1 and CTLA-4 targeting antibodies show higher response rates, a very significant part of patients experiences substantial immune-related toxicity (Larkin et al., 2015; Postow et al., 2015). Interestingly, immune-related adverse events are associated with increased overall survival (Topalian et al., 2019). This exemplifies how responses to immunotherapy are associated with increased immune activity.

CTLA-4 Targeting

CTLA-4 is related to the co-stimulatory receptor CD28, and they also share the same ligands called B7-1 and B7-2 (CD80 and CD86). CTLA-4 is released from intracellular vesicles upon APC recognition and thereby mediates its effects directly at the immunological synapse (Egen & Allison, 2002). CTLA-4 outcompetes CD28 by its superior affinity to their shared ligands and therefore inhibits T cell priming (Brunner-Weinzierl & Rudd, 2018; Linsley & Golstein, 1996; Sotomayor, Borrello, Tubb, Allison, & Levitsky, 1999). Most studies suggested that anti-CTLA-4 antibodies act mainly by relieving inhibition of effector T cells during priming and possibly by reducing the suppressive capacity of regulatory T cells (Tregs), which express high levels of CTLA-4. However, research by the group of Sergio A. Quezada demonstrated that in mice, anti-CTLA-4 antibodies lead to depletion of CTLA-4+ Tregs in an Fc-dependent manner, and this was essential for the therapeutic benefit (Simpson et al., 2013). However, it is a matter of great controversy, whether this effect also occurs in humans. Recent studies did not detect a decrease in Treg frequency in the tumor with both

clinically approved anti-CTLA-4 antibodies ipilimumab and tremelimumab (A. Sharma et al., 2019). This could, however, indicate ways to improve CTLA-4 targeting antibodies for humans in the future.

PD-1 Targeting

PD-1 is a transmembrane glycoprotein with limited sequence homology to CD28, CTLA-4, and ICOS (T. Okazaki & Honjo, 2007). Similarly to CTLA-4, PD-1 is expressed mainly on activated and dysfunctional T cells (D. S. Thommen et al., 2015). Importantly, different levels of PD-1 expression distinguish intratumoral T cells with significant functional differences (D. S. Thommen et al., 2018). There is also a considerable expression on tumor-associated macrophages (Gordon et al., 2017), B, NKT, and interestingly also on NK cells, on which I will report in this thesis (Keir, Francisco, & Sharpe, 2007). Engagement of PD-L1 or PD-L2 by PD-1+ T cells transduces inhibitory signals and reduces T cell activation (Freeman et al., 2000; Keir et al., 2007). PD-1 signaling also impacts T cell metabolism directly by enhancing fatty acid oxidation through elevated levels of carnitine-palmitoyltransferase (CPT1A) and lipases (Patsoukis et al., 2015). This is considered to affect their differentiation and longevity.

PD-L1 can engage B7-1 expressed on T cells by itself (Butte, Keir, Phamduy, Sharpe, & Freeman, 2007). This adds another layer of complexity, especially when comparing PD-L1 with PD-1 targeting antibodies, which have small but significant biochemical differences (De Sousa Linhares et al., 2019). Nevertheless, both PD-1 and PD-L1 blocking antibodies are used in the clinics and show similar activity, however, with no direct comparisons available. PD-1's immunoreceptor tyrosine-based inhibitory motif (ITIM) and primarily its immunoreceptor tyrosine-based switch motif (ITSM) domain are considered to be essential for its function and couple to Tyrosine-protein phosphatase non-receptor type 11 (PTPN11, referred to as SHP-2) (Taku Okazaki & Wang, 2005). While initially believed to regulate TCR signaling, recent data suggest that PD-1 mainly inhibits CD28 signaling (Hui et al., 2017; Kamphorst et al., 2017). Interestingly, SHP-2 deficient mice did not show superior tumor control and responded to anti-PD-1 therapies (Rota et al., 2018). Thus remarkably, despite the enormous clinical success of PD-1 pathway-targeting antibodies, the precise signaling events that underlie PD-1's repressive activity remain unclear.

1.2.2.   Adoptive Therapies

In addition to checkpoint blockade, adoptive transfers of T cells enriched for tumor reactivity or genetically engineered with natural or synthetic receptors have shown impressive anti-tumor efficacy (Guedan, Ruella, & June, 2019; June et al., 2018; June & Sadelain, 2018; Lim & June, 2017; Rohaan, Wilgenhof, & Haanen, 2019; Steven A. Rosenberg & Restifo, 2015).

TIL Expansion

T cells can be expanded from tumor biopsies using high doses of IL-2, antibody stimulation, and feeder cells. Such protocols allow for the *ex vivo* amplification of autologous T cells harboring tumor-reactive T cells, which can then be transfused back to the patients after lymphodepletion (Dudley, Wunderlich, Shelton, Even, & Rosenberg, 2003; Dudley et al., 2005). By creating a tumor-specific T cell compartment that is otherwise lacking in patients (Spranger, Dai, Horton, & Gajewski, 2017; Spranger & Gajewski, 2018), adoptive T cell therapies potentially address an entirely

different need compared to checkpoint blockade. They are used either as a stand-alone treatment or increasingly in combination with other cancer immunotherapies (Rohaan, van den Berg, Kvistborg, & Haanen, 2018). Adoptive transfer with TILs have been continuously developed and these efforts were pioneered by the group of Steven Rosenberg (Rosenberg et al. 1986; Rosenberg et al 2001; Dudley et al. 2002; Dudley et al. 2008; Rosenberg et al 2011; Chandran et al. 2017; Dudley et al. 2005; Morgan et al. 2006). Recently, more personalized approaches to engineer neoantigen reactivity have further boosted efficacy, even in patients with immunologically silent tumors such as breast cancer using neoepitope prediction algorithms (Zacharakis et al., 2018). New approaches that utilize tumor organoids could have the potential to expand these tumor antigen-specific T cells even from peripheral blood (Dijkstra et al., 2018).

Currently, 20 phase II trials (NCT-02500576; NCT03610490; NCT02421640; NCT03638375; NCT03645928; NCT00604136; NCT03108495; NCT03083873; NCT02360579; NCT03419559; NCT03467516; NCT02414945; NCT01993719; NCT01174121; NCT02621021; NCT02133196; NCT03449108; NCT03296137; NCT00338377; NCT01740557), and one phase III trial (NCT02278887) are recruiting patients with different types of cancer diagnoses, reflecting the attempt to move the path towards regulatory approval of adoptive cell therapy with TILs.

Chimeric Antigen Receptor Therapies

Several studies employed T cell receptor (TCR) engineered T cells for the targeted treatment of tumors. One of the most successful trials used an NY-ESO-1 specific TCR and showed encouraging clinical responses in 80% of patients (Rapoport et al., 2015). Recently, the highly promising technology of chimeric antigen receptors (CARs) has emerged. First-generation CARs consisted of CD3ζ chain stimulatory domains, a transmembrane domain, and an antigen-recognition domain derived from an antibody variable region. These first-generation CARs without co-stimulatory domains suffered from T cell depletion and induction of anergy (Grosser, Cherkassky, Chintala, & Adusumilli, 2019). Newer generation CARs either contain a single or multiple co-stimulatory domains, mainly derived from CD28 and 4-1BB (CD137) (June et al., 2018). CARs targeting CD19 proved immensely successful in the therapy of B cell acute lymphoblastic leukemia and refractory chronic lymphocytic leukemia (Davila et al., 2014; Kalos et al., 2011; Kochenderfer et al., 2010; Park et al., 2018; Porter, Levine, Kalos, Bagg, & June, 2011). CARs act so rapidly and effectively that severe immune-related adverse events such as cytokine storms are frequent and can lead to fatalities (Park et al., 2018; Porter et al., 2011). Moreover, CD19 CARs also cause profound B cell aplasia, which, however, can be managed by immunoglobulin replacement therapy (June et al., 2018). While CARs against other B cell antigens show similar efficacies, CARs against solid tumors remain a big challenge. The first trials with HER2-targeting CARs caused a deadly cytokine storm and off-target toxicity in the lung (Morgan et al., 2010). Nevertheless, numerous improvements to the CAR modality have been proposed, including combinatorial specificities and suicide switches (Lim & June, 2017).

1.3. Resistance Mechanisms to Immunotherapy

1.3.1.   Resistance to Checkpoint Inhibition

Cancer immunotherapies have shown remarkable clinical responses and already improved the lives of many cancer patients. However, only a fraction of patients profit from the currently approved immunotherapies. For example, the response rate of unselected patients with metastatic melanoma or NSCLC is between 19-45% with PD-1 blockade monotherapy (Syn, Teng, Mok, & Soo, 2017). Many entities, including pancreatic ductal adenocarcinoma, prostate, or breast cancer, show poor response rates. PD-1 blockade monotherapy trials in metastatic breast cancer reported objective responses in only 5-24% of patients (Esteva, Hubbard-Lucey, Tang, & Pusztai, 2019). Even when combining anti-CTLA-4 antibodies with PD-1 blockade in melanoma, which is a highly responding entity, the response rate in all patients was 55% (Larkin et al., 2015). Thus, the fraction of patients that do not show any objective response (called primary resistance) is very high. While responses to immunotherapy are generally considered to be more durable than with conventional targeted therapies, up to a quarter of patients with an initial response to pembrolizumab in melanoma later show disease progression – termed acquired resistance (Ribas et al., 2016).

This lack of clinical benefit highlights the urgent need for more preclinical and clinical research into the mechanisms behind resistance in immunotherapy. The questions which define current research efforts in the field can be grouped in the following categories: Identification of patients that respond to current immunotherapies (biomarkers), improvements and combinations of existing immunotherapies, and the discovery of novel therapeutic options.

Several attempts have been made to classify tumor immune microenvironments. The Immunoscore, initially defined in colorectal cancer, describes the presence of total and CD8 positive T cells at the tumor center and at the tumor margin (Pagès et al., 2018). In a large clinical study, the classification of colorectal cancers according to the Immunoscore provided the highest risk prediction and led to its implementation in the TNM-Immune classification (Pagès et al., 2018). This exemplifies that tumors can be classified into categories by differences in their immune status. In simple terminology, "cold" tumor microenvironments are devoid of immune infiltration, and "hot" microenvironments display the presence of immune cells and correlate with an ongoing immune response (Fridman et al., 2017; Palucka & Coussens, 2016; P. Sharma, Hu-Lieskovan, Wargo, & Ribas, 2017).
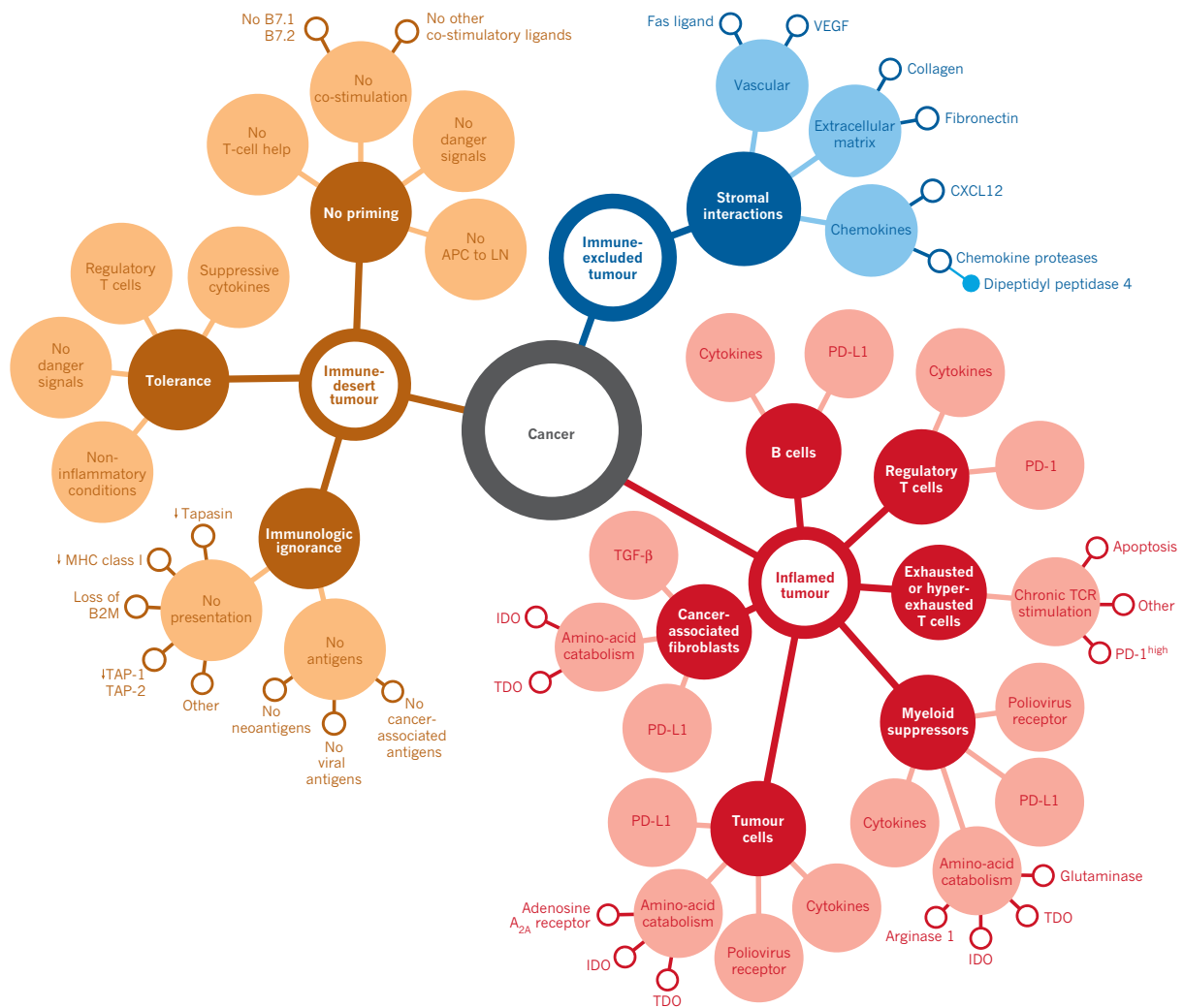
Figure 2 Cancer-Immune Phenotypes by Chen and Mellman
From D. S. Chen & Mellman, 2017. Three categories of mechanisms to resistance are shown. T cells and molecules involved are shown in interconnected spheres.

Chen and Mellman classified the mechanisms of resistance to immunotherapy in three categories depicted in Figure 2 (D. S. Chen & Mellman, 2017). The first category is represented by "immune deserts", which lack an ongoing immune response, which is an equivalent of a "cold" tumor. The second is "immune excluded" tumors, against which there would be an immune response, but the immune cells do not efficiently penetrate the tumor mass. The third category is the "inflamed" tumor with an ongoing immune response in the tumor mass, but this does not (yet) lead to rejection. For the remaining introduction, I will present a summary of current knowledge on potential mechanisms and ways to overcome resistance in cancer immunotherapy. I will split the introduction into the three categories described by Chen and Mellman above. However, there are no sharp borders, and mechanisms can be shared between categories.

I will lay some focus on PD-1 blockade as this constitutes the backbone for most current immunotherapy trials (Tang et al., 2018) and has been the main topic of my experimental work.

1.3.2.   Immune Desert Tumors

Tumor Mutational Burden

Tumor mutational burden (TMB) is one of the strongest predictors of response to checkpoint blockade. There is an impressive bandwidth of mutational frequencies among cancer types (Lawrence et al., 2013). This variability is amplified by the heterogeneity within the same disease spanning several orders of magnitude. Additionally, the types of mutations correlate with disease risk factors such as smoking in lung cancer or UV exposure in melanoma. Cancer entities associated with higher mutation rates, such as melanoma and lung cancer, tend to show higher response rates than cancer types with lower mutation rates (Jenkins, Barbie, & Flaherty, 2018). There is robust evidence that tumor mutational burden, usually defined as the frequency of non-synonymous mutations, is associated with response to CTLA-4 blockade in melanoma (Van Allen et al., 2015), PD-1 blockade in NSCLC (Carbone et al., 2017; Rizvi et al., 2015) and CTLA-4 plus PD-1 blockade in NSCLC (Hellmann et al., 2018). Along the same line, tumors with microsatellite-instability or mismatch repair deficiencies, which have very high mutation rates, also show high response rates (Le et al., 2017). Therefore, an important reason for primary resistance appears to be the lack of suitable antigens. In agreement, a central feature of immunotherapy responses is the reactivation and expansion of tumor-antigen specific T cells (Gubin et al., 2014; Snyder et al., 2014).

Consequently, one potential strategy to circumvent this type of low-TMB resistance would be to introduce new mutations. Chemotherapy and radiation can induce DNA damage and are considered as combination approaches (Tang et al., 2018), although not only for this reason, as discussed below. However, there are several problems surrounding this hypothesis. Radiation and chemotherapy induce random mutations, which are very unlikely to occur in the same loci in different cells (Lhuillier, Rudqvist, Elemento, Formenti, & Demaria, 2019). Therefore, any new mutations are likely to present only on a minor subclonal population. This would be disadvantageous because a high proportion of clonal mutations are associated with higher response rates to checkpoint blockade (Gejman et al., 2018; McGranahan et al., 2016; Wolf et al., 2019). Additionally, a recent study failed to detect higher levels of mutational burden after chemotherapy or radiotherapy in lung cancer patients (Jonna et al., 2019). Nevertheless, these therapies are important to release tumor antigens and reduce tumor burden, which is another potential predictor of primary resistance (A. C. Huang et al., 2017).

Lack of Immunogenic Cell Death

Chemotherapies

Chemotherapies were used for decades as a stand-alone treatment to kill tumor cells directly. With the rise of immunotherapeutics, the important question arose, whether these chemotherapies can act in synergy with immunotherapies. Importantly, some but not all chemotherapeutics, radiotherapy, and oncolytic virus immunotherapy probably involve immunogenic cell death and thereby promote a more inflamed "hot" tumor microenvironment (Bommareddy, Zloza, Rabkin, & Kaufman, 2019; Fridman et al., 2017; Nagarsheth, Wicha, & Zou, 2017). For example, doxorubicin is known to induce immunogenic cell death and induces vaccination responses when applied to tumor cells before injection and requires no adjuvants (Dudek, Garg, Krysko, De Ruysscher, & Agostinis, 2013). Oxaliplatin and cyclophosphamide are other widely used

therapeutics that can elicit immunogenic cell death (Casares et al., 2005). Importantly this is probably tumor type-specific, as only certain combinations of the supposedly immunogenic chemotherapeutics led to immunogenic cell death and synergized with PD-1 and CTLA-4 blockade in murine lung tumor models (Pfirschke et al., 2016). Therefore, systematic comparisons of different chemotherapies in combination with immunotherapeutics are warranted.

Some chemotherapeutic agents also have direct immunostimulatory effects. Specifically, the microtubule-destabilizing agent ansamitocin P3 directly promoted dendritic cell maturation, and this resulted in enhanced T cell priming (Martin et al., 2014). This was confirmed with HER2-directed ado-trastuzumab emtansine, which similarly triggered both innate and adaptive immunity and synergized with dual-checkpoint blockade (Müller et al., 2015). This effect is specific to a range of microtubule-destabilizing agents and depends on the microtubule-associated protein GEF-H1 (Kashyap, Fernandez-Rodriguez, et al., 2019). Clinical trials are ongoing that combine microtubule-destabilizing chemotherapies as antibody-drug conjugates (Beck, Goetsch, Dumontet, & Corvaïa, 2017).

A creative way to increase the immunogenicity of tumors was recently presented by the group of Sidi Chen. They activated multiple or even thousands of genes within a CRISPR-activation system, which leads to improved antigen presentation and co-stimulation by tumor cells (G. Wang et al., 2019). When they transduced tumor cells either *ex vivo* or *in vivo* with their adeno-associated virus (AAV) system, they noted an improved immune-mediated tumor rejection. Interestingly, their system also allowed the upregulation of previously identified neoantigens.

Radiation and Endogenous Retroviruses

The DNA damage caused by radiotherapy leads to DNA damage and the accumulation of cytosolic DNA. Remarkably, cytosolic DNA triggers an "anti-viral" response through the DNA sensors cyclic GMP-AMP synthase (cGAS) and stimulator of interferon genes protein (STING) (Cai, Chiu, & Chen, 2014). Through this pathway, radiation can induce the secretion of interferon-β which recruits basic leucine zipper transcriptional factor ATF-like 3 (Batf3) positive DCs and synergizes with checkpoint blockade (Vanpouille-Box et al., 2017). Interestingly, the DNA exonuclease three-prime repair exonuclease 1 (Trex1) can be induced as a negative feedback mechanism and cause resistance. Similarly, this pathway is vital for spontaneous CD8 T cell responses (Seng-Ryong Woo et al., 2014), and STING deficiency may cause resistance to checkpoint blockade and oncolytic viruses (Bommareddy et al., 2019).

The reactivation of endogenous retroviruses in tumor cells was similarly reported to correlate with responses in immunotherapy (Smith et al., 2018). It remains unclear how those are reactivated, but changes in the epigenome are probably involved. Unexpectedly, endogenous retroviral elements were also induced by CDK4/6 inhibition, then led to type-III interferon secretion and increased antigen presentation (Deng et al., 2018; Goel et al., 2017). This discovery raises hopes for immunotherapy-resistant entities such as breast cancer, for which CDK4/6 inhibitors are already approved (Goel, DeCristo, McAllister, & Zhao, 2018).

Anti-Tumor Vaccinations

A possibility to circumvent the inefficient priming of tumor antigens consists of anti-tumor vaccinations. While anti-viral prophylactic vaccinations are highly successful in

preventing HPV-associated tumors (Roden & Stern, 2018), therapeutic anti-tumor vaccines face several obstacles. While some initial vaccination trials showed beneficial effects (Jocham et al., 2004; Romero et al., 2016), another phase III trial failed to detect clinical benefit (Morton et al., 2007). A complication with more defined synthetic vaccines is that tumor-antigens often resemble self-antigens, and as a consequence, vaccine responses are generally lower compared to anti-viral vaccinations (Pedersen, Sørensen, Buus, Christensen, & Thomsen, 2013). An additional problem for anti-tumor vaccines lies in lower precursor frequencies for these antigens (Rizzuto et al., 2009). However, improved adjuvants that induce CpG-mediated TLR9 triggering are capable of inducing more potent CD8 T cell responses (Baumgaertner et al., 2012; Speiser et al., 2005). Importantly the anti-tumor vaccine Sipuleucel-T with limited but significant patient benefit has been approved for prostate cancer (Cheever & Higano, 2011).

Cancer vaccination protocols were reshaped by the discovery that a large part of the anti-tumor immune response is often MHC-II restricted and mediated by CD4 T cells (Kreiter et al., 2015). Additionally, improvements in neoantigen identification enable personalized approaches against less these tolerogenic epitopes (Romero et al., 2016; Schumacher & Schreiber, 2015). Recent studies have demonstrated potent expansions of tumor-specific T cells in patients with personalized modified RNA or long-peptide neoantigen-directed vaccination protocols (Ott et al., 2017; Sahin et al., 2017). These studies used both MHC-I and MHC-II epitopes with improved adjuvants. Importantly there is increasing evidence that vaccination reduces the frequency of primary resistance with PD-1 blockade both in preclinical models (Ali, Lewin, Dranoff, & Mooney, 2016; J. Fu et al., 2015; Martínez-Usatorre, Donda, Zehn, & Romero, 2018) and human trials (Massarelli et al., 2019).

Oncolytic Viruses

Another promising approach to simultaneously reduce tumor mass and trigger both innate and adaptive immunity is oncolytic viruses (Bommareddy, Shettigar, & Kaufman, 2018). Either through their capsule proteins, cytosolic DNA, or dsRNA, these viruses trigger many important anti-viral pathways inside the tumor cells, which lead to cytokine secretion, antigen presentation, and immune cell recruitment (Bommareddy et al., 2018; Dai et al., 2017). Thereby such viruses could be especially beneficial for immunologically "cold" tumors. The oncolytic virus product named T-VEC has been approved for melanoma immunotherapy for the first time by the FDA in 2015 (Pol, Kroemer, & Galluzzi, 2016).

Neoantigen Specific TIL Expansion

As described above, TIL transfer is a promising method to amplify a tumor-specific T cell compartment. In some instances, even infrequent but clonal mutations can mediate responses to checkpoint blockade after *ex vivo* amplification. For example, a new strategy to combat primary resistance in low-TMB or inefficiently primed tumors is to expand T cells against predicted tumor antigens *ex vivo*. This was recently tested in a patient with metastatic breast cancer and led to complete durable remission (Zacharakis et al., 2018). Even without predicting the antigens, TIL products could be enriched for tumor-specific T cells by co-culture with tumor organoids (Dijkstra et al., 2018).

1.3.3.   Immune Excluded Tumors

Immune cell exclusion is a crucial factor for resistance to immunotherapy (Jiang et al., 2018; Mariathasan et al., 2018), whereas T cell infiltration can indicate responding patients (Daud, Loo, et al., 2016; Tumeh et al., 2014).

Tumor Genetics

Interestingly, genetic tumor-intrinsic factors can be responsible for differences in the tumor immune environment (J. Li et al., 2018; Spranger, Bao, & Gajewski, 2015). Spranger and colleagues discovered that human melanomas with an absence of T cell infiltration displayed elevated β-catenin in 48% of cases (Spranger et al., 2015). In murine models, β-catenin^{high} tumors lost their capacity to secrete CCL4, which led to an abrogation of dendritic cell recruitment. The hyperactivation of β-catenin also caused resistance to PD-1 and CTLA-4 blockade. Similarly, using a library of pancreatic cancer cell clones, Li et al. demonstrated that the oncogene c-myc drives CXCL1 expression, which leads to T cell exclusion and mediates resistance to checkpoint blockade in mice (J. Li et al., 2018).

Chemokines and Cytokines

Chemokines can have multiple roles in the tumor microenvironment from the attraction of cytotoxic and regulatory cells to direct effects on tumor cell migration (Nagarsheth et al., 2017). The secretion of CXCL9 and CXCL10 by tumor cells can be inhibited by epigenetic silencing, which causes a lack of T$_{h1}$ and CD8 T cell recruitment to the tumor (Peng et al., 2015). Contrastingly, multiple chemokines are associated with adverse prognosis by the exclusion of effector cells and the recruitment of regulatory cells. For example, CCL22 and CCL28 can attract regulatory T cells to tumor sites (Nagarsheth et al., 2017). Similarly, two recent studies confirmed that TGFβ signaling in the tumor microenvironment is associated with immune exclusion, and blocking TGFβ synergized with checkpoint blockade (Mariathasan et al., 2018; Tauriello et al., 2018). A recent study in mice found that prostate cancer bone metastases induced the release of TGFβ by osteoclasts, which suppressed T$_{h1}$ differentiation and mediated resistance to immune checkpoint blockade (Jiao et al., 2019). Blockade of either TGFβ or RANKL acted synergistically with PD-1 blockade in their murine models. Macrophages can be attracted by CCL2 expressed by tumor cells and inhibit T cell responses or promote cancer metastasis (Nagarsheth et al., 2017). Intratumoral reactive nitrogen species are capable of modifying CCL2 in the tumor microenvironment and leading to an abrogation of TIL migration to the tumor core (Molon et al., 2011).

Tumor Stroma

Cancer-associated fibroblasts (CAFs) are well known for their effects on tumor progression and metastasis by remodeling of the tumor stroma mainly by the deposition of extracellular matrix (Östman & Augsten, 2009). The stroma is critical to restrict the immune-mediated destruction of tumors (Singh, Ross, Acena, Rowley, & Schreiber, 1992). In their study, Singh et al. showed that tumor cells injected as suspensions were rapidly cleared, whereas cells embedded as blocks or in a synthetic matrix would engraft and avoid immune destruction. A recent study created CAR T cells that express Heparanase, which allows them to degrade the extracellular matrix and invade into the tumor (Caruana et al., 2015). Interestingly, T cells are able to recognize and kill the surrounding stroma, which internalized tumor antigens (Zhang et al., 2008).

CAFs, together with tumor-associated macrophages, are also important to induce angiogenesis (Kammertoens, Schüler, & Blankenstein, 2005). The tumor vasculature is a frequent target of conventional therapies, and drugs targeting the vasculature are increasingly combined with immunotherapies. Indeed, normalizing the tumor vasculature by an anti-VEGFR2 antibody synergizes with TIL transfer in mice (Y. Huang et al., 2012), and it might be even possible to target the vasculature by anti-VEGFR2 CAR T cells (Chinnasamy et al., 2013) or vaccination (Nair et al., 2003). Interestingly, activated T cells themselves can inhibit angiogenesis through IFNγ secretion (Qin et al., 2003). The established anti-angiogenic drug axitinib even has two beneficial roles by preventing VEGFR signaling and decreasing tumor-associated mast cells and macrophages (Läubli et al., 2018).

1.3.4.   Inflamed Tumors

Loss of Antigen Presentation

Already during tumor development, mutations in human leukocyte antigens (HLA, MHC-I) and beta-2-microglobulin (B2M) correlated with higher immune infiltration and increased suppressive activity (Pereira et al., 2017; Rooney, Shukla, Wu, Getz, & Hacohen, 2015; Zhao et al., 2016). This demonstrates that these tumors probably underwent immunoediting, during which the loss of HLA and B2M represented a growth advantage. Similarly, defects in antigen presentation are associated with primary and secondary resistance to immunotherapy.

For example, Zaretsky and colleagues found that some patients with relapses after initial responses to PD-1 blockade in melanoma acquired mutations in B2M (Zaretsky et al., 2016) and the same was observed in a patient that initially responded to an anti-tumor RNA mutanome vaccine (Sahin et al., 2017). Similarly, low expression of B2M and TAP1/2 correlated with resistance to CTLA-4 blockade in melanoma (S. J. Patel et al., 2017). Using a genome-wide CRISPR-Cas9 screen on tumor cells, the group of Nicolas Restifo systematically evaluated genetic alterations that lead to T cell immune escape *ex vivo*. They identified a spectrum of genes that were essential in T cell recognition ranging from B2M and HLA but also the proteasome and antigen import into the endoplasmatic reticulum (S. J. Patel et al., 2017). Another study also linked MHC-I loss with resistance to CTLA-4 and PD-1 therapies, and MHC-II loss to PD-1 blockade (Rodig et al., 2018).

Effector Cytokine Signaling and Tumor Heterogeneity

Some of the studies, which described the loss of HLA and B2M (S. J. Patel et al., 2017), also identified mutations in JAK1/2. Similar mutations had already been observed in relapsing melanoma patients (Zaretsky et al., 2016). JAK1/2 mutations hamper IFNγ signaling in tumor cells and were also linked to primary resistance in melanoma in two other studies (Rodig et al., 2018; D. S. Shin et al., 2017). Notably, these mutations can be found at frequencies of around 10% in breast, colorectal, prostate, and lung cancers (D. S. Shin et al., 2017). Increased risk for resistance was also observed for a number of mutations in the IFNγ response pathway in melanoma patients undergoing CTLA-4 blockade (Zhao et al., 2016).

Contrastingly, there is completely opposing evidence from the laboratory of Andy Minn, who reported that the loss of IFN receptors IFNGR and IFNAR increased response to

checkpoint blockade in mice, and even in humans they found correlations between checkpoint blockade response and decreased IFNγ signaling (Benci et al., 2016). They argue that chronic IFNγ signaling induces the expression of PD-L1 and alternative inhibitory ligands such as TNFRSF14 (HVEM), which then decreased intratumoral T cell activation. IFNγ thus seems to contribute to both pro-tumorigenic processes such as inhibitory ligand expression, while also mediating direct effector toxicity. Indeed, IFNγ is a critical cytokine in negative and positive feedback loops to both upregulated inhibitory ligands and the antigen presentation machinery on tumor cells (Benci et al., 2016; S. J. Patel et al., 2017). Moreover, Garris and colleagues found that IFNγ also induced IL-12 secretion by dendritic cells in the tumor (Garris et al., 2018). IFNγ-induced secretion of IL-12 was required for an effective T cell response, and this could be exploited therapeutically by intratumoral IL-12 delivery.

A new study that performed CRISPR-Cas9 screens in murine tumor cell lines indicated that TNFα was essential to both CD8 T cell and NK cells mediated cytotoxicity and in their hands even more important than IFNγ (Kearney et al., 2018). Even co-culture of tumor cells with perforin knock out (KO) CD8 T cells led to the selection of TNFα pathway mutations, which included mutations in Casp8, Tradd, and Fadd. However, when they performed the screen with a human HER2+ cell line and human HER2-directed CAR T cells, they did not detect any enrichment for IFNγ or TNFα pathway mutations. This indicates that either CAR T cells or more generally human T cells could differ in their mechanisms of tumor cell killing.

A recent study reported that intra-tumor heterogeneity is associated with resistance to checkpoint blockade (Wolf et al., 2019). They demonstrated that mixtures of genetically similar tumor cell lines could be rejected, while mixtures of highly diverse clones showed outgrowth and resistance to spontaneous anti-tumor immunity and PD-1 blockade. They could confirm their observations in four published datasets on human checkpoint blockade studies, in which increased tumor heterogeneity correlated with resistance.

PD-L1 and Alternative Inhibitory Ligands

The expression of PD-L1 is the most obvious candidate as a biomarker for the effectivity of PD-(L)1 targeting antibodies. A prime example of its predictive capacity is represented by Hodgkin's Lymphoma, where 97% of tumors have genetic alterations in the PD-L1/2 locus (Ansell, 2017). This entity has one of the highest response rates to nivolumab monotherapy of 66.3%, even in extensively pre-treated patients (Younes et al., 2016). In several other cancer types, there is an association of PD-L1 with responses to immunotherapy, for example, in non-small cell lung cancer (Fehrenbacher et al., 2016). In this study, patients with less than 1% PD-L1 staining on both tumor cells and immune cells, did not show a significant benefit from atezolizumab treatment.

A complication of these associations is that different trials used different PD-L1 antibody clones and evaluated staining either on tumor cells alone or in combination with the expression on immune cells (S. P. Patel & Kurzrock, 2015; Savic Prince & Bubendorf, 2019). Importantly, different inclusion criteria including different thresholds of PD-L1 expression are thought to be responsible for the observed discrepancy between two phase III trials of untreated NSCLC patients, one which showed therapeutic benefits (Reck, Rodríguez-Abreu, et al., 2016) while the other trial failed to

detect those in the total population (Carbone et al., 2017; Havel, Chowell, & Chan, 2019). After all, the predictive potential of PD-L1 is far from perfect, and non-responding patients are still frequent among patients with high levels of PD-L1. Vice versa, even a considerable number of patients with PD-L1 negative tumors show durable responses in melanoma (Daud, Wolchok, et al., 2016). Thus, more predictive approaches than PD-L1 staining are required. Understanding the mechanisms of primary resistance is crucial in this endeavor.

The upregulation of inhibitory ligands is often a direct consequence of immune activity and represents an important resistance mechanism in response to PD-1 blockade (Benci et al., 2016; Koyama et al., 2016). Co-targeting for example TIM-3 (Sakuishi et al., 2010), LAG-3 (S.-R. Woo et al., 2012), TIGIT (Johnston et al., 2014), B7-H4 (Sica et al., 2003) and VISTA (Xu, Hiếu, Malarkannan, & Wang, 2018), can increase T cell functionality and may act synergistically with PD-1 blockade by improving T cell functionality. Many clinical trials are ongoing or planned to test such combinations (Melero et al., 2015). Vice versa, the upregulation of PD-L1 represents a mechanism for acquired resistance to agonistic anti-CD40 immunotherapy (Zippelius, Schreiner, Herzig, & Muller, 2015). PD-L1 upregulation was induced mainly by IFNγ, and PD-1 blockade could relieve this inhibitory axis.

Another important, yet less explored, alternative immune checkpoint is the hypersialylation of tumors (Läubli et al., 2014; Rodríguez, Schetters, & Van Kooyk, 2018). This pathway is recognized as a driver for NK cell-dependent tumor escape (Hudak, Canham, & Bertozzi, 2014; Jandus et al., 2014). Importantly these sialoglycans also inhibit tumor-infiltrating T cells by engaging upregulated Siglec receptors (Stanczak et al., 2018). Blocking sialoglycan interactions could be an attractive new way to boost therapeutic efficiency in combination with PD-1 and CTLA-4 blockade.

Macrophages

Infiltration of M2-like macrophages is associated with worse prognosis in most tumor entities (Fridman et al., 2017). Remarkably, CD8 T cell reactivity, more precisely IFNγ and TNFα release, induced colony stimulation factor 1 (CSF1) secretion in melanoma, which recruits macrophages to the tumor (Neubert et al., 2018). Moreover, non-responding patients had increased expression of CD163 and CD68, showing a protumoral role for tumor-associated macrophages in checkpoint blockade. Indeed, anti-CSF1R-mediated depletion of macrophages synergized with PD-1 blockade in murine models (Neubert et al., 2018). Tumor-associated macrophages may even express PD-1, which was found to inhibit phagocytosis and anti-tumor immunity (Gordon et al., 2017). Moreover, intratumoral macrophages are able to sequester anti-PD-1 antibodies in an FcR-dependent manner, thus limiting antibody delivery to T cells (Arlauckas et al., 2017).

PI3Kγ signaling seems to play a vital role to induce an anti-inflammatory protumoral phenotype in macrophages and targeting PI3Kγ synergized with PD-1 blockade in mice (Kaneda et al., 2016). Tumor-associated macrophages have a distinct metabolic phenotype and accumulate in hypoxic areas and display a highly glycolytic phenotype that causes high ROS production (Pitt et al., 2017). These cells could be targeted by chemotherapy or by inhibition of their specific metabolic program high in fatty acid oxidation (Al-Khami et al., 2015; Yan et al., 2013). Moreover, myeloid-derived suppressor cells are attracted by granulocyte macrophage colony-stimulating factor

20

(GM-CSF), and they inhibit T cell responses and antigen-presenting cells in tumors (Bronte et al., 1999; Umansky & Sevko, 2013).

Metabolic Enzymes and Endonucleases

Targeting metabolic enzymes represent another important resistance mechanism that modulates the tumor microenvironment. The enzyme indoleamine 2,3-dioxygenase (IDO) is frequently expressed by tumor cells and regulatory immune cells in the tumor and inhibits immune responses by depleting tryptophan from the tumor microenvironment (Friberg et al., 2002; Uyttenhove et al., 2003; R. Wang & Green, 2012). Additionally, IDO leads to the secretion of its degradation product kynurenine, which in synergy with TGFβ , induces regulatory T cell differentiation via the aryl hydrocarbon receptor (Abdel-Malek & Swope, 2011). Many studies reported that inhibition of IDO in murine models changes the tumor microenvironment and leads to improved anti-tumor immunity (Friberg et al., 2002; Xiangdong Liu et al., 2010; Uyttenhove et al., 2003). Despite promising results in early clinical trials, a large phase III trial of an IDO inhibitor in combination with the PD-1 inhibitor pembrolizumab did not meet its primary endpoints and led to the halt of other trials (Komiya & Huang, 2018; Roy Baynes, 2018). Improved targeting or patient selection may improve future clinical trials.

Extracellular ATP and AMP are released by immunogenic cell death and stimulate P2YR receptors or P2XR channels. This mainly induces pro-inflammatory cytokine secretion and dendritic cell maturation (Silva-Vilches, Ring, & Mahnke, 2018). Both CD73 and CD39 (ENTPD1) ectonucleotidases are expressed on diverse immune cells and convert extracellular ATP to AMP, and finally into adenosine. Adenosine has many regulatory functions in the immune system and enhances the proliferation and the immunosuppressive functions of regulatory T cells (Tregs) (Allard, Longhi, Robson, & Stagg, 2017). CD39 is highly expressed by Tregs (Sun et al., 2010) and remarkably also by dysfunctional CD8 T cells in tumors (Canale et al., 2018; Thelen, Lechner, Wennhold, von Bergwelt-Baildon, & Schlößer, 2018). Interestingly, Tregs are especially sensitive to ATP induced cell death via P2X7 (Aswad, Kawamura, & Dennert, 2005). Thus, inhibiting CD39 and CD73 is an attractive way to reduce immunosuppressive functions and numbers of regulatory T cells in the tumor. Inhibiting the CD39/CD73 pathway shows promising effects by restoring T cell functionality and synergizes with oxaliplatin chemotherapy or CTLA-4 and PD-1 blockade in murine tumor models (Allard, Pommey, Smyth, & Stagg, 2013; Perrot et al., 2019; Waickman et al., 2012). CD39 can also be targeted *in vivo* by anti-sense oligonucleotides, which reduced intratumoral Tregs and synergized with PD-1 blockade (Kashyap, Thelemann, et al., 2019).

Tumor Metabolism

Tumor cells have an increased demand for energy and profoundly transform their metabolism. Remarkably, the metabolic reprogramming of expanding effector T cells resembles the metabolic needs of tumor cells in having a higher demand for glucose, glutamine, and lipid oxidation (Bantug, Galluzzi, Kroemer, & Hess, 2018). Therefore, T cells in the tumor compete with cancer cells for the scarce nutrients in the microenvironment. Changes in the tumor microenvironment induced by metabolic activity can hamper immune cell function, for example, by hypoxia (Masoud & Li, 2015; N. E. Scharping, Menk, Whetstone, Zeng, & Delgoffe, 2017), or the lack of glucose (Ho et al., 2015). The secretion of lactate additionally induces an acidic microenvironment, which is detrimental to T cell proliferation and cytokine secretion (Neri & Sondel, 2016).

High levels of lactate dehydrogenase in the serum strongly correlated with resistance to PD-1 and CTLA-4 immunotherapy (Dick et al., 2016; Kelderman et al., 2014). Possibly this axis can be targeted by the pyruvate dehydrogenase kinase inhibitor dichloroacetate (Ohashi et al., 2013). Moreover, changes in nutrient availability, such as glutamine deprivation, skews CD4 T cell differentiation towards Treg development and thereby changes the tumor microenvironment (Gerriets et al., 2016). Similarly, depletion of L-Arginine leads to an expansion of myeloid-derived suppressor cells and inhibits T cell functionality (Fletcher et al., 2015; Rodriguez, Quiceno, & Ochoa, 2007).

B Cells

Only very recently, a report linked activated B cells, which were expanded via IL-21 secretion by T follicular helper cells, to responses in checkpoint blockade in murine models (Hollern et al., 2019). The depletion of B cells in mutagenized murine models led to the abrogation of responses to PD-1 and CTLA-4 combination treatment. Using mRNA signatures, they correlated the infiltration of B cells with response rates in human melanoma and breast cancer patients. This is especially interesting, given that PD-1^T cells often reside in tertiary lymphoid follicles and thereby might be involved in B-cell interactions (D. Thommen et al., 2018). Indeed, dysfunctional intratumoral CD8 T cells have many epigenetic similarities to T_{fh} cells and can secrete the B-cell recruiting chemokine CXCL13 (Satpathy et al., 2019; D. S. Thommen et al., 2018; Workel et al., 2019). How they might be involved in B cell activation or maturation remains to be elucidated.

Microbiome

In a series of publications, the group of Laurence Zitvogel has shown that differences in the microbiome are associated with resistance to cancer immunotherapy. They first reported that the intestinal microbiome was associated with a T_{h17}-dependent immune response to cyclophosphamide chemotherapy (Viaud et al., 2013). Afterward, they found that mice housed under germ-free conditions did not show responses to CTLA-4 blockade in comparison to mice under specific pathogen-free conditions (Vétizou et al., 2015). CTLA-4 blockade induced changes in the microbiome and they proposed an association of several bacterial species with the response to this treatment. Moreover, they could transfer feces from responding and non-responding human patients to mice and recapitulate their clinical response. Similar findings have since been presented in PD-1 blockade in melanoma both in mice and patients by multiple groups (Chaput et al., 2017; V Gopalakrishnan et al., 2018; Matson et al., 2018; Routy et al., 2018). Interestingly the use of antibiotics in patients was negatively linked with response to immunotherapy (Routy et al., 2018). A complication of these associations is that these studies found minimal overlap of species or genus of the bacteria found to be associated with responses. Thus, interventions based on single bacterial strains might not yield the desired effects. Additionally, the mechanisms remain unclear but likely involve priming, induction of tolerance, or cross-reactivity (V Gopalakrishnan et al., 2018; Vancheswaran Gopalakrishnan, Helmink, Spencer, Reuben, & Wargo, 2018; Matson et al., 2018; Routy et al., 2018). As the intestinal microbiome is highly linked with food composition and lifestyle, it could be beneficial to combine lifestyle interventions with cancer immunotherapy (Vancheswaran Gopalakrishnan et al., 2018).

T Cell Dysfunction

T cell dysfunction is the main topic of the third manuscript presented in this thesis. A more detailed introduction and an extensive discussion can be found in section 2.3.5. T cell dysfunction is an essential ta[...] so a major limitation for cancer immunotherapies. PD-(L)1 targeting [...] s cause the expansion and reinvigoration of exhausted T cells (A. C[...] l., 2017) and especially the TCF7+ stem-like cells (Im et al., 2016; Kurtulu[...] chroo, Regev, & Anderson, 2018; Sade-Feldman et al., 2018; Siddiqui e[...] Thus finding ways to improve the effector function of TCF7- cells could represent an attractive additive strategy. The epigenetic stability of the dysfunctional phenotype limits the durability of T cell responses (Ghoneim et al., 2017; Pauken et al., 2016; Philip et al., 2017; Sen et al., 2016). Dysfunction is also a major conce[...] t al., 2013) and CAR T cells (Long et al., 2015; Rott[...] al., 2015). Avoiding the induction of dysfunction is c[...] lerstanding the mechanisms of T cell dysfunction wil[...] nts.

Our group recently demonstrated that T[...] pression in human lung cancer (PD-1^T, tumor-associa[...] criptionally distinct subset that expresses a broad [...] (Figure 3). Importantly, this subset contains a largely unique TCR repertoire with highly enriched tumor reactivity (D. S. Thommen et al., 2018), and the frequency of PD-1^T correlated with response to immunotherapy. The frequency of PD-1^T likely reflects an ongoing immune response ("hot" tumor) and could potentially be used as a biomarker complimentary to PD-L1, TMB, and an Immunoscore.
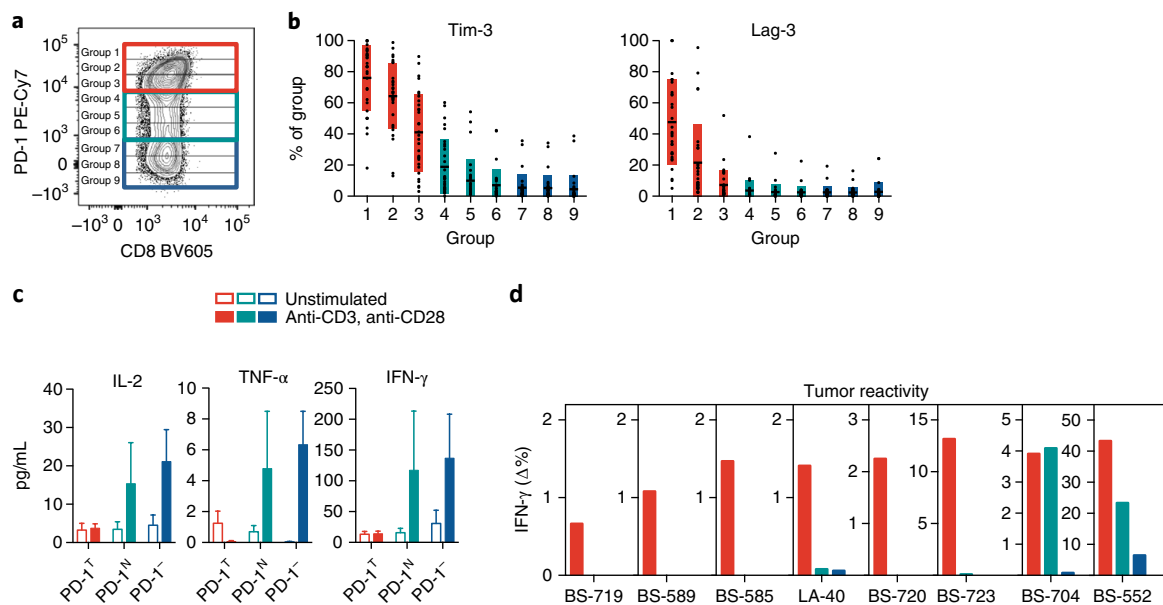

Figure 3 PD-1 Expression Identifies a Subset of Distinct Tumor-reactive T Cells in NSCLC
Adapted from (D. S. Thommen et al., 2018) (a*) Gating for PD-1^T (red), PD-1^N (green), and PD-1$^-$ (blue). (b) Co-expression of inhibitory receptors Tim-3 (left) and LAG-3 (right) within the PD-1 populations. (c) Effector cytokine secretion after anti-CD3/CD28 stimulation in sorted TIL fractions. (d) IFN-γ production by rapidly expanded PD-1 fractions after co-culture with autologous tumor digests.*

Many of the strategies discussed above to enhance checkpoint blockade ultimately affect T cell functionality, such as the reduction of immunosuppressive cytokines, improving co-stimulation, inhibiting inhibitory ligands, and enhancing antigen-presentation. In addition, ways to improve T cell functionality more directly have been proposed. Prominently the intratumoral application of IL-12 boosts T cell responses and could be used to ameliorate T cell dysfunction (Garris et al., 2018).

Another increasingly applied approach is to design bispecific antibodies that redirect and activate T cells to their target. The first bispecific T cell engager (BiTE) blinatumomab is approved for the treatment of refractory precursor B-cell acute lymphoblastic leukemia (Nagorsen & Baeuerle, 2011; Przepiorka et al., 2015), and other BiTEs are being developed (M. Fu et al., 2019). Claus and colleagues recently presented a combination between a tumor antigen-targeted T cell stimulatory bispecific antibody and a FAP-targeted 4-1BB agonist. This could provide selective stimulation and co-stimulation to T cells only in the tumor and may help to reduce off-target toxicity (Bacac, Klein, & Umana, 2016; Claus et al., 2019). Similarly, targeting of cytokines or cytokine-receptor agonists to the tumor site can provide additional stimulus to prevent T cell dysfunction (Neri & Sondel, 2016). Many targeted compounds incorporating parts of IL-2, IL-12 or TNF are being tested in clinical trials (Neri & Sondel, 2016). Current approaches mainly target tumor antigens, but binding moieties to PD-1 are also being explored (Klein et al., 2019).

Resistance Against CAR T cell Therapies

CAR T cell therapy is used to circumvent inefficient priming or tolerance against tumors. They could be inhibited by many of the resistance mechanisms described above, especially for solid tumors. Here, I will elaborate on some CAR T cell-specific mechanisms of resistance.

First-generation CAR T cells suffered from a specific type of T cell-intrinsic resistance mechanism reminiscent of T cell exhaustion or anergy (O'Donnell, Teng, & Smyth, 2019). Even in vitro, scFv-CD3ζ chimeric receptors induce only suboptimal cytokine production, and such CAR T cells did not persist in patients (Brocker, 2000; Kershaw et al., 2006). This was substantially improved with the addition of co-stimulatory domains derived from CD28 or 4-1BB (termed 2nd generation CARs) (Kowolik et al., 2006; Milone et al., 2009). Even though both are used in clinical trials, they appear to have significant differences in murine models (Kawalekar et al., 2016). In their study, Kawalekar et al. demonstrate that the 4-1BB domain induced enhanced T cell signaling to maintain higher persistence and a central memory-associated metabolic phenotype with increased mitochondrial respiration (Kawalekar et al., 2016). Similarly, a detrimental feature of certain CAR constructs is chronic tonic signaling that leads to exhaustion and lack of persistence (Long et al., 2015). The authors showed that this was ameliorated by using a 4-1BB instead of a CD28 co-stimulatory domain. However, summarized clinical data tends to show higher activity for CARs with a CD28 co-stimulatory domain (Weinkove, George, Dasyam, & McLellan, 2019). Therefore, a direct comparison is urgently required to guide future developments, and this will be addressed in two ongoing clinical trials (NCT03191773 and NCT03076437, clinicaltrials.gov). Understanding T cell dysfunction is critical for the improvement of CAR T cell therapies, which was demonstrated by the finding that ablation of the exhaustion-associated transcription factor NR4A1 can improve CAR T cell therapies (J. Chen et al., 2019; Xindong Liu et al., 2019). An intriguing strategy could also be to fuse antigen-recognition domains directly to TCR domains instead of CD8

24

transmembrane regions and CD3ζ domains, which improved co-stimulation and reduced excessive cytokine release in murine models (Baeuerle et al., 2019).

Nevertheless, the primary cause for adaptive resistance with 2nd generation CARs is the loss of its targeting tumor antigen. Several studies with CD19-targeting CARs reported cases of CD19 negative escaping tumor blasts (Grupp et al., 2013; Yu et al., 2017). Even splice variants of CD19 have the potential to cause tumor escape (Sotillo et al., 2015). Importantly, dual-targeting of CD19 with CD123 or CD20 may be able to circumvent or delay this resistance mechanism (Ruella et al., 2016; Zah, Lin, Anne, Jensen, & Chen, 2016).

A multitude of other improvements to CARs have been proposed, including the expression of a dominant-negative TGFβ receptor to improve the infiltration into the tumor, cytokine secretion, and persistence in murine models (Boudreau et al., 2016). Similarly, disruption of PD-1 may also enhance the efficiency of CARs (Rupp et al., 2017). A major limitation of CAR T cells is their infiltration into solid tumors, but checkpoint blockade could be beneficial (Grosser et al., 2019). Efforts to increase tissue-specific homing have been overshadowed by a case of alleged scientific misconduct and led to the retraction of a publication on brain-targeting CARs (Samaha et al., 2018; Schneider, 2019). Other studies found beneficial effects for the regional delivery of CAR T cells (Adusumilli et al., 2014), or the expression of extracellular matrix-degrading enzyme heparanase by CAR T cells themselves (Balkhi, Ma, Ahmad, & Junghans, 2015).

1.3.5. Genetic Predisposition

While tumor genetics have been studied in detail, the contribution of germline host genetics to resistance against cancer immunotherapy remains uncertain. A large study that investigated HLA genotypes discovered that HLA homozygosity is accompanied by an increased risk for progression independently of tumor mutational burden (Chowell et al., 2018). Interestingly, this effect was mainly dependent on HLA-B and HLA-C homozygosity, which either bind a more diverse peptide repertoire or are expressed at higher levels than HLA-A on dendritic cells. Similarly, the same study associated tumor HLA loss of heterozygosity with resistance. They even linked specific HLA-B subtypes to resistance, but this probably requires further validation.

In addition to HLA types, we recently described that the killer cell immunoglobulin-like receptor KIR3DS1 polymorphism is associated with resistance to PD-1 blockade in lung cancer, and I will present this work in the next chapter.

2. Results

2.1. A Variant of a Killer Cell Immunoglobulin-like Receptor is Associated with Resistance to PD-1 Blockade in Lung Cancer

Marcel P. Trefny[1][*], Sacha I. Rothschild[1, 2][*], Franziska Uhlenbrock[1], Dietmar Rieder[3], Benjamin Kasenda[2], Michal Stanczak[1], Fiamma Berner[4], Abhishek S. Kashyap[1], Monika Kaiser[1], Petra Herzig[1], Severin Poechtrager[5], Daniela S. Thommen[6], Florian Geier[7], Spasenija Savic[8], Philip Jermann[8], Ilaria Alborelli[8], Stefan Schaub[9], Frank Stenner[1, 2], Martin Früh[10], Zlatko Trajanoski[3], Lukas Flatz[4], Kirsten D. Mertz[5], Alfred Zippelius[1, 2#], and Heinz Läubli[1, 2#]

[1] Laboratory of Cancer Immunology, Department of Biomedicine, University Hospital and University of Basel, Hebelstr. 20, 4031 Basel, Switzerland, [2] Division of Oncology, Department of Internal Medicine, University Hospital Basel, Petersgraben 4, 4031 Basel, Switzerland, [3] Biocenter, Division of Bioinformatics, Medical University of Innsbruck, Innsbruck, Austria, [4] Institute of Immunobiology and Oncology, Cantonal Hospital St. Gallen, Switzerland,, [5] Cantonal Hospital Liestal, Switzerland, [6] Division of Molecular Oncology and Immunology, Oncode Institute, The Netherlands Cancer Institute, Amsterdam, The Netherlands, [7] Division of Bioinformatics, Department of Biomedicine, University Hospital and University of Basel, Switzerland, [8] Institute of Pathology, University Hospital Basel, Basel, Switzerland, [9] HLA-Diagnostic & Immunogenetics, Department of Laboratory Medicine, University Hospital Basel, Switzerland, [10] Department of Medical Oncology/Hematology, Cantonal Hospital of St. Gallen, St. Gallen, Switzerland. [*]These authors equally contributed to the work. [#]These authors equally supervised the work.

Corresponding Authors: Heinz Läubli & Alfred Zippelius, University Hospital Basel, Petersgraben 4, 4031 Basel, Switzerland, Phone: +41 61 265 5074, Fax: +41 61 265 5316, Email: heinz.laeubli@unibas.ch or alfred.zippelius@usb.ch

2.1.1.   Abstract

Purpose

PD-(L)1 blocking antibodies have clinical activity in metastatic non-small cell lung cancer (NSCLC) and mediate durable tumor remissions. However, the majority of patients are resistant to PD-(L)1 blockade. Understanding mechanisms of primary resistance may allow prediction of clinical response and identification of new targetable pathways.

Experimental Design

Peripheral blood mononuclear cells were collected from 35 NSCLC patients receiving nivolumab monotherapy. Cellular changes, cytokine levels, gene expression, and polymorphisms were compared between responders and non-responders to treatment. Findings were confirmed in additional cohorts of NSCLC patients receiving immune checkpoint blockade.

Results

We identified a genetic variant of a Killer Cell Immunoglobulin-like Receptor (KIR) *KIR3DS1* that is associated with primary resistance to PD-1 blockade in NSCLC patients. This association could be confirmed in independent cohorts of patients with NSCLC. In a multivariate analysis of the pooled cohort of 135 patients the progression-free survival was significantly associated with presence of the *KIR3DS1* allele (HR 1.72, 95 % CI 1.10 to 2.68, *P*=0.017). No relationship was seen in cohorts of NSCLC patients who did not receive immunotherapy. Cellular assays from patients before and during PD-1 blockade showed that resistance may be to NK cell reactivity.

Conclusion

We identify an association of the *KIR3DS1* allelic variant with response to PD-1 targeted immunotherapy in patients with NSCLC. This finding links NK cells with response to PD-1 therapy. While the findings are interesting, a larger analysis in a randomized trial will be needed to confirm KIRs as predictive marker for response to PD-1 immunotherapy.

2.1.2.   Translational Relevance

Only a minority of patients with NSCLC respond to PD-(L)1 therapy. The identification of resistance mechanisms to PD-(L)1 therapy can identify biomarkers of response and potential new targets for cancer immunotherapy. Here, we identify an allelic variant of an NK cell receptor to be associated with resistance to PD-1 targeted immunotherapy in NSCLC. Based on this finding, further exploratory analyses show that NK cells could be potential mediators of resistance to PD-1 blocking antibodies. The described KIR variant is not associated with outcome differences in patients undergoing chemotherapy for stage IV or in the potentially curative setting of stage I-III disease.

2.1.3. Introduction

Adaptive immune escape of tumor cells by upregulation of ligands for programmed death 1 (PD-1) has been identified as an important and targetable pathway in many cancer types (D. S. Chen & Mellman, 2017; Topalian, Drake, & Pardoll, 2015). Many clinical trials have demonstrated that targeting PD-1 or its ligand PD-L1 with immune checkpoint inhibitors (ICI) can restore anti-tumor immunity and induce durable remission (D. S. Chen & Mellman, 2017; Topalian et al., 2015). In patients with non-small cell lung cancer (NSCLC), several trials have demonstrated a survival benefit with PD-(L)1 blocking antibodies in patients with metastatic (Borghaei et al., 2015a; Brahmer et al., 2015; Fehrenbacher et al., 2016; Herbst et al., 2016; Reck, Rodríguez-Abreu, et al., 2016) and locally advanced NSCLC (Antonia et al., 2018). Yet, most patients have primary resistance to PD-(L)1 blockade: approximately 20-25% of unselected patients with NSCLC achieve an objective response while 40-50% have progressive disease. Understanding mechanisms of primary resistance to PD-(L)1 blockade is important in the search for potentially targetable pathways and may ultimately allow discrimination between patients that derive benefit from PD-(L)1 blockade and those requiring combination strategies or alternative treatment approaches.

Different mechanisms of primary and acquired resistance to PD-(L)1 blockade have been described, including defects in human leukocyte antigen (HLA) class I presentation, cellular adaptation of the tumor microenvironment, low mutational burden, and mutations or defects in the interferon gamma (IFNγ) pathway (Syn et al., 2017). To date, most of the focus of investigations has been on how T cells interact with tumor cells, while other immune cells may be critical as well. Recently, cross talk between natural killer (NK) and dendritic cells has been associated with response to PD-1 blockade in melanoma (Barry et al., 2018). In this study, we aimed to identify mechanisms of resistance and potential new targetable pathways in patients with metastatic NSCLC that received PD-1 blockade using a comprehensive analysis of peripheral blood from responding and non-responding patients. We found that the allelic variant *KIR3DS1*, referred to as *KIR3DS1* allelic variant, is associated with primary resistance to PD-1 blockade and is mainly expressed on NK cells. *KIR3DS1* is an alternative allele at the *KIR3DL1* locus coding for an activating receptor unlike the *KIR3DL1* alleles which encode for inhibitory receptors. *KIR3DS1* mainly differs from *KIR3DL1* in its signaling binding domains at the cytoplasmatic tail (Parham, Norman, Abi-Rached, & Guethlein, 2011)p . In addition, peripheral NK cell reactivity is enhanced in patients responding to PD-1 blockade, suggesting that NK cells are involved in response to immunotherapy.

2.1.4.   Materials and Methods

Patients and Sample Preparation

Serum and peripheral blood mononuclear cells (PBMCs) were prospectively collected from 35 metastatic NSCLC patients (discovery cohort) immediately before the first administration and after two cycles (week 4) of treatment with PD-1 blockade at the University Hospital in Basel, Switzerland. All patients that were planned for immunotherapy after progression on chemotherapy were asked to participate. Ethics approval was obtained from the local ethical committee to analyze the tissue and blood samples (Ethikkomission Nordwestschweiz, EK321/10) and written informed consent was obtained from all patients prior to sample collection. Objective radiologic response was determined by RECIST by a thoracic radiologist, with scans performed every 6-8 weeks. Single cell suspensions of primary NSCLC tumor samples were prepared by digestion after surgical removal.

For validation and comparison, we examined whole exome sequencing data from a previously published cohort of patients with metastatic NSCLC treated with pembrolizumab (Rizvi et al., 2015). In addition, we examined a third independent cohort of patients from St. Gallen with NSCLC with PD-(L)1 inhibitors by PCR (approved by the local ethical committee, Ethikkommission Ostschweiz, EKOS). Finally, early stage NSCLCs in the TracerX study cohort not treated with immunotherapy were analyzed by whole exome sequencing (Jamal-Hanjani et al., 2017).

Multicolor Flow Cytometry

PBMCs were isolated as published previously (D. S. Thommen et al., 2015). Multicolor flow cytometry was performed after staining dead cells with live/dead fixable Blue and various panels of antibodies (Supplementary Table 10). Corresponding isotype antibodies were used as controls. Tumor samples were analyzed by flow cytometry with a Fortessa LSR II flow cytometer (BD Biosciences). For intracellular cytokine staining, cells were fixed and permeabilized using IC-Fixation or Fix/Perm kit (eBioscience). For RNA sample collection, peripheral CD8$^+$ T cells were sorted by fluorescence-activated cell sorting using a BD FACS AriaIII.

Molecular Analysis of KIR3DS1/L1 and HLA Locus

The *KIR3DS1/L1* locus was analyzed from germ-line DNA isolated from peripheral blood by polymerase chain reaction as previously described (Uhrberg et al., 1997). The *HLA-A, -B* and *−C* were typed by molecular methods (FluoGene; Inno-train) and the presence of Bw4 and Bw6 within the *HLA-A* and *HLA-B* determined.

Bioinformatic Analysis of KIR3DS1/L1 and HLA Status from Whole-Exome Sequencing Data

To identify polymorphisms and genetic variants in *KIR* alleles from whole exome sequencing data, germline whole exome sequencing data from dataset EGAD00001003206 was obtained under a data access agreement through the European Genome Archive (https://ega-archive.org). Sequence alignments were first sorted by read name using SAMtools 1.3.1 (H. Li et al., 2009) and separated into paired FASTQ files using picard 2.9.2 (http://broadinstitute.github.io/picard). Parts of the KIR genome region (GRCh37; KIR3DL1 +/- 100bp chr19:55327793-55342333, KIR3DS1 +/- 100bp chr19_gl000209_random:69997-84758) were extracted from the provided

sequence alignments using SAMtools 1.3.1. We used BLAST to identify three unique sequence regions distinguishing KIR3DS1/L1 (Supplementary Table 9). We then used featureCounts (Liao, Smyth, & Shi, 2014) to quantify the number of sequencing reads from each individual normal sample aligning to these three distinguished regions (primary, concordant paired-end alignments, having >90% region overlap and no CIGAR operations). We calculated the LogR ratio for the individual counts and used these measures to assess the *KIR3DS1/L1* genotype (the script for the analysis is deposited at https://github.com/mui-icbi/KIRcaller). We used the "Pushing Immunogenetics to the Next Generation" (PING) method developed by Norman and colleagues (Norman et al., 2016) in an independent cohort (TracerX) to cross-validate the genotyping of the KIR alleles.

Natural Killer Cell Degranulation and Cytotoxicity Assay

Whole bulk PBMCs containing NK cells from patients with NSCLC before and during PD-1 blockade treatment were thawed. 10,000 K562 target cells were co-cultured with 200,000 PBMCs (effector to target ratio 20:1) in the presence of fluorochrome-coupled anti-CD107a antibody. After 1 h of co-incubation, Monensin and Brefeldin were added to the culture to accumulate cytokines intracellularly. After 5 h of additional co-incubation, the cells were fixed and stained for IFNγ and TNFα. The samples were then analyzed by flow cytometry gated on CD56+ CD3- NK cells. NK effector functions were further assessed by a cytotoxicity assay performed using whole bulk PBMCs at an effector to target ratio of 20:1 using K562 cells previously labeled by Vybrant DiO Dye (Thermo Fisher). The cytotoxic capacity of the NK cells was determined after 6 h co-incubation by measuring the percentage of PI$^+$/DiO dye$^+$ K562 target cells by flow cytometry taking into account non-specific K562 cell death.

Multiplex Cytokine Measurements

Serum samples before and during treatment were used. NK and T cell cytokines were measured by a flow cytometry bead assay that allows measurement of 13 cytokines (LEGENDplex^{TM}; BioLegend). Binding of cytokines to the beads was measured using a Fortessa II analyzer (BD Biosciences).

HLA-F Immunohistochemistry

Tissue sections from patients were analysed by immunohistochemistry for HLA-F expression. Paraffin sections were incubated with a monoclonal rabbit anti-human HLA-F IgG (Abcam, clone EPR6803).

Statistical Analysis

We used multivariable Cox regression models to investigate the association between *KIR3DS1/L1* status and progression-free survival (PFS) adjusted for age and smoking status in the in the pooled analysis (discovery and confirmation cohort). An additional sensitivity analysis was conducted on the discovery cohort with PD-L1 in the model (considering expression levels of 0%, 1-50% and >50%). All analyses were conducted on complete cases, no techniques for multiple imputations were applied. We used the statistical program R (version 3.4.3) for all multivariable analyses and creating the Kaplan-Meier plots. GraphPad Prism version 6.05 was used for statistical analysis of flow cytometry data. All reported *P*-values are two sided and considered exploratory.

2.1.5.   Results

Minimal Cellular Changes in Peripheral Blood of NSCLC Patients Undergoing PD-1 Blocking Antibody Therapy

PBMCs and serum samples were collected from 35 patients with NSCLC immediately before and after two cycles (week 4) of treatment with nivolumab (Table 1). All patients had progressed on or after at least one prior platinum-containing chemotherapy regimen. Median age was 62 years, 20% of patients were female, 14.3% had squamous cell histology, and 74.3% adenocarcinoma histology (Table 1). Eastern Cooperative Oncology Group (ECOG) performance status (PS) was 0 or 1 in 77.1% of patients.

Changes in immune cells in the peripheral blood were analyzed in 19 patients with available serial samples. After two cycles of treatment, there were no significant changes in numbers of $CD8^+$ and $CD4^+$ T cells during treatment (Figure 4A), but a slight increase in $CD4^+$ $CD25^+$ $FoxP3^+$ regulatory T cells was seen (Figure 4A). No changes were observed in $CD56^+$ $CD3^-$ NK cell numbers or naïve T cells ($CD45RA^+$ $CCR7^+$ T cells; Figure 4A). Since $CD8^+$ T cells are considered the main effectors of checkpoint blockade and cancer immunotherapies (D. S. Chen & Mellman, 2017; Topalian et al., 2015), we analyzed differentially expressed genes in peripheral $CD8^+$ T cells before and during treatment in 5 patients with partial response and 5 patients with primary progressive disease to identify mechanisms of resistance to PD-1 therapy (Supplementary Table 1). Messenger-RNA sequencing revealed alterations in very few genes in total peripheral $CD8^+$ T cells during treatment (Supplementary Table 2) Only one gene – the gene for the killer immunoglobulin-like receptor *KIR3DS1* - was clearly differently expressed between responders and non-responders (Figure 4B).

Table 1 Patient Characteristics of NSCLC Patients in the Discovery Cohort. *

Characteristic	Discovery Cohort (N = 35)
Median age — yr (range)	62 (35–83)
Male sex — no. (%)	20 (57.1)
Histology — no. (%)	
Adenocarcinoma	26 (74.3)
Squamous cell carcinoma	5 (14.3)
Large cell carcinoma	1 (2.9)
NOS	3 (8.5)
Smoking history — no. (%)	
Never	7 (20)
Former	14 (40)
Current	14 (40)
Molecular markers — no. (%)	
No markers detected	22 (62.8)
KRAS mutation	9 (25.6)
EGFR mutation	1 (2.9)
ALK translocation	1 (2.9)
MET exon 14 deletion	1 (2.9)
HER2 mutation	1 (2.9)
Previous therapy lines — no. (%)	
1	33 (84.6)
2	3 (7.7)
>2	3 (7.7)
ECOG PS — no. (%)	
0	9 (25.7)
1	18 (51.4)
2	7 (20)
3	1 (3)

Patients all received nivolumab monotherapy for at least 3 cycles. ALK denotes anaplastic lymphoma kinase, ECOG PS Eastern Cooperative Oncology Group Performance Status, EGFR epidermal growth factor receptor, NOS not otherwise specified.
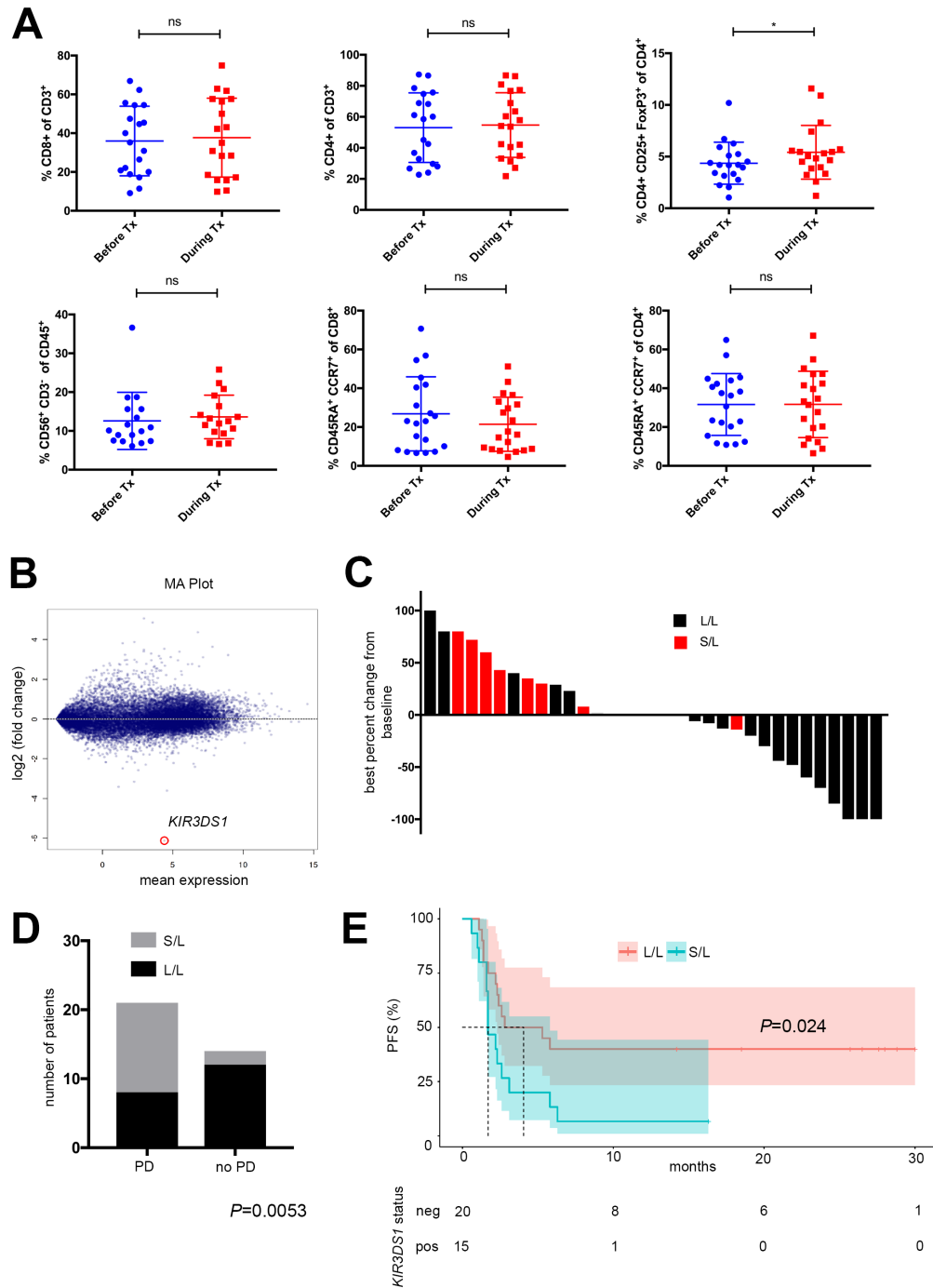
Figure 4 Presence of KIR3DS1 Polymorphism is Associated with Resistance to PD-1 Blockade

(**A**) Frequency of peripheral CD8+ T cells, CD4+ T cells, regulatory CD4+ CD25+ FoxP3+ T cells, NK (CD56+ CD3-) cells, naïve CD8+ T cells, and naïve CD4+ T cells in the peripheral blood of NSCLC patients undergoing PD-1 blocking treatment (Tx) with nivolumab determined by flow cytometry, N = 19, *P<0·05 by paired Student's t test. Data represented as Mean±SD. (**B**) MA plot of the expression analysis in patients responding to PD-1 blockade vs patients not responding. (**C**) Best radiographic response determined by RECIST in NSCLC patients treated with nivolumab. Response assessment was performed in homozygous KIR3DL1 (L/L) and heterozygous KIR3DS1/L1 (S/L) patients. (**D**) Number of NSCLC patients in the discovery cohort with the KIR3DS1 allele present or absent that have progressive disease (PD) or not progressive disease (no PD) in the discovery cohort. Fisher's exact test was used for statistical analysis. (**E**) PFS of discovery cohort (N = 35), according to KIR3DS1 status. Statistical analysis by Wilcoxon signed-rank test.

Association of KIR3DS1 *Genetic Variant with Resistance to PD-1 Blockade*

KIRs are a polymorphic family of NK cell receptors that bind to HLAs (Chiossone, Vienne, Kerdiles, & Vivier, 2017; Malmberg, Sohlberg, Goodridge, & Ljunggren, 2017). The gene product of *KIR3DS1* is an activating variant of the inhibitory *KIR3DL1* receptor that binds to Bw4 epitope-containing HLAs (Chiossone et al., 2017; Malmberg et al., 2017). The *KIR3DS1* allele was present in the germline of 4/5 patients with primary progressive disease and 0/5 patients with partial response, prompting us to study the allelic variant in the full cohort.

Genotyping of the discovery cohort (n=35) revealed that 15 (42.9%) patients carried the *KIR3DS1* variant while 20 (57.1%) were homozygous for *KIR3DL1*. The whole cohort had an overall response rate of 22.8% (8/35) and a PFS of 2.4 months (Supplementary Figure 1). No patient was homozygous for *KIR3DS1* in our cohort. Clinical characteristics were similar between these two groups (Table 2). Thirteen of 17 (76.5%) patients with primary progression carried the activating receptor KIR3DS1 compared with 2 of 10 (20%) of patients with partial response (*P*=0.007). Patients with the *KIR3DS1* allele present had a significantly higher chance for disease progression (Figure 4C). The overall response rate (ORR) in patients homozygous for the *KIR3DL1* allele was 40% (7/20 partial response [PR], 35%; 1/20 complete response [CR], 5%). In contrast, the response rate in patients with the *KIR3DS1* allele was 0% (*P*=0.01). PFS to PD-1 blockade was also worse in patients carrying the *KIR3DS1* allele (Figure 4E; hazard ratio [HR], 2.68; 95% confidence interval [CI], 1.58 to 4.61; *P*=0.03). Patients carrying either the *KIR3DS1* allele or carrying no allele for Bw4-containing *HLAs* showed a lower risk of progression compared with patients carrying *KIR3DS1* alone, but the consideration of Bw4-containing *HLA*s (ligands for KIR3DL1) did not better discriminate between progressing and non-progressing patients (Supplementary Figure 1B and C). In addition, the PFS of prior chemotherapy regimen did not differ between patients with or without the *KIR3DS1* allele (Supplementary Figure 2A; HR, 0.80; 95% CI, 0.41 to 1.55; *P*=0.50).

We next explored two cohorts of patients with metastatic NSCLC treated with PD-(L)1 blocking antibodies as confirmation cohorts. First, we analyzed a cohort of 34 patients with metastatic NSCLC treated with pembrolizumab (Rizvi confirmation cohort). We selected this cohort because whole exome sequencing data were available (Rizvi et al., 2015). Seven of 13 patients with primary progression carried the allele for the activating receptor *KIR3DS1* compared with 1 of 12 of patients with PR (*P*=0.03). All other responders (11 of 12) were homozygous for *KIR3DL1*. In this cohort, the response rate in the patients with *KIR3DS1* was 9.1% (1/11) and without *KIR3DS1* 47.8% (11/23). Similarly, PFS to PD-1 blockade was worse in patients carrying the *KIR3DS1* allele (Figure 5A; HR, 2.64; 95% CI, 1.58 to 4.61; *P*=0.01). KIR types in this cohort were determined by a new bioinformatics algorithm that has been developed by us and successfully validated in an independent cohort (TracerX) against a well-characterized published method (Norman et al., 2016). In addition, we examined by PCR the presence for *KIR3DS1* of another new cohort of 66 metastatic NSCLC patients that received a PD-(L)1 inhibitor (St. Gallen confirmation cohort). There was a trend with a median time to progression of 5.1 months in the KIR3DS1 positive group versus 10.2 months in the *KIR3DS1* negative group. Yet, we did not observe a statistically significant difference of the PFS in this cohort (Figure 5B, HR, 1.37; 95% CI, 0.69 to 2.70; *P*=0.36). In this cohort, the response rate in the patients with *KIR3DS1* was 7.1% (2/28) and 21.1% (8/38) without *KIR3DS1*. The overall response rate of the

whole cohort is lower than would be expected in such a treatment group (15.1%). This could be a possible explanation for the lack effect in this independent group alone. Unlike in the discovery cohort, *KIR3DS1* homozygous patients were found in the confirmation cohorts (2 in the Rizvi cohort, 4 in the St. Gallen cohort).

Table 2 Patient Characteristics of the Discovery Cohort, According to KIR3DS1/L1 Status

Characteristic	KIR3DL1/L1 (N = 20)	KIR3DS1/L1 (N = 15)	P value
Median age — yr (range)	61 (49–83)	61 (35–75)	0.43[*]
Male sex — no. (%)	10 (50)	11 (73.3)	0.30[†]
Histology — no. (%)			
Non-squamous	17 (85)	13 (86.6)	>0.99[†]
Squamous	3 (15)	2 (13.4)	
Smoking history — no. (%)			
Yes	17 (85)	11 (73.3)	0.43[†]
No	3 (15)	4 (26.7)	
ECOG status — no. (%)			
0–1	15 (75)	12 (80)	>0.99[†]
2–3	5 (15)	3 (20)	
PD-L1 status — no. (%)			
Negative	6 (30)	8 (53.3)	0.11[‡]
1–50%	5 (25)	2 (13.4)	
>50%	5 (25)	0 (0)	
Missing	4 (20)	5 (33.3)	

[*] *Student's t test,* [†]*Fisher's exact test,* [‡]*Chi-Square test. ECOG PS denotes Eastern Cooperative Oncology Group Performance Status; PD-L1 programmed death-ligand 1.*
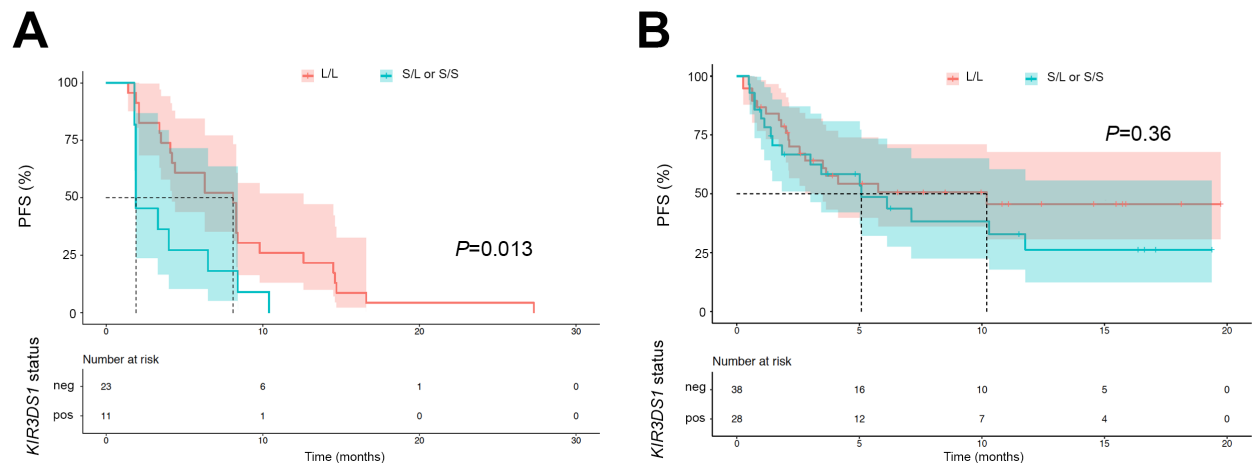

A

B

Figure 5 KIR3DS1 Association with PFS in NSCLC Checkpoint Inhibitor Confirmation Cohorts

(*A*) *PFS of confirmation cohort according to KIR3DS1 status (N = 34) from Rizvi et al. Statistical analysis by Wilcoxon signed-rank test. (B) PFS of confirmation cohort according to KIR3DS1 status (N = 66) of an additional cohort from the cantonal hospital in St. Gallen. Statistical analysis by Wilcoxon signed-rank test.*

Univariate analysis of PFS of the combined cohorts (discovery cohort plus the two confirmation cohorts) confirms a significantly worse outcome when *KIR3DS1* was present with a median PFS of only 2.6 months compared to 6.3 months (Figure 5 and

Supplementary Table 5, HR 1.89, 95% CI, 1.24 to 2.87; *P*=0.0029). Multivariate analysis considering age and smoking status demonstrated a significantly increased risk of progression in patients with the *KIR3DS1* allele (Supplementary Table 6, HR 1.91, 95% CI, 1.25 to 2.91; *P*=0.0027). When a multivariate analysis was performed that included tumor PD-L1 status considering three groups of expression (0%, 1-50% and >50%), the significant effect of the *KIR3DS1* status on the PFS remained (Supplementary Table 7, HR 1.72, 95% CI, 1.10 to 2.68; *P*=0.017). In contrast to this finding, among patients (n=99) with early stage NSCLCs who were not treated with immunotherapy (TracerX cohort) there was no difference in disease-free survival according to *KIR3DS1* status (Supplementary Figure 2B; HR, 1.41; 95% CI, 0.58 to 3.24; *P*=0.44). We could not observe an association between PD-L1 expression and the *KIR3DS1* status (Table 3). We could also not observe an association with the tumor mutational burden (TMB) of patients that had TMB data available (Table 3).

Table 3 Association of PD-L1 Status and TMB with Pooled Cohort

KIR3DS1 status	L/L	S/L or S/S	P value
PD-L1 status – no. (%)			
0%	23 (36)	17 (39.5)	0.92[‡]
1-50%	18 (28)	12 (27.9)	
>50%	23 (36)	14 (32.6)	
TMB– no. (%)			
Low (0-11 mutations/Mb)	13 (39.4)	9 (60)	0.22[†]
High (>11 mutations/Mb)	20 (60.6)	6 (40)	

[‡]*Chi-Square test.* [†]*Fisher's exact test, TMB denotes tumor mutational burden. Mb megabase.*

The KIR3DS1 Receptor Associates NK Cells with Resistance to Immune Checkpoint Blockade

To provide mechanistic insights into the association of KIR3DS1 expression and immune checkpoint blockade resistance, we determined the expression of KIR3DS1 on peripheral immune cells by flow cytometry. KIR3DS1/L1 was mainly expressed on NK cells compared to CD8 T cells both in the peripheral blood and in the tumor (Figure 6A). Both *KIR3DL1/L1* and *KIR3DS1/L1* patients showed similar NK cell numbers and expression of PD-1, CD56, TBET, EOMES and KI67 in NK cells (Supplementary Figure 4). PD-1 expression on peripheral NK cells was very low, but higher and significantly decreased upon treatment in patients homozygous for *KIR3DL1*. TIM-3 was higher before treatment in *KIR3DL1/L1* patients compared with *KIR3DS1/L1* patients (Supplementary Figure 4F). Expression of other inhibitory and activating receptors on NK cells remained unchanged during treatment (Supplementary Figure 4).

To test the functional potential of NK cells in patients treated with PD-1 blockade, we incubated peripheral NK cells with K562 target cells and analyzed degranulation by CD107a surface staining and production of intracellular cytokines. Patients homozygous for *KIR3DL1* showed increased cytokine production after PD-1 blockade monotherapy compared to those carrying the *KIR3DS1* allele (Figure 6B and Supplementary Figure 5A). Similarly, more *KIR3DL1/L1* patients had an increase in tumor cell killing (63%) during treatment compared with patients carrying the *KIR3DS1* allele (28%) (Supplementary Figure 5B). Multiplex analysis of NK and T cell cytokines in the peripheral blood showed a tendency towards reduced IFNγ and significantly increased IL-6 levels in NSCLC patients with *KIR3DS1/L1* heterozygosity (Figure 6C). There were no significant changes of peripheral T cells depending on the *KIR3DS1* status (Supplementary Figure 5C-5H). The presence of activating ligands for KIR3DS1 could lead to continuous stimulation of NK cells and potential NK cell exhaustion. We

therefore stained available tissue for the KIR3DS1 ligand HLA-F. Indeed, several tumors showed a clear positivity for HLA-F immunohistochemical staining (Figure 6D, Supplementary Table 8). In general, most NSCLC samples demonstrated an intermediate to high staining score suggesting that HLA-F upregulation in lung tumors is a common phenomenon (Supplementary Figure 6, Supplementary Table 8).
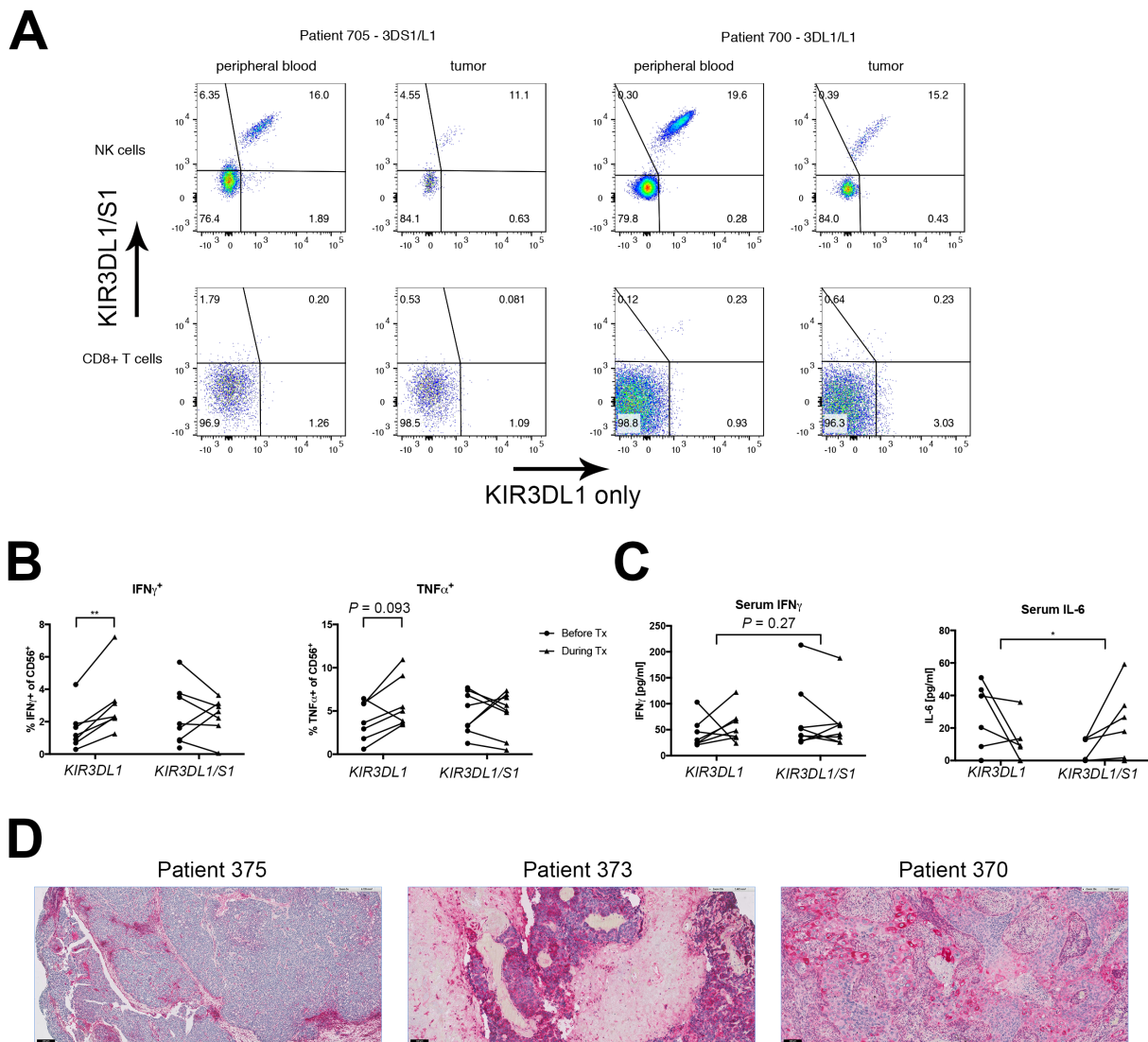

Figure 6 KIR3DS1 on NK Cells is Involved in the Association with Resistance to PD-1 Blockade

(*A*) Two representative flow cytometric analyses of peripheral and intratumoral NK cells and CD8$^+$ T cells for KIR3DL1 and KIR3DS1 (y-axis: antibody that recognizes both KIR3DS1 and KIR3DL1, x-axis: antibody that recognizes only KIR3DL1). (*B*) Functional analysis of peripheral NK cells before and during treatment with PD-1 blockade. Peripheral NK cells were incubated with K562 target cells and intracellular cytokine production was determined by flow cytometry. N=7, ** P<0·01 by paired two-way ANOVA with Sidak's multiple comparison testing. (*C*) Changes of IFNγ and IL-6 in the peripheral sera of NSCLC patients during PD-1 blockade therapy. N = 7, * P<0·05 for the interaction between genotype and treatment by paired two-way ANOVA with Sidak's multiple comparison testing. (*D*) Representative images of HLA-F staining for NSCLC tissue by immunohistochemistry in red coloring (Bars, 100 μm).

2.1.6.   Discussion

We identified a receptor gene variation, which is known to modulate NK cell activation, being associated with worse clinical outcome in patients with metastatic NSCLC treated with PD-1 blockade. We confirmed our findings in a combined analysis of cohorts of metastatic NSCLC patients treated with PD-(L)1 blocking antibodies. We also show that the genetic variation is not associated with prognosis in patients with localized NSCLC after resection (TracerX) cohort. In general, *KIR3DS1* seems to be rather a predictive marker for PD-(L)1 therapy than a prognostic marker, although further studies including prospective trials would be needed to definitively answer this question.

The *KIR3DS1/L1* genetic variation has been previously linked to the outcome of treated cancer patients (Boudreau et al., 2017; Chiossone et al., 2017; Forlenza et al., 2016; Gabriel et al., 2010; Venstrom et al., 2012). In one study, the presence of the *KIR3DS1* allele predicted increased risk of progression in patients receiving autologous stem cell transplantation for multiple myeloma (Gabriel et al., 2010). In another study, the *KIR3DL1/S1* status was associated with outcomes in neuroblastoma patients treated with anti-GD2 monoclonal antibody (Forlenza et al., 2016). Recent mechanistic studies in a humanized mouse model have shown that the presence of inhibitory KIR3DL1 and Bw4-containing HLA ligands can educate NK cells to be more responsive to the loss of MHC-I molecules on tumor cells (Boudreau et al., 2016).

We have identified the *KIR3DS1* allele to be associated with resistance to PD-1 blockade by expression analysis in peripheral CD8$^+$ T cells. Although expression was different between responders and non-responders on a transcript level, only minimal protein expression was found by flow cytometry on CD8+ T cells compared to NK cells. We therefore focused further analysis on NK cells. NK cell education describes a process by which the chronic interaction of inhibitory KIRs (e.g. KIR3DL1) with their MHC ligands (e.g. Bw4) promotes NK cell responsiveness through yet unknown mechanisms (Elliott & Yokoyama, 2011; Raulet & Vance, 2006; Shifrin, Raulet, & Ardolino, 2014). Our correlative analysis suggests that NK cells are involved in the mechanism of KIR3DS1-associated resistance to PD-1 blockade, since KIR3DL1 or KIR3DS1 were only minimally expressed on peripheral and intratumoral T cells. NK cell education mediated by KIR3DL1-Bw4 ligation seems unlikely to be the primary cause of resistance, because the predictive value of *KIR3DS1* was reduced when the Bw4 ligands were considered. Thus, the presence or absence of KIR3DL1-binding Bw4-containing HLA's does not improve the discrimination between responders and non-responders in patients homozygous for *KIR3DL1*. In addition, differences in peripheral NK cell functionality were only observed after initiation of PD-1 blockade and not prior treatment, which should also be different if education was involved.

Recent analysis of *HLA* types and response to immune checkpoint inhibitors suggests an association with certain *HLA-B* types, mainly linked to presentation capacities of specific *HLA-B* types (Chowell et al., 2018). It is possible that these *HLA* types also associate with differences in NK functionality, which would need further investigation in larger cohorts given the vast numbers of possible combinations. Another possible underlying mechanism might be the induction of dysfunctional or 'exhausted' NK cells by continuous KIR3DS1 stimulation by its ligand HLA-F, which was found to be highly expressed in lung cancer (Lin et al., 2011). Indeed, we confirmed strong expression of HLA-F in selected patients, although this could not be performed in all patients due to unavailability of tumor tissue. Yet, we currently lack a deeper mechanistic

understanding of the cellular network that mediates resistance in patients expressing KIR3DS1. Complex human *in vitro* systems or humanized mouse models would be required for functional studies, as *KIR* receptors and *HLAs* both are very weakly conserved between mice and humans. In addition, larger prospective trials are needed to validate the presence of *KIR3DS1* as predictive marker for primary resistance in tumors other than lung cancer and combination treatments such as PD-1/ CTLA-4 blockade.

Our results support the hypothesis that NK cells are involved in resistance to PD-1 blockade. NK cells have been known to be important players in the immunosurveillance of cancers and recent efforts have led to the development of checkpoint inhibitors that target inhibitory receptors on NK cells for cancer immunotherapy (Chiossone et al., 2017; Guillerey, Huntington, & Smyth, 2016). Lirilumab, for example, targets the immunoglobulin-like domain 2 (2D) of KIR2DL1, 2 and 3, which is engaged by HLA-C epitopes (Chiossone et al., 2017; Guillerey et al., 2016). Our findings suggest that NK cells play an important role in mediating the effect of PD-1 blocking immunotherapy. It is conceivable that crosstalk between NK cells and the tumor microenvironment, rather than an independent effect of NK cells, could be responsible for our observations. Indeed, a recent publication described the interaction of NK cells with dendritic cells within the tumor to induce a PD-1 checkpoint inhibitor responsive microenvironment (Barry et al., 2018). A recent analysis in a mouse model has additionally provided evidence that NK cells dictate the infiltration of classical dendritic cells into tumors and thereby play an important role in anti-tumor immunity (Böttcher et al., 2018).

In summary, we provide evidence that the *KIR3DS1* genetic variant is associated with the outcome in NSCLC patients treated with PD-1 directed immunotherapy (summarized in Figure 7). Our findings suggest an important role of NK cells to modulate the therapeutic efficacy of PD-(L)1 targeted therapies. As NK cell targeted therapies are available, they might be particularly useful in patients with the *KIR3DS1* allele present. Thus, it will be of utmost clinical relevance to dissect the cellular mechanisms how NK cells interact with other immune effectors in the tumor microenvironment.
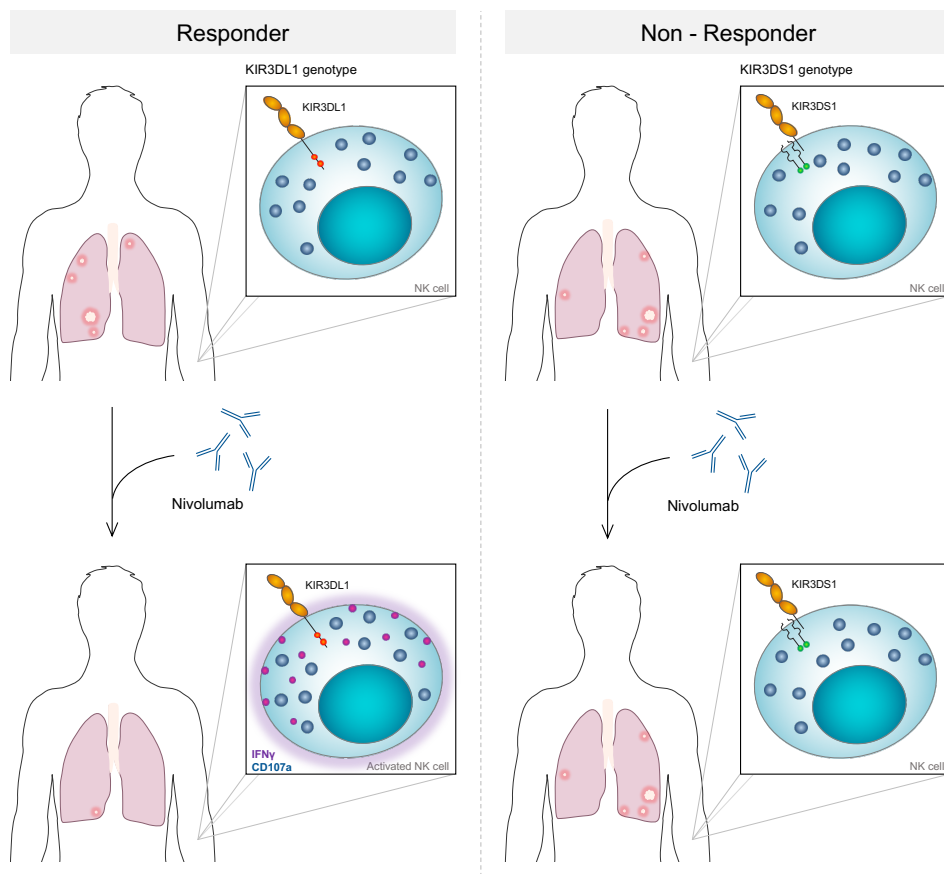
Figure 7 Summary of the Findings

Patients with a KIR3DS1 allele, which codes for an activating receptor on NK cells, are more likely not to respond to PD-(L)1 blocking agents such as Nivolumab compared to KIR3DL1 homozygous patients. Correspondingly, in KIR3DL1 homozygous patients we see an increased production of effector molecules such as IFNγ by NK cells after treatment with PD-1 targeted therapy.

Contributions

H.L. and A.Z. conceived the idea for the study. H.L., M.P.T., and A.Z. interpreted the data and wrote the manuscript. H.L., M.P.T. F.U., M. K., and A. S. K. planned the experiments. M.P.T., M. K., F.U., M.S., S.S., K.M., P.J. and I.A. and P.H. performed and analyzed the experiments. H.L., D. S. T., B.K., S.P., F.S and S.I.R. collected and analyzed the clinical data. D.R., Z.T., F.G and M.P.T. performed the bioinformatic analysis of the confirmation and discovery cohorts. St.S. performed the HLA analysis and interpretation.

Acknowledgment

2.1.7. Supplementary Methods

Multicolor Flow Cytometry

Multicolor flow cytometry was performed after staining dead cells with live/dead fixable Zombie UV (Biolegend) and various panels of antibodies.

Antibody target (all human)	Fluorochrome	company	catalog Nr.	clone
CCR7	Alexa Fluor 647	Biolegend	3532218	G043H7
CD16	FITC	eBioscience	11-0168	eBioCB16
CD3	PE-CF594	BD	562280	UCHT1
CD45	APC-H7	BD	560178	2D1
CD45RA	BV421	Biolegend	304130	HI100
CD56	BV785	BioLegend	362550	5.1H11
CD8	FITC	eBioscience	11-0087	SK1
EOMES	PerCP eFluor	eBioscience	46-4877	WD1928
Human IgG4	PE	Southern Biotech	9200-09	HP6025
IFNγ	BV421	BD	564791	4S.B3
KI67	APC	BioLegend	350514	Ki-67
KIR2DL3	APC	BioLegend	312611	DX27
KIR3DL1	Alexa700	BioLegend	312712	DX9
KIR3DS1/L1	PE	Beckmann Coulter	IM3292	Z27.3.7
LAMP-1 (CD107a)	PE	BD	555801	H4A3
NKG2D	BV605	BD	743559	1D11
NKp30	BV711	BD	563383	p30-15
NKp46	BV421	BioLegend	331913	900
NKp80	APC	BioLegend	346708	5D12
PD-1	PE-Cy7	BD	561272	EH12.1
TBET	BV421	BioLegend	644815	4B10
TIGIT	PE	eBioscience	2776179	MBSA43
TIM-3	BV605	BioLegend	345018	F38-2E2
TIM-3	BV421	BioLegend	345008	F38-2E2
TNFα	APC	eBioscience	17-7349	MAb11

2.1.8. Supplementary Figures and Tables
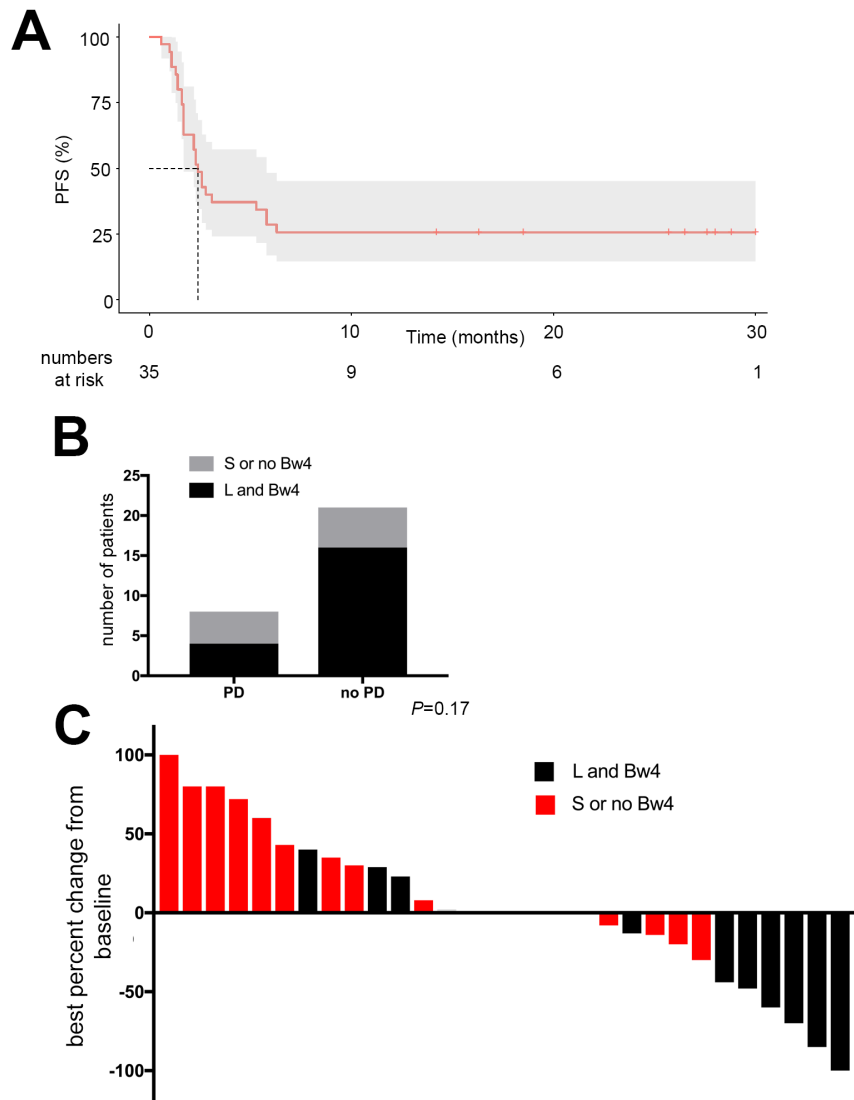
Supplementary Figure 1 Association of Response to PD-1 Therapy with KIR3DS1 Status or Absence of KIR3DL1 Ligands

*A) PFS curve of the whole discovery cohort (N = 35). The median PFS was 2.4 months in the whole cohort. (**B**) Presentation of number of patients with the KIR3DS1 allele or no ligands for KIR3DL1 (no Bw4) with primary progression (PD) or no primary progression (no PD). (**C**) Best percent change of target lesions from baseline according to the presence of KIR3DS1 and absence of the KIR3DL1 ligand Bw4.*
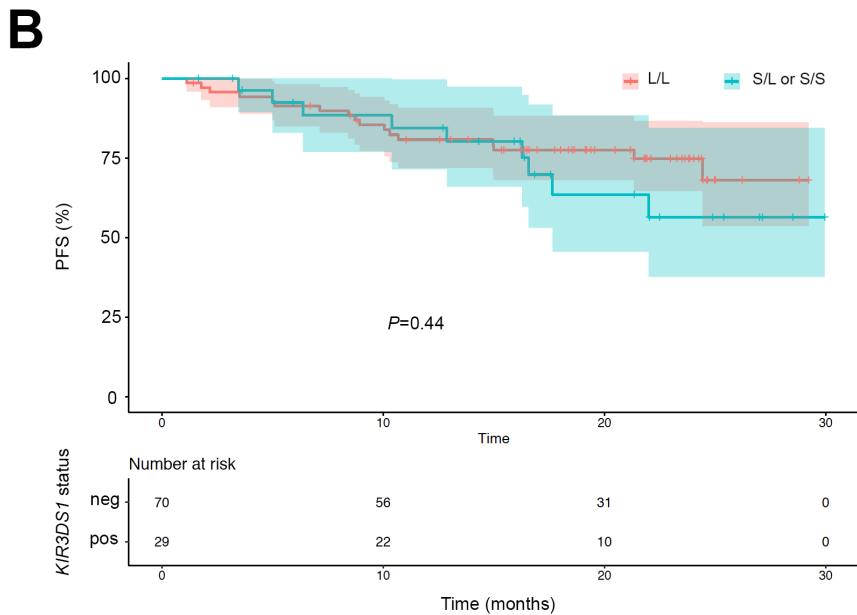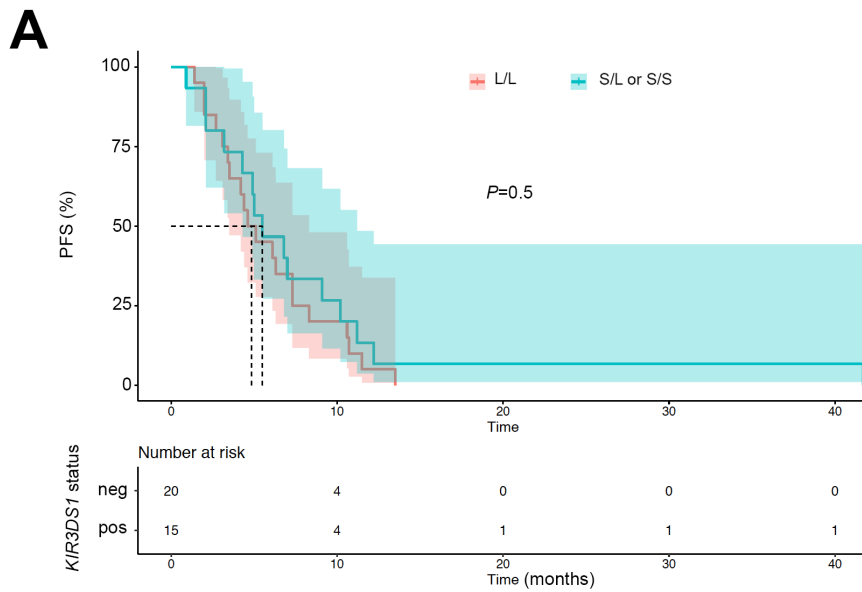
Supplementary Figure 2 KIR3DS1 is not Associated with Worse PFS in NSCLC Patients Receiving Chemotherapy or Adjuvant Treatment.
(A) Progression-free survival of the NSCLC patients from the discovery cohort undergoing first line chemotherapy. (B) Progression-free survival of NSCLC patients with early disease undergoing adjuvant platinum-containing chemotherapy (TracerX cohort). In this cohort, three patients were homozygous for the KIR3DS1.
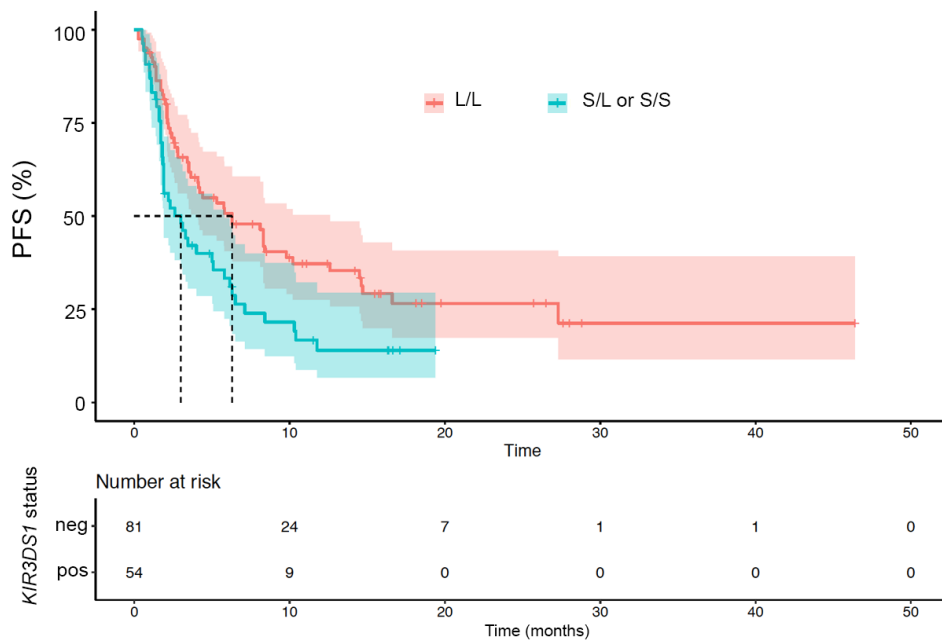
Supplementary Figure 3 Progression-free Survival According to Presence of the KIR3DS1 Allele (Pooled Discovery and Confirmation Cohorts, N = 135)

Probability of PFS over time (months) in NSCLC patients receiving PD-1 blockade monotherapy of the pooled cohort.
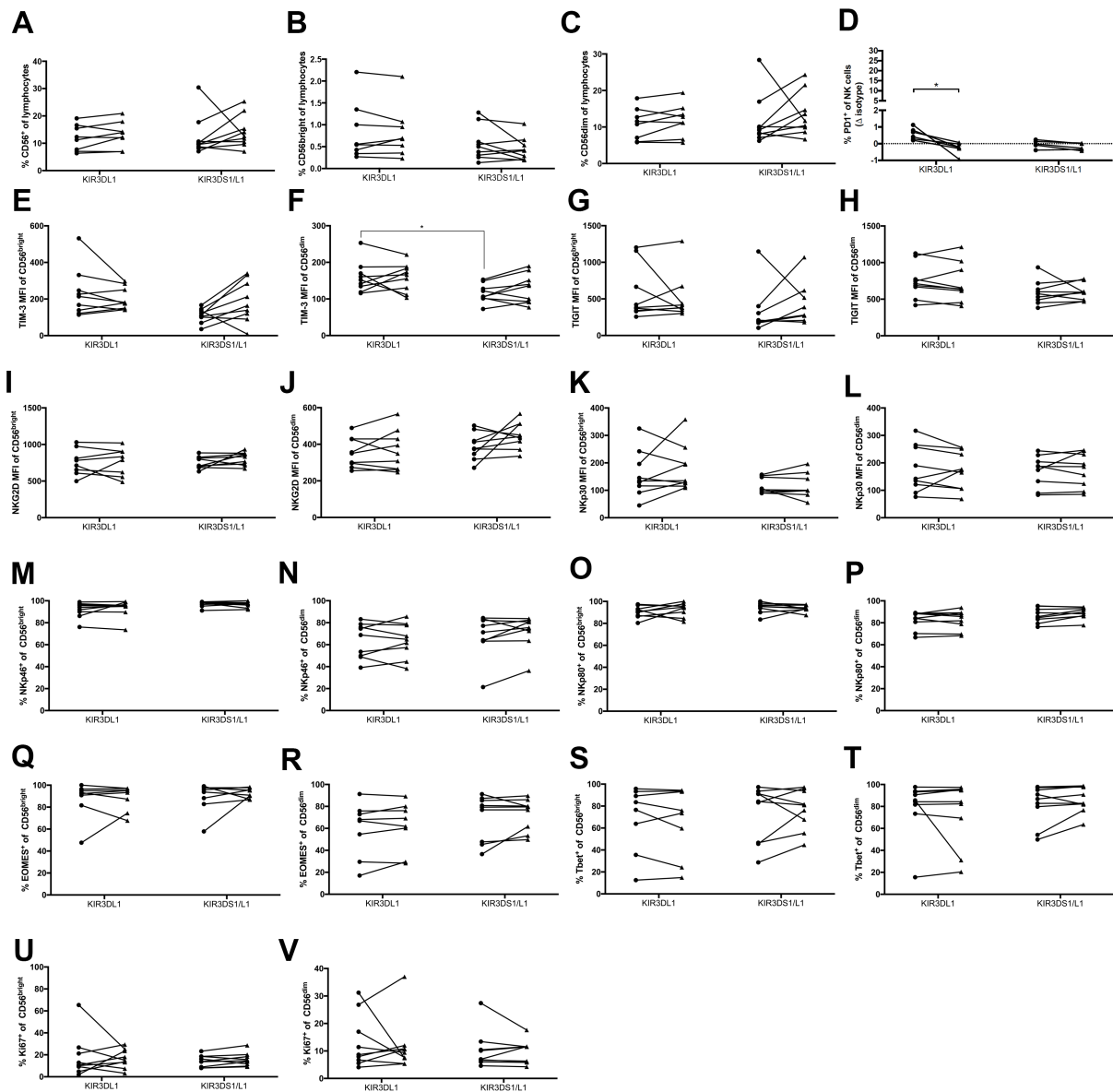
Supplementary Figure 4 Characterization of NK Cells According to the KIR3DS1 Status
*(A-D) Frequency of peripheral NK cells (A), CD56^bright^ NK cells (B), CD56^dim^ NK cells (C), and PD-1 positive NK cells (D) before and during the treatment according to KIR3DL1 homozygosity or KIR3DL1/S1 heterozygosity. PD-1 is significantly decreasing in KIR3DS1 negative patients (D). (E-P) geometric mean fluorescent intensity (MFI) of TIM-3 expression on CD56^bright^ (E) and CD56^dim^ (F) NK cells, of TIGIT expression on CD56^bright^ (G) and CD56^dim^ (H) NK cells of NKG2D expression on CD56^bright^ (I) and CD56^dim^ (J) NK cells, of NKp30 expression on CD56^bright^ (K) and CD56^dim^ (L) NK cells, of NKp46^+ CD56^bright^ (M) and CD56^dim^ (N) NK cells, of NKp80^+ CD56^bright^ (O) and CD56^dim^ (P) NK cells. (Q-V) Frequency of EOMES^+ CD56^bright^ (Q) and CD56^dim^ (R) NK cells, of Tbet^+ CD56^bright^ (S) and CD56^dim^ (T) NK cells, and of Ki67^+ CD56^bright^ (U) and CD56^dim^ (V) NK cells. N = 8, * P<0·05 by 2-way ANOVA and multiple comparison.*
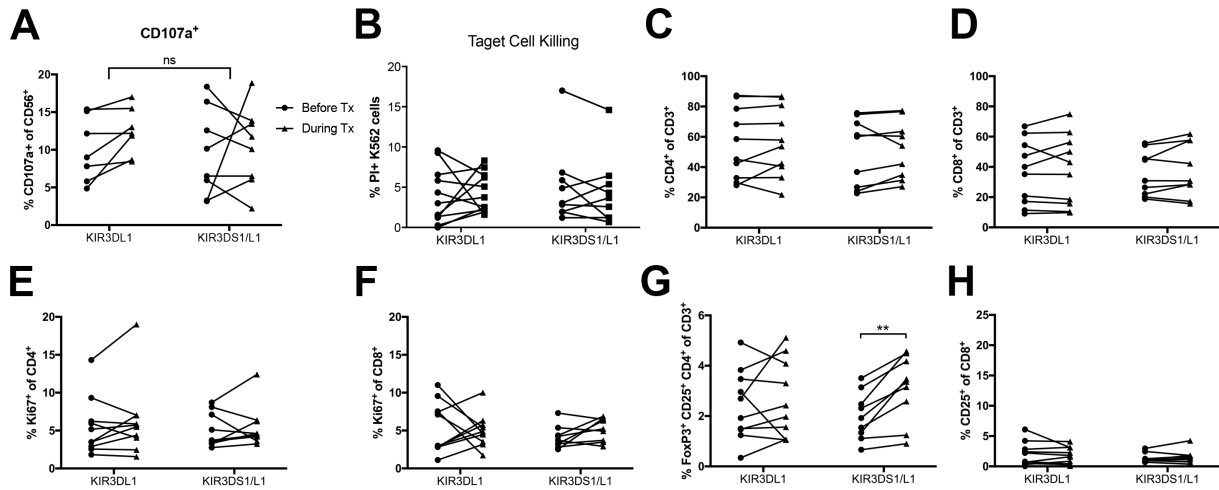
Supplementary Figure 5 NK Functionality and Characterization of Peripheral T Cells According to the KIR3DS1 Status.

(*A*) Accumulation of CD107a on the surface of peripheral NK cells from NSCLC patients before (circles) and during (triangles) treatment with nivolumab incubated with K562 cells. Samples are grouped according to the KIR3DS1 status. (*B*) Determination of K562 cell killing by incubation with peripheral NK cells from NSCLC patients. Killing of K562 cells was determined by propidium iodide staining of prelabeled K562 and analysis by flow cytometry. The data is arranged according to the KIR3DS1 status (N = 9 (L1) and 11 (S1/L1)). (*C-*) Frequency of peripheral CD4$^+$ T cells (*C*), CD8$^+$ T cells (*D*), KI67$^+$ CD4$^+$ (*E*), KI67$^+$ CD8$^+$ (*F*), CD4$^+$ regulatory T cells (CD25$^+$ FoxP3$^+$) (*G*), and CD25$^+$CD8$^+$ (*H*) before and during the treatment according to KIR3DL1 homozygosity or KIR3DL1/S1 heterozygosity. N = 8, ** P<0.01 by 2-way ANOVA and multiple comparison.

| HLA-F negative | HLA-F intermediate | HLA-F high |
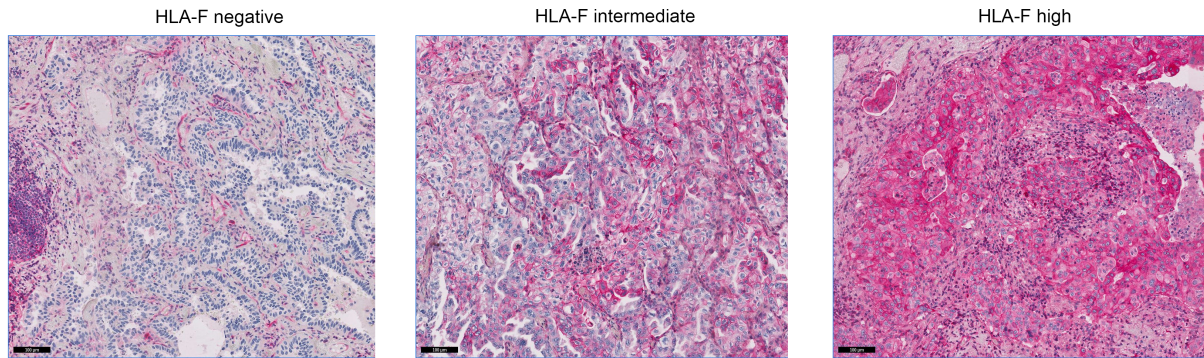
Supplementary Figure 6 Scoring of HLA-F Immunohistochemistry.

Supplementary Table 1 Overview of Characteristics of NSCLC Patients Used for the RNAseq Analysis of Peripheral CD8+ T cells.

patient ID	response	age	histology	line of therapy	therpapies	brain metastasis	type of metatasis
BS373	PR	59	Squamous	4th	Cb, Vaccination, Gem	yes	brain, bone, lymphatic
BS381	PR	51	Adeno	2nd	Cis, pem	no	pleural, pulm, bone, peritoneal
BS385	PR	65	Adeno	2nd	Cb, paclitaxel	no	pulmonal, muscle
BS394	PR	61	Adeno	2nd	Cis, pem	no	lymphatic
BS395	PR	71	Adeno	2nd	Cb, pem	yes	brain, pulm, adrenal
BS375	PD	62	Adeno	2nd	Cb, pem	no	liver, pulm
BS379	PD	75	NOS	2nd	Cb, pem	no	bone, lymphatic
BS391	PD	54	Adeno	2nd	Cis, pem	yes	brain, bone, lymphatic, adrenal
BS409	PD	79	Adeno	2nd	Cb, pem	yes	liver, pulm, brain
BS418	PD	72	NOS	2nd	Cb, pem	no	bone, lymphatic, pleural

Supplementary Table 2 Most Significantly Changed Genes in the RNAseq Analysis.

PR. vs PD. N1							
EntrezID	Symbol	Gene Name	log2FC	log2A	P.Value	adj.P.Val	Interpretation
3813	KIR3DS1	killer cell immunoglobulin like receptor, three Ig domains and short cytoplasmic tail 1	-6.12	4.40	2.4E-07	5.1E-03	up-regulated PD
136	ADORA2B	adenosine A2b receptor	1.55	-0.55	2.9E-05	3.1E-01	up-regulated PR
85463	ZC3H12C	zinc finger CCCH-type containing 12C	1.32	-1.07	5.0E-05	3.5E-01	up-regulated PR
PR. vs PD. N2							
EntrezID	Symbol	Gene Name	log2FC	log2A	P.Value	adj.P.Val	Interpretation
3813	KIR3DS1	killer cell immunoglobulin like receptor, three Ig domains and short cytoplasmic tail 1	-6.56	4.40	3.3E-07	6.8E-03	up-regulated PD
6696	SPP1	secreted phosphoprotein 1	4.73	2.27	6.6E-06	6.9E-02	up-regulated PR
5210	PFKFB4	6-phosphofructo-2-kinase/fructose-2,6-biphosphatase 4	2.61	1.96	1.2E-05	8.3E-02	up-regulated PR

Supplementary Table 3 Patient Characteristics of the Rizvi Confirmation Cohort, According to KIR3DS1/L1 Status.

Characteristic	KIR3DL1/L1 (N = 23)	KIR3DS1/L1 KIR3DS1/S1** (N = 11)	P value
Median age — yr (range)	63 (51-80)	59 (41-78)	0.09*
Sex — no. (%)			
Male	8 (34.8)	8 (72.7)	0.06†
Female	15 (65.2)	3 (27.3)	
Histology — no. (%)			
Non-squamous	20 (87)	9 (81.8)	>0.99†
Squamous	3 (13)	2 (18.2)	
Smoking history — no. (%)			
Yes	21 (91.3)	8 (72.7)	0.35†
No	3 (8.7)	3 (27.3)	
PD-L1 status — no. (%)			
Negative	4 (17.4)	2 (18.2)	0.45‡
1-50%	8 (34.8)	6 (54.5)	
>50%	7 (30.4)	3 (27.3)	
Missing	4 (17.4)	0 (0)	

* Student's t test, †Fisher's exact test, ‡Chi-Square test. **2/11 (18.2%) patients are KIR3DS1/S1; PD-L1 programmed death-ligand 1.

Supplementary Table 4 Patient Characteristics of the St. Gallen Confirmation Cohort, According to KIR3DS1/L1 Status.

Characteristic	KIR3DL1/L1 (N = 38)	KIR3DS1/L1 KIR3DS1/S1** (N = 28)	P value
Median age — yr (range)	69 (47-84)	65 (51-81)	0.27*
Sex — no. (%)			
Male	27 (71.1)	11 (39.3)	0.01‡
Female	11 (28.9)	17 (60.7)	
Histology — no. (%)			
Non-squamous	30 (78.9)	21 (75)	0.77†
Squamous	8 (21.1)	7 (25)	
Smoking history — no. (%)			
Yes	34 (89.5)	27 (96.4)	0.44‡
No	2 (5.3)	0 (0)	
unknown	2 (5.3)	1 (3.6)	
PD-L1 status — no. (%)			
Negative	12 (31.6)	7 (25)	0.84‡
1-50%	6 (15.8)	4 (14.3)	
>50%	11 (28.9)	11 (39.3)	
Missing	9 (23.7)	6 (21.4)	

*Student's t test, †Fisher's exact test, ‡Chi-Square test. **4/28 (14.3%) patients are KIR3DS1/S1; PD-L1 programmed death-ligand 1.

Supplementary Table 5 Pooled Cohort Univariable Regression Analysis

Univariable Cox regression analysis with a random effect for centre for progression free survival based on all 135 patients (been treated with anti-PD1 agents) and 95 events of progression or death.

Variable	HR	95% CI	P-value
KIR3DS1 (positive vs negative)	1.8894	1.2436 to 2.871	0.0029

Supplementary Table 6 Pooled Cohort Multivariable Regression

Multivariable Cox regression analysis with a random effect for center for progression free survival based on all 135 patients (been treated with anti-PD1 agents) and 95 events of progression or death.

Variable	HR	95% CI	P-value
KIR3DS1 (positive vs negative)	1.9067	1.2515 to 2.905	0.0027
Age (continuous)	1.0031	0.9803 to 1.026	0.7900
Smoking status (yes vs no)	0.7308	0.4123 to 1.295	0.2800

Supplementary Table 7 Pooled Cohort Multivariable Regression Including PD-L1

Multivariable Cox regression analysis with a random effect for center for progression free survival based on all 122 patients (been treated with anti-PD1 agents) and 83 events of progression or death.13 patients were not included because of missing PD-L1 status

Variable	HR	95% CI	P-value
KIR3DS1 (positive vs negative)	1.7183	1.1014 to 2.6807	0.017
Age (continuous)	1.0037	0.9792 to 1.0288	0.770
Smoking status (yes vs no)	0.6731	0.3586 to 1.2634	0.220
PD-L1 (positive vs negative)	0.5401	0.3358 to 0.8686	0.011

Supplementary Table 8 HLA-F Staining in two Different Cohorts of NSCLC

	Discovery Cohort (N = 11)	*Independent Coh*ort (N = 16)
HLA-F staining (IHC, %)		
Negative	3 (27.2)	5 (31.3)
Intermediate (1-2+)	5 (45.5)	5 (31.3)
High (3+)	2 (18.2)	6 (37.4)
Not evaluable	1 (9.1)	0 (0)

Supplementary Table 9 Unique Sequences used for KIR3DS1/L1 Analysis of Whole Exome Sequencing Data

Chromosome	Start	End	Name	Description
19	55341521	55341761	KIR3DL1_uniq.0	not present in KIR3DS1
19	55340738	55341276	KIR3DL1_uniq.1	different from KIR3DS1_uniq.1 in blast alignment
19	55341397	55341696	KIR3DL1_uniq.2	different from KIR3DS1_uniq.2 in blast alignment
chr19_gl000209	83291	83830	KIR3DS1_uniq.1	different from KIR3DL1_uniq.1 in blast alignment
chr19_gl000209	83951	84228	KIR3DS1_uniq.2	different from KIR3DL1_uniq.2 in blast alignment

2.2. PD-1+ NK Cells in Human Non-Small Cell Lung Cancer Can Be Activated by PD-1 Blockade

Marcel P. Trefny[1], Monika Kaiser[1], Michal A. Stanczak[1], Petra Herzig[1], Spasenija Savic[3], Mark Wiese[4], Didier Lardinois[4], Heinz Läubli[1,2], Franziska Uhlenbrock[1,#] and Alfred Zippelius[1,2,#]

[1]Laboratory of Cancer Immunology, Department of Biomedicine, University of Basel and University Hospital of Basel, Basel, Switzerland; [2]Department of Internal Medicine, Division of Oncology, University Hospital Basel, Basel, Switzerland.; [3]Institute of Pathology, University Hospital Basel, Basel, Switzerland; [4]Department of Surgery, University Hospital Basel, Basel, Switzerland
[#]These authors jointly directed this work

Running title: NK cells in NSCLC and PD-1 blockade
Keywords: cancer immunotherapy, immune checkpoint inhibitor, inhibitory receptor, resistance, innate immunity

Corresponding authors: Marcel Trefny and Alfred Zippelius, M.D., Laboratory of Cancer Immunology, Department of Biomedicine, University of Basel and University Hospital of Basel, Hebelstrasse 20, 4031 Basel, Switzerland, Phone: +41 61 265 23 55, marcel.trefny@unibas.ch or alfred.zippelius@usb.ch

2.2.1.   Abstract

Natural killer (NK) cells are critically involved in anti-tumor immunity by targeting tumor cells. In this study, we show that intratumoral NK cells from NSCLC patients expressed elevated levels of the immune checkpoint receptor PD-1 on their cell surface. In contrast to the expression of activating receptors, PD-1+ NK cells co-expressed more inhibitory receptors compared to PD-1- NK cells. Intratumoral NK cells were less functional compared to peripheral NK cells, and this dysfunction correlated with PD-1 expression. Tumor cells expressing PD-L1 inhibited the functionality of PD-1+ NK cells in *ex vivo* models and induced PD-1 clustering at the immunological synapse between NK cells and tumor cells. Notably, treatment with PD-1 blockade was able to reverse PD-L1 mediated inhibition of PD-1+ NK cells. Our findings highlight the therapeutic potential of PD-1+ NK cells in immune checkpoint blockade and could guide the development of NK cell-stimulating agents in combination with PD-1 blockade.

2.2.2.   Précis

We demonstrate that natural killer (NK) cells in lung cancer frequently overexpress the inhibitory receptor PD-1 on their cell surface. Blocking the PD-1/PD-L1 axis enhances NK cell functions required for tumor cell killing.

2.2.3.   Introduction

Cancer immunotherapy targeting the PD-1/PD-L1 inhibitory axis is nowadays considered to be one of the treatment pillars of non-small cell lung cancer (NSCLC) (Antonia et al., 2018; Borghaei et al., 2015a; Brahmer et al., 2015; Gandhi et al., 2018; Hellmann et al., 2018; Paz-Ares et al., 2018; Reck, Rodriguez-Abreu, et al., 2016; Socinski et al., 2018). Despite significant improvements in survival and durability of responses, the majority of patients are still resistant to PD-1/PD-L1 blockade (Garon et al., 2019). Several markers and mechanisms of resistance to ICB have been described, but the determinants of responses and/or failures are still poorly defined. There is increasing evidence that a lower burden of nonsynonymous somatic mutations or genomic alterations in individual genes correlates with a lack of clinical benefit and immune resistance (Odorizzi, Pauken, Paley, Sharpe, & Wherry, 2015; Skoulidis et al., 2018; Snyder et al., 2014). Recent data on patients with melanoma indicate that attenuation of MHC class I protein expression does not predict responsiveness to PD-1 blockade. This finding suggests that immune recognition beyond MHC restriction may be necessary for successful responses and other cell types than T cells might be involved in mediating anti-tumor immunity upon PD-1 blockade (Rodig et al., 2018).

Natural killer cells, a subset of innate lymphoid cells, constitute a first line of defense against microbial infections and cancer development (López-Soto, Gonzalez, Smyth, & Galluzzi, 2017; Morvan & Lanier, 2016). They can control cancers directly by rapid killing of tumor cells through perforin and granzymes (Voskoboinik, Smyth, & Trapani, 2006) and/or the ligation of death receptor-mediated pathways (Screpanti, Wallin, Grandien, & Ljunggren, 2005). Moreover, NK cells secrete a wide array of cytokines and chemokines to regulate the activities of other immune cells in the tumor microenvironment (Fauriat, Long, Ljunggren, & Bryceson, 2010). While their role in cancer immunosurveillance has been demonstrated in models of primary and metastatic tumors (Guillerey & Smyth, 2016), NK cell density in human tumors and their prognostic impact is largely dependent on the histological origin of the malignant cell (Delahaye et al., 2011; Remark et al., 2013; Sconocchia et al., 2012). In lung cancer, NK cells accumulate mainly in the tumor stroma without direct contact with tumor cells and appear not to impact the clinical outcome of chemo- or radiotherapy (Carrega et al., 2008; Platonova et al., 2011). Nevertheless, their involvement in the response to immunotherapy remains to be determined.

NK cell effector functions are tightly controlled by a balance of signals from both activating and inhibitory receptors (Carrega et al., 2008). Inhibitory killer immunoglobulin-like receptor family (KIRs), Ly49 and CD94/NKG2A receptors function to detect MHC class I self-ligands and inhibit NK cell activation to prevent the destruction of non-transformed cells (K. C. Hsu, Chida, Geraghty, & Dupont, 2002). In turn, activating receptors including NKG2D, the natural cytoxicity receptors NKp46, NKp30, NKp44, as well as DNAM-1 and CD16 may induce an immune response (Moretta et al., 2001). We recently found that allelic variants of *KIR3DS1/L1* correlate with resistance to PD-1/PD-L1 blockade in lung cancer which indicates that NK cells may be implicated in the generation of anti-tumor immune responses during checkpoint inhibitor therapy (Trefny et al., 2019). There is indeed evidence that NK cells upregulate inhibitory receptors such as PD-1, T-cell immunoreceptor with Ig and ITIM domains (TIGIT), and T-cell immunoglobulin and mucin-3 (TIM-3) during cancer progression (da Silva et al., 2014; Xin-guang Liu, Hou, & Liu, 2017; Pesce et al., 2017). A comprehensive characterization of the abundance, phenotype and functional significance of tumor-infiltrating NK cells expressing those inhibitory receptors, particularly in NSCLC, is still missing.

The tumor environment can suppress NK cell functionality through different mechanisms (Vitale, Cantoni, Pietra, Mingari, & Moretta, 2014). Like T cells, intratumoral NK cells may become dysfunctional, which prevents them from displaying optimal anti-tumor responses, while their counterparts in the peripheral circulation maintain full or only slightly reduced effector functions (Mamessier et al., 2011; Platonova et al., 2011). Dysfunctional NK cells in cancer are characterized by a high expression of NK cell-associated inhibitory receptors, reduced expression of activating receptors, as well as a decreased expression of the transcription factors TBET and EOMES (da Silva et al., 2014; Gill et al., 2012; Mamessier et al., 2011). The higher levels of inhibitory receptors expressed on NK cells have been associated with more aggressive and invasive tumors (Mamessier et al., 2011).

In this study, we show that tumor-infiltrating NK cells from NSCLC patients expressed the immune checkpoint receptor PD-1 on their surface. Moreover, we investigated the expression of other inhibitory and activating receptors on PD-1^{+} and PD-1^{-} NK cell subsets and found that PD-1^{+} NK cells co-expressed more inhibitory receptors compared to PD-1^{-} NK cells. We also provide evidence that the dysfunction of intratumoral NK cells correlates with increasing levels of PD-1 surface expression. Notably, treatment with PD-1 blocking antibodies was able to reverse PD-L1 mediated inhibition of NK cells, highlighting the therapeutic potential of PD-1^{+} NK cells in immune checkpoint blockade.

2.2.4. Material and Methods

Cell Lines

K562 cells (ATCC CCL-243) and HEK293T cells (ATCC CRL-3216) were purchased from ATCC, cultured in IMDM and DMEM, respectively, and supplemented with 10% heat-inactivated FBS (PAN Biotech), 100 ng/ml penicillin/streptomycin (Sigma), 2 mM L-Glutamine (Sigma), 1 mM Sodium Pyruvate (Sigma) and 1% MEM non-essential amino acids (Sigma). The melanoma cell line NA8-Mel was kindly provided by Dr. Romero (University of Lausanne) and cultured in RPMI-1640 (Sigma) supplemented as described above for IMDM and DMEM. NK92 cells (ATCC CRL-2407) were kindly provided by Dr. Bentires-Alj (University of Basel, Switzerland) and cultured in αMEM (w/o ribo/deoxyribonucleosides, with 2 mM L-glutamine and 1.5 g/l sodium bicarbonate) (Thermo Fisher) supplemented with 0.2 mM inositol, 0.1 mM 2-mercaptoethanol, 0.02 mM folic acid, 300 U/ml recombinant human IL-2 (Peprotech), 12.5% horse serum (Thermo Fisher), 12.5% heat-inactivated FBS and 100 ng/ml penicillin/streptomycin. Cells were confirmed to be negative for mycoplasma by PCR as described after every freeze-thaw cycle and then passaged every 2-3 days for a maximum of 10 passages (Choppa, Vojdani, Tagle, Andrin, & Magtoto, 1998).

Cloning of PD-1 and PD-L1 Expression Vectors

The human PD-1/PD-L1 open reading frames (ORFs) were amplified by PCR from a pCMV6 human cDNA clone (RC210364, Origene) and a pCMV-XL4 human cDNA clone (SC115168, Origene), respectively. The ORFs were extended with overlapping ends (both sides) complementary to the pRRL.PPT.SFFV.EGFP.pre expression vector (kindly provided by Drs. Baum and Schambach at Hannover Medical School, Germany (Zychlinski et al., 2008)) together with an XbaI cut site and a Kozak sequence element. The amplified fragments were fused into the pRRL.PPT.SFFV.EGFP.pre expression vector between the sFFV promotor and the IRES-EGFP fragment using the InFusionHD kit (Clonetech Takara Bio). Both plasmids were amplified in Stbl3 *E. coli* (in-house) and purified using NucleoBond Xtra Midi Plus kits (Machery Nagel). Inserts were sequenced by Sanger sequencing (Microsynth AG) to confirm correct integration. Empty IRES-GFP vectors were used as controls.

Production of Lentivirus

Low passage HEK293T cells were cultured in DMEM medium and transfected with the packaging plasmid pCMV-delta8.9, the envelope plasmid VSV-G and either PD-1-GFP, PD-L1-GFP or empty GFP sFFV transfer plasmids, respectively, in combination with PEI 25K (Polysciences Inc.) at a ratio of 1:3. After two days, supernatants were collected and filtered through a 0.45 μm PES filter. Supernatant containing lentiviral PD-L1 particles were stored at -80°C until usage. Supernatant containing lentiviral PD-1 particles were concentrated by ultra-centrifugation at 40'000 x g for 2 h at 4°C, resuspended in complete αMEM medium and immediately used for transduction.

Generation of PD-1$^+$GFP$^+$-NK92 Cell Line

One day prior to transduction, NK92 cells were expanded in fresh complete αMEM medium containing 300 U/ml IL-2. The following day, cells were re-stimulated with 100 U/ml IL-2 and 100 ng/ml IL-12 (Peprotech) for 2 h without medium exchange. Cells were then collected by centrifugation and resuspended in freshly concentrated supernatant containing lentiviral PD-1 particles or the vector control particles. Cells were seeded in 96-well flat bottom plates coated with 5 μg/cm^2 Retronectin (Takara

Bio). Afterwards, cells were expanded in complete αMEM medium containing 300 U/ml IL-2 for 2 weeks. GFP$^+$/PD-1$^+$GFP$^+$ NK92 cells were then sorted by flow cytometry and the pool of sorted cells was used in all subsequent experiments.

Generation of PD-L1$^+$ GFP$^+$ K562 and PD-L1$^+$ GFP$^+$NA8-Mel Cell Lines

K562 cells were collected by centrifugation and resuspended in supernatant containing either lentiviral particles coding for sFFV-PD-L1-IRES-GFP or sFFV-IRES-GFP control as well as 8 μg/ml polybrene. Nine days post transduction, several clones of GFP$^+$/PD-L1$^+$GFP$^+$ K562 cells were sorted by flow cytometry. Cell lines from these single cell clones were validated for expression of GFP and GFP+PD-L1. NA8-Mel cells were transduced by replacing media with lentiviral supernatants and polybrene as described above followed by medium replacement one day after transduction. Seven days post transduction, pools of GFP$^+$/PD-L1$^+$GFP$^+$ NA8-Mel cells were sorted and cultured for 1 week. The expression of PD-L1 and GFP was validated by flow cytometry.

Isolation of Healthy Human Blood Cells and Tumor-infiltrating Lymphocytes

Human peripheral blood mononuclear cells (PBMCs) were isolated by density gradient centrifugation using Histopaque-1077 (Sigma) from buffy coats obtained from 23 healthy blood donors (HD) (Blood Bank, University Hospital Basel) and from 19 NSCLC patients. Fresh tumor tissues were collected from 16 patients with NSCLC undergoing surgery at the University Hospital Basel, Switzerland. Detailed HD/patient characteristics are provided in Table 1. The study was approved by the local ethical review board (Ethikkommission Nordwestschweiz, EK321/10), and all patients consented in writing to the analysis of their tumor samples. Staging was based upon the 7th edition of the AJCC/UICC tumor–node–metastasis (TNM) staging system. Tumor lesions were mechanically dissociated and digested using accutase (PAA), collagenase IV (Worthington), type V hyaluronidase from bovine testes (Sigma), and DNAse type IV (Sigma), directly after excision. Single-cell suspensions were prepared. All samples were stored in 10% DMSO/90% FCS in liquid nitrogen until further usage.

Antibodies and Flow Cytometry

Cryopreserved tumor digests or PBMCs were thawed, washed, resuspended in PBS, and blocked with human Fc-receptor-inhibitor (eBioscience). Dead cells were stained with Fixable Viability Dyes (Biolegend or eBioscience). For surface staining, cells were washed, resuspended in FACS buffer (PBS supplemented with 2 mM EDTA, 0.1% Na-Azide, 2% FCS), and stained with appropriate antibodies for 30 min at 4°C. All antibodies used in this study are listed in Supplementary Table S1. For intracellular (cytoplasmic) staining, cells were fixed and permeabilized using IC Fixation Buffer and Permeabilization Buffer (eBioscience). For staining of the nuclear proteins, the Fixation/Permeabilization kit (eBioscience) was used. After staining, cells were analyzed on a BD LSR Fortessa Cell analyzer (BD Bioscience). Data were collected using the BD FACS Diva Software version 7 and further analyzed with FlowJo v10.1.6 (Tree Star Inc.) and GraphPad Prism v7.0a (GraphPad Software Inc.). An example gating strategy can be found in Supplementary Figure 7. All results show integrated fluorescence area on a biexponential scale.

54

Baseline Characterization of NK Cells

Patient samples (PBMCs and TILs) and PBMCs from HDs were comprehensively characterized by multicolor flow cytometry. NK cells were identified by gating for live CD45$^+$, CD3$^-$, CD56$^+$, and then divided into subpopulations based on the expression of the described markers.

FACS-based Cell Sorting

For functional assays, NK cells from PBMCs and TILS were isolated by flow cytometry-based sorting. In brief, cells were thawed, washed and stained with appropriate antibodies for 30 min at 4°C. Following incubation, cells were washed, resuspended in FACS buffer and filtered. Sorting of cells was performed using a FACSAria III (BD) and the purity of sorted populations was routinely tested.

FACS-based NK Cell Killing Assay

One day prior to the experiment, 20'000 sorted NK cells from TILs or PBMCs were seeded into 96-well U bottom plates and cultured in complete RPMI-1640 in the presence or absence of 20 ng/ml IL-15 (Peprotech). The next day, K562 cells were stained with Vybrant DiO Dye (Molecular Probes) according to the manufacturer's instructions for 25 min at 37°C, then washed in complete medium. NK cells from HDs/patients and K562 cells were then co-cultured at an E:T ratio of 2:1 for 6 h at 37° C (duplicates). NK cells cultured without target cells were used as spontaneous cell death control. Following incubation, cells were washed and resuspended in FACS buffer. Shortly before sample acquisition Propidium Iodide (PI; BD) was added to each sample to stain for dead cells and samples were acquired using a Beckmann Cytoflex flow-cytometer. Cells were gated as shown in Supplementary Figure 9a. Specific NK cell killing was determined by the following equation:

$$\% \, specific \, lysis = \left(\frac{\% \, PI^+ (dead) \, targets - \% \, spontaneous \, PI^+ \, targets}{100 - \% \, spontaneous \, PI^+ targets} \right) \times 100\%$$

Calcein Release-based NK Cell Killing Assay

GFP$^+$/PD-1$^+$GFP$^+$ NK92 cells were cultured as described above. Cells were stimulated with 20 ng/ml IL-15 overnight and the next day they were washed in serum-free RPMI-1640 and stained with Calcein-AM Viability Dye (eBioscience) for 30 min 37°C. Stained cells were resuspended in assay medium (RPMI-1640 with 10% FBS and 5 mM HEPES) and seeded into a 96-well V-bottom plate. Next, 10 µg/ml nivolumab (Opdivo, Bristol-Meyer-Squib) or IgG4 isotype control (Ultra-LEAF purified, Biolegend) was added to the wells and incubated for 15 min at 37°C. Pre-stimulated GFP$^+$/PD-1$^+$GFP$^+$ NK92 cells were washed, resuspended in assay medium and added to the wells at an E:T ratio of 2:1. Maximum lysis was induced with assay medium containing 2% Triton-X100 (Sigma). Cells were co-cultured for 4 h. Following incubation, Calcein was measured from supernatants using a Biotek Plate Reader at 490 nm ex / 520 nm em. Specific NK cell killing was determined by the following equation:

$$\% \, specific \, lysis = \left(\frac{Calcein \, release \, samples - spontaneous \, release}{maximum \, release - spontaneous \, release} \right) \times 100\%$$

NK Cell Degranulation

Sorted NK cells from TILs or PBMCs were co-cultured with K562 cells for 6 h at 37°C as described in the FACS-based NK cell killing assay. In addition, 20 ng/ml anti-CD107a antibody was added. After 1 h of incubation, degranulation was blocked using 1X Monensin (Biolegend) and 1X Brefeldin A (eBioscience). Following incubation, the accumulation of IFNγ and TNFα within NK cells was investigated by flow cytometry. Cells were gated as shown in Supplementary Figure 9b.

Cytokine-mediated PD-1 Upregulation on Peripheral NK Cells

Frozen PBMCs from HDs were thawed, washed, and resuspended in complete RPMI-1640 medium. Cells were seeded into 96-well round bottom plates and rested for 2h at 37°C. Afterwards, various combinations of recombinant human IL-15 (25 ng/μl), IL-18 (20 ng/μl) and IL-12 (25ng/μl) were added to the cells and incubated for 48h at 37°C. PD-1 upregulation was investigated by flow cytometry (Cytoflex, Beckmann Coulter).

Immune Synapse Analysis

Two days prior to the experiment, GFP$^+$/PD-1$^+$GFP$^+$ NK92 cells were cultured at 0.5*10^6 cells/ml in complete αMEM medium containing 300 U/ml IL-2. One day prior, GFP$^+$/PD-L1$^+$GFP$^+$ K562 cells were stained with 1 μM Cell Trace Violet (Thermo Fisher Scientific) according to the manufacturers' instructions for 15 min at 37°C. Stained cells were resuspended in serum-free RPMI-1640, and incubated with 20 μg/ml of atezolizumab (Tecentriq, Roche) for 15 min at 37°C. GFP$^+$/PD-1$^+$GFP$^+$ NK92 cells were washed, resuspended in serum-free RPMI-1640, and co-cultured with K562 at an E:T of 2:1 at 37°C. After 15 min, cells were immediately fixed for 20 min at RT using 4 % PFA. Cell clusters were washed with permeabilization buffer (eBioscience) and subsequently stained with anti-PD-1-AlexaFluor647 antibody (clone EH12.1, BD Phosphoflow) for 30 min at RT. Cells were analyzed using an MKII Imagestream Analyzer (EMD Milipore). One to one cell ratio clusters were gated as shown in Supplementary Fig. S4a using the IDEAS software (EMD Milipore). An interface mask between Cell Trace Violet$^+$/PD-1$^+$ cells (synapse between PD-1+ GFP+ NK92 cells and PD-L1+GFP+ K562 target cells) of width 6 was created. Next, an intensity concentration ratio feature for the PD-1 signal was calculated for this interface and compared to the total PD-1 mask (immune synapse versus total cell). The geometric mean of the intensity concentration ratio distribution of one to one cell clusters was used for further analysis.

Statistical Analysis

The statistical analysis and graph preparation were performed using the software package Prism version 8.0 a (GraphPad Software, La Jolla, CA). Functional data are representative of at least three experiments. Data were considered statistically significant with p values < 0.05. Normality tests were used to choose parametric or non-parametric tests. Data are shown as mean ± standard deviation with symbols representing individual patients or donors where applicable.

2.2.5.   Results

NK Cells of NSCLC Patients Express the Immune Checkpoint PD-1

We previously showed that a variant of a killer immunoglobulin receptor expressed on NK cells may mediate resistance to PD-1 blockade in NSCLC (Trefny et al., 2019). Here, we aimed to obtain a broader overview of the expression of activating and inhibitory receptors including immune checkpoints PD-1, TIM-3, TIGIT on NK cells from NSCLC patients. We characterized NK cells from PBMCs and tumors of 16 patients by flow cytometry for the expression of PD-1, TIM-3, TIGIT, as well as NK cell inhibitory/activating receptors KIR3DL1, KIR2DL3, CD16, NKG2D, NKp30, NKp46, NKp80, and transcription factors TBET and EOMES (Supplementary Figure 7). PBMCs from healthy donors (HD) served as controls (Table 4).

Table 4 Cohort of Healthy Donors and NSCLC Patients

	Healthy Donors PBMCs	NSCLC PBMCs	NSCLC TILs
Characteristic	N=23	N=19	N=16
Age, median years (range)	48 (19-72)	67.6 (42-80)	68.2 (54-83)
Sex **-male (%)** **-female (%)**	12 (52.2%) 11 (47.8%)	11 (58%) 8 (42%)	9 (56%) 7 (44%)
Stage **-I (%)** **-II (%)** **-III (%)** **-IV (%)**	NA	8 (42.1%) 6 (31.6%) 4 (21%) 1 (5.3%)	4 (25%) 7 (43.8%) 4 (25%) 1 (6.3%)

NK cells comprised 0.56 ± 0.58 % (mean ± standard deviation, range 0.31 – 4.16 %) of all CD45+ lymphocytes in the tumor (Figure 8a). Cell surface PD-1 expression was observed on 11.2 ± 6 % (1.59 – 21.4 %) of intratumoral NK cells. In contrast, only 2.5 ± 2.5 % (0.39 – 7.8 %) of NK cells in PBMCs from NSCLC patients expressed PD-1, while PD-1 was absent on NK cells from HDs (Figure 8b-c). PD-1 expression on NK cells did not correlate with PD-1 expression on CD8 T cells (Supplementary Figure 8a). The expression of TIM-3 was similar in NSCLC TILs compared to NSCLC PBMCs (Figure 8c), while fewer intratumoral NK cells expressed TIGIT compared to peripheral blood NK cells of NSCLC patients. NK cells from patients' PBMCs expressed higher levels of KIR3DL1 compared to both intratumoral NK cells and healthy donor NK cells, while higher levels of KIR2DL3 were observed on intratumoral NK cells only (Figure 8c). We detected significantly lower expression of activating receptors CD16 and NKp80 on intratumoral NK cells (Figure 8d), while the expression of NKG2D and NKp30 was similar on intratumoral NK cells compared to peripheral NK cells from NSCLC patients. The expression of NKp46 was lower in peripheral NK cells from patients compared to both intratumoral and healthy donor NK cells. The transcription factors TBET was significantly reduced in intratumoral NK cells compared to peripheral NK cells of NSCLC patients, whereas EOMES was unchanged (Figure 8e).
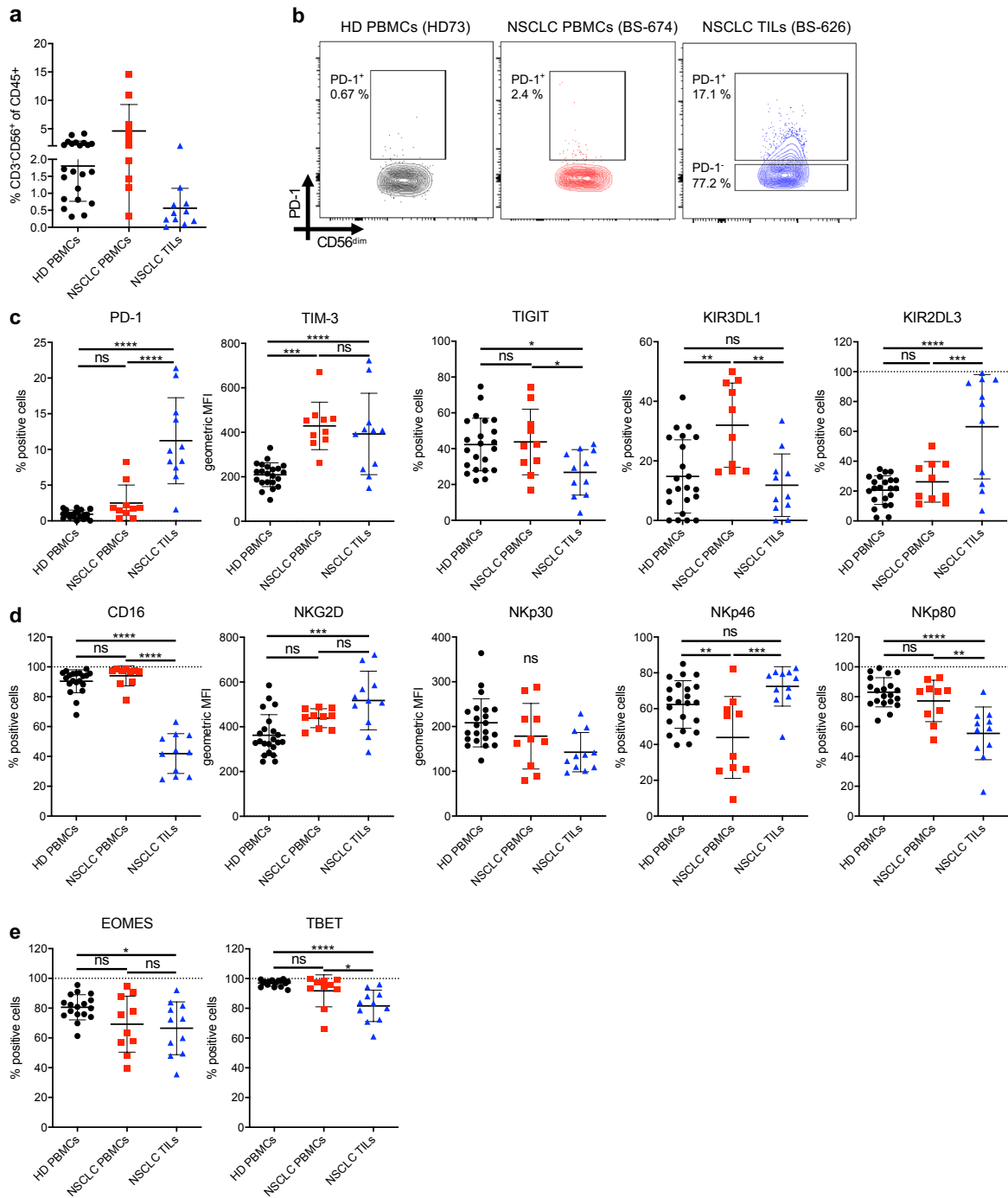
Figure 8 Characterization of NK Cell Infiltration and Immune Checkpoint Expression in NSCLC Patients

(a) Frequency of NK cells in HD PBMCs, NSCLC PBMCs and NSCLC TILs relative to CD45+ cells. (b) Contour plot for PD-1 flow cytometry staining from one representative HD PBMC, NSCLC PBMC, and NSCLC TIL sample. (c) Expression of inhibitory receptors, (d) Expression of activating receptors and (e) Expression of transcription factors by NK cells from HD PBMCs, NSCLC PBMCs and NSCLC TILs measured by flow cytometry. p<0.05, ** p<0.01, *** p<0.001, **** p<0.0001

PD-1⁺ NK Cells Co-express More Inhibitory Receptors than PD-1⁻ NK Cells in NSCLC Patients

PD-1 expressed on NK cells could be a direct target of therapeutic PD-1 blocking antibodies which supports a potential role for NK cells in immunotherapy. We hypothesized that the expression of PD-1 on NK cells may correlate with the expression pattern of other receptors and therefore influence functionality as observed with tumor-infiltrating T cells in NCSLC (D. S. Thommen et al., 2015). Therefore, we investigated the co-expression of TIM-3, TIGIT, KIR3DL1, KIR2DL3, the activating receptors CD16, NKG2D, NKp30, and NKp80, as well as the transcription factors TBET and EOMES on intratumoral PD-1⁺ or PD-1⁻ NK cell subsets. As seen in Figure 9a, PD-1⁺ NK cells more frequently co-expressed other inhibitory receptors (TIM-3, TIGIT, KIR2DL3 and KIR3DL1) compared to PD-1⁻ NK cells (p = 0.018). NK cells that co-expressed none of the four inhibitory receptors ("+ 0 Co-Expression", light shading) were more than twice as frequent in the PD-1⁻ NK cell subset (Supplementary Table 11). Notably, the co-expression of activating receptors (Figure 9a, Supplementary Table 12) and of the two transcription factors Supplementary Figure 8b) did not differ significantly between PD-1⁺ and PD-1⁻ NK cells.
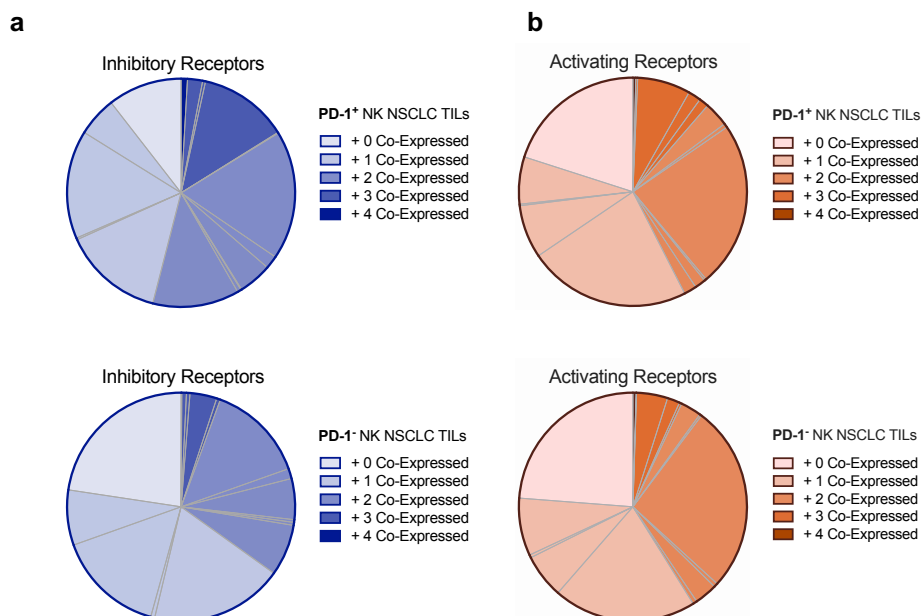

Figure 9 Co-expression of Inhibitory and Activating Receptors in PD-1+ vs. PD-1- NK Cell Subpopulations in NSCLC Patients

Co-expression of inhibitory (a) and activating (b) receptors in PD-1⁺/PD-1⁻ NK cell subpopulations in NSCLC TILs. The number of receptors co-expressed on either population is indicated by color opacity within the pie chart. The individual subpopulations described in Supplementary Tables S2 and S3 are delimited by grey lines.

Tumor-infiltrating NK Cells Display Impaired Functionality Compared to NK Cells from Healthy Donors

We next explored how the difference in the receptor repertoire between tumor-infiltrating and peripheral NK cells impacts NK cell functionality. We noted a trend for lower cytotoxic activity of intratumoral NK cells (p = 0.12) against the MHC-I deficient tumor cell line K562 compared to peripheral patient NK cells (Figure 10a). In addition, degranulation measured by CD107a accumulation on the cell surface upon co-culture

with K562 cells was decreased on intratumoral NK cells from NSCLC patients compared to peripheral NK cells from healthy donors (Figure 10b). Similarly, intratumoral NK cells produced less IFN-γ (Figure 10b, Supplementary Fig. S3c). We detected no significant difference in TNF-α production (Figure 10b). Notably, polyfunctionality, defined as the combined capacity for cytotoxicity, IFN-γ, and TNF-α release, was reduced in intratumoral NK cells (Figure 10c, Supplementary Figure 9d) and correlated with PD-1 expression (Figure 10d). We could not detect a correlation between functionality and age (Supplementary Figure 9e). In the absence of PD-L1 on K562 target cells, no functional difference between intratumoral PD-1$^+$ and PD-1$^-$ NK cells could be detected (Supplementary Figure 9f).
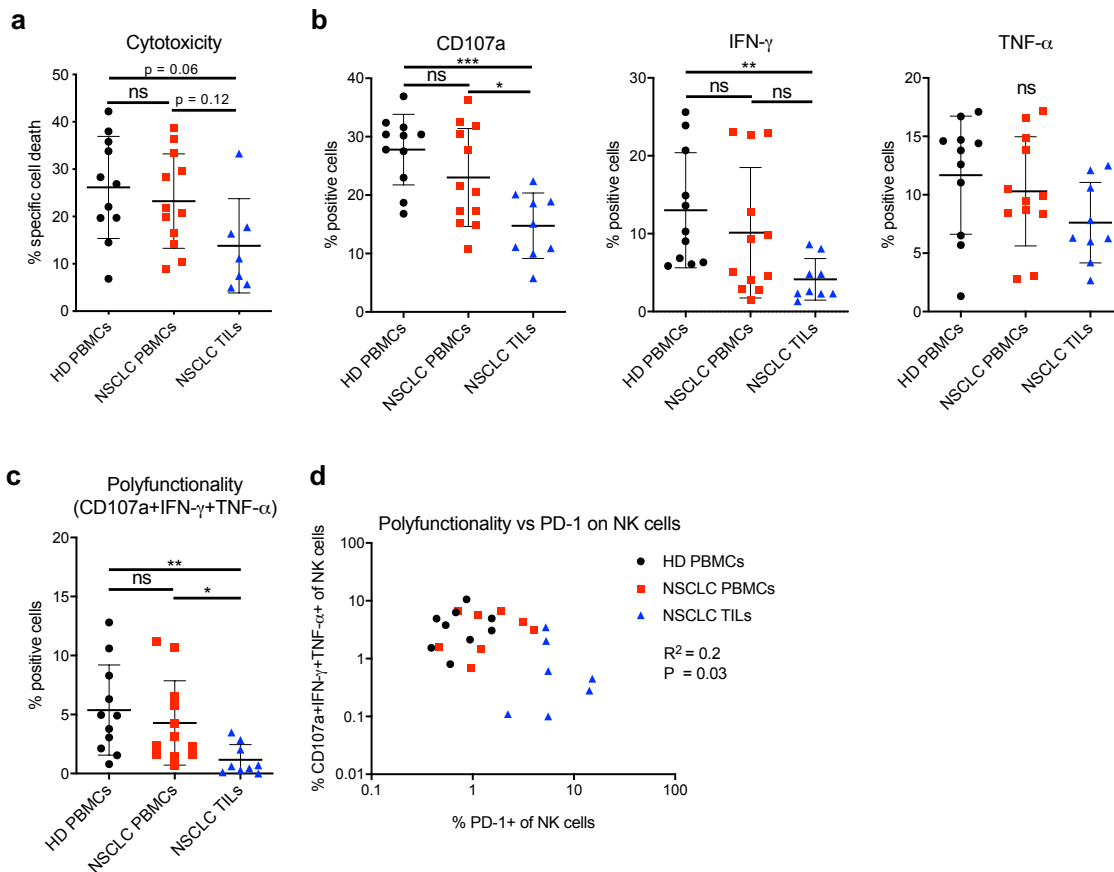

Figure 10 Cytotoxicity, Degranulation and Cytokine Production by NK Cells in Response to K562 Cells

(a) Cytotoxicity analyzed using a flow cytometry-based killing assay with sorted NK cells from HD PBMCs, NSCLC PBMCs and NSCLC TILs co-cultured with K562 wildtype cells for 4 h at an E:T ratio of 1:2. (b) Sorted NK cells from HD PBMCs, NSCLC PBMCs and NSCLC TILs co-cultured with K562 wildtype cells for 6 h at an E:T ratio of 2:1. NK cell degranulation (CD107a exposure), secretion of IFN-γ and TNF-α was measured by flow cytometry. (c) Polyfunctionality (CD107a+ IFN-γ+ and TNF-α+ NK cells) from the same data as in B. (d) Polyfunctionality of NK cells correlated with cell-surface expression of PD-1 on CD56+ NK cells. Linear correlation was performed on logarithmically transformed data. A normality test (Anderson-Darling test) was performed on the data in graphs (a) and (b). For data that passed the test (cytotoxicity, CD107a and TNF-α) an unpaired 1-way ANOVAs with Tukey's multiple comparison test was performed. When the normality test failed (p < 0.05) a non-parametric Kruskal-Wallis test was performed with Dunn's multiple comparison correction (IFN-γ+, polyfunctionality). * p<0.05, ** p<0.01, *** p<0.001, **** p<0.0001

PD-1 Blockade Can Rescue PD-L1-mediated Inhibition of PD-1+ NK Cells

To assess whether PD-1+ NK cells can be inhibited by PD-L1 on tumor cells, we established an NK92 cell line model with overexpression of PD-1. In addition, we generated PD-L1-IRES-GFP or GFP-only overexpressing tumor cell lines from MHC-I deficient K562 cells and MHC-I proficient NA8-Mel cells (
Figure 11a, hereafter called K562-PD-L1/GFP cells or NA8-Mel-PD-L1/GFP cells, respectively). When NK92-PD-1 cells were exposed to PD-L1 overexpressing K562 and NA8-Mel, the cytotoxic capacity was profoundly decreased (
Figure 11b). This effect could be relieved with increasing concentrations of nivolumab (
Figure 11b). We observed no difference in cytotoxicity between NK92-PD-1 and NK92-GFP cells against K562-GFP cells, while cytotoxicity was slightly decreased against NA8-Mel-GFP cells, which was antagonized by nivolumab treatment. This is likely explained by the endogenous expression of PD-L1 on NA8-Mel cells (
Figure 11a-b).

To study how PD-1 on NK cells interacts with PD-L1 on tumor cells, we next analyzed the clustering of PD-1 at the NK92 cell/tumor cell immunological synapse. Doublets of single NK92 and K562 cells were readily identified by imaging flow cytometry (Supplementary Figure 10). The clustering of PD-1 at the cell-cell interface increased when NK92-PD-1 cells were co-cultured with K562-PD-L1 cells compared to K562-GFP cells. Moreover, the clustering of PD-1 was abrogated when the PD-L1 blocking antibody atezolizumab was present during the co-culture
Figure 11c-d).

To investigate the reinvigoration of freshly obtained PD-1+ NK cells after PD-(L)1 blockade, we exposed NK cells from healthy donors to cytokines previously associated with PD-1 upregulation (Y. Liu et al., 2017; Quatrini et al., 2018). Of note, the combination of IL-15 and IL-12 led to a robust PD-1 upregulation on NK cells (
Figure 11e). Whereas IL-15 only led to a minimal change in PD-1 expression, treatment with IL-18 had no effect on PD-1 expression. Upon co-incubation with PD-L1+ tumor cells, atezolizumab specifically enhanced the degranulation of ex vivo generated PD-1+ NK cells (
Figure 11f). This data further indicates that PD-1/PD-L1-targeting immunotherapies can target and impact the functionality of primary human PD-1+ NK cells.

a

NK92 / K562 / NA8-Mel

PD-1 / PD-L1 / PD-L1

b

K562 Killing / NA8-Mel Killing

c PD-1 clustering at synapse

d

PD-1   K562-PDL1

high ratio
NK92-PD-1 + K562-PD-L1

low ratio
NK92-PD-1 + K562-GFP

e PD-1 Upregulation

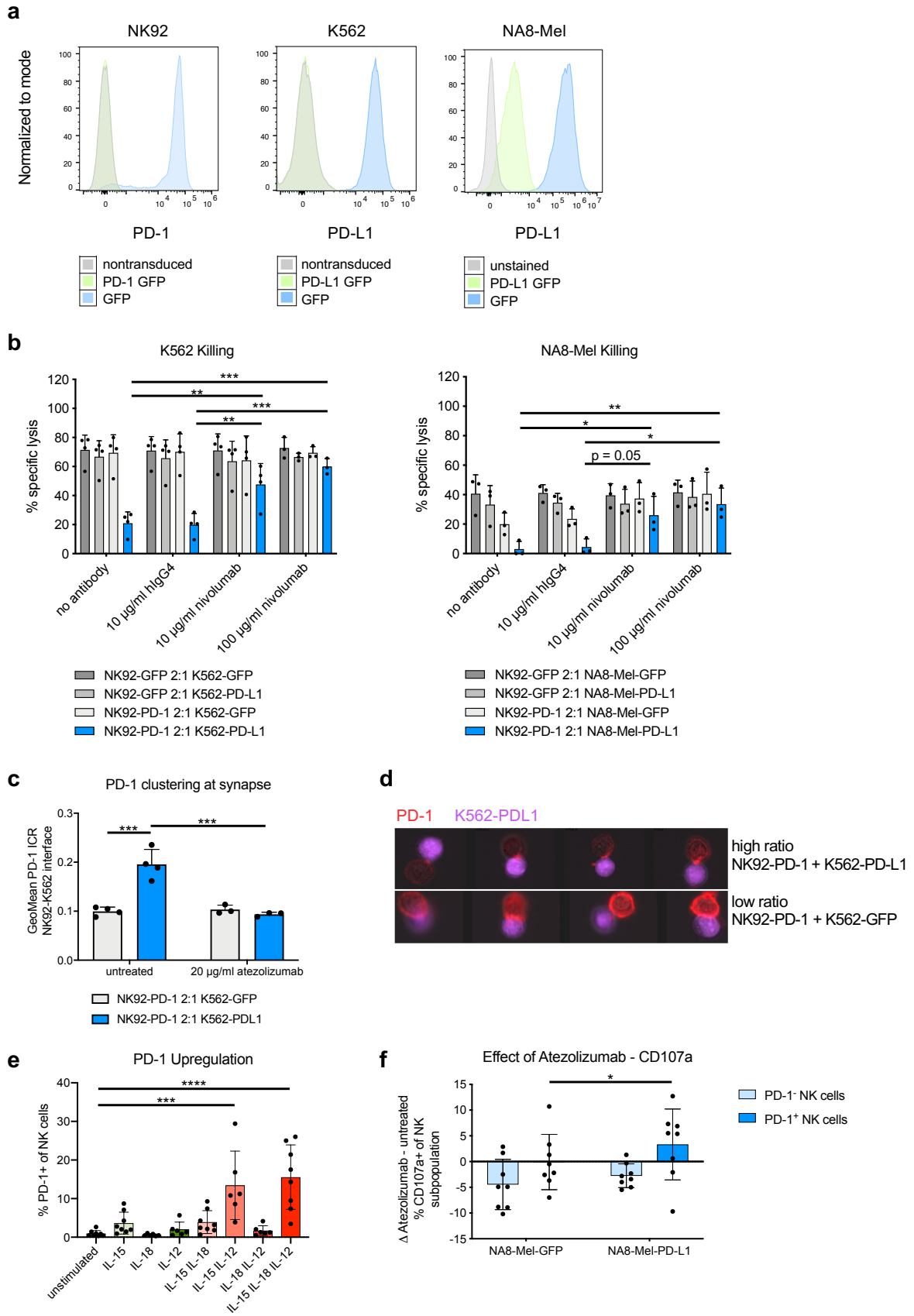**f** Effect of Atezolizumab - CD107a

Figure 11 PD-1 Blockade Restores NK Cell Functionality Ex Vivo

(a) Histogram of PD-1 and PD-L1 measured by antibody-based staining and flow cytometry. Left panel: PD-1 on NK92 cells transduced with a lentiviral vector encoding for PD-1 GFP or GFP alone. Middle and right panel: PD-L1 expression of the different K562 and NA8-Mel cell lines transduced with PD-L1 GFP or GFP lentiviral vectors. (b) Effects of nivolumab on specific target cell lysis measured by Calcein-AM release after 2 h of coculture of NK92-PD-1/GFP effector cells with K562 (left) or NA8-Mel (right) target cells expressing either PD-L1 GFP or GFP only. Paired 2-way ANOVA with Tukey's multiple comparison test. (c) PD-1 clustering measured by ImageStream at the cell-cell synapse between NK92-PD-1 cells and K562-PD-L1/GFP cells. Quantified geometric mean of the intensity concentration ratio between the cell-cell interface and the total cell area. 2-way ANOVA with Tukey's multiple comparison test. (d) Representative images from the ImageStream analysis quantified in (c) showing NK92-K562 interactions with a high intensity concentration ratio (top panel, PD-1 clustered at synapse) or low ratio (bottom, no clustering). (e) Upregulation of PD-1 on peripheral NK cells from healthy donors after in vitro stimulation with the indicated combinations of recombinant human IL-15 (25 ng/µl), IL-18 (20 ng/µl) and IL-12 (25 ng/µl). Unpaired 1-way ANOVAs with Tukey's multiple comparison test (f) Change in degranulation between atezolizumab (20 µg/ml) and untreated PD-1+ and PD-1- NK cells pre-cultured for 2 days with recombinant human IL-15 (25 ng/µl) and IL-12 (25 ng/µl), which were then co-cultured with NA8-Mel-PD-L1/GFP. Paired 2-way ANOVA with Tukey's multiple comparison test. * p<0.05, ** p<0.01, *** p<0.001, **** p<0.0001

2.2.6.   Discussion

NK cells are key mediators of anti-tumor immunity and express a variety of activating and inhibitory receptors, which are critical for their effector functions (Guillerey et al., 2016). Although NK cell infiltration in NSCLC has been investigated (Platonova et al., 2011), little is known about the expression of immune checkpoint receptors on intratumoral NK cells. In this study, we found that a significant fraction of NK cells infiltrated in NSCLC expressed PD-1 and co-expressed other inhibitory receptors such as TIM-3 or TIGIT. In addition, we provide evidence that PD-L1 mediated inhibition of PD-1$^+$ NK cells can be reversed by clinically used PD-1/PD-L1 blocking antibodies.

PD-1$^+$ NK cells were previously identified in patients with multiple myeloma (Benson et al., 2010), lymphoproliferative disorders (Wiesmayr et al., 2012), renal cell carcinoma (MacFarlane et al., 2014), Kaposi sarcoma (Beldi-Ferchiou et al., 2016), digestive cancers (Y. Liu et al., 2017), and in pleural effusions of ovarian cancer patients (Pesce et al., 2017). In contrast to a recent work that identifies a rare subset of peripheral PD-1 expressing NK cells in healthy individuals (Pesce et al., 2017), we were only able to detect some expression of PD-1 in circulating NK cells from NSCLC patients. In contrast, though with substantial inter-patient variability, up to 21% of intratumoral NK cells of NSCLC patients expressed PD-1, which is comparable to findings in other cancer types (Y. Liu et al., 2017; MacFarlane et al., 2014; Pesce et al., 2017). Interestingly, PD-1 expression on NK cells and CD8 T cells appears to be independently regulated in the tumor as the expression of PD-1 on both subsets did not correlate. Furthermore, we observed increased expression of TIM-3 both in peripheral and intratumoral NK cells of NSCLC patients. TIM-3$^+$ NK cells were previously identified in the peripheral blood of advanced melanoma patients and TIM-3 blockade was reported to rescue dysfunctional NK cells (da Silva et al., 2014).

NK cells are known to stochastically vary the expression of activating and inhibitory receptors. The integration of negative and positive stimuli together with cell-intrinsic fine-tuning determines whether NK cells are activated and mediate their effector functions (Guillerey et al., 2016). The observation that PD-1$^+$ NK cells more frequently expressed other inhibitor receptors may have implications for their response when exposed to tumor cells expressing inhibitory ligands. The increase of certain KIRs such as KIR2DL3 on intratumoral NK cells is particularly interesting as KIR-targeting agents such as lirilumab (KIR2DL1/2/3 targeting mAb) are tested in multiple clinical trials for different cancer types, often together with PD-(L)1 inhibitors (Chiossone et al., 2017). In agreement with observations in patients with Kaposi sarcoma (Beldi-Ferchiou et al., 2016), we found substantial expression of the investigated activating receptors CD16, NKG2D, NKp30 and NKp80 on PD-1$^+$ and PD-1$^-$ NK cell subsets. Therefore, we believe that these findings further support the clinical development of novel NK cell engagers which have demonstrated activation of NK cells when co-targeting activating NK cell receptors (Gauthier et al., 2019).

The mechanisms which drive the upregulation of PD-1 on NK cells in cancer patients are unclear. PD-1 expression correlated with human cytomegalovirus seropositivity, which suggests a link between PD-1 upregulation and NK cell-mediated anti-viral activity (Pesce et al., 2017). In agreement with previous work (Y. Liu et al., 2017; Quatrini et al., 2018), combined treatment with IL-15 and IL-12 caused a significant upregulation of PD-1 on human NK cells. The synergistic effect of these cytokines is intriguing because IL-12 is typically produced by dendritic cells and was recently found to be essential for a successful response to PD-1 blocking agents (Garris et al., 2018).

We speculate that PD-1$^+$ NK cells may be involved in interactions between NK cells and stimulatory DCs in the tumor microenvironment as recently observed for human cancer, particularly for patients responding to immunotherapy (Barry et al., 2018).

NK cell hyporesponsiveness has previously been described for a fraction of NK cells that did not express ligands for MHC-I molecules or in humans that lack MHC-I presentation (Anfossi et al., 2006; Zimmer et al., 1998). We found that NK cells from NSCLC patients were mostly limited in their degranulation capacity and polyfunctionality, whereas cytokine secretion and cytotoxicity were less affected. Moreover, our findings indicate that the expression of PD-1 on NK cells might correlate with NK hyporesponsiveness. However, in the absence of PD-L1 expression on target cells, we detected no functional differences between PD-1$^+$ or PD-1$^-$ NK cells in response to MHC-I deficient K562 cells. Interestingly, in a recent study, PD-1$^+$ NK cells in murine tumor models were even more functional than PD-1$^-$ NK cells in the absence of PD-L1 (J. Hsu et al., 2018). Our experiments showed that PD-L1 expressing tumor cells substantially inhibited cytotoxic killing by PD-1$^+$ NK cells. This inhibition could be reversed by a PD-L1 blocking antibody. We additionally observed PD-1 clustering at the NK-tumor cell-cell interface, which indicates that modulation of the activating and inhibitory signals at the immunological synapse is likely involved in PD-1 signaling in NK cells.

Our findings highlight the importance of PD-1 expression on NK cells and show that PD-1 blockade in patients may directly result in NK cell re-activation. In agreement with our data, Hsu and colleagues recently showed that PD-1$^+$ NK cells in murine tumor models are necessary to mediate the full therapeutic benefit of PD-1 blocking antibodies (J. Hsu et al., 2018). A limitation of our study is that the functional assays were performed either in a model system or with healthy donor human NK cells due to the low abundance of NK cells in patient tumors. Further investigations should aim at analyzing intratumoral NK cells from patients undergoing immunotherapy and increasing the resolution to a single-cell level. These investigations will shed further light on the exact role of PD-1$^+$ NK cells upon immune checkpoint blockade with PD-1/PD-L1 targeting agents.

2.2.7.   Disclosure of Potential Conflict of Interest

2.2.8.   Financial Support

2.2.9.   Ethical Approval:

All procedures performed in studies involving human participants were in accordance with the ethical standards of the institutional and/or national research committee (Ethikkommission Nordwestschweiz, EK321/10) and with the 1964 Helsinki declaration and its later amendments or comparable ethical standards. Informed consent was obtained from all individual participants included in the study. This article does not contain any studies with animals performed by any of the authors.

2.2.10.   Contributions

F.U., A.Z. and M.P.T conceived the idea for the study. F.U., M.P.T, and A.Z. interpreted the data, made the figures and wrote the manuscript. M.P.T, M.K., M.A.S., F.U. and A.Z. planned the experiments. M.P.T, M.K., M.S. and P.H. performed and analyzed the experiments. D.L., M.W. and S.S. provided samples. H.L. and A.Z. collected the clinical data and ethical board approvals.

2.2.11.   Acknowledgement

2.2.12. Supplementary Material
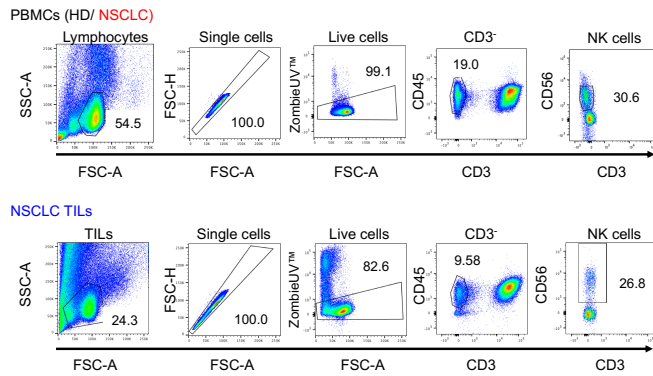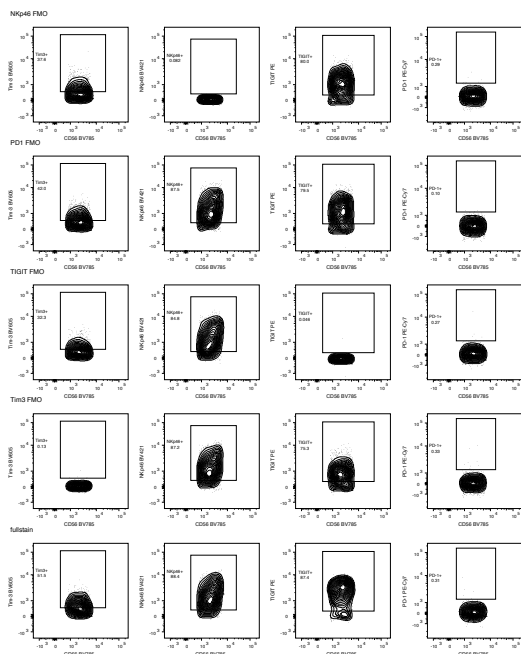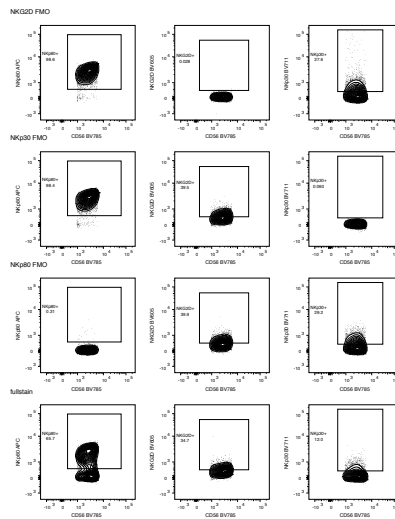
Supplementary Figure 7 Gating Strategy and FMO Controls

(a) *Gating strategy to define CD56+ NK cells in PBMCs (HD/NSCLC) and TILs (NSCLC). (b) Fluorescence minus one (FMO) controls for baseline characterization, activation receptors and inhibitory receptors. (c) FMO controls for baseline characterization, second panel.*

a

b
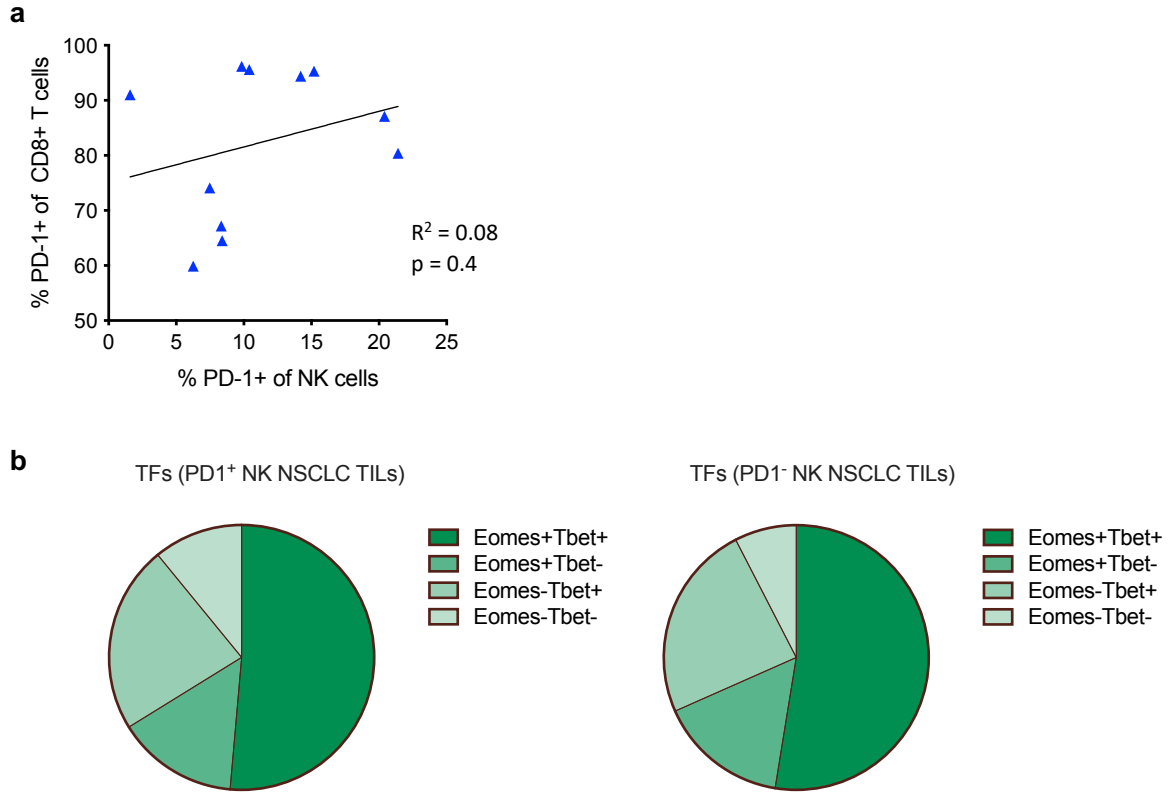
Supplementary Figure 8 Correlation PD1 and Transcription Factors

(a) *Correlation of PD-1 expression in intratumoral CD8 T cells and NK cells. (b) Co-expression of transcription factors of PD-1⁺/PD-1⁻ NK cell subsets in NSCLC TILs.*
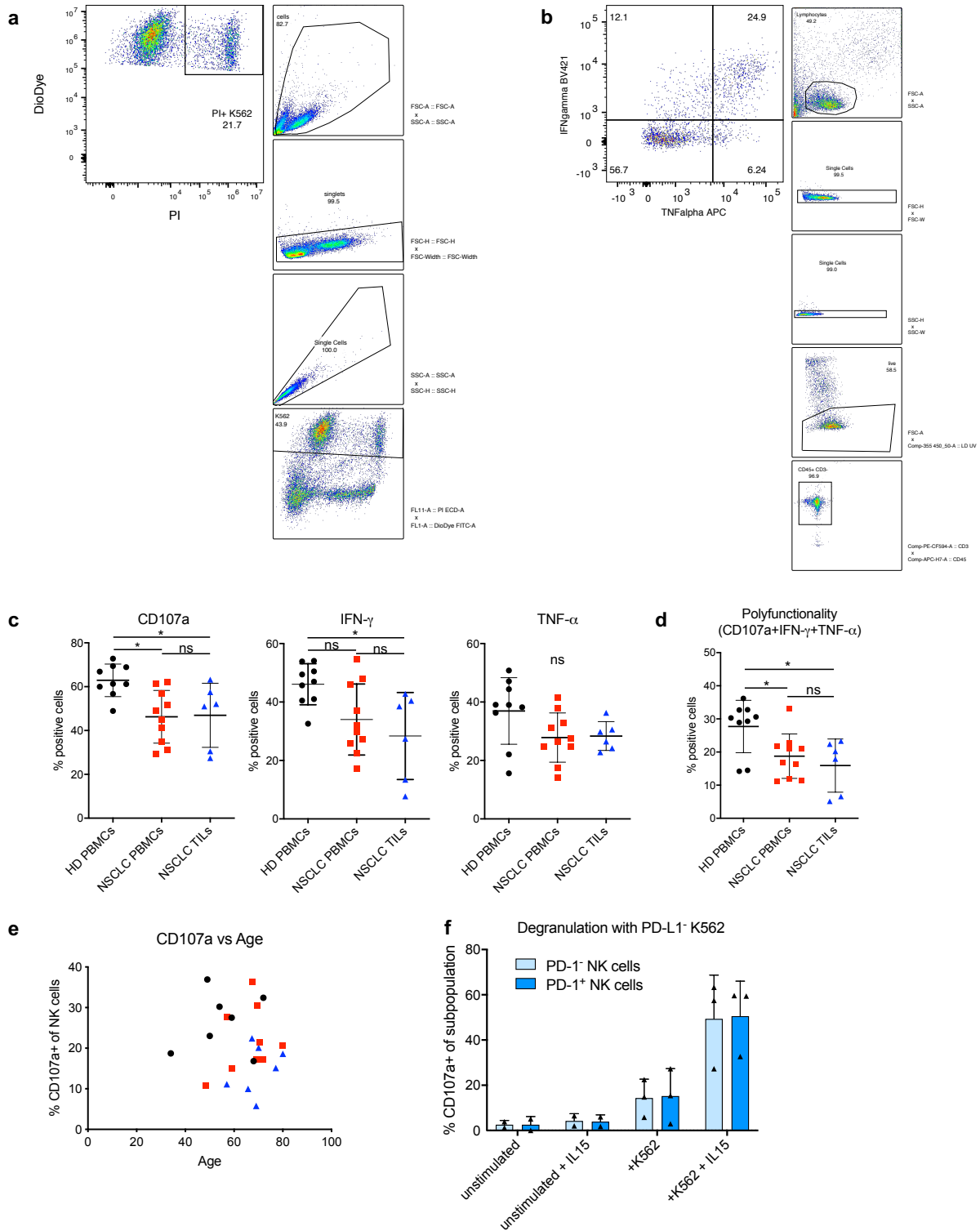
Supplementary Figure 9 Functional Assays

(a) Gating strategy applied for FACS-based killing assay. (b) Gating strategy applied for degranulation assay. (c) Sorted NK cells from HD PBMCs, NSCLC PBMCs and NSCLC TILs were stimulated over night with IL-15 and co-cultured with K562 wt cells for 6h at an E:T ratio of 2:1. NK cell degranulation (CD107a), secretion of IFN-γ and TNF-α was assessed by FACS. (d) Polyfunctionality of NK cells stimulated with IL-15 overnight. (e) Correlation of polyfunctionality with age of patients. (f) Same data as in B gated on PD-1+ and PD-1- NK cells for the three NSCLC tumor samples, in which more than 100 evens were recorded for PD-1+ NK cells. Statistics in all graphs are unpaired 1-way ANOVAs with Tukey's multiple comparison test.

a
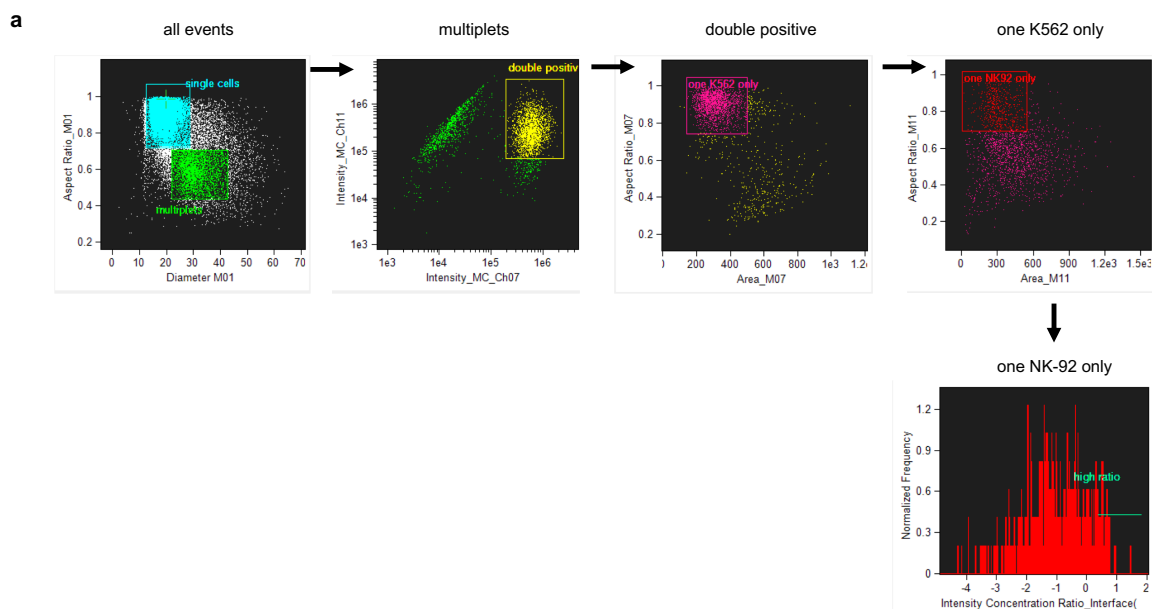
Supplementary Figure 10 Gating Imaging Flow Cytometry PD1 Clustering
(a) PD1/PD-L1 clustering at immunological synapse – gating strategy.

Supplementary Table 10 Antibodies
List of antibodies used throughout this manuscript

Source	Antibody	Clone
BD Biosciences	Anti-CD3-PE-CF594	UCHT1
BD Biosciences	anti-CD45-APC-H7	2D1
BD Biosciences	anti NKG2D-BV605	1D11
BD Biosciences	anti-PD-1-PE-Cy7	EH12.1
BD Biosciences	anti-PD-1-AlexaFluor647	EH12.1
BD Biosciences	anti-IFNgamma-BV421	4S.B3
BD Biosciences	anti-CD107a-PE	H4A3
BD Biosciences	anti-CD4-BV711	SK3
BD Biosciences	anti-CD56-BV786	5.1H11
Biolegend	anti-KIR2DL3-APC	DX279
Biolegend	anti-KIR3DL1-Alexa700	DX9
Biolegend	anti-NKp46-BV421	9E2
Biolegend	anti-NKp80-APC	5D12
Biolegend	anti-TIM3-BV605	F38-2E2
Biolegend	anti-TIM3-BV421	F38-2E2
Biolegend	anti-Tbet-BV421	4B10
Biolegend	anti-CD19-PerCP-eFluor710	SJ25C1
Biolegend	anti-CD14-PerCP-eFluor710	61D3
Biolegend	anti-CD3-FITC	HIT3a
Biolegend	anti-CD8-BV605	RPA-T8
eBioscience	anti-CD16-FITC	eBioCB16
eBioscience	anti-TIGIT-PE	MBSA43
eBioscience	anti-TNFalpha-APC	Mab11
eBioscience	anti-EOMES-eFluor660	WD1928
eBioscience	anti-CD274-APC (PD-L1)	MIH1
eBioscience	anti-CD11c-PerCP-Cy5.5	3.9
eBioscience	anti-CD3-PE	SK7
Miltenyi Biotech	anti-CD8-FITC	SK1
Miltenyi Biotech	anti-CD56-APC	AF12-7H3

Supplementary Table 11 Inhibitory Receptors Co-Expression

Average co-expression of inhibitor receptors on intratumoral PD-1$^+$ versus PD-1$^-$ NK cells (n = 4). Co-Expression of none of the four inhibitory receptors is highlighted in bold letters.

Subset	PD-1$^+$ NK cells	PD-1$^-$ NK cells
KIR2DL3+KIR3DL1+TIGIT+TIM-3+	0.90%	0.10%
KIR2DL3+KIR3DL1+TIGIT+TIM-3-	2.15%	0.65%
KIR2DL3+KIR3DL1+TIGIT-TIM-3+	0.41%	0.50%
KIR2DL3+KIR3DL1-TIGIT+TIM-3+	12.72%	3.81%
KIR2DL3-KIR3DL1+TIGIT+TIM-3+	0.10%	0.54%
KIR2DL3+KIR3DL1+TIGIT+TIM-3-	18.30%	13.99%
KIR2DL3+KIR3DL1+TIGIT-TIM-3-	1.85%	1.43%
KIR2DL3+KIR3DL1-TIGIT-TIM-3+	4.74%	5.79%
KIR2DL3-KIR3DL1+TIGIT+TIM-3-	0.10%	0.39%
KIR2DL3-KIR3DL1+TIGIT-TIM-3+	0.55%	0.42%
KIR2DL3-KIR3DL1-TIGIT+TIM-3+	12.29%	7.28%
KIR2DL3+KIR3DL1-TIGIT-TIM-3-	14.30%	18.85%
KIR2DL3-KIR3DL1+TIGIT-TIM-3-	0.25%	0.56%
KIR2DL3-KIR3DL1-TIGIT+TIM-3-	15.39%	15.28%
KIR2DL3-KIR3DL1-TIGIT-TIM-3+	5.63%	7.81%
KIR2DL3-KIR3DL1-TIGIT-TIM-3-	**10.54%**	**22.62%**
KIR2DL3+	55.36%	45.11%
KIR3DL1+	6.10%	4.58%
TIGIT+	61.74%	42.02%
TIM-3+	37.24%	26.25%

Supplementary Table 12 Activating Receptors Co-Expression

Average co-expression of activating receptors on intratumoral PD-1$^+$ versus PD-1$^-$ NK cells (n = 4).

Subset	PD-1$^+$ NK cells	PD-1$^-$ NK cells
CD16+NKG2D+NKp30+NKp80+	0.41%	0.45%
CD16+NKG2D+NKp30+NKp80-	0.27%	0.06%
CD16+NKG2D+NKp30-NKp80+	7.52%	4.41%
CD16+NKG2D-NKp30+NKp80+	1.81%	1.78%
CD16-NKG2D+NKp30+NKp80+	1.37%	0.34%
CD16+NKG2D+NKp30-NKp80-	3.48%	2.95%
CD16+NKG2D-NKp30+NKp80-	0.57%	0.27%
CD16+NKG2D-NKp30-NKp80+	23.48%	26.50%
CD16-NKG2D+NKp30+NKp80-	0.28%	0.55%
CD16-NKG2D+NKp30-NKp80+	1.54%	3.23%
CD16-NKG2D-NKp30+NKp80+	1.78%	0.59%
CD16+NKG2D-NKp30-NKp80-	23.04%	20.28%
CD16-NKG2D+NKp30-NKp80-	7.51%	6.24%
CD16-NKG2D-NKp30+NKp80-	0.21%	0.41%
CD16-NKG2D-NKp30-NKp80+	6.68%	8.16%
CD16-NKG2D-NKp30-NKp80-	20.06%	23.78%
CD16+	60.57%	56.69%
NKG2D+	22.37%	18.22%
NKp30+	6.69%	4.45%
NKp80+	44.58%	45.45%

2.2.13. Extended Outlook KIR3DS1 and PD-1+ NK Cells

In the presented studies, I first described a polymorphism in the *KIR3DS1/L1* locus that we associated with resistance to PD-1 blockade in NSCLC. This study also linked an increase in NK cell functionality with the response to PD-1 blockade. In the second manuscript, I elaborated on the expression of PD-1 and other co-inhibitory receptors on NK cells in NSCLC and described how PD-1+ NK cells respond to PD-(L)1 blockade *ex vivo*. As discussed above, many questions remain and will build the basis for future studies on NK cells and cancer immunotherapy in our laboratory. Therefore, I would like to discuss some of the proposed next steps.

The relationship between *KIR3DS1* and response to PD-1 blockade in NSCLC should be corroborated in larger cohorts and preferentially in prospective clinical trials to determine the predictive potential. Furthermore, this should be extended to other cancer entities and treatments. For example, we started to investigate whether *KIR3DS1* also might predict resistance to immunotherapy in melanoma. However, the number of available published studies with a sufficient number of patients and accessible sequencing data is low (Hugo et al., 2016), especially for paired-end whole-exome sequencing data. Therefore, studies that include genomic sample collection will need to be initiated. Additionally, we seek to investigate if this association can be confirmed for PD-1 + CTLA-4 combination treatment as well, as this becomes more frequent in clinical practice.

Clinical studies would optimally combine full *KIR* locus genotyping, tumor mutational burden analysis, *HLA* locus genotyping, and staining for PD-1, NK markers, PD-L1, and HLA-F on tumor biopsies before and after therapy. This would allow us to investigate the interaction between these variables and might provide more suggestions on the potential mechanism behind *KIR3DS1* and PD-1+ NK cells. Moreover, multiplexed imaging or single-cell sequencing could be critical to dissect the interactions of NK cells with other cells such as DCs and T cells in the tumor microenvironment.

To investigate the proposed HLA-F-induced NK cell exhaustion hypothesis, we will try to establish an *ex vivo* model of NK cells exhaustion similar to what I propose in the next chapter for T cells. We will investigate whether repetitive stimulation of KIR3DS1+ or KIR3DS1- NK cells in the presence or absence of HLA-F on tumor cells induces changes in NK cell functionality and phenotype.

Interestingly, another hypothesis on the role of KIR3DS1+ NK cells involves interactions with activated T cells. A study by Waggoner and colleagues indicated that during LCMV infections, activated NK cells can kill activated CD4 T cells (Waggoner, Cornberg, Selin, & Welsh, 2012). This leads to a lack of CD4 T cells, followed by CD8 T cell dysfunction and chronic viral persistence. The depletion of NK cells either induced complete viral clearance or fatal immune-related toxicity, depending on the viral load. They did not find a ligand-receptor pair that mediates this effect but they indicated that the 2B4-CD48 axis might be involved. This study implies a regulatory role for NK cells in chronic infections and a similar mechanism might be involved in tumor-associated T cell dysfunction.

Importantly, HLA-F, the ligand for KIR3DS, is upregulated on activated CD4 T cells (Garcia-Beltran et al., 2016). Moreover, the same study found that HLA-F was upregulated following HIV infection in CD4 T cells, which triggered KIR3DS1+ NK cell-mediated elimination of infected CD4 T cells. I speculate that CD4 (and possibly CD8) T cells increase their HLA-F expression during an ongoing anti-tumor immune response, for example, after PD-1 blockade. We seek to investigate this in serial blood or tumor biopsies of patients undergoing PD-1 blockade treatment. The upregulation of HLA-F might lead to KIR3DS1+ NK-mediated elimination of the reinvigorated anti-tumor T cell response. I further speculate that PD-1 expression on NK cells could be involved via inhibition by PD-L1+ tumor cells. We will investigate this hypothesis in human cell culture models with sorted NK and T cells. Possibly, murine tumor models could be investigated, although neither the *KIR3DS1* nor *HLA-F* genes are present in mice. Alternative pathways, such as the 2B4-CD48 axis described for LCMV above, might fulfill similar roles. However, Hsu et al. described that NK cell depletion in murine tumor models led resistance towards PD-L1 blockade (J. Hsu et al., 2018). However, in all except one model, they used a rat IgG2b anti-PDL1 antibody that has been shown to mediate its effects mainly through antibody-dependent cellular cytotoxicity, which is an important function of NK cells (Seidel, Schlegel, & Lang, 2013). If PD-1 blockade without ADCC also depends on or is inhibited by NK cells remains to be investigated.

2.3. An *ex vivo* Model for T Cell Dysfunction Reveals Potential Targets for Cancer Immunotherapy

Led by:
Marcel P. Trefny[1] and Alfred Zippelius[1,5]

Contributions in alphabetical order:
Abhishek Kashyap[1]
Daniela S. Thommen[1,6]
Didier Lardinois[4]
Dominic Schmid[1]
Gillian Griffiths[3]
Heinz Läubli[1,5]
Jane Stinchcombe[3]
Laura Fernandez Rodriguez[1]
Mark Wiese[4]
Michal Stanczak[1]
Nicole Kirchhammer[1]
Petra Herzig[1]
Priska Auf der Maur[2]

[1]*Laboratory of Cancer Immunology, Department of Biomedicine, University of Basel and University Hospital of Basel, Basel, Switzerland;* [2]*Laboratory of Tumor Heterogeneity, Metastasis and Resistance, Department of Biomedicine, University of Basel and University Hospital of Basel, Basel, Switzerland;* [3]*Cambridge Institute for Medical Research, Addenbrooke's Hospital, Cambridge CB2 0XY, England, UK;* [4]*Department of Surgery, University Hospital Basel, Basel, Switzerland;* [5]*Department of Internal Medicine, Division of Oncology, University Hospital Basel, Basel, Switzerland;* [6]*Division of Immunology, The Netherlands Cancer Institute, Amsterdam, The Netherlands*

Corresponding authors: Marcel Trefny and Alfred Zippelius, M.D., Laboratory of Cancer Immunology, Department of Biomedicine, University of Basel and University Hospital of Basel, Hebelstrasse 20, 4031 Basel, Switzerland, Phone: +41 61 265 23 55, marcel.trefny@unibas.ch or alfred.zippelius@usb.ch

2.3.1.   Abstract

Tumor-specific T cells are frequently rendered dysfunctional by chronic stimulation and an immunosuppressive environment. While targeting the PD-1 axis can ameliorate T cell dysfunction, only a minority of patients undergo sustained responses. In the present study, we developed a human *ex vivo* model for T cell dysfunction. In this model, repetitive antigen-specific stimulation with tumor cells leads to T cell dysfunction highly resembling T cells found in human tumors on a phenotypic and transcriptional level. Through a targeted CRISPR screen and functional validation, we discovered that the genomic ablation of several target proteins, including the scaffold protein SNX9, led to improved T cell effector functions. Our *ex vivo* model provides the community with a versatile tool to study different aspects of human T cell dysfunction and shows a role for novel targets such as SNX9 in the modulation of T dysfunctionality.

2.3.2.   Introduction

Cancer immunotherapy is increasingly considered to be the most critical advance in the field of oncology in the last decades, following outstanding clinical successes with immune checkpoint blockade and adoptive T cell therapies (June et al., 2018; Ribas & Wolchok, 2018; Wei et al., 2018). Monoclonal antibodies against immune checkpoints such as programmed death receptor 1 (PD-1) or cytotoxic T-lymphocyte associated protein 4 (CTLA-4) can block inhibitory signaling in immune cells and display remarkable clinical efficacy. Multiple antibodies are now approved for the treatment of a broad range of tumor types including melanoma (Robert, Long, et al., 2015; Robert, Schachter, et al., 2015) and non-small cell lung cancer (Borghaei et al., 2015b; Brahmer et al., 2015; Carbone et al., 2017; Reck, Rodríguez-Abreu, et al., 2016). These therapies mediate prolonged survival, but particularly often induce durable clinical benefits. However, therapeutic benefits are currently limited to a minority of treated patients, and many patients present with innate resistance or develop resistance through yet poorly understood mechanisms (O'Donnell et al., 2019; Syn et al., 2017). In addition to checkpoint blockade, adoptive transfers of T cells enriched for tumor reactivity, or genetically engineered with natural or chimeric receptors, have shown impressive anti-tumor efficacies (Guedan et al., 2019; June et al., 2018; Rohaan et al., 2019). Recently, more personalized approaches to enhance neoantigen reactivity has further boosted efficacy, even in patients with immunologically silent tumors such as breast cancer (Zacharakis et al., 2018).

Intra-tumoral T cell dysfunction is considered a hallmark of cancer. Experimental studies in murine models of chronic lymphocytic choriomeningitis virus (LCMV) infections provided critical insights into a specific functional state commonly referred to as T cell exhaustion or T cell dysfunction (Wherry, 2011). Detailed mechanistic investigations revealed that a persistently high antigen burden is necessary to induce T cell dysfunction in chronic infections (Bucks, Norton, Boesteanu, Mueller, & Katsikis, 2009; Mueller & Ahmed, 2009; Streeck et al., 2008; Utzschneider et al., 2016). Similarly to chronic viral infections, several studies have demonstrated that tumor-infiltrating CD8 T cells are impaired in their production of effector cytokines such as IFNγ (Baitsch et al., 2011; Zippelius et al., 2004). Recent work from our group revealed that a subpopulation of tumor-infiltrating T cells (TILs) expressing high levels of PD-1, are enriched for tumor reactivity, co-express multiple inhibitory receptors, and are exceptionally dysfunctional (D. S. Thommen et al., 2018, 2015). Nevertheless, there is increasing evidence that these intratumoral T cells are not fully "exhausted" but fulfill

other functions in the tumor microenvironment such as CXCL13 secretion (D. S. Thommen et al., 2018; D. S. Thommen & Schumacher, 2018). Therefore, we and others instead refer to these cells as "dysfunctional" (Blank et al., 2019). Although chronic murine infections are a validated and valuable research tool, differences between T cell dysfunction in chronic viral infections and tumors have been described (Baitsch et al., 2011; D. S. Thommen & Schumacher, 2018). Beyond chronic TCR triggering, tumor-infiltrating T cells are shaped by a multi-faceted and highly heterogeneous immunosuppressive environment that includes engagement of inhibitory and costimulatory receptors, presence of immunosuppressive cytokines, metabolic restriction, hypoxia, diverse cell populations, and alterations in glycosylation patterns (Binnewies et al., 2018; Stanczak et al., 2018).

T cell dysfunction is a significant hurdle to improve cancer immunotherapy. For example, targeting the PD-1/PD-L1 pathway by monoclonal antibodies leads to an expansion and reinvigoration of PD-1+ T cells (A. C. Huang et al., 2017), especially the TCF7+ compartment of stem-like dysfunctional T cells (Im et al., 2016; Kurtulus et al., 2018; Sade-Feldman et al., 2018; Siddiqui et al., 2019). However, epigenetic stability of the dysfunctional phenotype can limit therapeutic efficacy (Ghoneim et al., 2017; Pauken et al., 2016; Philip et al., 2017; Sen et al., 2016), which is linked to a combination of transcription factors including TOX (Alfei et al., 2019; Khan et al., 2019; Scott et al., 2019). Importantly, T cell dysfunction is also a limiting factor for cellular therapies, such as adoptive T cell transfer (Ma et al., 2013) and chimeric antigen receptor (CAR) T cells (Long et al., 2015; Rottman & Horvath, 2017; Weigelin et al., 2015). As many aspects of T cell dysfunction remain unclear, the development of novel cancer immunotherapies urgently requires a comprehensive understanding of the molecular mechanisms underlying T cell dysfunction.

Here, we developed an *ex vivo* human model system to mimic tumor-specific T cell dysfunction. For this purpose, healthy-donor T cells transduced with an NY-ESO-1 T cell receptor construct are exposed to repetitive stimulation using tumor cells presenting antigenic peptides. We can demonstrate that this procedure stably renders CD8 T cells dysfunctional and induces a state that highly resembles CD8 T cells found in human tumors on a phenotypic and transcriptional level. Importantly, this model can produce a high number of antigen-specific dysfunctional T cells, which overcomes the restraints imposed by the limited availability of tumor-infiltrating T cells with unknown antigen specificity obtained from cancer patients. Using bioinformatic target prioritization and a targeted pooled-CRISPR-Cas9 gRNA screen, we discovered a role for SNX9 in the regulation of T cell effector functions. SNX9 accumulates at the immune synapse during tumor cell recognition and impairs tumor cell recognition.

2.3.3. Methods

Reagents and Resources

Name	Source	Identifier
Critical reagents		
NY-ESO-9C peptide SLLMWITQC >95% purity	EZ Biolabs	custom
NY-ESO-9V peptide SLLMWITQV >95% purity	EZ Biolabs	Custom
Recombinant human IL-2	Peprotech	
CD8 microbeads human	Miltenyi	130-045-201
T cell stimulation and expansion kit	Miltenyi	130-091-441
Polyethylenimine > 25kDa	Poly Sciences Inc.	23966-1
Nucleospin plasmid miniprep	Machery Nagel	740588.250
NucleoBond Xtra Midi Kit	Machery Nagel	740410.50
NucleoBond Xtra Maxi Kit	Machery Nagel	740414.50
Precision Count Beads	Biolegend	424902
ALT-R crRNA	Integrated DNA Technologies (IDT)	Sequence specific
ALT-R tracrRNA	Integrated DNA Technologies (IDT)	1072533
16 % para-formaldehyde	Electron Microscopy Services	15710-S
Vectashield Mounting Media Vibrance	Reactolab SA	H-1700-10
5 well microscopy slides	Hendly-Essex	PH299 B230615
Retronectin	Takara	T100B
NucleoSpin Gel and PCR Clean-up	Machery Nagel	740609.50
QIAamp DNA Blood Mini Kit	Qiagen	51104
Plasmids		
pRRL094 WT LAU155 NY-ESO-1 TCR	Kindly provided by Dr. Michael Hebeisen and Dr. Natalie Rufer (Hebeisen et al., 2013; Schmid et al., 2010)	Request at the indicated source
LentiCRISPRv2-mCherry	Addgene, was as a gift from Agata Smogorzewska	99154
pcDNA3.1(+)/Luc2=tdT	Addgene, was a gift from Christopher Contag	32904
Biological Samples		
Human Peripheral Blood Buffy Coat	Blood Donation Center Basel, Switzerland	NA
Human non-small cell lung cancer	University Hospital Basel, Switzerland	NA
Human AB+ male serum	Blood Donation Center Basel, Switzerland	NA
Dyes		
Zombie UV	Biolegend	423107
Fixable Viability Dye eF450	ThermoFisher	65-0863-14
Cell Trace Violet	ThermoFisher	C34557
Phalloidin-AF647	ThermoFisher	A22287
Mitotracker Deep Red	ThermoFisher	M22426
Mitotracker Green	ThermoFisher	M7514

Bodipy493	ThermoFisher	D2922	
Bodipy500	ThermoFisher	D3823	
2-NBDG	ThermoFisher	N13195	
Software and algorithms			
PinAPL-py	(Spahn et al., 2017)	http://pinapl-py.ucsd.edu/	
Huygens Deconvolution	Scientific Volume Imaging https://svi.nl/HomePage	Huygens Remote Manager 3.6.0-3-g0891e1e	
OMERO	openmicroscopy.org University of Dundee	OMERO.web 5.4.10-ice36-b105	
R Studio Version 1.2.1335	https://rstudio.com		
Graphpad Prism 8.3.0	Graphpad Software LLC		
R version 3.5.1	https://rstudio.com		
Imaris 9	Bitplane, Oxford Instruments		

Antibodies

Antibody target (all human)	Fluorochrome	Company/Provider	catalog Nr.	clone
CCR7	Alexa Fluor 647	Biolegend	3532218	G043H7
CD3	PE-CF594	BD	562280	UCHT1
CD45	APC-H7	BD	560178	2D1
CD56	BV785	BioLegend	362550	5.1H11
CD8	FITC	eBioscience	11-0087	SK1
EOMES	PerCP eFluor710	eBioscience	46-4877	WD1928
TNFα	APC	eBioscience	17-7349	MAb11
IFNγ	BV421	BD	564791	4S.B3
KI67	APC	BioLegend	350514	Ki-67
LAMP-1 (CD107a)	PE	BD	555801	H4A3
PD-1	PE-Cy7	BD	561272	EH12.1
TBET	BV421	BioLegend	644815	4B10
TIM-3	BV605	BioLegend	345018	F38-2E2
TIM-3	BV421	BioLegend	345008	F38-2E2
TCR Vbeta13.1	FITC	Biolegend	362404	H131
TCR Vbeta13.1	PE-Cy7	Biolegend	362406	H131
TCF7	AF647	Biolegend	655203	7F11A10
CD28	PE-Cy7	eBioscience	25-0289.42	CD28.2
CD57	BV421	BD	563896	NK-1
LAG-3	APC	eBioscience	17-2239-41	3DS223H
SNX9	None	ThermoFisher	PA5-56734	polyclonal
SNX9	None	Kindly provided by Dr. Jennifer Hirst (Hirst, Motley, Harasaki, Peak Chew, & Robinson, 2003)	SNX9-1 (Sully)	polyclonal
SNX9	None	Kindly provided by Dr. Jennifer Hirst (Hirst et al., 2003)	SNX9-2 (Shrek)	polyclonal
CD8α	AF488	R&D	37006	FAB1509G
LAMP1	none	Biolegend	328602	H4A3
Goat-anti-mouse IgG	AF488	ThermoFisher	A32723	polyclonal
Goat-anti-rabbit IgG	AF647	ThermoFisher	A21246	polyclonal
Goat-anti-rabbit IgG	AF488	ThermoFisher	A11034	polyclonal

CRISPR-Cas9 Guide Sequences

CRISPR-screen guides will be deposited separately

guide	gene	Guide RNA sequence
sgIntergenic19822	Intergenic region control	GAGAGGGTGGCGACAGAGCG
sgSNX9-1	SNX9	GAAACATCAAAGGAGAACGA
sgSNX9-2	SNX9	GAGGTAGGATAAACCCACAT

Peptides

Peptides were purchased in >95% purity from EZ Biolabs. Lyophilized peptides were resuspended at 10mM in sterile dimethyl sulfoxide (DMSO) and stored at -20°C until use. For the NY-ESO-9C peptide and to keep conditions equal, 2 mM of the reducing agent TCEP was added to a 20 μM predilution of all peptides for 1h in PBS to reduce cysteine bridges. The endogenous NY-ESO-1 peptide SLLMWIQC was shown to elicit half-maximal response by LAU155 TCR transduced T cells at an EC50 of 12 nM (Romero et al., 2001). The NY-ESO-9V peptide has a 4500-fold relative competitor activity towards HLA-A2010 and 200-fold higher antigenic activity (half-maximal dose required for killing of T2 tumor cells) compared to the NY-ESO-9C endogenous peptide (Romero et al., 2001).

Cell Culture Media

For the culture of T2, Jurkat and NA8-Mel cells, RPMI1640 (Sigma) was supplemented with 10% heat-inactivated (56°C 30min) fetal calf serum (PAN Biotech), 100 ng/ml penicillin/streptomycin (Sigma), 2 mM L-Glutamine (Sigma), 1 mM Sodium Pyruvate (Sigma) and 1% MEM non-essential amino acids (Sigma), 50 nmol/l beta-mercaptoethanol (Thermo Fisher) and 10mM HEPES (Sigma).
For the culture of human T cells, RPMI1640 was supplemented as described above, but FCS was replaced with 10% heat-inactivated AB+ male donor serum. Recombinant human IL-2 (Peprotech or Proleukin) was always added freshly at the indicated doses. For the culture of HEK293T cells, DMEM (Sigma) was supplemented with 5% heat-inactivated (56°C 30min) fetal calf serum (PAN Biotech), 100 ng/ml penicillin/streptomycin (Sigma), 2 mM L-Glutamine (Sigma), 1 mM Sodium Pyruvate (Sigma) and 1% MEM non-essential amino acids (Sigma) and 10mM HEPES (Sigma).

Cell Lines

T2 cells (ACC598) and Jurkat (ACC282) were purchased from DSMZ, Leibnitz Institute. HEK293T cells (ATCC CRL-3216) were purchased from ATCC.
T2 and Jurkat cells were cultured in supplemented RPMI as described above. The melanoma cell line NA8-Mel was kindly provided by Dr. Romero (University of Lausanne) and cultured in RPMI-1640 supplemented as described above. All cells were confirmed to be negative for mycoplasma by PCR as described (Choppa et al., 1998) after every freeze-thaw cycle and then passaged every 2-3 days for a maximum of 15 passages.

Isolation of Primary Immune Cells

Human peripheral blood mononuclear cells (PBMCs) were isolated by density gradient centrifugation using Histopaque-1077 (Sigma) from buffy coats obtained from healthy blood donors (HD) (Blood Bank, University Hospital Basel). Briefly, buffy coat was diluted in PBS and layered on top of Histopaque-1077 and spun in SepMate (Stem Cell) according to manufacturer's instructions. Red blood cells were lysed using Red Blood Cell Lysis Kit (eBiosciences), washed and frozen in 10% DMSO 90% FCS in a

Styrofoam container to -80°C. For long term storage, cells were transferred to liquid nitrogen.

Fresh tumor tissues were collected from patients with NSCLC undergoing surgery at the University Hospital Basel, Switzerland. The study was approved by the local ethical review board (Ethikkommission Nordwestschweiz, EK321/10), and all patients consented in writing to the analysis of their tumor samples. The staging was based upon the 7th edition of the AJCC/UICC tumor–node–metastasis (TNM) staging system. Tumor lesions were mechanically dissociated and digested using accutase (PAA), collagenase IV (Worthington), type V hyaluronidase from bovine testes (Sigma), and DNAse type IV (Sigma), directly after excision. Single-cell suspensions were prepared and frozen as above.

T Cell Receptor Construct

The lentiviral construct encoding for the codon-optimized WT LAU155 NY-ESO-1 T cell receptor alpha and beta chains under an hPGK promotor separated by an IRES domain was kindly provided by Dr. Michael Hebeisen and Dr. Natalie Rufer at the University of Lausanne(Hebeisen et al., 2013; Schmid et al., 2010). This TCR has a K_D = 21.4 μM for its endogenous NY-ESO-1 SLLMWITQC peptide.

Generation of Lentivirus

To generate lentivirus, 2.5 million low passage HEK293T cells were cultured in DMEM medium and seeded into a 15cm tissue-culture treated dish. Three days late 2nd generation LTR-containing donor plasmid, packaging plasmid pCMV-delta8.9, the envelope plasmid VSV-G and were mixed at a ratio of 4:2:1 ratio in unsupplemented Opti-MEM (ThermoFisher) and sterile filtered. This solution was then mixed with polyethyleneimine 25 kDa (Polysciences Inc.), also diluted in Opti-MEM at a DNA:PEI ratio of 1:3. 28 μg of DNA was transfected per 15cm dish. After two days, supernatants were collected from cells (exchange medium) and filtered through a 0.45 µm PES filter. Supernatants were stored for 1 day at 4°C until the second batch of supernatant was collected 24h later. The supernatant containing lentiviral particles was concentrated by ultra-centrifugation at 40'000 x g for 2 h at 4°C, resuspended in 0.1% BSA in PBS, and frozen to -80°C.

Transduction of Human T Cells

To generate NY-ESO-1 TCR specific T cells, human healthy donor PBMCs were thawed and washed in PBS. CD8 T cells were then isolated using the CD8 microbeads kit (Miltenyi, positive selection) according to the manufacturer's instructions on an AutoMACS. Isolated cells were washed and resuspended in suppl. RPMI with 10% human Serum as described above and plated at 1.5 mio/ml. T cell activation and expansion kit (Miltenyi) anti-CD3+anti-CD28 stimulatory magnetic beads were coated overnight at 4°C on a rotator shaker according to the manufacturer's instructions. These beads were washed in medium and added to the CD8 T cells at a 1:1 ratio together with 150 U/ml IL-2. 24h later, NY-ESO-1 TCR lentiviral particles produced as above were added at a multiplicity of infection (MOI) of 2. Cells were then expanded every 2 days with fresh medium and replenishing 50 U/ml IL-2 for 5 days. The percentage of transduced cells was then calculated by staining for TCR Vbeta13.1+ T cells in comparison to non-transduced cells.

Repetitive Stimulation

NY-ESO-1 TCR specific T cells were plated at 0.125mio/ml specific cells. T2 tumor cells were irradiated at 3000 rad using a GammaCell irradiator. Irradiated cells were loaded with the indicated dose of NY-ESO-9C/9V peptides and added to the T cells at an effector to target ratio of 1:3 in the presence of 50 U/ml IL-2. This procedure was repeated (with IL-2 stimulation only on the first and third stimulation) according to the scheme in Suppl. Fig. 1b. Acute stimulation controls were only stimulated with tumor cells on day 9 after plating. After 12 days (thus 3 days after last stimulation), cells were stained and analyzed by flow cytometry including counting bead normalization. Functional assays were performed the next day according to these cell numbers.

Immunofluorescence Staining for Flow Cytometry

At the indicated time points, T cells were stained with the following protocol. Cells are washed in PBS, resuspended in PBS, and blocked with 1:100 human Fc-receptor-inhibitor (eBioscience) in PBS and stained with Fixable Viability Dyes (Biolegend or eBioscience) 1:200 for 20min on ice. For surface staining, cells were washed and resuspended in FACS buffer (PBS supplemented with 2 mM EDTA, 0.1% Na-Azide, 2% FCS), and stained with the appropriate antibodies for 30 min at 4°C. All antibodies used in this study are listed above. For intracellular (cytoplasmic) staining, including SNX9 and cytokines, cells were fixed and permeabilized using IC Fixation Buffer (eBioscience) for 20min at room temperature. Intracellular antibodies were then stained in 1x Permeabilization buffer (eBioscience) for 30min at 4°C. For secondary staining, this procedure was repeated, including washing steps. For staining of nuclear proteins, the Fixation/Permeabilization kit (eBioscience) was used for 30min at room temperature followed by two wash cycles in 1x permeabilization buffer and antibody staining in 1x permeabilization buffer for 45min at room temperature. We added 10'000 Precision counting beads (Biolegend) to each sample before the first washing step to adjust cell counts after acquisition based on the bead count (population high in SSC and positive in any channel <640 lasers). After staining, cells were analyzed on a BD LSR Fortessa Cell analyzer (BD Bioscience) or Cytoflex S (Beckmann) flow cytometer. Data were collected using the BD FACS Diva Software version 7 or Beckmann Culture CytExpert and further analyzed with FlowJo v10.1.6 (Tree Star Inc.) and GraphPad Prism v8 (GraphPad Software Inc.). All results unless indicated show integrated fluorescence area on a biexponential scale.

Flow Cytometry-based Cell Sorting

For cell sorting, cells were kept on ice, washed in PBS, and stained with appropriate antibodies for 30 min at 4°C in PBS + 2% FCS and 2 mM EDTA (without Azide). Following incubation, cells were washed, resuspended in the same buffer and filtered through a 70um mesh. Sorting of cells was performed using a FACSAria III or FACS SorpAria (BD), and the purity of sorted populations was routinely tested to be >98%.

Mitochondria and Metabolism Stainings

Mitochondrial stainings were performed with Mitotracker Green (MTG, ThermoFisher) and Mitotracker Deep Red (MTDR, ThermoFisher). Cells were washed in fresh medium as described above and incubated in 50 nM MTG and 10 nM MTDR in prewarmed medium for 15 min at 37°C. Cells were then washed two times in FACS buffer and acquired directly using a Fortessa 2 flow cytometer. Similarly, staining for glucose uptage and lipid uptake cells were incubated separately in 100 μM 2-NBDG (ThermoFisher) or 1 μM Bodipy500 (ThermoFisher) in fresh medium for 15 min at

37°C. Cells were washed and stained as above. For neutral lipid staining, antibody stained cells were fixed for 20 min with IC fixation buffer and then incubated with 1 μg/ml of Bodipy493 (ThermoFisher) in PBS for 1h on ice. Cells were washed twice with FACS buffer and acquired on a flow cytometer.

Degranulation and Cytokine Production Assay

We performed a co-culture of peptide-loaded T2 cells with T cells in the presence of CD107a antibodies to assess the degranulation of cytokine production of T cells. For this purpose, T2 cells were incubated at a density of 1mio/ml with the respective peptides diluted in full RPMI supplemented medium. Afterward, 10'000 NY-ESO-1 specific T cells (measured by TCR Vβ13.1 staining as above) were co-cultured with 10'000 of these peptide-loaded T2 cells for 5h in the presence of 20 ng/ml anti-CD107a-PE/APC-H7 antibody and 1x Monensin (Biolegend). Following incubation, the cells were stained for dead cells, surface antibodies, fixed using IC fixation buffer (eBioscience), and then stained for the accumulation of IFNγ and TNFα within cells. Samples were analyzed on a Fortessa LSR (BD).

Killing Assay

Killing capacity was measured using a luminescence-based cell system. T2 cells expressing Luciferase and tdTomato (abbreviated "T2-Luc") were generated by the transduction of a lentivirus made with the pFU-Luc2-tdTomato construct and sorting for tdTomato expression. T2-Luc2 cells were washed and resuspended at 1 mio/ml with 1 μM NY-ESO-9V peptides (if indicated 9C instead) and incubated at 37°C for 30 min. T2-Luc cells were then washed and plated at 20'000 cells per well of a V-bottom 96-well white plate. 20'000 (or else according to the E:T ratio) NY-ESO-1 specific T cells were then added to these cells and incubated for the indicated time. Afterward, 0.15mg/ml D-Luciferase (Perkin Elmer) was added to each well and immediately analyzed on a BioTek H1 Spectro/luminometer, acquiring for 1 sec / well. Averages of three successive reads were used. Controls without T cells (maximal signal) and one with 0.1% Triton-X100 (minimal signal) were used to calculate % specific lysis:

$$\% \: specific \: lysis = (1 - \left(\frac{signal - minimal \: signal}{maixmal \: signal - minimal \: signal} \right)) \times 100\%$$

Proliferation and Stability Assay

To measure proliferation and stability after repetitive stimulation, cells on day 13 after the first stimulation, were washed and plated at 10'000 specific cells per 96-well with 50 U/ml IL-2. Cells were then either left to rest or stimulated again with a 1:1 ratio of irradiated NY-ESO-9V loaded T2 tumor cells as above. The medium was exchanged three days later, and cells were stained and analyzed 6 days later. The next day, the degranulation capacity and production of cytokines of the cells was measured as above.

Transcriptomics Analysis

Minimally 41'000 (most samples 200'000) repetitively stimulated antigen-specific T cells were sorted on day 12 as described above directly into Trizol LS (Sigma).

The 24 purified RNA was quality-checked on the Bioanalyzer instrument (Agilent Technologies, Santa Clara, CA, USA) using the RNA 6000 Pico Chip (Agilent, Cat# 5067-1513) - Average RIN (RNA Integrity Number) was 7.4±0.5. RNA was quantified by Fluorometry using the QuantiFluor RNA System (Cat# E3310, Promega, Madison, WI, USA). Library preparation was performed, starting from 150ng total RNA (except for Sample 93.2), using the TruSeq Stranded mRNA Library Kit (Cat# 20020595, Illumina, San Diego, CA, USA) and the TruSeq RNA CD Index Plate (Cat# 20019792, Illumina, San Diego, CA, USA). 15 cycles of PCR were performed. Libraries were quality-checked on the Fragment Analyzer (Advanced Analytical, Ames, IA, USA) using the Standard Sensitivity NGS Fragment Analysis Kit (Cat# DNF-473, Advanced Analytical) revealing the excellent quality of libraries (average concentration was 51±16 nmol/L and average library size was 350±8 base pairs). Samples were pooled to equal molarity. The pool was quantified by Fluorometry using the QuantiFluor ONE dsDNA System (Cat# E4871, Promega, Madison, WI, USA). Libraries were sequenced Single-reads 76 bases (in addition: 8 bases for index 1 and 8 bases for index 2) using 2 NextSeq 500 High Output Kit 75-cycles (Illumina, Cat# FC-404-1005) loaded at 1.4 pM and 1.9 pM respectively and including 1% PhiX. Primary data analysis was performed with the Illumina RTA version 2.4.11 and Base-calling Version bcl2fastq-2.20.0.422. Two Nextseq runs were performed to compile enough reads (on average per sample: 35.7±2.6 million pass-filter reads).

Reads were aligned to the human genome (UCSC version hg38AnalysisSet) with STAR (version STAR/2.5.2a-goolf-1.7.20) using the multi-map settings '--outFilterMultimapNmax 10 --outSAMmultNmax 1'. The output was sorted and indexed with samtools (version SAMtools/1.3.1-goolf-1.7.20), and picard markDuplicates (version picard/2.9.2) was used to collapse samples run on different sequencing lanes. Coverage tracks per sample were generated by tiling the genome in 20bp windows, counting overlapping reads per window using the function bamCount from the bioconductor package bamsignals (bioconductor version 3.6) and exporting these window counts in bigWig format using the export function of the bioconductor package rtracklayer. Read and alignment quality was evaluated using the qQCReport function of the bioconductor package QuasR. The qCount function of QuasR was used to count the number of read (5'ends) overlapping with the exons of each gene assuming an exon union model.

The results of the RNA sequencing have been deposited on Gene Expression Omnibus (GEO) under the number (Thesis comment: Will be deposited upon completion of the manuscript).

Cloning gRNA CRISPR Screen Library

In addition to the 25 selected genes from the RNA-Sequencing analysis described above, four genes with known roles in T cell dysfunction (PTPN22, DUSP4, ENTPD1, SPRY1)(Sade-Feldman et al. 2018; Collins et al. 2012; Zheng et al. 2017; Maine et al. 2016; Singer et al. 2016) and three genes essential to T cell functionality (ZAP70, LAT, LAMP1)(Shifrut et al. 2018) were used as positive and negative controls for the CRISPR-Cas9 screen. 5 gRNA sequences for each of the selected genes and 20 intergenic controls were extracted from a published highly optimized gRNA library (Wang et al. 2017) and ordered with the required overlaps for assembly as a DNA oligo

pool from Twist Biosciences according to Wang et al. (T. Wang, Lander, & Sabatini, 2016). gRNA DNA oligonucleotides were amplified by high fidelity PCR, purified over a 2% agarose Tris-acetate EDTA gel, and extracted using Machery Nagel PCR cleanup kit. LentiCRISPRv2-mCherry (Addgene 99154) was digested by BsmBI and cut plasmid extracted from a 1% TAE agarose gel. This fragment was fused with the PCR amplified gRNAs at a 1:30 molar ratio by Hifi-DNA Assembly for 1h at 50°C (New England Biolabs, failed using Gibson Assembly standard kit). The product was amplified by the transformation of Stbl3 *E. coli* with over 1000 colonies per guide, cultured in LB with 100 μg/ml ampicillin (Sigma), and extracted using Midi Prep (Machery Nagel). The plasmid library was barcoded by PCR and sequenced at the D-BSSE Genomics Facility on an Illumina MiSeq 50 cycle v2 run, which proved successful cloning and representation of all guides (Gini index 0.188). 2nd generation lentivirus was then prepared on a larger scale (>1000 cells / guide) from the library and the NY-ESO-1 TCR, which were then concentrated by ultracentrifugation and titrated on Jurkat cells.

Co-transduction of a CD3E-targeted LentiCRISPRv2-mCherry construct and the NY-ESO-1 TCR was optimized for the multiplicity of infection (0.5 to minimize multiple KO per cell), delivery method (TCR in suspension and KO on retronectin coated plates), stimulation (1:1 with anti-CD3/28 beads) and timing of infection (24h post-stimulation) (not shown).

CRISPR Screen and Analysis

Freshly isolated healthy donor CD8 T cells were stimulated as above. In addition, cells were co-transduced with LentiCRISPRv2-mCherry virus at an MOI of 0.5. For this purpose, non-treated 6-well polystyrene plates were coated with 2 μg/cm^2 Retronectin (Takara) overnight in PBS at 4°C and then blocked using 2% BSA in PBS for 20 min at room temperature. The LentiCRISPRv2-mCherry virus was diluted according to the desired MOI in PBS with 0.1% BSA and added to the plates in 2ml per well. Plates were then centrifuged 90min at 2000 g at 32°C. Plates were then washed with 0.1% BSA in PBS, and CD8 T cells were added on top. Then the NY-ESO-1 TCR virus was added, and cells were incubated for 2 days. Fresh medium and 50 U/ml IL-2 was added every 2 days, and after 6 days, cells were sorted for live CD8+ TCR+ mCherry+ cells (co-transduction efficiency for the two donors was 0.57% and 0.99% respectively). An initial cell fraction was frozen for the "d0 control" sample at >415 cells / guide representation. The remaining cells were then repetitively stimulated with NY-ESO-9V peptide, as described above. After four rounds of stimulation, cells were re-stimulated with NY-ESO-9V loaded T2 cells in the presence of an anti-CD107a-APC-H7 antibody. 4h later, cells were stained and sorted based on live CD8+ Vbeta13.1+ CD19- CD4- CD56- CD107a+/- fractions into 200ul PBS. Genomic DNA from these samples was extracted using the Qiagen Blood DNA mini kit, including a Proteinase K digestion step. DNA was eluted in 5mM Tris-HCl (no EDTA), and a barcoded PCR amplification of gRNA sequences was performed as described (T. Wang et al., 2016) with PCR cycles: 95°C 2'; 35x: 98°C 10', 60°C 15'', 72°C 30''; 72°C 5'. gRNA PCR product was isolated from a 2% agarose in Tris-Acetate-EDTA gel and eluted using Machery Nagel PCR cleanup kit and dried for 10min at 56°C. DNA was eluted in 25 μl 5mM Tris-HCl. This DNA library was loaded onto a 50 cycle MiSeq v2 Illumina Run on an Illumina MiSeq.

gRNA sequencing reads retrieved from this sequencing were demultiplexed and uploaded to PinAPL-py.ucsd.edu(Spahn et al., 2017). PinAPL-py was then used to align, control for quality, and count guides with the 5' adapter ATTTTAACTTGCTATTTCTAGCTCTAAAAC. Bioconductor EdgeR (within R Studio) was then used to perform differential gRNA analysis based on these counts based on a generalized linear model, including batch effects for cell donors. From gRNA statistics, gene enrichment analysis using its camera function was performed and mean log-fold changes were calculated. Given the low number of genes and replicates, we found this to be more informative than the aRRA (MAGECK) algorithm designed for much larger whole-genome CRISPR screens.

Cas9-RNP-mediated KO

To knock out genes using Cas9-crRNA-tracrRNA ribonuclear protein complexes, the Lonza Nucleofector 4D system was used. Both gene-specific crRNA and tracrRNA were mixed at 44 μM in nuclease-free duplex buffer (IDT) and heated to 95°C for 5min, then cooled to 25°C at -0.1°C per minute. 1.5 μl of these aligned crRNA-tracrRNA complexes was then incubated with 1.5 μl of 40 μM Cas9-NLS protein (Berkeley, QB3) for 30min at room temperature in the dark and used immediately (referred to as Cas9-RNP). CD8 T cells were stimulated for 1 day using anti-CD3+anti-CD28 stimulatory beads (Miltenyi) with 150 U/ml of IL-2 in 10% human serum containing supplemented RPMI as described above. The next day, beads were removed by magnetic separation. Cells were spun down at 500g 3min and resuspended in 1:4.5 supplemented electroporation P3 buffer at 1 mio / 20 μl according to manufacturer's instruction. 20 μl of this solution containing 1 million cells was then mixed with the 3 μl of Cas9-RNP and electroporated using the EH115 setting in an X-unit Lonza Nucleofector 4D. Immediately after electroporation, 80 μl prewarmed medium was added, and cell incubated for 20 min. Cells were then transferred to 24 well plates at 1mio/ml in fresh medium with 50 U/ml IL-2 1:4 anti-CD3+anti-CD28 stimulatory beads and if indicated additional NY-ESO-1 TCR virus at 2 MOI.

Immunofluorescence Staining for Imaging

To perform immunofluorescence images of T cell – tumor cell conjugates, T2 tumor cells were loaded with 1 μM NY-ESO-9V peptide for 30min at 37°C. Then T2 tumor cells were washed 2x in serum-free prewarmed RPMI and resuspended at 1 mio/ml in the same medium. Similarly, repetitively stimulated NY-ESO-1 TCR transduced T cells produced as above, were washed 2x in serum-free prewarmed RPMI and resuspended at 1 mio/ml. Both cells were then mixed at a 1:1 ratio and incubated for 5min at 37°C. 50 μl of this cell mixture was then plated per microscopy slide well (25'000 T cells and tumor cells respectively). Cells were then incubated on the slide for 30min and then fixed with -20°C 100% Methanol for 5min. For LAMP1 and phalloidin stainings, cells were instead fixed for 20min at room temperature in 4% PFA (Electron Microscopy Services, diluted with PBS), extracted with 0.1% Triton-X100 in PBS for 5min and quenched with 50mM Glycine in PBS for 20min. Both fixation procedures were then followed by blocking in 1% 0.2 μm filtered bovine serum albumin (Sigma) in PBS (blocking buffer) for 15 min. Primary antibodies were then incubated in the same blocking buffer for 1h at room temperature or overnight at 4°C. Samples were then washed 4x times with blocking buffer, incubated for 2x 5min in blocking buffer, and then incubated for 1h with secondary antibody in blocking buffer at room temperature. Samples were washed again as above and incubated with 1:500 dilution of DAPI in blocking buffer for 5min. Samples were washed again and mounted with Vectashield

Vibrance mounting medium and Nr 1.5 coverslips and sealed with clear nail polish. Samples were stored at 4°C until acquisition.

Imaging

Images from immunofluorescence images were recorded on a Nikon Ti with a Yokogawa CSU-W2 spinning disk module on a Photometrics 95B (22mm back-illuminated sCMOS) camera. A Nikon CFI Apo TIRF NA 1.49 100x objective together with a 1.5x additional magnification unit was used with1.515 oil mounted samples. Diode-pumped solid-state lasers at 405, 488, 561, and 647nm were used together with filters for DAPI (ET460/50nm), AF488 (ET525/50nm), AF568 (ET630/75nm) and AF647 (ET700/75nm) with a Quad BS Dichroic mirror.

Raw nd2 format image stacks of 110x110x100nm were deconvoluted using Huygens using a theoretical point spread function classical maximum likelihood estimation using 100 iterations and a quality stop criterion of 0.01.

Deconvoluted images were visualized using Imaris 9 (Bitplane). Single slices or sections are shown with linear display adjustments (brightness). Images were exported by the snapshot function at 300dpi resolution.

Statistics and Data Visualization

The statistical analysis and graph preparation was performed using the software package Prism version 8.0a (GraphPad Software, La Jolla, CA). Functional data are representative of at least two experiments. Data is displayed as scatter dot plots where applicable and single points represent individual healthy donor replicates. Data were considered statistically significant with p values < 0.05. Normality tests were used to choose parametric or non-parametric tests. Data are shown as mean ± standard deviation with symbols representing individual patients or donors where applicable.

Data availability

Deposited Data	Source	Identifier
FASTQ and processed data for bulk RNA sequencing	This paper	Will be deposited upon submission
FASTQ and processed data for CRISPR-Screen gRNA sequencing	This paper	Will be deposited upon submission
Confocal Imaging Data	This paper	Will be deposited upon submission

2.3.4.   Results

Repetitive Antigen-specific Stimulation of T Cells with Tumor Cells Results in Dysfunction

Chronic stimulation of T cells in the tumor microenvironment is considered to be a significant cause of T cell dysfunction (Bucks et al., 2009; Mueller & Ahmed, 2009; Streeck et al., 2008; Utzschneider et al., 2016). To develop an *ex vivo* model for human T cell dysfunction, we transduced CD8 T cells with a viral construct to express a T cell receptor recognizing the aa157-165 peptide of the cancer-testis antigen NY-ESO-1 (Irving et al., 2012; Romero et al., 2001; Schmid et al., 2010). Next, we stimulated these TCR-transduced CD8 T cells with NY-ESO-1 peptides pulsed on irradiated HLA-A2+ T2 tumor cells (Figure 12a, Supplementary Figure 11a). We chose T2 tumor cells (also known as 174xCEM.T2) because they are TAP deficient and present only minimal amounts of endogenous peptides on their surface (Salter & Cresswell, 1986). Using T2 cells enabled us to better dissect the contribution of TCR dependent and independent effects on T cell functionality. To determine the impact of repetitive exposure to tumor antigens on T cell dysfunction, we performed this stimulation either once, twice, or four times ("repetitive") every three days at an effector to target (E:T) ratio of 1:3 (Supplementary Figure 11b). A high tumor load was chosen to induce serial triggering of T cells because high antigen loads are necessary to induce T cell dysfunction in murine LCMV models (Utzschneider et al., 2016). Controls included cells that only received medium and IL-2 ("rested") and cells that received only T2 tumor cells without peptides ("tumor only"). All replicates throughout this study represent individual healthy donor-derived T cells.

In contrast to a single or double antigen-specific stimulation, repetitive stimulation induced significant co-expression of PD-1, LAG-3, and TIM-3 on day 12 (Figure 12b, Supplementary Figure 11f). These repetitively stimulated T cells were also found to be CD28+ CD57- and thus do not resemble senescent T cells (Supplementary Figure 11g-h) (Brenchley et al., 2003). Importantly, repetitively stimulated T cells were highly impaired in their production of the effector cytokines IFNγ and TNFα upon antigen-specific re-stimulation (Figure 12c-d). Already the presence of T2 tumor cells without peptide led to a decrease in cytokine production, indicative of possible TCR independent effects. T2 tumor cells express low levels of PD-L1, both unstimulated and after the addition of IFNγ, implying these to be mostly PD-L1 independent effects (Supplementary Figure 11i). As reported for non-terminally dysfunctional murine TILs (Philip et al., 2017), repetitively NY-ESO-9V cells showed an increase in degranulation capacity after 18h of stimulation with IL-15 or IL-2 (Supplementary Figure 11j). Repetitively stimulated cells maintained their capacity to produce IFNγ in response to the Phorbol 12-Myristate 13-Acetate (PMA) plus ionomycin, whereas only minor differences in TNFα production could be observed (Supplementary Figure 11k-l). Thus, repetitive stimulation with tumor cells seems to induce a phenotype resembling tumor-infiltrating T cells on an expressional and functional level (Baitsch et al., 2011; D. S. Thommen et al., 2018; Zippelius et al., 2004).

We sought to confirm these results using two different NY-ESO-1 peptides (endogenous SLLMWITQC "NY-ESO-9C"; SLLMWITQV "NY-ESO-9V" with 4500-fold higher MHC affinity and 200-fold higher antigenic activity, Supplementary Figure 12a-b). Additionally, a control condition that was stimulated three days before the readout ("acute") was included to observe the differences between acute versus repetitive

stimulation. Both the acute and repetitive stimulation with both peptides resulted in the upregulation of PD-1, TIM-3, and LAG-3 (Figure 12e, Supplementary Figure 12c-d). Similarly, the capacity to degranulate was decreased by repetitive stimulation with either peptide (Figure 12f), whereas only NY-ESO-9V stimulation significantly decreased the co-production of IFNγ and TNFα compared to previously rested cells (Figure 12g). Despite their inhibitory receptor expression, acutely stimulated cells were highly functional (Figure 12f-g) and were superior in their capacity to secrete cytokines, degranulate and lyse tumor cells compared to repetitively stimulated cells (Figure 12e-h, Thesis comment: We will include the NY-ESO-9C and tumor only conditions in the next killing experiments). Also, TOX expression was highest in acutely stimulated cells, while after repetitive stimulation, only minor differences could be observed (Supplementary Figure 12f, Thesis comment: this will be replicated and quantified). Importantly, we observe similar effects of repetitive stimulation on T cell dysfunction when using the NA8-Mel melanoma cell line instead of T2 tumor cells (Supplementary Figure 13a-f). With this melanoma cell line, however, we observed significantly higher inhibitory receptor expression and decreased degranulation capacity only with the higher affinity NY-ESO-9V repetitive stimulation. Additionally, the expansion with these cells over 12 days of culture was smaller than with T2 tumor cells (Supplementary Figure 13g). Overall, repetitive stimulation leads to inhibitory receptor expression and impaired effector functions.
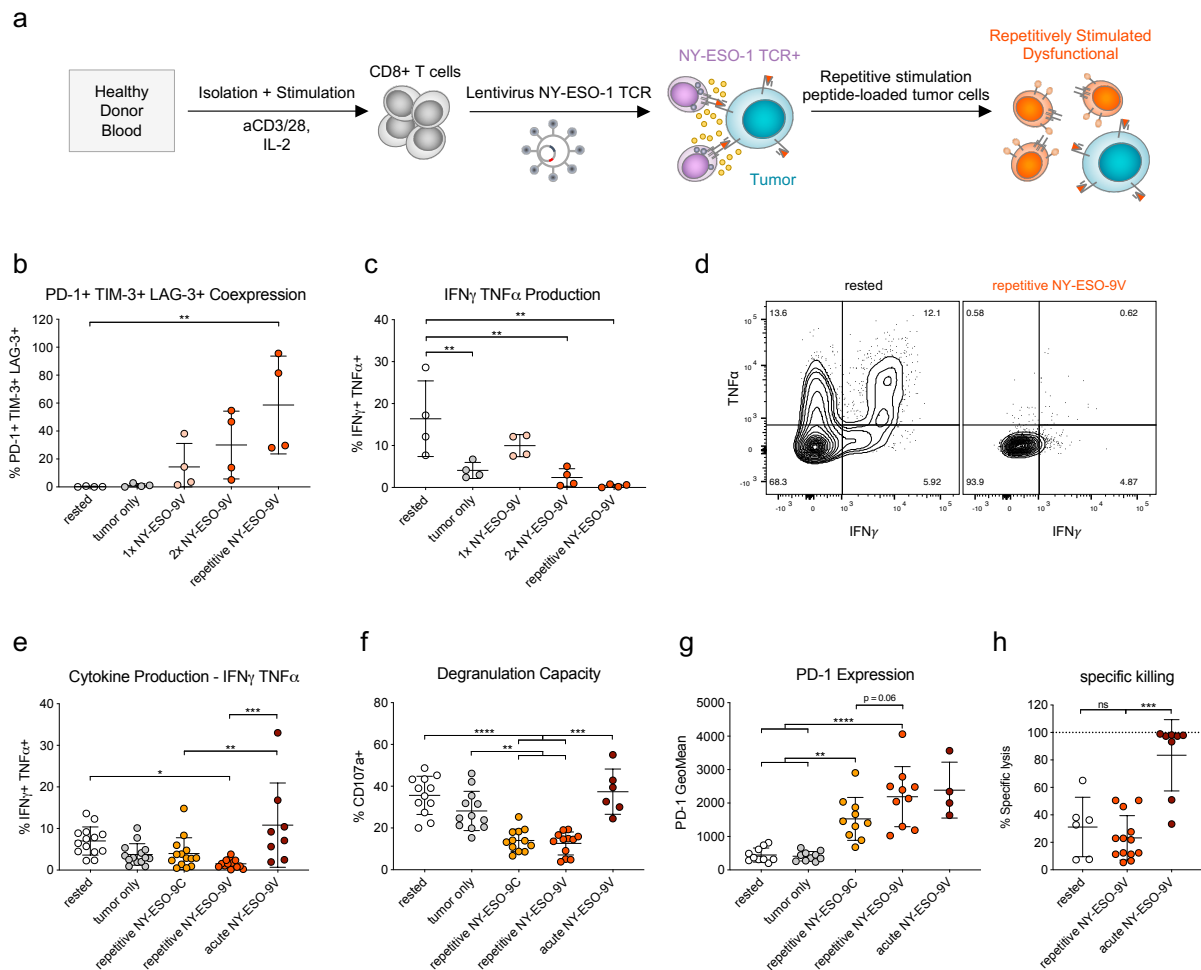
Figure 12 Repetitive Stimulation of CD8+ T Cells with Tumor Cells and Antigen Leads to Dysfunction

(a) Scheme representing the principle of the exhaustion model. A T2 tumor cell is shown in turquoise with peptide-loaded MHC molecules on its surface. (b) Co-Expression of PD-1, TIM-3, and LAG-3 measured by antibody staining and flow cytometry on day 12 after first stimulation. (c) & (e) Production of IFNγ and TNFα measured by intracellular cytokine staining and (f) degranulation measured by CD107a staining after re-stimulation of all cells after 13 days of culture in the indicated conditions. (d) Exemplary flow cytometry plot of the results in c. (g) PD-1 expression measured by flow cytometry after antibody staining on day 12 after first stimulation. (h) Specific lysis of T2-Luc+ tumor cells pulsed with 1 μM NY-ESO-9V peptide after 5 hours of co-incubation measured by luminescence intensity. 1-way ANOVA statistics with Holm-Sidak correction for multiple comparison, not all significant comparisons are shown, * p<0.05, ** p <0.01, *** p < 0.001, **** p < 0.0001. Dots represent individual healthy donor biological replicates and mean + SD is indicated.

Multiple studies connected T cell dysfunction with defective mitochondria and altered metabolic needs (Bengsch et al., 2016; Ho et al., 2015; Patsoukis et al., 2015; N. E. E. Scharping et al., 2016; Siska et al., 2017). Therefore, we next evaluated the changes in metabolism and mitochondria after repetitive stimulation (Thesis comment: should be replicated). We only measured higher glucose uptake for acutely stimulated but not for repetitively stimulated cells (Supplementary Figure 13a). Contrastingly, the uptake of lipids and the neutral lipid content was significantly higher in repetitively stimulated cells than in rested cells (Supplementary Figure 13i-j). Acutely activated cells also displayed a non-significant trend towards increased lipid uptake and lipid content but with higher variability. Furthermore, we sought to investigate mitochondrial mass by

mitotracker green staining, functional mitochondria by mitotracker deep red staining, and mitochondrial membrane potential (MMP) by the ratio between the two dyes. We detected a significant increase in mitochondrial mass only for acutely stimulated cells (Supplementary Figure 13k). On the other hand, co-culture with tumor cells alone and repetitive stimulation both induced a trend towards decreased content of functional mitochondria (Supplementary Figure 13l). Similarly, the MMP was reduced for tumor only and repetitive stimulation conditions (Supplementary Figure 13m). These experiments indicate that repetitive stimulation induces a shift towards fatty acid metabolism and a decrease in mitochondrial function.

Ex vivo *Generated Dysfunctional Cells Resemble Human Tumor-Infiltrating T Cells*

Next, we sought to investigate the transcriptional changes that are induced by repetitive stimulation. Therefore, we performed bulk RNA sequencing to compare rested, tumor only, and repetitively NY-ESO-9C and NY-ESO-9V stimulated T cells (Thesis comment: at the time, we did not sequence acutely stimulated cells due to cell restrictions, we will, however, get this information soon). Samples mainly clustered according to stimulation condition, but only minor differences between 9C and 9V repetitive stimulation were observed (Figure 13a, Supplementary Figure 14a-c). Already, the stimulation with tumor cells without peptides led to many differentially regulated genes (Supplementary Figure 14b). To compare our results, we compiled a list of published gene sets for dysfunctional T cells ranging from publications on murine LCMV, murine tumors, human hepatitis to human tumor patient gene sets, including single-cell sequencing datasets (Supplementary Table 13). Next, we performed gene set enrichments between our dysfunctional cells with these published gene sets (Figure 13b). We observed high enrichment (FDR < 10^{-7}, fold change > 2) for several gene sets of human TILs for repetitively stimulated T cells (Supplementary Table 14, Supplementary Figure 14c). For example, gene sets previously generated in our lab from PD-1^{high} lung cancer TILs (D. Thommen et al., 2018) showed high enrichment in the repetitive NY-ESO-9V stimulation condition (Figure 13b). Additionally, gene sets from dysfunctional CD8 T cells in hepatocellular carcinoma (Zheng et al., 2017), melanoma (Hanjie Li et al., 2018), and another lung cancer study (Guo et al., 2018) enriched in repetitively stimulated T cells.

When we compared enrichments within different subsets of intratumoral CD8 T cells in lung cancer (Guo et al., 2018), we observed that repetitively stimulated cells enrich positively within the dysfunctional C6_LAYN compartment, whereas the naïve C1_LEF and intermediate-effector C4_GZMK subsets were negatively enriched (Figure 13c). Repetitive NY-ESO-9V stimulation induced more enrichment than NY-ESO-9C in the C6_LAYN cluster. The effector C3_CX3CR1 and pre-exhaustion C5_ZNF683 clusters did not show significant enrichment in repetitively stimulated cells. Surprisingly, even tumor only stimulated cells showed positive enrichment in the C6_LAYN cluster. However, they also enriched in the C3_CX3CR1 and C4_GZMK effector clusters.

The same pattern is visible within melanoma-infiltrated CD8 T cells (Sade-Feldman et al., 2018), where repetitively stimulated T cells positively enrich for the 2_ExhaustionHeatshock and 3_Exhaustion clusters (Figure 13d). The higher enrichment in exhausted clusters was more pronounced with NY-ESO-9V than with NY-ESO-9C stimulation. Both repetitive stimulations similarly negatively enrich for the 6_MemoryEffector cluster (Figure 13d). Also, the transcriptional changes in repetitively stimulated T cells correlated more with the B_Exhaustion cluster, associated with

patients that did not respond to PD-1 blockade, than with the G_MemoryActivationSurvival cluster (Sade-Feldman et al., 2018). Again, the tumor only condition showed enrichment in the 3_Exhaustion and 2_ExhaustionHeatshock cluster. One possible explanation is that this 3_Exhaustion cluster represents an intermediate population between effectors and dysfunctional T cells because it significantly overlaps with the C4_GZMK and C3_CX3CR1 clusters of the Guo et al. data set (Supplementary Table 15). Besides, tumor only treated cells did not negatively enrich in the 6_MemoryEffector cluster, unlike the repetitively stimulated conditions. This indicates that stimulation with tumor cells without any antigenic peptide only partially induces a transcriptional phenotype associated with T cell dysfunction. Overall, these results confirm a high degree of similarity between our *ex vivo* generated dysfunctional T cells and patient-derived dysfunctional TILs.
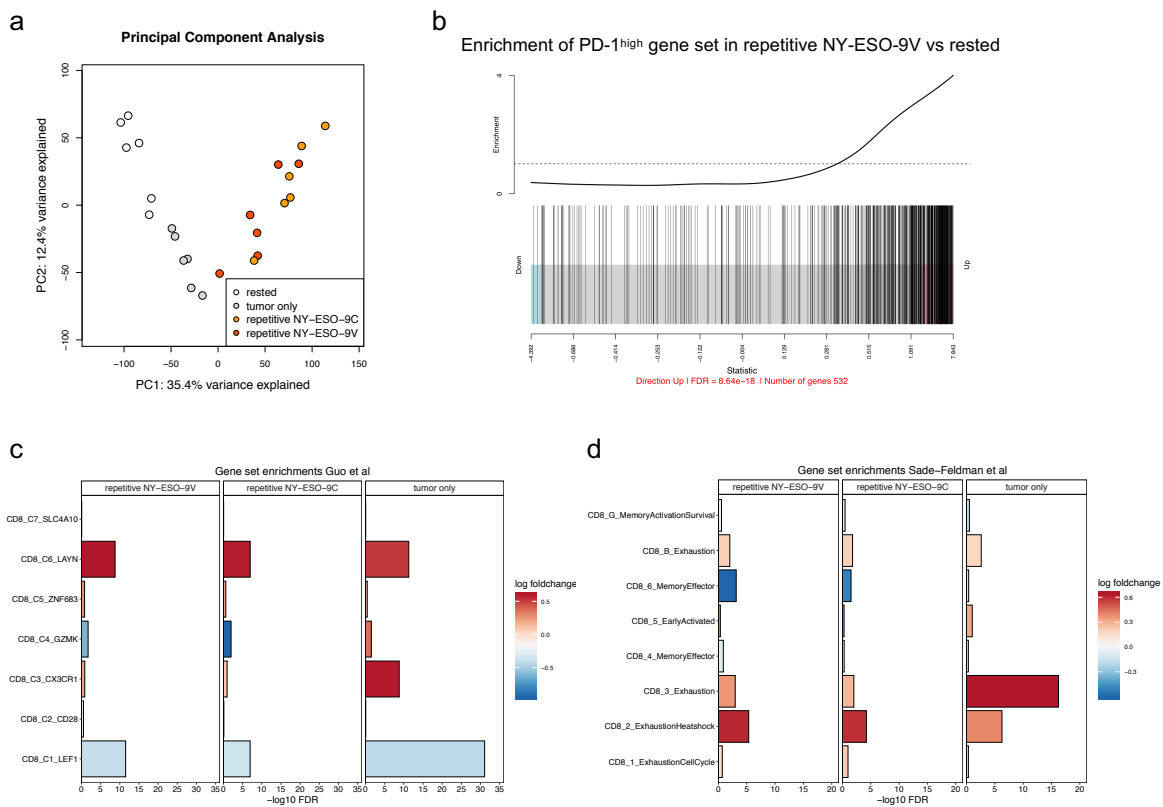

Figure 13 Transcriptomics Reveals Similarity to Patient-derived Tumor-infiltrating T Cells
(a) Principal component analysis of individual replicates (n = 6) for the four investigated conditions. Axis indicate components and percentage of variance explained by these. (b) Barcode plot of the gene set enrichment analysis performed with NY-ESO-9V repetitively stimulated cells and PD-1high vs. PD-1int cells in human lung cancer samples. Horizontal lines indicate the position along a z-score axis where genes within the PD-1high gene set were found. Genes to the right indicate enrichment towards the repetitively stimulated condition, also indicated by the line plot above. The direction, false discovery rate (FDR), and the number of genes are described below. (c) Gene set enrichment for scRNAseq data sets of lung cancer TILs by Guo et al. and in (d) with melanoma infiltrating TILs by Sade-Feldman et al. Conditions on the y-axis indicate the gene set whereas the x-axis indicates the -log10 false discovery rate of the enrichment analysis. The color gradient indicates the directionality and average fold change of the enrichment. The three panels per plot indicate the comparisons of the three conditions to the rested condition.

Repetitive Stimulation Leads to Loss of Expansion Potential and Mediates Sustained T Cell Dysfunction

Multiple studies describe that dysfunctional T cells generally show a loss of proliferation potential (Wherry & Kurachi, 2015). However, intratumoral dysfunctional PD-1^{high} T cells still express multiple markers of active cell cycling (D. Thommen et al., 2018). For these reasons, we pursued to determine the proliferative capacity of the repetitively stimulated cells. There was significant cell expansion during the four stimulation cycles, and a high proportion of cells expressed KI67 (Figure 14a, Supplementary Figure 15a). Next, we investigated the potential of these cells to proliferate over a six-day resting period in fresh medium with 50 U/ml IL-2. Moreover, a part of the cells was stimulated again with an additional cycle of NY-ESO-9V stimulation. Previously rested cells and tumor only-stimulated cells highly expanded with this stimulus, whereas repetitively stimulated cells decreased in cell numbers (Figure 14a). Cells stimulated with NA8-Mel cells instead of T2 cells showed higher cell numbers after re-stimulation, however this was only enough to approximately maintain cell numbers for repetitively NY-ESO-9V NA8-Mel stimulated cells (Supplementary Figure 15b). Despite their lack of cell expansion, repetitively stimulated cells showed signs of Cell Trace Violet label dilution, indicative of ongoing cell divisions (Supplementary Figure 15c-d). Repetitively NY-ESO-9V stimulated cells also retained higher expression levels of PD-1 during this resting period (Figure 14c, Supplementary Figure 15e; same effects for NA8-Mel stimulated cells: Supplementary Figure 15f). Next, we observed that NY-ESO-9C repetitively stimulated cells re-gained their degranulation capacity when rested for seven days (Figure 14d). Contrastingly, repetitively NY-ESO-9V stimulated cells maintained low levels of functionality (Figure 14d) implying a more stable dysfunctional phenotype.

To better distinguish the effects of peptide affinity versus concentration, we titrated the amounts of both NY-ESO-9C and NY-ESO-9V peptides in four cycles of repetitive stimulation. The expression levels of the inhibitory receptors PD-1 and LAG-3 were significantly dependent on peptide concentration and affinity (Figure 14e, Supplementary Figure 16a-b). Degranulation capacity was affected by both peptide affinity and concentration (Figure 14f), while IFNγ and TNFα production was almost absent even with low concentrations of NY-ESO-9C repetitive stimulation (Supplementary Figure 16c-d). With higher concentrations of the peptides, the frequency of cells expressing the stemness-associated transcription factor TCF7 decreased, while the percentage of TBET+ cells increased (Figure 14g, Supplementary Figure 16e-f). Overall, these results led us to the assumption that repetitive stimulation with NY-ESO-9V peptide-loaded tumor cells leads to a more stable dysfunctional phenotype.
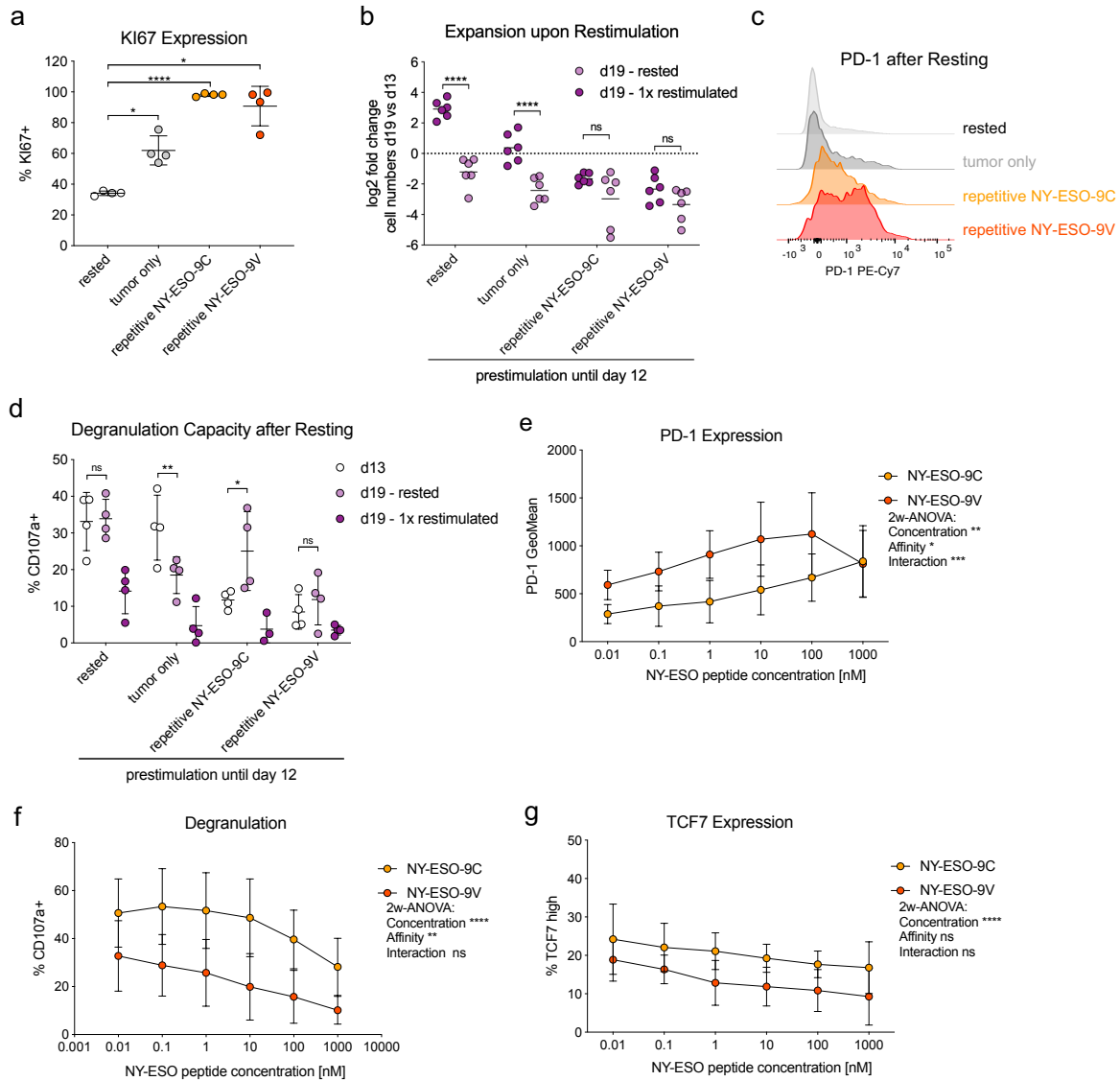
Figure 14 Stability of T Cell Dysfunction and TItration of Peptide Concentration

(a) Percentage of cells expressing KI67 on day 12 after the first stimulation measured by intra-nuclear antibody staining and flow cytometry. 1-way ANOVA statistics with Holm-Sidak correction for multiple comparisons. (b) Fold change of cell numbers during the six-day resting with or without an additional re-stimulation with T2 and NY-ESO-9V started on day 13. Measured by flow cytometry using counting beads. (c) An exemplary plot of PD-1 expression after six days of resting after 12 days of culture in the indicated conditions. Counts were normalized according to mode. (d) Degranulation capacity measured by CD107a exposure upon re-stimulation with T2 tumor cells pulsed with NY-ESO-9V. Measurements were performed before and after six days of resting. (a-d) 2-way ANOVA with Holm-Sidak correction. Dots represent individual healthy donor biological replicates and mean + SD is indicated. (e) PD-1 expression, (f) degranulation capacity upon re-stimulation and (g) TCF7 expression after repetitive stimulations with T2 tumor cells and the indicated antigen-dose and type. (e-g) 2-way ANOVA with Holm-Sidak correction, mean + SD is shown. The significance of concentration, affinity, and the interaction term are indicated.

A Targeted CRISPR-Cas9 Screen Reveals Genes with Potential Functions in T Cell Dysfunction

Next, we sought to test the potential of our model system to investigate uncharacterized genes associated with T cell dysfunction. To prioritize genes for further investigations, we generated gene clusters from the RNAseq data by pairwise comparison representing three categories of transcriptional changes (Figure 15a). These clusters represent transcriptional changes specific to NY-ESO-9V repetitive stimulation (High Affinity), changes associated with repetitive stimulation indiscriminate of peptide affinity (Repetitive Stimulation), and genes already regulated by the presence of tumor cells without antigen (Tumor Co-Culture). Within each list, we ranked genes according to their overlap with published patient TIL datasets available at the time, and we required at least one overlap with genes from our PD-1^{high} NSCLC TIL gene set (Supplementary Table 16) (D. Thommen et al., 2018). From the top 20 selected genes per cluster, we focused our analysis on genes with more than two counts per million reads after repetitive NY-ESO-9V stimulation and at least two-fold upregulation compared to rested cells. Of this list of genes, we further only selected those that were not previously studied in T cell dysfunction (for example, excluding HAVCR2 encoding TIM-3). Through this prioritization, we selected the 25 genes shown in Figure 15b (Supplementary Figure 17a).

To investigate these genes, we decided to perform a targeted pooled CRISPR-Cas9 screen in our primary human CD8+ T cells. To this aim, we chose five guides per gene in addition to 20 guides targeting intergenic regions as controls. Additionally, we included the negative control genes LAT, LAMP1 (= CD107a), and ZAP70, of which a genetic KO should lead to dysfunctionality (Shifrut et al., 2018). In addition some genes with described regulatory functions in T cells were included DUSP4 (C.-Y. Huang et al., 2012), SPRY1 (Collins et al., 2012), PTPN22 (Maine, Teijaro, Marquardt, & Sherman, 2016) and ENTPD1 (Takenaka, Robson, & Quintana, 2016; Yost et al., 2019). Briefly, we transduced primary human CD8+ T cells with the NY-ESO-1 T cell receptor construct and with a pooled library of LentiCRISPRv2-mCherry (LCv2) lentivirus that encodes the gRNAs and Cas9. (Figure 15c). As recently described (Shifrut et al., 2018), the co-transduction efficiency of the LCv2 library in human T cells was low at 0.57% and 0.99%, for the two biological replicates, which hindered the use of a whole-genome CRISPR-Cas9-gRNA library. Next, we sorted cells that expressed both the TCR and KO construct and repetitively stimulated these with NY-ESO-9V peptide. Then, cells were re-stimulated with tumor cells and NY-ESO-9V and sorted based on their degranulation capacity measured by CD107a staining (Figure 15c).

The genomic DNA-based guide sequencing revealed that we maintained all gRNAs in all conditions and that the guide distribution changed after sorting for functional cells (Gini coefficient: input d0 "control" = 0.24, d12 "CD107a positive" = 0.28, Supplementary Figure 17b). The multi-dimensional scaling plot shows that samples cluster according to functionality, however, with substantial inter-donor variability (Figure 15d). Guides leading to genetic knock-out (KO) of the negative controls were significantly enriched in the CD107a negative (dysfunctional) fraction as expected (Figure 15e, Supplementary Figure 17c). Next, we calculated the mean fold change per gene and ranked genes according to the enrichment of their guides in the functional fraction (Figure 15e, Supplementary Figure 17c-d). The genes with the highest negative enrichment were the three negative controls (LAT, LAMP1, and ZAP70), while intergenic controls had an average fold change near zero. DUSP4 showed a trend towards positive enrichment in d12 vs. d0 input samples irrespective of functionality.

94

This indicates a role for DUSP4 in the regulation of cell expansion, which had been reported for CD4 and CD8 T cells (C.-Y. Huang et al., 2012; Shifrut et al., 2018) validating our screen results. Guides for ENTPD1 (CD39) showed no enrichment in either fraction. Several candidate genes including SLC29A2, SNX9, SERPINE1, GEM, FAM3C, PHEX, and SRGAP3, showed a non-significant trend towards positive enrichment (Supplementary Figure 17d). None of these genes had been associated with changes in T proliferation capacity by Shifrut and colleagues (Shifrut et al., 2018). Overall, despite its high variability, the targeted CRISPR-Cas9 screen enabled us to narrow down gene candidates involved in T cell dysfunction. (Thesis Comment: We will replicate this screen with at least three more donors).
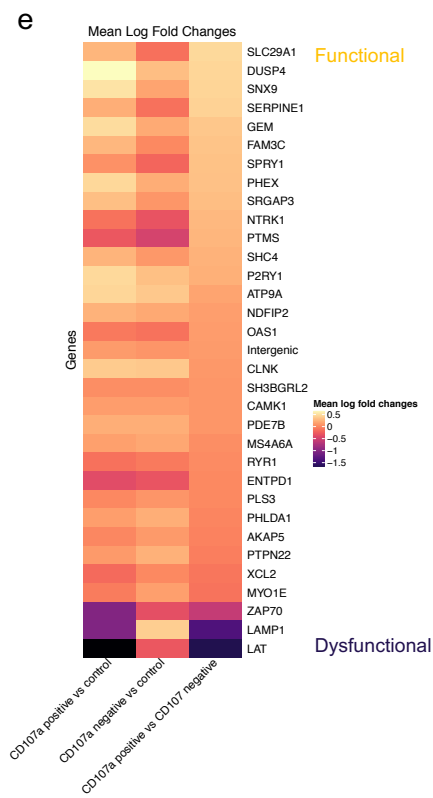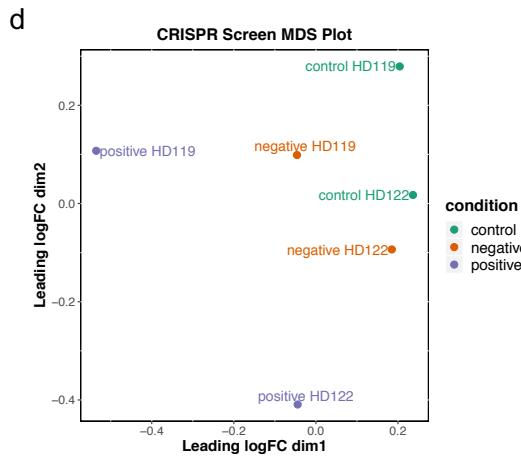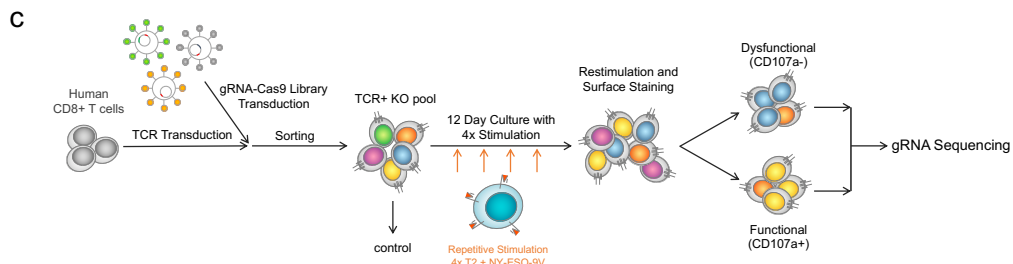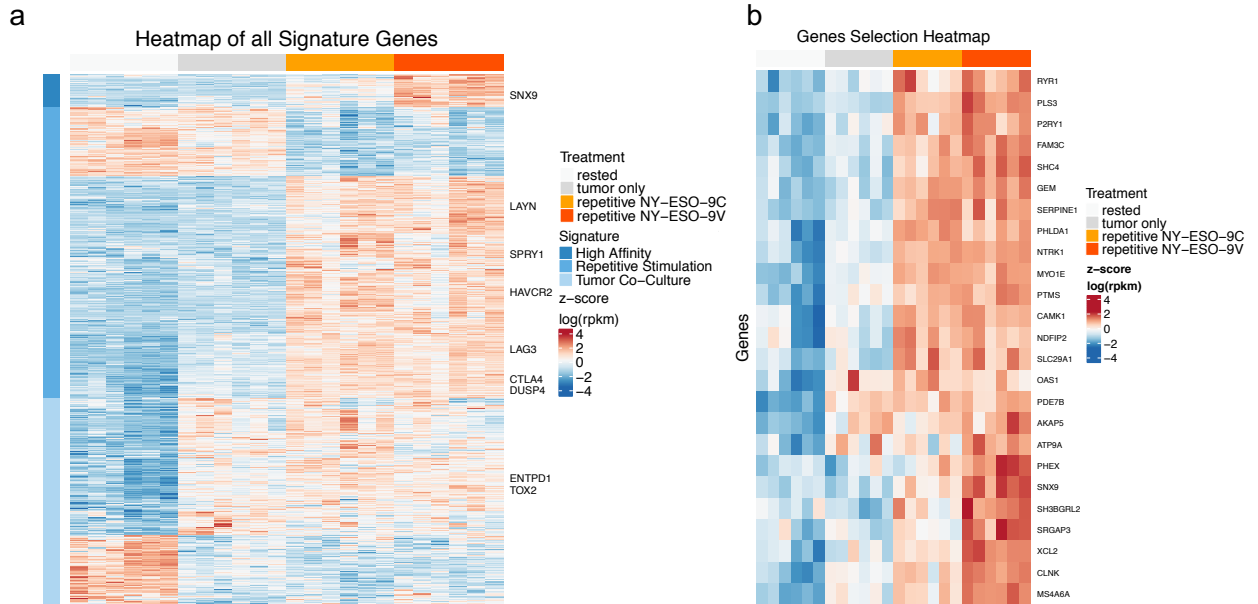
a
Heatmap of all Signature Genes

b
Genes Selection Heatmap

c

d
CRISPR Screen MDS Plot

e
Mean Log Fold Changes

(a) Heatmap of expression values of genes in the clusters «High Affinity», «Repetitive Stimulation» and «Tumor Co-Culture». The heatmap displays z-score scaled log(rpkm) values in a red-white-blue color gradient. We indicated selected genes known to be involved in T cell exhaustion and SNX9. (b) Heatmap of the expression of selected gene targets to follow-up in a targeted CRISPR screen. Gene names are indicated to the right of the plot. (c) Schematic description of the targeted-pooled CRISPR-Cas9 KO screen. (d) A multi-dimensional scaling plot done using edgeR and ggplot2 to visualize overall changes in guide counts. The axes denote leading log fold change dimensions of n = 2 donor replicates ("HD119" and "HD122"). "positive" indicates CD107a+ functional cells, "negative" CD107a- dysfunctional fraction, (e) Mean log fold changes of each gene (rows, averaging guides and donors) for the three comparisons (columns). Genes are ranked according to mean fold change between the CD107a+ functional and CD107a- dysfunctional fractions.

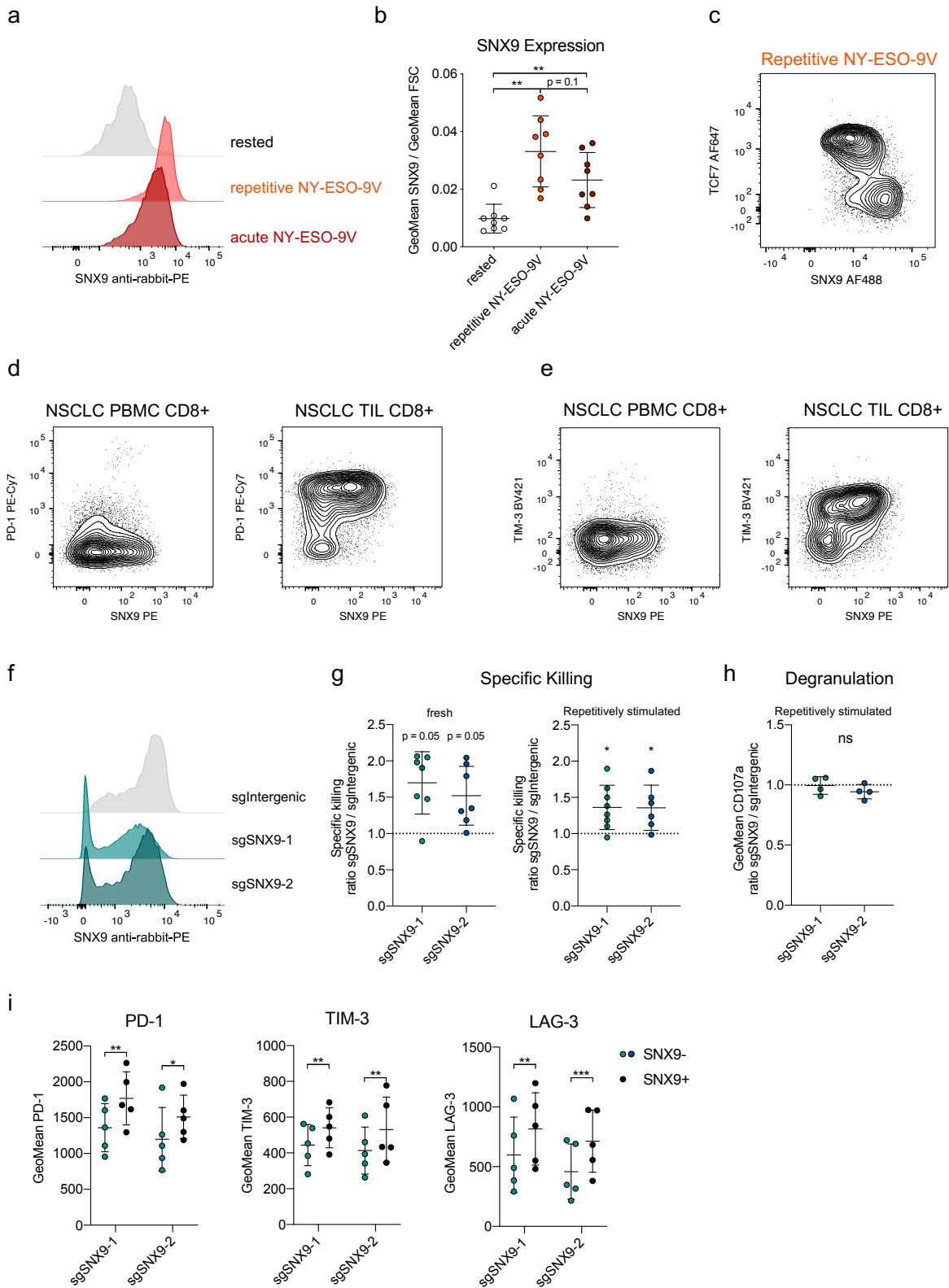## Upregulation of SNX9 Contributes to T Cell Dysfunction

The ranked list of genes from the CRISPR-Cas9 screen provided us with several interesting genes to pursue. For this study, we decided to study the scaffold protein SNX9 because it had the most overlaps with published gene sets for T cell dysfunction (Supplementary Figure 17a). Indeed, SNX9 expression was associated with dysfunctional TILs in lung cancer (Guo et al., 2018; D. Thommen et al., 2018), hepatocellular carcinoma (Zheng et al., 2017), melanoma (Baitsch et al., 2011; Tirosh et al., 2016), basal cell carcinoma (Yost et al., 2019) and early dysfunctional murine TILs (Schietinger et al., 2016). Expression levels of SNX9 on a transcriptional level were highest in NY-ESO-9V repetitively stimulated T cells (Supplementary Figure 18a). Other studies reported partially redundant roles for SNX18, which was, however, expressed at lower levels and was not upregulated by repetitive stimulation (Supplementary Figure 18a). On the other hand, repetitive NY-ESO-9V stimulation induced expression of the less characterized family member SNX33 but at lower expression levels (Supplementary Figure 18a). On a protein level, both repetitively and acutely stimulated T cells increased their staining for SNX9 (Figure 16a-b, Supplementary Figure 18b). However, when normalizing for forward scatter area as a surrogate for cell size, there was a non-significant trend for higher normalized SNX9 density in repetitively stimulated cells (Figure 16b).

Interestingly, SNX9 expression was higher in the TCF7- compartment of repetitively stimulated cells (Figure 16c, Thesis comment: will be replicated and quantified). Next, we investigated the expression of SNX9 in human patient TILs and observed expression of SNX9 mainly on PD-1+ and TIM-3+ cells, whereas there was lower staining on peripheral blood CD8 T cells (Figure 16d-e, Thesis comment: will be validated and quantified). When we reanalyzed recently published single-cell ATACseq data of TILs in basal cell carcinoma, we found an open chromatin region (OCR) within the *SNX9* gene locus that is specific to intermediate and late dysfunctional cells, T follicular helper cells (T_{fh}) and T regulatory cells (T_{reg}), which are known to share some transcriptional regulation (Supplementary Figure 18d) (Satpathy et al., 2019). Accordingly, this study detected lower chromatin accessibility approximately +7 kbp downstream of the transcriptional start site (TSS) in naïve, memory, or early-dysfunctional T cells, which indicates some state-specific chromatin regulation.

To determine the role of SNX9 in T cell functionality, we adapted a Cas9-ribonucleoprotein (RNP) electroporation-based KO protocol (Shifrut et al., 2018). With this approach, we achieved SNX9 KO on protein level in approximately 20 to 40% of cells using two independent guides (sgSNX9-1 designed by T. Wang et al., 2017 and sgSNX9-2 by IDT) (Figure 16e, Supplementary Figure 18c). Despite the incomplete KO, the unsorted sgSNX9-1 and sgSNX9-2 cell populations showed a non-significant trend towards increased killing capacity (Figure 16, Thesis comment: more replicates will follow). We observed a significant increase in killing capacity when we then assessed these cells after repetitive stimulation (Figure 16f). We could not observe a significant effect on degranulation capacity on the bulk population (Figure 16g, (Thesis comment: Having an SNX9 antibody, we will replicate this and gate on SNX9 KO). SNX9 KO cells also showed lower levels of PD-1, TIM-3, and LAG-3 after repetitive stimulation (Figure 16h) compared to unedited cells. In summary, dysfunctional T cells, including PD-1+ TILs, express SNX9, and its genetic ablation in the *ex vivo* model led to improved tumor cell killing and lower inhibitory receptor expression.

Figure 16 Correlating SNX9 Expression with Markers of Exhaustion and Functionality

(a) Exemplary flow cytometry plots of (b) showing SNX9 expression measured by antibody staining. Expression in (b) was normalized to mean forward scatter (FSC) area signal to approximate cell size. (c) Exemplary flow cytometry plot showing expression of TCF7 and SNX9 in NY-ESO-9V stimulated cells on day 12 after first stimulation. (d) Exemplary flow cytometry plots of SNX9 expression vs. PD-1 and (e) TIM-3 expression in CD8+ T cells of non-small cell lung cancer (NSCLC) patient's PBMCS (left) and tumor-infiltrating cells (right). (f) Expression of SNX9 in NY-ESO-9V repetitively stimulated cells 12 days after the first stimulation with or without Cas9-RNP mediated KO six days before the first stimulation. Specific killing capacity ratio (g) or degranulation (h) of cells transduced six days before ("fresh") or NY-ESO-9V repetitively stimulated cells on day 13 after first stimulation. The ratio of killing between cells electroporated with a crRNA against an intergenic region versus crRNAs targeting two different sites in SNX9 exons. We performed a paired 1-way ANOVA on non-normalized data with Holm-Sidak correction and indicated the significance in a plot showing the normalized data. (i) Expression of PD-1, TIM-3, and LAG-3 after NY-ESO-9V repetitive stimulation measured by flow cytometry gated on either SNX9-KO or SNX9+ cells. Paired 2-way ANOVA with Holm-Sidak correction.

a

rested

repetitive NY-ESO-9V

acute NY-ESO-9V

SNX9 anti-rabbit-PE

b

SNX9 Expression

Sample Name	Subset Name	Count
HD127 nonelectro d12_0x_029.fcs	Vbeta13.1+	3126
HD127 nonelectro d12_4xV_027.fcs	Vbeta13.1+	10423
HD127 nonelectro d12_1xV d9_028.fcs	Vbeta13.1+	15074

GeoMean SNX9 / GeoMean FSC

** p = 0.1
**

rested
repetitive NY-ESO-9V
acute NY-ESO-9V

c

Repetitive NY-ESO-9V

TCF7 AF647

d

NSCLC PBMC CD8+   NSCLC TIL CD8+

PD-1 PE-Cy7

SNX9 PE

e

NSCLC PBMC CD8+   NSCLC TIL CD8+

TIM-3 BV421

SNX9 PE

f

sgIntergenic

sgSNX9-1

sgSNX9-2

SNX9 anti-rabbit-PE

g

Specific Killing

fresh

Subset Name	Count
HD127 4xV d12	Vbeta13.1+ 5246
HD127 4xV d12	Vbeta13.1+ 12144
HD127 4xV d12	Vbeta13.1+ 8085

Specific killing ratio sgSNX9 / sgIntergenic

p = 0.05   p = 0.05

sgSNX9-1   sgSNX9-2

Repetitively stimulated

Specific killing ratio sgSNX9 / sgIntergenic

*   *

sgSNX9-1   sgSNX9-2

h

Degranulation

Repetitively stimulated

GeoMean CD107a ratio sgSNX9 / sgIntergenic

ns

sgSNX9-1   sgSNX9-2

i

PD-1

GeoMean PD-1

**   *

sgSNX9-1   sgSNX9-2

TIM-3

GeoMean TIM-3

**   **

sgSNX9-1   sgSNX9-2

LAG-3

GeoMean LAG-3

**   ***

sgSNX9-1   sgSNX9-2

SNX9-
SNX9+

99

SNX9 Colocalizes to the Immune Synapse

To investigate how SNX9 negatively regulates T cell-mediated tumor killing, we stained SNX9 in repetitively stimulated cells by immunofluorescence. Deconvoluted spinning disk confocal images show that SNX9 accumulates at the T cell – tumor cell synapse (Figure 17a, Supplementary Figure 19a-b). T cells exhibiting polarized LAMP1+ granules showed a clustered localization of SNX9 protein at the interface between the T cell and the tumor cell (Figure 17b). SNX9 has been shown to bind N-WASP and trigger Arp2/3 dependent polymerization of actin filaments (Yarar, Waterman-Storer, & Schmid, 2007). Therefore, we co-stained T cell tumor interactions with F-actin by phalloidin and observed some colocalization of SNX9 around cortical actin (Figure 17c-d, white color). However, we detected most of the SNX9 signal in the core of the cell-cell interface (Figure 17d *en face* view). These results warrant further investigation into the role of SNX9 into possible modulations of the immune synapse (Thesis comment: we will systematically quantify this).
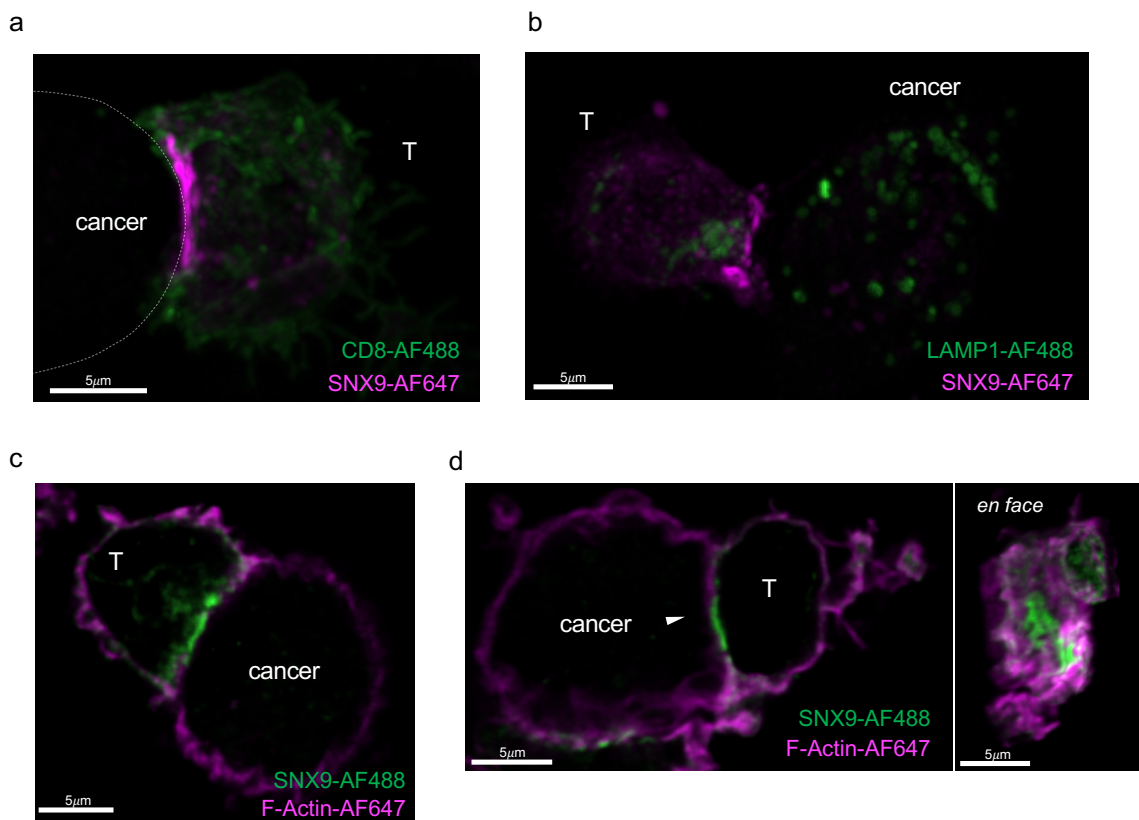
Figure 17 SNX9 Localizes to the Immunological Synapse

Spinning disk confocal images acquired on a 150x CSU-W1 Nikon using a Photometrics camera. 110x110x100 (x, y, z in nm) stacks were deconvoluted using Huygens Deconvolution. NY-ESO-9V repetitively stimulated cells on day 13 after were co-incubated with NY-ESO-9V peptide-pulsed T2 cells for 30 min in serum-free medium. (a) 3D slice representation rendered using IMARIS of a T cell ("T") in contact with a T2 cancer cell ("cancer", indicated by a dotted white line, based on brightfield image) fixed in Methanol. CD8 (in AF488 in green) and SNX9 (AF647 in magenta, SNX9-1 'shrek' antibody batch) were stained with primary and secondary antibodies. (b) 3D representation was done using IMARIS of a T cell - cancer cell conjugate stained with SNX9 in AF647 and LAMP1 = CD107a in AF488. (c) and (d) are single z-stack slices of a T cell contacting a cancer cell with F-actin stained by phalloidin-AF647 and SNX9 in AF488. In (d), an additional 3D representation of the contact site is shown "en face" (cut across in the z dimension) looking from the cancer cell side. Colocalization of green and magenta appears in white color.

2.3.5. Discussion

Models for T Cell Dysfunction

T cell exhaustion has been extensively studied in murine models of chronic viral infections (Wherry & Kurachi, 2015). Nevertheless, mice and humans have remarkable differences in their immune responses (Mestas & Hughes, 2004; Shay et al., 2013) and cancer development (Rangarajan & Weinberg, 2003). Additionally, murine models require special laboratory facilities, trained personnel, and are troubled by ethical and regulatory constraints. Scalable human *ex vivo* systems are essential for drug discovery and simplify small molecule or antibody development in the frequent case of non-conserved targets. Recently, the advent of single-cell technologies has re-shaped our understanding of the tumor-infiltrating immune compartment in human patients and discovered differences compared to murine models (Azizi et al., 2018; Gubin et al., 2018; Guo et al., 2018; Sade-Feldman et al., 2018; Savas et al., 2018; Tirosh et al., 2016; Zheng et al., 2017). For example, the B-cell-recruiting chemokine CXCL13 and the surface receptor Layilin (LAYN) are prominently expressed by CD8 and CD4 T cells in human tumors (De Simone et al., 2016; Guo et al., 2018; Hanjie Li et al., 2018; D. Thommen et al., 2018; Workel et al., 2019; Zheng et al., 2017), but had not been reported in murine models.

Yet, model systems to investigate human dysfunctional T cells and their interaction partners are lacking. Simple *ex vivo* models were suggested to induce a dysfunctional T cell phenotype by continuous anti-CD3/anti-CD28-coated bead stimulation. These models, however, neglect many vital aspects of cancer infiltrating T cells such as cell-cell interactions, inhibitory receptor signaling, and metabolic restrictions imposed by cancer cells (McKinney, Lee, Jayne, Lyons, & Smith, 2015). A model developed by Chiu et al. to mimic the loss of polyfunctionality in HIV-specific T cells shows that high antigen doses presented by dendritic cells (DCs) are capable of inducing dysfunctionality in cytokine secretion (Chiu et al., 2014). Interestingly, their DC-based model does not lead to a decrease in degranulation and killing capacity.

Apart from reductionist approaches, relying on healthy donor cells and cell lines only, complex models of the tumor microenvironment have been developed using patient-derived organoids and immune cells in an air-liquid interface (Neal et al., 2018) or embedded in 3D microfluidic devices (Jenkins, Aref, et al., 2018). Such personalized models hold great promise to understand complex cell-cell interactions, test multiple therapeutics simultaneously and can be used to expand tumor-specific T cells for adoptive therapies (Dijkstra et al., 2018). These models can capture important interactions between different cell types such as DCs and T cells. Nevertheless, these systems require a supply of patient tumors, complex and expensive growth media supplements, long culturing times, and suffer from heterogeneity and limited infiltration. These requirements hamper the use of high-throughput technologies such as CRISPR-Cas9 screens and extensive drug screening.

I here propose a model system that purely relies on healthy donor T cells in combination with tumor cell lines and thereby enables the generation of millions of dysfunctional T cells with high flexibility. Besides, both T cells and perspectively tumor cells can be modified to knock-out or overexpress receptor-ligand pairs. In patient-based models, the pathways that have led to the establishment of specific immune cell phenotypes cannot be easily reverse-engineered. In contrast, our model enables us to investigate the establishment of dysfunction over time. On the other hand, our model

bears other limitations, for example, the lack of an intact tumor microenvironment, including helper and regulatory immune cells. A way to tackle this limitation could be to combine the benefits of both systems and build an artificial 3D tumor microenvironment based on heterogeneous cancer (organoid) cultures, extracellular matrix scaffolds, and exogenously added immune cells. Repetitively stimulated T cells could be generated in such a system or added to established structures to observe their integration into the tumor microenvironment. Although still artificial, such models could enable spatiotemporal tracking of differently labeled immune populations and still enable larger screens. We believe that future studies will utilize reductionist approaches dissecting the molecular mechanisms in combination with complex patient-based co-culture systems that more closely represent the *in vivo* situation to better understand immune responses against cancer.

Mechanisms Leading to T Cell Dysfunction

T cell dysfunction is associated with a gradual loss of effector functions under chronic stimulation in an inflammatory environment. Nonetheless, it is related to other states of T cell hypofunctionality such as peripheral tolerance and senescence. Although senescent T cells can occur in the tumor microenvironment, the majority of dysfunctional T cells do not show the hallmarks of senescence such as CD57 and KLRG1 expression (Angelosanto, Blackburn, Crawford, & Wherry, 2012; Crespo, Sun, Welling, Tian, & Zou, 2013; Wherry & Kurachi, 2015). Accordingly, we noted that *ex vivo* repetitively stimulated cells did not express CD57 and remained CD27 positive. Peripheral tolerance (sometimes referred to as peripheral anergy) and clonal anergy has been mostly studied in CD4 T cells and can be induced by antigen recognition in a tolerogenic environment with insufficient co-stimulation (Schietinger & Greenberg, 2014; Schwartz, 2003). Peripheral tolerance shares some functional and phenotypical traits with dysfunctionality, such as reduced production of cytokines and proliferation, and probably plays a role in early tumorigenesis (Kim & Ahmed, 2010). Nevertheless, melanoma-specific TILs do not express many of the described markers for peripheral tolerance and anergy (Baitsch et al., 2011).

During the lentiviral transduction with the TCR construct, we stimulate the cells with anti-CD3/anti-CD28 stimulation beads in the presence of IL-2, which should provide the cells with sufficient co-stimulation. In agreement, when we exposed these transduced cells to an acute stimulation with T2 cells and antigen, the cells show high expansion and functional capacity. Thus, it is unlikely that insufficient priming is the cause of hypofunctionality in our model. Interestingly, T2 cells express the co-stimulatory molecules CD80 and CD86, which influences the amount of co-stimulation the T cells receive. We do not fully understand how this affects the establishment of T cell dysfunction in our model, but we assume that the presence of some co-stimulatory molecules resembles the situation in inflamed tumors. Interestingly, activated T cells themselves, including our repetitively stimulated cells, express elevated levels of CD80 and CD86, which was shown to dampen T cell functionality via CTLA-4 (Taylor et al., 2004). We observe comparable induction of dysfunction and inhibitory receptor expression when we used the CD80$^-$ CD86$^-$ NA8-Mel cell line instead of T2 tumor cells. Thus, co-stimulation with CD80 and CD86 *in trans* does not seem to be essential during repetitive stimulation after efficient priming.

We used total CD8+ T cells for our lentiviral transduction, and therefore, our starting material contained both naïve and antigen-experienced T cell populations. It would be of interest to compare whether naïve and antigen-experienced populations respond differently to repetitive stimulation with or without co-stimulation. In murine infections, memory T cells are either able to clear subsequent chronic infections or experience clonal deletion (Angelosanto et al., 2012; Wherry, 2011). Naïve cells, but also effector and early-memory cells, on the other hand, are susceptible to dysfunction in mice (Angelosanto et al., 2012). Therefore, I would assume that human memory cells do not become as dysfunctional as naïve cells because of their epigenetically imprinted functional state (Henning, Roychoudhuri, & Restifo, 2018). However, we chose to use total CD8 T cells as this is a more accessible source of cells. This might even represent a more physiological situation, during which multiple clones respond to a tumor and not all undergo the same extent of exhaustion.

The induction of T cell dysfunction involves a gradual loss of effector function and epigenetic imprinting (Blank et al., 2019; C. Wang, Singer, & Anderson, 2017; Wherry & Kurachi, 2015). In chronic murine viral infections, the expression of inhibitory receptors such as PD-1 is rapidly induced and reaches a stable plateau approximately after 20 days (Wherry et al., 2007). This dysfunctional phenotype of CD8 T cells is still reversible eight days after infection but became stable 15 days after infection (Angelosanto et al., 2012). It appears that the induction of T cell dysfunction in murine tumors also occurs in the first eight days and becomes stably imprinted between 12 to 30 days post tumor challenge (Philip et al., 2017; Schietinger et al., 2016). In our *ex vivo* model, we observe a relatively stable induction of T cell dysfunction 12 days after the first stimulation with tumor cells, and this was dependent on the strength of TCR triggering. Nevertheless, we observed that IL-2 and IL-15 stimulation could partially reinvigorate these repetitively stimulated cells, unlike what was reported for terminally dysfunctional T cells (Philip et al., 2017). We believe this potential of functional reinvigoration is beneficial for the model, as it enables us to screen for genetic or pharmacological ways to relieve exhaustion before the cells are irreversibly differentiated. Lately, several groups described a prominent role for a TCF7+ stem-like population within dysfunctional T cells with higher reinvigoration potential (Kurtulus et al., 2018; B. C. Miller et al., 2019; Sade-Feldman et al., 2018). In our model, we find a remaining TCF7+ population in repetitively stimulated cells, but its frequency is reduced with increasing doses of antigen-specific stimulation. It remains to be investigated whether these remaining TCF7+ cells in our model also retain more functional and proliferative capacity.

TCR-independent Effects and Metabolism

Already the co-culture with tumor cells led to many transcriptional changes associated with TILs. This highlights that tumor co-culture is an important factor in our model, although it remains to be investigated by which mechanisms. As T2 cells are TAP deficient, they present very little antigens to which an allogeneic response could be triggered by T cells (Salter & Cresswell, 1986). The absence of inhibitory receptor expression by T cells that only received tumor cells without antigen supports the hypothesis that these effects are mainly TCR-independent. In contrast, the tumor cells could induce an altered metabolic environment in our culture system. Importantly, metabolic competition is a critical limiting factor for anti-tumor immune responses (Chang et al., 2015; Delgoffe & Powell, 2015). For example, the insufficiency of the metabolic product phosphoenolpyruvate caused by the depletion of glucose in the tumor microenvironment can drive T cell dysfunction through decreased Ca^{2+}-NFAT

signaling (Ho et al., 2015). Similarly, hypoxia diminishes the response to PD-1 blockade, which can be rescued by metformin (N. E. Scharping et al., 2017). T cell dysfunction in tumors is also linked to a loss in mitochondrial functions, and this could be rescued by overexpression of PPAR-gamma coactivator 1α (PGC1α) in murine models (Bengsch et al., 2016; N. E. E. Scharping et al., 2016). Interestingly, both studies implicate chronic TCR signals in the establishment of mitochondrial dysfunction but disagreed on the contribution of PD-1 signaling in this mechanism.

Our preliminary results indicate that repetitive stimulation *ex vivo* induces higher lipid metabolism and content, whereas functional mitochondria are decreased. This is in agreement with our previous study, in which NSCLC TILs with high PD-1 expression exhibited higher lipid content and uptake and displayed a lower mitochondrial membrane potential (D. Thommen et al., 2018). Our model does not seem to replicate the minor but significant increase in mitochondrial mass detected in NSCLC PD-1^{high} TILs. A higher mitochondrial mass was, however, seen in acutely activated T cells. Remarkably, there were already significant differences in lipid uptake and mitochondrial membrane potential with the co-culture of tumor cells alone without peptide, which could be caused by TCR-independent effects on metabolic reprogramming. It is likely that the T2 cells, which we used to stimulate the T cells, cause glucose deprivation and lactate accumulation, which is indicated by substantial medium discoloration. However, we have not investigated the contribution of metabolic insufficiency to dysfunctionality in our model. (Thesis comment, a ^{13}C-Glucose tracing experiment comparing acute vs. repetitively stimulated cells is ongoing). The contribution of local hypoxia might also play a role, but normal cell culture conditions often do not adequately reflect physiological oxygen levels in tissues (Place, Domann, & Case, 2017). It would also be interesting to compare our model using T2 cells with repetitive stimulations by anti-CD3/anti-CD28 antibodies or peptide-loaded mature dendritic cells. This could help to indicate the contribution of tumor-specific factors to T cell dysfunction.

Transcription Factors in T Cell Dysfunction

Our knowledge of the regulatory network and epigenetic imprinting underlying the dysfunctional T cell state has been massively expanded in recent years. The transcription factors Eomes and Tbet (Tbx21) have long been the focus of investigations in murine chronic viral infections (Doering et al., 2012; Wherry & Kurachi, 2015). Evidence suggests that naïve T cells differentiate first to effector T cells, then they either differentiate into one of the mutually exclusive phenotypes of memory or dysfunctional T cells (Wherry & Kurachi, 2015). Nevertheless, this model has been challenged by data that instead suggests that KLRG1^{low} memory precursor cells develop into dysfunctional cells (Angelosanto et al., 2012). Moreover, Siddiqui et al. provide evidence that a Tcf1+ memory-like population is established early in dysfunction without an intermittent effector state, and this population continuously replenishes the bulk of dysfunctional CD8 cells (Siddiqui et al., 2019). Additionally, recent single-cell RNA sequencing data indicates that effector and dysfunctional cells in human tumors do not frequently share T cell clonotypes (Yost et al., 2019). This implies that the differentiation towards either state is mutually exclusive.

104

Either way, dysfunctional T cells in chronic murine infections contain a progenitor-like Tbet[high] PD1^{int} and a terminal Eomes[high] PD1^{high} population (Wherry & Kurachi, 2015). In contrast to chronic LCMV models, Eomes expression was instead lost during tumor progression in murine tumor models, and there was no correlation with effector functions (Schietinger et al., 2016). Moreover, in human lung cancer TILs, there is very little correlation between EOMES and TBET levels with PD-1 expression (D. S. Thommen et al., 2018). This was again elegantly shown in a recent single-cell ATACseq study, where EOMES and TBET were rather implicated in CD8 memory formation than exhaustion (Satpathy et al., 2019). Similarly, we find no correlation of EOMES with functionality in repetitively stimulated cells.

On the other hand, a multitude of studies have now implicated the transcription factors NFATC1 (NFAT2), IRF4, NFKB1/2, BATF, NR4A1, and TOX, among others, in the induction and/or maintenance of T cell dysfunction (Alfei et al., 2019; J. Chen et al., 2019; Khan et al., 2019; Xindong Liu et al., 2019; Man et al., 2017; Martinez et al., 2015; Satpathy et al., 2019; Scott et al., 2019). We find a slightly higher expression of TOX in repetitively stimulated cells, but it is upregulated more strongly on acutely stimulated cells. It would be interesting to investigate at which stage of our model, TOX expression is required to induce dysfunction. Importantly, KO of TOX massively decreased the absolute numbers of TILs in murine tumor models and did not improve effector functions (Alfei et al., 2019). This is in line with the hypothesis, termed "functional adaptation", that exhaustion is established early during infection or tumor recognition and might have evolved to avoid immunopathology during chronic infections while still maintaining some limited effector functions (Speiser et al., 2014).

The Role of Antigen Affinity in T Cell Dysfunction

Our system allowed us to repetitively stimulate the T cells with different antigen concentrations and affinities. We noted that at high antigen concentrations, the difference in functionality between repetitive stimulation with the endogenous NY-ESO-9C peptide and the higher affinity NY-ESO-9V peptide was rather small. The differences in RNA expression were also small, although some genes, including SNX9, were more elevated with higher affinity stimulation. We also observed increased enrichment for some but not all of the dysfunctional scRNAseq populations with the NY-ESO-9V peptide. Repetitive NY-ESO-9V stimulation also induced a more stable dysfunctional phenotype. When we then titrated the peptide concentration during repetitive stimulation, we observed a dose-dependency for degranulation capacity, PD-1 and TCF7 expression. As expected, repetitive stimulation with low concentrations of peptide led to reduced PD-1 expression and improved effector functions. Because the differences between the two peptides were smallest at high peptide concentrations, antigen density is probably more important in these experiments than the peptide-MHC's affinity to the TCR. Supporting this argument, at lower peptide concentrations, the effects on expression and functionality scaled approximately linearly to the difference in peptide to MHC affinity (relative competitor activity 4'500-fold) rather than to the difference in functional avidity (200-fold EC50)(Romero et al., 2001). To conclusively answer this question, however, stable overexpression of equal levels of different peptides would be required, preferably over a more extensive affinity range. Additionally, our model would also allow us to exchange the TCR rather than the peptide to investigate this question.

Still, it remains an intriguing question, whether the antigen concentration on each cell or the frequency of antigen-presenting cells is more critical for dysfunction. Utzschneider et al. presented compelling data on this issue by using mixtures of otherwise identical gp33-epitope positive and negative chronic LCMV stains (Utzschneider et al., 2016). They observed that the infection of mice with a mixture of gp33+ and gp33- LCMV induced almost no exhaustion on gp33-specific T cells compared to the purely gp33+ strain. This comparison implies that the antigen dose is a critical determinant of T cell dysfunction. Nevertheless, in murine tumor models, either a low-affinity peptide expressed on all tumor cells or a low-affinity TCR, both led to diminished peripheral expansion and tumor control while maintaining higher effector functions and lower PD-1 levels (Martínez-Usatorre et al., 2018). Interestingly, we observed a higher expansion of T cells with repetitive NY-ESO-9C stimulation. One important consideration is that the NY-ESO-9C peptide, although of lower affinity than NY-ESO-9V, still has a relatively high functional avidity (EC50 12 nM (Romero et al., 2001)), compared to the SIITFEKL variant with the OT-I TCR used in their studies (EC50 70.7 nM (Zehn, Lee, & Bevan, 2009)). Thus, these two situations cannot be directly compared. Our data might suggest that repetitive stimulation lowers the optimal range of TCR to peptide-MHC affinity, above which T cell responses are known to be impaired (Hebeisen et al., 2013; Schmid et al., 2010). Another possible explanation could be that *in vivo,* there are differences in recruitment to the tumor vs. *in situ* expansion, which our *ex vivo* model would not capture.

Understanding the contribution of antigen affinity to the response to PD-1 blockade remains critical, as recent data in mice suggest that PD-1 blockade unleashes both low and high-affinity T clones and thereby broadens the T cell response against tumors (Martínez-Usatorre et al., 2018; Memarnejadian et al., 2017). An interplay between PD-1 blockade and TCR affinity is further suggested by the discovery that T cell clones derived from PD-1^{+} TILs in melanoma were of higher affinity than those from PD-1^{-} TILs (Simon et al., 2016). Intriguingly, recent data from basal and squamous cell carcinoma samples suggests that there were minimal shared clonotypes between effector and dysfunctional T cells (Yost et al., 2019). In addition, they report a correlation between specificity groups and T cell phenotype, which could suggest that TCR signaling strength determines the T cell phenotype. Also, there was substantial 'clonal replacement' of T cells in the tumor following PD-1 blockade. Yet, if these novel T cell clones harbor different TCR affinities remains to be elucidated. Our model provides a basic framework to test the impact of different TCR and peptide affinities on T cell dysfunction in more detail.

Genetic Screens to Discover Pathways in Cancer Immunology

Pooled CRISPR-Cas9 screens represent a versatile tool to investigate many to thousands of genes in an unbiased fashion and have been prominently used to discover essential genes in cancer cells (T. Wang et al., 2015; T. Wang, Wei, Sabatini, & Lander, 2014; T. Wang et al., 2017). CRISPR-Cas9 KO screens are considered to be equally or more robust than RNAi or CRISPRi screens (Evers et al., 2016; Morgens, Deans, Li, & Bassik, 2016). Given its high potential, multiple CRISPR-Cas9 screens have been used to determine which genes are essential to immune recognition of tumor cells. The genes important in tumor cells prominently feature include the IFNγ, TNFα signaling, and antigen-presentation pathways (Burr et al., 2017; Kearney et al., 2018; Manguso et al., 2017; Pan et al., 2018; S. J. Patel et al., 2017). Nevertheless, the first assays performed in T cells in murine tumor models employed targeted shRNA libraries instead (Zhou et al., 2014). Only very recently, two in vivo CRISPR-Cas9 KO

screens, one using lentiviruses, and one using adeno-associated viruses on murine TILs have been published (Dong et al., 2019; Ye et al., 2019). In these studies, Cas9+ OT-I T cells were transduced with a gRNA library before adoptive transfer into E0771-mCh-OVA tumor-bearing mice. The advantage of these systems is that they include multiple important aspects of tumor immunology, such as T cell trafficking and recruitment, as well as an intact tumor microenvironment. Despite the important discoveries made with such *in vivo* screens, they often suffer from underrepresentation of guides, which is evident in a complete loss of many guides in TILs (Ye et al., 2019).

CRISPR-Screens using primary human cells were long considered to be very difficult because of low transduction rates. For this reason, we decided to perform a targeted approach, which allowed us to investigate fewer selected genes but with a sufficient guide representation. Importantly, Shifrut and colleagues recently reported an improved protocol, which replaced virus-encoded Cas9 with electroporation-based delivery (Shifrut et al., 2018). This system allowed them to perform genome-wide screens, even in primary human T cells, and they uncovered networks that regulate T cell proliferation. Interestingly, SNX9 was not identified in this screen, presumably because its effects on proliferation are minimal. Interestingly, according to a recent tumor-cell CRISPR-Cas9 screen, human CAR T cells displayed substantial differences in their cytotoxic mechanisms compared to murine CD8 T cells (Kearney et al., 2018). This shows that investigating human T cells or CAR T cells directly has essential advantages. A significant limitation of our screen is the high inter-donor variability, which highlights the need for more replicates than with cell lines or inbreed mice. Any future screening attempts using our *ex vivo* model will undoubtedly profit from improved screening protocols and should include more replicates. Recently, multiple groups described methods to detect guide RNAs as well as mRNA with single-cell sequencing platforms (Datlinger et al., 2017; Hill et al., 2018; Jaitin et al., 2016). These technologies open a wide variety of possibilities to study transcriptional changes after gene perturbation.

SNX9 and its Potential Functions

SNX9 (also called SH3PX1) is a multi-domain scaffold-protein that is well known to be involved in clathrin-mediated endocytosis, during which it binds clathrin and AP2 followed by recruitment of dynamin. Clathrin-independent endocytosis by actin polymerization also involves SNX9 through binding of N-WASP, which then triggers Arp2/3 dependent actin polymerization (Yarar et al., 2007). Interestingly, SNX9 frequently featured on gene lists associated with T cell dysfunction in tumors but it has never been investigated in this context (Baitsch et al., 2011; Guo et al., 2018; Schietinger et al., 2016; D. Thommen et al., 2018; Tirosh et al., 2016; Zheng et al., 2017). *SNX9* ranked among the genes with the highest correlation with T cell exhaustion in basal cell carcinoma and squamous cell carcinoma in human patient samples and clustered together with *HAVCR2* (TIM-3), *ENTPD1* (CD39), *CXCL13* and *TIGIT* (Yost et al., 2019). It was not discovered in the *ex vivo* model for HIV-specific dysfunction (Chiu et al., 2014), which indicates the added value of our model. In the murine *in vivo* CRISPR screens described above, Snx9 was not discovered to regulate T cell effector functions or infiltration. Both the shRNA and the AAV-CRISPR-Cas9 library did not include guides for Snx9, whereas the lentiviral screen detected no reads for Snx9 guides in the tumor (Chow et al., 2017; Dong et al., 2019; Ye et al., 2019). Apart from their apparent loss in guide representation, SNX9 could be more important in human cells, while mice may have replaced its function by redundant proteins.

Satpathy et al. describe an open chromatin region at the *SNX9* locus that is specific to dysfunctional CD8 T cells, T_{reg}, and T_{fh} cells (Satpathy et al., 2019). This peak is reminiscent of a TSS + 5kbp OCR they describe for the *PDCD1* locus (encoding PD-1). Further analysis into this specific *SNX9* OCR should provide more details on the state-specific regulators behind elevated SNX9 expression because many transcription factor binding sites in this region have been described in other cell types (ENCODE Project Consortium, 2012). A genomic KO of SNX9 led to improved functionality after repetitive stimulation, and we observe a similar trend already for functional T cells. Ablation of SNX9 expression could be of interest to CAR-T cells and rapidly expanded TIL transfer products to improve their effector functions. Further experiments to test this hypothesis are ongoing.

SNX9 prominently localized to the contact site between T cells and tumor cells, which could indicate involvement in synapse formation or the regulation of T cell signaling. T cell synapse formation requires extensive actin polymerization and depletion to allow centrosome docking and polarized granule release (Ritter et al., 2015, 2017). There is limited literature on the modulation of the immune synapse in T cell dysfunction. One report describes that TILs suffer from defects in microtubule-organization cluster mobilization to the immunological synapse (Radoja et al., 2001). This prevents directed granule release and leads to decreased killing capacity. Our model will allow us to study the kinetics of synapse formation and polarization in more detail. SNX9 was shown to be involved in actin polymerization and exocytosis in cell biology model systems, however, there is no information whether it directly regulates the immune synapse (Bendris & Schmid, 2017; Lundmark & Carlsson, 2009). Intriguingly, SNX9 coordinated synaptic vesicle endocytosis through interactions with dynamin1 and N-WASP in cultured hippocampal neurons (N. Shin et al., 2007). In their study, both overexpression and knock-down of SNX9 had a negative effect on vesicle formation.

SNX9 also binds most phosphatidylinositol-phosphate (PIP) isoforms (Bendris & Schmid, 2017; Yarar et al., 2007), although there is a controversy on its specificity towards $PI(3,4,5)P_3$ (Badour et al., 2007). Interestingly, all these lipids are highly involved in immune synapse formation. For example, $PI(3,4)P_2$ accumulates at the immune synapse core because of SHIP1 activity on $PI(3,4,5)P_3$, whereas $PI(4,5)P2$ was depleted (Gawden-Bone et al., 2018; Ritter et al., 2015). Whether these phospholipids directly recruit SNX9 to the synapse requires further investigation. Additionally, T cell receptor complexes are known to internalize and recycle via clathrin-mediated endocytosis (Das et al., 2004), which involves N-WASP and Arp2/3. In cell lines models of T cells, SNX9 appears to be necessary for CD28 internalization and NFAT signaling (Badour et al., 2007). Contrastingly, our results point towards lower functionality in cells with high SNX9 levels. SNX9 seems to be downmodulated in murine models of chronic inflammation and colorectal cancer patients (Ish-Shalom et al., 2016). However, this study has several limitations, as they only investigated bulk-lysates of splenocytes and whole-blood by Western-blot for SNX9. Nevertheless, they also find SNX9 localization at cell-cell contacts.

We speculate that SNX9 could be not only involved in CD28 but also inhibitory receptor endocytosis, recycling, and signaling. This would explain why SNX9 KO cells have lower levels of PD-1, TIM-3, and LAG-3. This hypothesis could also be relevant for CTLA-4 expression, as it is stored in intracellular vesicles and trafficked to the synapse upon stimulation (Egen & Allison, 2002). Interestingly, a recent study presented a mechanism for PD-1 degradation by the E3 ligase FBX038 through ubiquitination (Meng et al., 2018). FBX038 was downregulated in human tumor tissues, but IL-2 stimulation restored its expression and led to reduced PD-1 levels. Similarly, it will be interesting to determine the role of SNX9 in both inhibitory and activating receptor signaling.

Despite its upregulation in dysfunctional TILs, SNX9 is rather ubiquitously expressed in humans (Bendris & Schmid, 2017; Lundmark & Carlsson, 2009). The expression in other cell types complicates the direct targeting of SNX9 for cancer immunotherapy. However, deletion or downmodulation of SNX9 could improve CAR-T and TIL transfer therapies and ameliorate their dysfunction in the tumor. A similar approach was proposed by Rupp et al., where they deleted PD-1 before adoptive CAR-T cell therapy (Rupp et al., 2017). PD-1 blockade is thought to mainly affect the TCF7+ population (Im et al., 2016; Kurtulus et al., 2018; Siddiqui et al., 2019), which expresses lower levels of SNX9 and, therefore, may be synergistic with the use of SNX9 KO CAR or TILs. On the other hand, more detailed investigations into the mechanisms behind SNX9 upregulation and its function could provide novel targets with a favorable drugability profile. Further investigations should shed more light on the role of the immune synapse and receptor recycling in T cell dysfunction.

2.3.6. Outlook

In summary, we developed and characterized a human *ex vivo* model for T cell dysfunction. We discovered that repetitive stimulation with tumor cells and antigen induces a T cell phenotype reminiscent of dysfunctional human TILs. Employing this system enabled us to perform genetic screening and led to the identification of a potentially new pathway involved in T cell dysfunction involving SNX9. We believe the *ex vivo* model for T cell dysfunction provides the community with a valuable tool to investigate the mechanisms leading to T cell dysfunction.

The work presented in this part of the dissertation is still ongoing, and therefore, I would like to elaborate on the planned and proposed work. The next experiments will include the determination of SNX9 protein levels in different human T cell populations in the periphery and the tumor. Similarly, Snx9 expression in murine TILs will be investigated. Furthermore, we will establish a murine adoptive transfer system allowing for KO of genes in OT-I T cells. Briefly, Cas9+ OT-I T cells are transduced with a retrovirus-based gRNA delivery system to enable efficient KO of selected genes (kindly provided by Prof. Ping-Chih Ho, University of Lausanne). These cells will then be transferred to OVA+ tumor-bearing mice (e.g. MC38-OVA, EG7-OVA). The effects on T cell infiltration, activation, cell recruitment, and tumor control will then be studied with different KOs. These experiments will be extended *ex vivo* and *in vivo* with CAR-T cell models. For example, human or mouse CD19 specific CAR-T cells will be generated *ex vivo* by viral transduction, followed Cas9-RNP mediated KO of SNX9. These cells will then be extensively studied *ex vivo,* and be used for adoptive transfer experiments into mice with CD19^{+} tumor xenografts or syngeneic tumors (J. Chen et al., 2019; Davila, Kloss, Gunset, & Sadelain, 2013; Ren et al., 2017).

Importantly we will further validate how SNX9 regulates T cells dysfunction. For this purpose, SNX9 protein will be co-stained in subsequent functional assays *ex vivo* to allow separation of KO from wild type cells. Also, we will generate Jurkat cell lines (and T cell clones if possible) with SNX9 KO and an HA-mApple-SNX9 fusion protein overexpression. This overexpression construct will provide us with a tool to follow SNX9 by live imaging and enable co-localization studies with fluorescent probes for different PIP_2 isoforms and actin. Using the Jurkat SNX9 KO and overexpression clones, we will determine the impact of SNX9 on receptor internalization, degradation, and recycling for the TCR, CD28 and inhibitory receptors. This could be extended to an unbiased surface biotinylation pull-down experiment. Additionally, we could perform co-immunoprecipitation experiments followed by protein mass spectrometry to determine SNX9's interaction partners in T cells.

We will also investigate whether repetitive stimulation leads to differences in synapse formation in general and if this involves SNX9. For this purpose, we will measure the kinetics of T cell – tumor cluster formation and their polarization state with repetitively stimulated T cells or TILs.

Until now, we focused our experiments on preventing dysfunction by generating KOs before repetitive stimulation. We will, however, try to reinvigorate established dysfunctional cells in our *ex vivo* model and TILs from cancer patients in a next step. To address this point, we will investigate the efficacy of SNX9 mRNA-targeting siRNA and antisense oligonucleotides (Kashyap, Thelemann, et al., 2019).

The regulation of SNX9 expression will be investigated by transcription factor motif analysis and gene regulatory network analysis by ISMARA (Balwierz et al., 2014) making use of the data published by Satpathy et al. Additionally, a bulk-ATACseq could be performed in repetitively stimulated cells to confirm exhaustion specific chromatin regulation. Additionally, we will investigate whether a KO of candidate transcription factors leads to reduced SNX9 levels.

All these experiments aim to validate the importance of SNX9 in T cell dysfunction and will undoubtedly spur new investigations into T cell signaling regulation in the context of cancer immunology. Furthermore, we will extend this work by performing whole-genome CRISPR-Cas9 KO screens and in parallel drug library screens on these dysfunctional T cells. This may uncover other targets and molecules for T cell reinvigoration.

2.3.7. Acknowledgments

2.3.8. Author Contributions

2.3.9. Ethics Declaration

2.3.10. Declaration of Interests

2.3.11. Financial Support
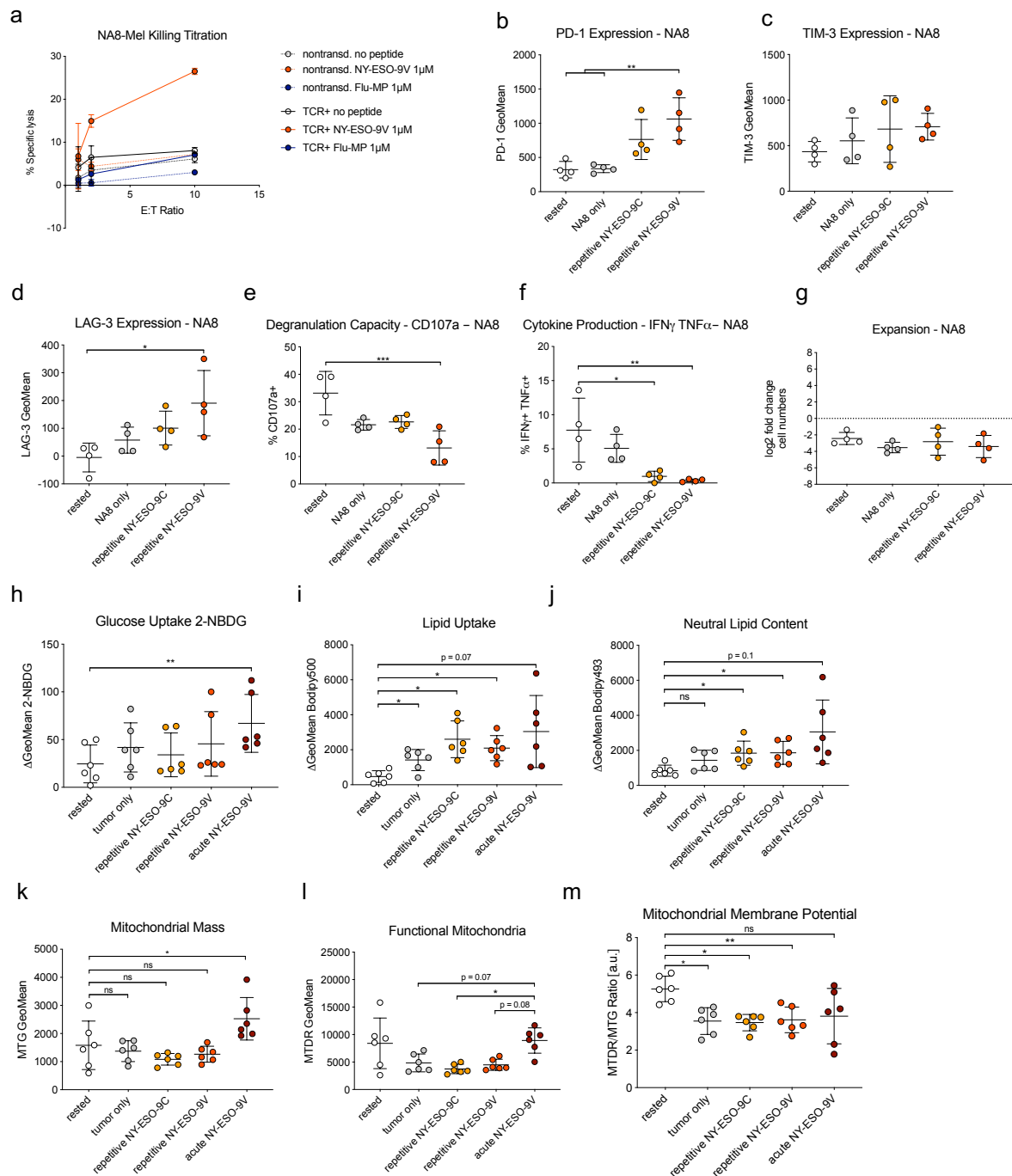
2.3.12. Supplementary Figures

Supplementary Figure 11

*(a) Degranulation measured by CD107a exposure after 4h stimulation with either NY-ESO-9V pulsed T2 cells or 50 nM PMA + 1 μM ionomycin. The time of first stimulation is indicated by "d0". (b) Representative scheme of the transduction and stimulation procedure underlying the ex vivo T cell dysfunction model. Days are indicated as circles with different treatments in different colors and shadings. (c) Expression of PD-1 and (d) TIM-3 and (e) LAG-3 on cells stimulated in the indicated conditions 12 days after the first stimulation (d12). (f) Representative plot of PD-1 and TIM-3 expression measured by flow cytometry on d12. (g) Expression of CD28 and CD57 on d12. (i) Exemplary plot of PD-L1 expression on T2 cells with and without incubation of the indicated doses of IFNγ for 24h. (j) Degranulation capacity in response to T2s with and without peptide. Repetitively stimulated cells were incubated with the indicated doses of IL-2 or IL-15 for 18h before the assay. The difference in CD107a labeling compared to unstimulated cells is shown. (k) The production of IFNγ and (l) TNFα was measured in response to PMA-ionomycin stimulation in presence of Monensin by intracellular staining. 1-way ANOVA statistics with Holm-Sidak correction for multiple comparisons. Unless indicated, only comparisons to rested condition are shown * p<0.05, ** p <0.01, *** p < 0.001, **** p < 0.0001. Dots represent individual healthy donor biological replicates and mean + SD are indicated.*
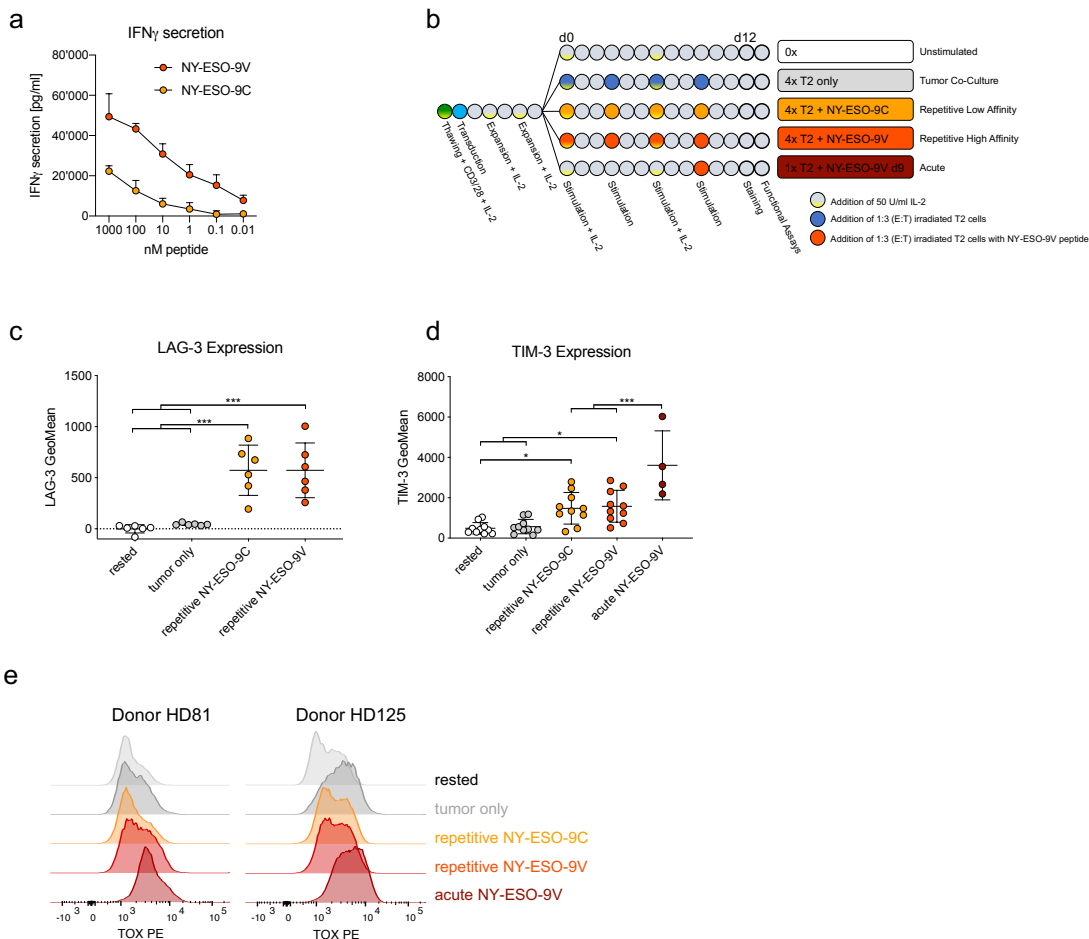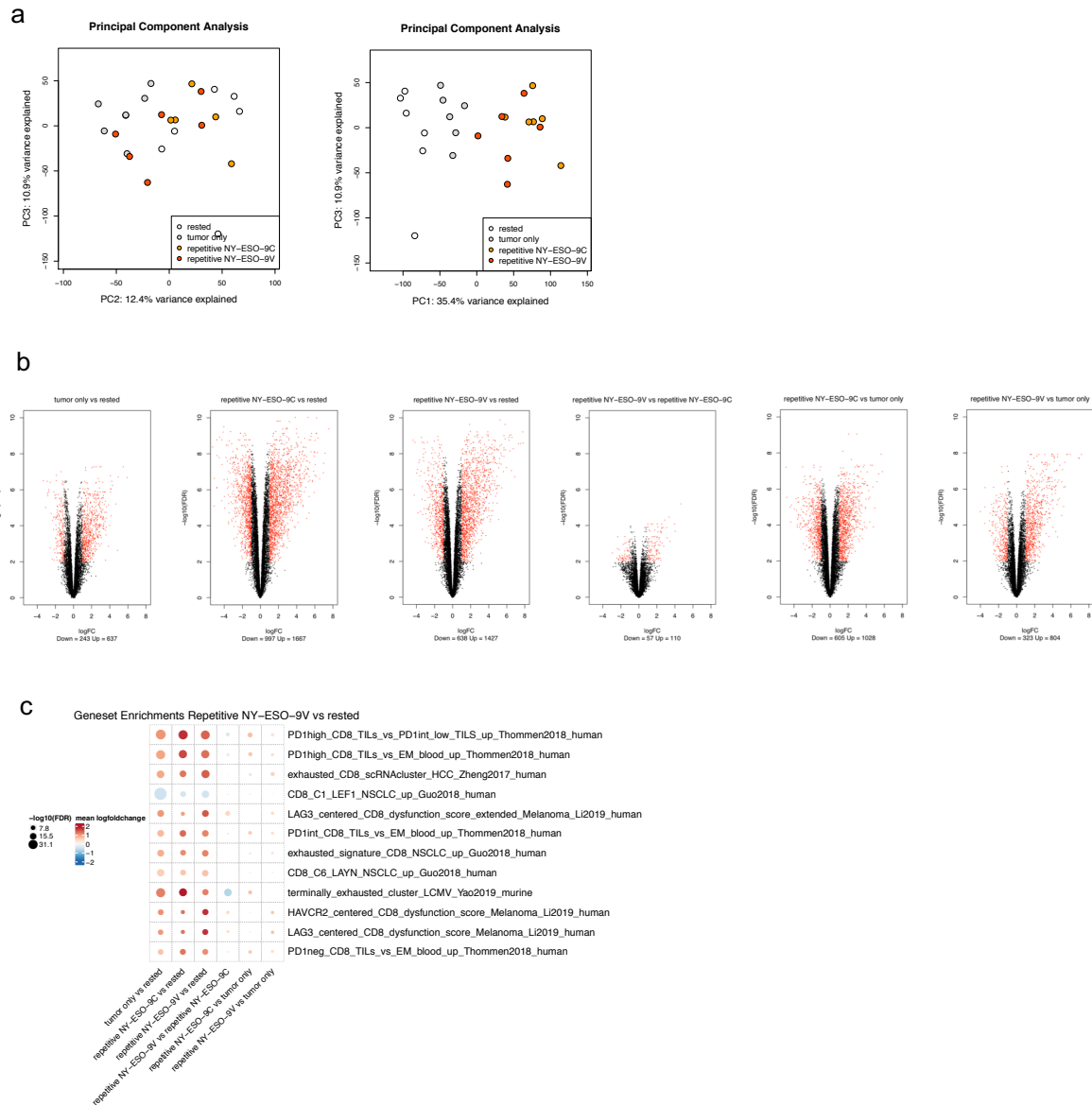

Supplementary Figure 12

(a) IFNγ secretion after three days of stimulation with T2 cells loaded with the indicated peptide dose measured by ELISA. (b) Representative scheme of the transduction and stimulation procedure underlying the ex vivo T cell dysfunction model for additional conditions. Days are indicated as circles with different treatments in different colors and shadings. (c) Expression of LAG-3 and (d) TIM-3 on T cells stimulated in the indicated conditions on day 12 (e) Exemplary plot of TOX expression measured by antibody staining and flow cytometry. Two biological donor replicates are shown as histograms with colors indicating the stimulation conditions.
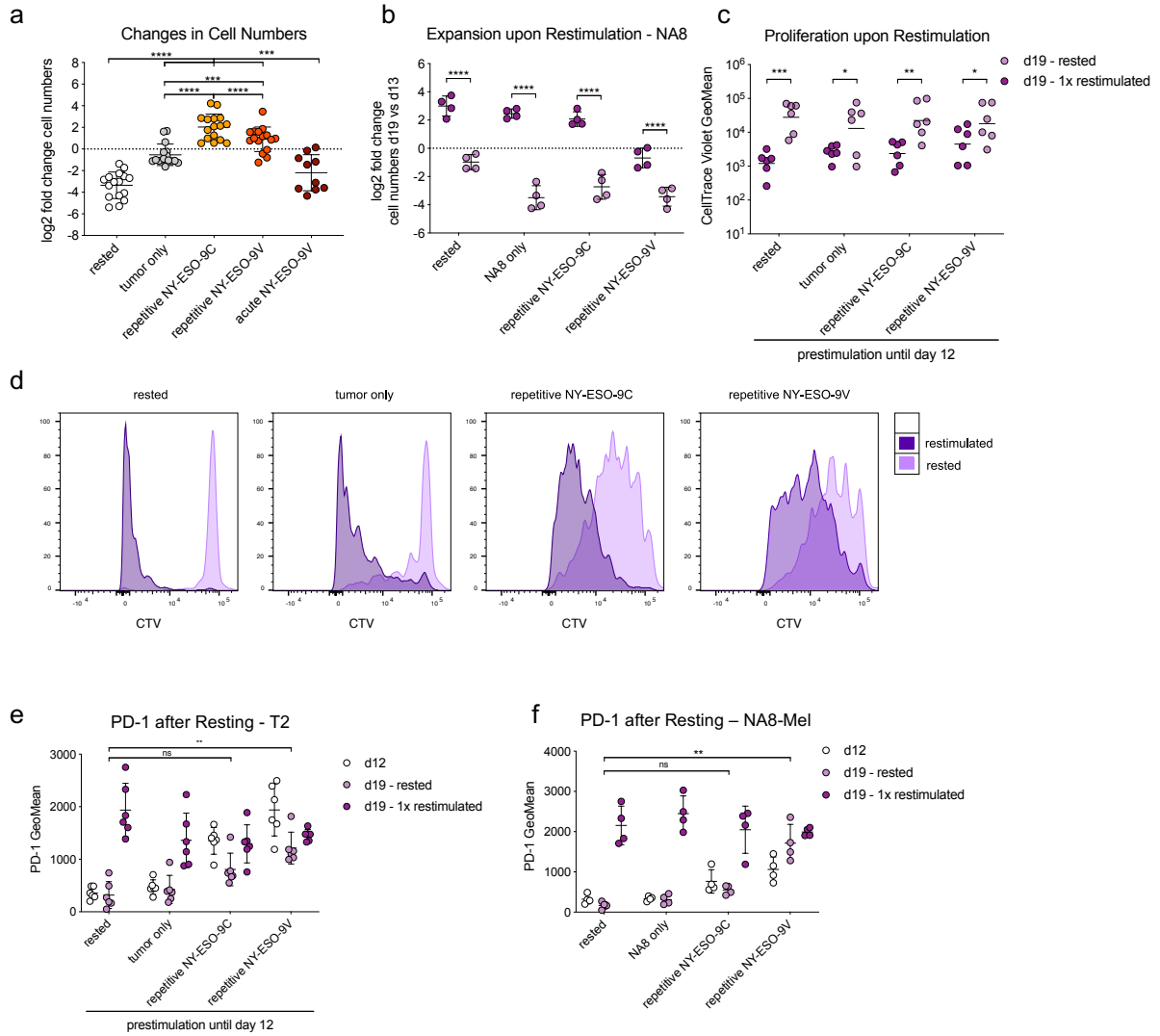
Supplementary Figure 13

(a) Specific Lysis of the HLA-A2+ NA8-melanoma cell line loaded with 1 μM of the indicated peptides after incubation with NY-ESO-1 TCR transduced or nontransduced T cells for 4h. Flu MP1 peptide was used as an irrelevant control. (b) Expression of PD-1, (c) TIM-3 and (d) LAG-3 on T cells stimulated with NA8-Melanoma cells for the indicated conditions.(e) Degranulation capacity and (f) co-production of IFNγ and TNFα and of T cells stimulated with NA8-Melanoma cells for 12 days, then re-stimulated for 5h with NY-ESO-9V loaded T2 cells in the presence of an anti-CD107a antibody and Monensin. (h) Glucose uptake measured by uptake of 100 μM 2-NBDG for 15 min at 37°C. Shown are the differences compared to unstained cells. (i) Lipid uptake measured by culture in 1 μM Bodipy500 for 15min at 37°C. (j) Neutral lipid content measured by staining of Bodipy493 on fixed cells. (k) Geometric mean signal intensity of Mitotracker Green staining by flow cytometry as a correlate to mitochondrial mass. (l) Geometric mean signal intensity of Mitotracker Deep Red staining by flow cytometry and (m) ratio between (k) and (l), as an approximation of mitochondrial membrane potential.

114

Supplementary Figure 14

(a) Principal component analysis of RNA sequencing data (b) k-means clustering of all significantly regulated genes (b) "Volcano" plot displaying -log10(FDR) in the y-axis and log-fold change (logFC) in the x-axis. Genes with a logFC > 1.5 and -log10(FDR) > 2 (<0.01 FDR) were considered significant and highlighted in red. Different comparisons are shown, first all against rested cells, then comparing 9V and 9C, and finally repetitively stimulated conditions against the tumor only condition. (c) Plot displaying the top 12 published gene sets for dysfunctional and control T cells enriched in our RNAseq data from ex vivo generated dysfunctional T cells. Performed using camera in edgeR with significance shown as dot size and mean log fold change of genes in this gene set shown as a color gradient. Columns indicate different comparisons between the four experimental conditions, whereas rows indicate gene sets. 1st column: tumor only vs. rested = effects of tumor cells alone. 2nd and 3rd column: repetitive NY-ESO-9C/9V vs. rested = effects of 9C/9V repetitive stimulation (total effects). 4th column: the difference between 9V and 9C affinity repetitive stimulation. 5th and 6th column: effects of 9V/9C repetitive stimulation compared to tumor cells alone (only TCR mediated effects).
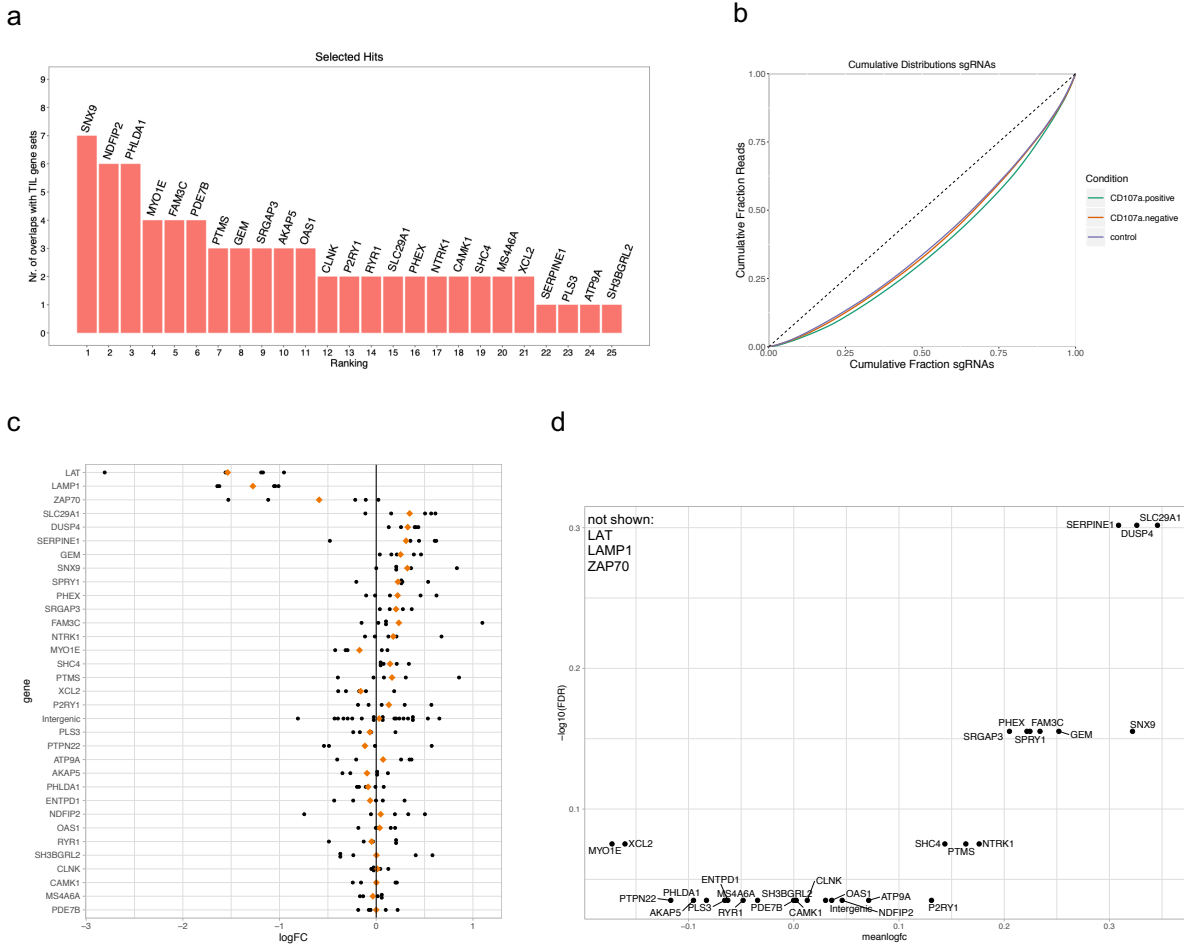
Supplementary Figure 15

(a) Log 2-fold changes of T cells in cell numbers over the 12 days of culture for the indicated conditions. (b) Expansion of T cells either rested or restimulated after repetitive stimulation with NA8-Mel cells. Shown as log 2-fold change in cell numbers during the six-day resting or restimulation period after repetitive stimulation. (c) Geometric mean signal and (d) exemplary plot of Cell Trace Violet labeled T cells on day 19 after six days of either resting or 1x restimulation on day 13. Lower signal indicates dilution and thus proliferation. The indicated conditions denote the stimulation between day 0 and 13. (e) Expression of PD-1 measured by flow cytometry on day 19 vs. day 12 with resting or restimulation between day 13 and day 19. (f) same as in d with cells repetitively stimulated with NA8-Mel cells instead of T2 for 12 days. Cells were either rested or restimulated with T2 loaded with NY-ESO-9V and assessed six days later. 2-way ANOVA statistics with Holm-Sidak correction for multiple comparisons. * p<0.05, ** p <0.01, *** p < 0.001, **** p < 0.0001. Dots represent individual healthy donor biological replicates and mean + SD is indicated.
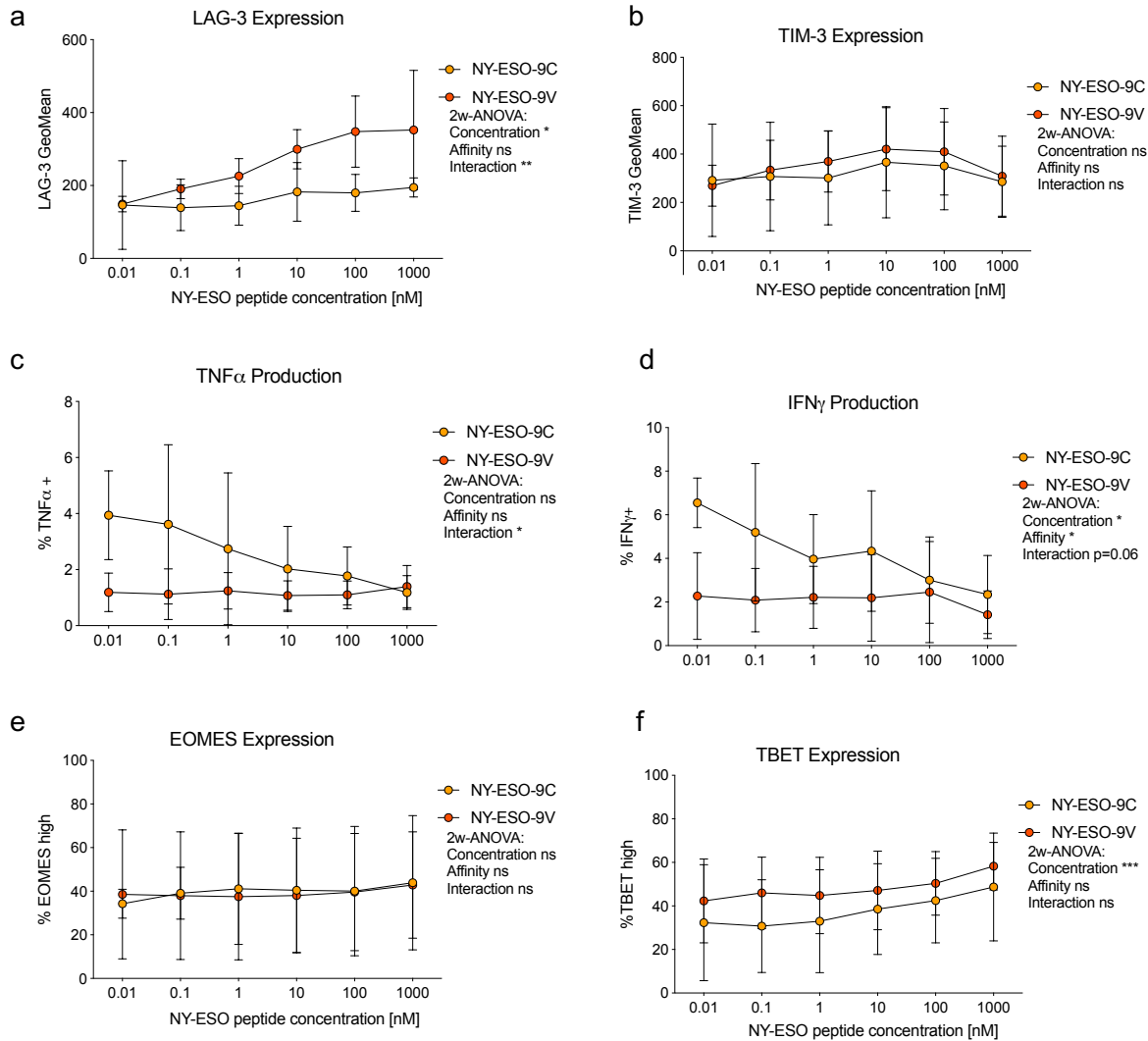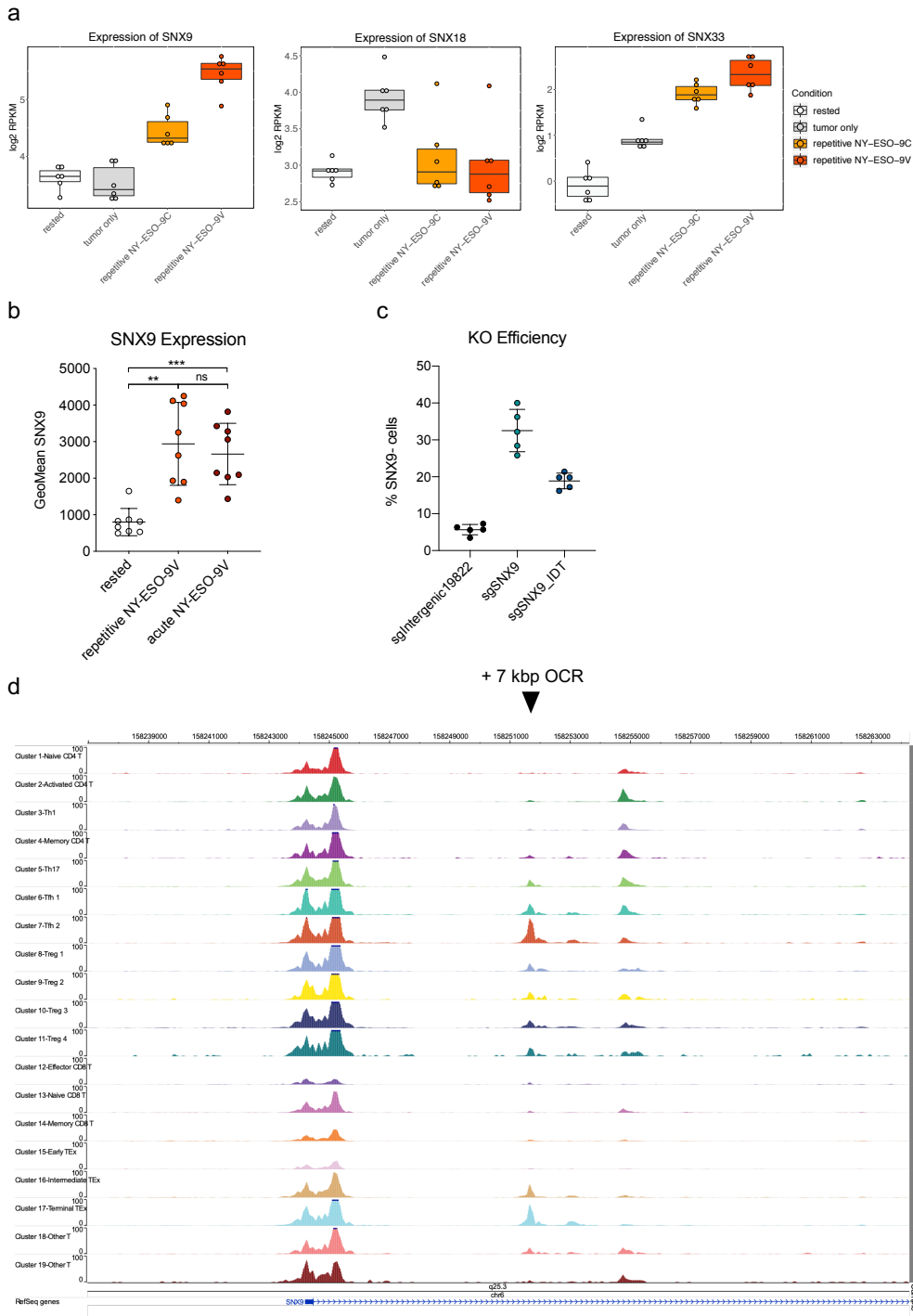
Supplementary Figure 16

*(a) LAG-3 and (b) TIM-3 expression 12 days after the first of four stimulations with T2 tumor cells and the indicated antigen-dose and type. (c) TNFα and (d) IFNγ production measured by intracellular cytokine staining after restimulation with NY-ESO-9V loaded T2 cells. Performed on day 13 day after repetitive stimulation with the indicated antigen dose. (e) EOMES and (f) TBET measured by antibody staining as in (a). 2-way ANOVA with Holm-Sidak correction, mean + SD is shown. The significance of concentration, affinity and their interaction term are indicated. * p<0.05, ** p <0.01, *** p < 0.001, **** p < 0.0001.*
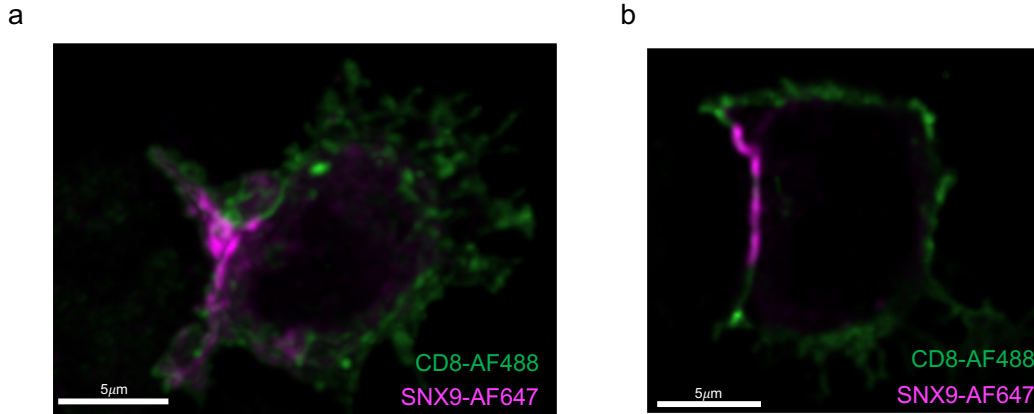
Supplementary Figure 17

(a) Ranked list of genes according to the number of overlaps per gene with published gene sets for T cell dysfunction in human tumors. (b) Cumulative distribution of all guide RNA reads determined by sequencing for each condition shown in different colors. A straight line with an area under the curve of 1 is shown as a comparison. (c) List of genes according to FDR with the log fold change in guide counts is shown for every single guide (black dots). The average fold change for all guides for each gene is shown as a yellow dot. (d) "Volcano" pot of -log10 FDR per gene shown in the y-axis and the mean log fold change per gene shown in the x-axis. FDR was determined by edgeR camera enrichment. Negative controls LAT, LAMP, and ZAP70 are not because they have a much higher -log10(FDR). None of the displayed genes reached statistical significance.

Supplementary Figure 18

(a) Expression of SNX9 and its family members SNX18 and SNX33 in the RNA sequencing of the indicated conditions. Log2 of rpkms normalized for library size is shown. Dots represent individual donors in addition to a Box-Whisker plot made using ggplot. (b) Geometric mean intensity of SNX9 expression by antibody staining and flow cytometry. 1-way ANOVA with Holm-Sidak correction, mean + SD is shown. * p<0.05, ** p <0.01, *** p < 0.001, **** p < 0.0001. (c) KO efficiency on protein level determined by flow cytometry after repetitive stimulation of cells. The crRNA construct used in the Cas9-RNP electroporation is indicated in comparison to the control sgIntergenic19822. (e) Single-cell ATAC seq tracks displaying open chromatin regions from BCC TILs of Satpathy et al. are displayed using the WashU Epigenome Browser. The human SNX9 locus is shown (RefSeq annotation of hg19) with the transcriptional start site found around the prominent OCR region to the left. An arrow indicates the OCR specific to dysfunction, Treg and Tfh specific + 7 kbp of the TSS.

Supplementary Figure 19

Spinning disk confocal images acquired on a 150x CSU-W1 Nikon using a Photometrics camera. 110x110x100 (x, y, z in nm) stacks were deconvoluted using Huygens software. NY-ESO-9V repetitively stimulated cells on day 13 after first stimulation were co-incubated with NY-ESO-9V peptide-pulsed T2 cells for 30 min. (a) 3D slice representation rendered using IMARIS of a T cell in contact with a T2 cancer cell fixed in Methanol. CD8 (in AF488 in green) and SNX9 (AF647 in magenta) were stained with primary and secondary antibodies. (b) Single z-stack slice of the same cell, as shown in Figure 6a.

2.3.13.   Supplementary Tables

Supplementary Table 13 Gene Sets for Dysfunction and Tumors

CD8_1_ExhaustionCellCycle_Sade_Feldman2018_human
CD8_2_ExhaustionHeatshock_Sade_Feldman2018_human
CD8_3_Exhaustion_Sade_Feldman2018_human
CD8_4_MemoryEffector_Sade_Feldman2018_human
CD8_5_EarlyActivated_Sade_Feldman2018_human
CD8_6_MemoryEffector_Sade_Feldman2018_human
CD8_B_exhaustion_Sade_Feldman2018_human
CD8_blood_PDL1Treatment_correlationMKi67_negative_Huang2017_human
CD8_blood_PDL1Treatment_correlationMKi67_positive_Huang2017_human
CD8_exhaustion_conserved_epigeneticORR_Down_Bengsch2018_human
CD8_exhaustion_conserved_epigeneticORR_Up_Bengsch2018_human
CD8_G_MemoryActivationSurvival_Sade_Feldman2018_human
CD8_TILs_DN_Tim3neg_CD39neg_OCRs_up_Sade_Feldman2018_human
CD8_TILs_DP_Tim3pos_CD39pos_OCRs_up_Sade_Feldman2018_human
CD8_C1_LEF1_NSCLC_up_Guo2018_human
CD8_C2_CD28_NSCLC_up_Guo2018_human
CD8_C3_CX3CR1_NSCLC_up_Guo2018_human
CD8_C4_GZMK_NSCLC_up_Guo2018_human
CD8_C5_ZNF683_NSCLC_up_Guo2018_human
CD8_C6_LAYN_NSCLC_up_Guo2018_human
CD8_C7_SLC4A10_NSCLC_up_Guo2018_human
CX3CR1_centered_CD8_cytotoxicity_score_Melanoma_Li2019_human
exhausted_signature_CD8_NSCLC_up_Guo2018_human
exhausted_CD8_scRNAcluster_HCC_Zheng2017_human
exhausted_CD8_TILs_d34_down_Schietinger2016_murine
exhausted_CD8_TILs_d34_up_Schietinger2016_murine
exhausted_CD8_TILs_d8_down_Schietinger2016_murine
exhausted_CD8_TILs_d8_up_Schietinger2016_murine
exhaustion_associated_variable_Tirosh2016_human
exhaustion_consistent_core_up_Tirosh2016_human
exhaustion_Mel75_up_Tirosh2016_human
FGFBP2_centered_CD8_cytotoxicity_score_extended_Melanoma_Li2019_human
FGFBP2_centered_CD8_cytotoxicity_score_Melanoma_Li2019_human
HAVCR2_centered_CD8_dysfunction_score_Melanoma_Li2019_human
HIVgag_specific_CD8_controller_top100_up_Quigley2010_human
HIVgag_specific_CD8_progressors_top100_up_Quigley2010_human
LAG3_centered_CD8_dysfunction_score_extended_Melanoma_Li2019_human
LAG3_centered_CD8_dysfunction_score_Melanoma_Li2019_human
LCMV_exhaustion_coremodule_CM4_Doering2012_mouse

LCMV_exhaustion_d30_differentially_sector4_Doering2012_mouse
LCMV_exhaustion_d30_differentially_sector5_Doering2012_mouse
memory_precursor_cluster_LCMV_Yao2019_murine
PBMCs_CD8_EM_EMRA_signature_up_Willinger2005_human
PBMCs_CD8_memory_signature_up_Willinger2005_human
PBMCs_CD8_naive_signature_up_Willinger2005_human
PD1hi_vs_HCM_OCRs_down_Philip2017_human
PD1hi_vs_HCM_OCRs_up_Philip2017_human
PD1hi_vs_HEM_OCRs_down_Philip2017_human
PD1hi_vs_HEM_OCRs_up_Philip2017_human
PD1hi_vs_HN_OCRs_down_Philip2017_human
PD1hi_vs_HN_OCRs_up_Philip2017_human
PD1high_CD8_TILs_vs_EM_blood_down_Thommen2018_human
PD1high_CD8_TILs_vs_EM_blood_up_Thommen2018_human
PD1high_CD8_TILs_vs_PD1int_low_TILS_down_Thommen2018_human
PD1high_CD8_TILs_vs_PD1int_low_TILS_up_Thommen2018_human
PD1int_CD8_TILs_vs_EM_blood_down_Thommen2018_human
PD1int_CD8_TILs_vs_EM_blood_up_Thommen2018_human
PD1neg_CD8_TILs_vs_EM_blood_down_Thommen2018_human
PD1neg_CD8_TILs_vs_EM_blood_up_Thommen2018_human
progenitor_like_cluster_LCMV_Yao2019_murine
terminally_exhausted_cluster_LCMV_Yao2019_murine
TOX_KO_8dpi_Cl13_down_Khan2019_murine
TOX_KO_8dpi_Cl13_up_Khan2019_murine
TOX_overexpression_invitro_down_Khan2019_murine
TOX_overexpression_invitro_up_Khan2019_murine
TOX_overexpression_in_vitro_down_Scott2019_murine
TOX_overexpression_in_vitro_up_Scott2019_murine
tumor_CD8_activation_module100_Singer2016_murine
tumor_CD8_activation_dysfunction_module100_Singer2016_murine
tumor_CD8_dysfunction_module100_Singer2016_murine
tumor_CD8_naive_memory_module100_Singer2016_murine
tumor_specific_vs_bystander_tumor_down_Scott2019_murine
tumor_specific_vs_bystander_tumor_up_Scott2019_murine
tumor_specific_blood_vs_CMV_blood_down_Baitsch2011_human
tumor_specific_blood_vs_CMV_blood_up_Baitsch2011_human
tumor_specific_blood_vs_EBV_blood_down_Baitsch2011_human
tumor_specific_blood_vs_EBV_blood_up_Baitsch2011_human
tumor_specific_TILs_vs_tumor_specific_blood_down_Baitsch2011_human
tumor_specific_TILs_vs_tumor_specific_blood_up_Baitsch2011_human

Supplementary Table 14 Gene Set Enrichment Repetitive NY-ESO-9V vs Rested

	NGenes	Direction	PValue	FDR	meanlogfc
PD1high_CD8_TILs_vs_PD1int_low_TILS_up_Thommen2018_human	532	Up	4.11E-19	3.25E-17	1.22108486
PD1high_CD8_TILs_vs_EM_blood_up_Thommen2018_human	692	Up	2.48E-16	9.78E-15	1.15294892
exhausted_CD8_scRNAcluster_HCC_Zheng2017_human	81	Up	5.62E-16	1.48E-14	1.25718016
CD8_C1_LEF1_NSCLC_up_Guo2018_human	295	Down	1.48E-13	2.93E-12	-0.4075224
LAG3_centered_CD8_dysfunction_score_extended_Melanoma_Li2019_human	57	Up	1.72E-11	2.71E-10	1.29283054
PD1int_CD8_TILs_vs_EM_blood_up_Thommen2018_human	483	Up	5.83E-11	7.67E-10	1.02620599
exhausted_signature_CD8_NSCLC_up_Guo2018_human	84	Up	1.09E-10	1.23E-09	1.0333707
CD8_C6_LAYN_NSCLC_up_Guo2018_human	385	Up	1.69E-10	1.67E-09	0.59208043
terminally_exhausted_cluster_LCMV_Yao2019_murine	221	Up	8.47E-10	7.43E-09	1.05526515
HAVCR2_centered_CD8_dysfunction_score_Melanoma_Li2019_human	30	Up	1.62E-09	1.28E-08	1.53272941
LAG3_centered_CD8_dysfunction_score_Melanoma_Li2019_human	30	Up	6.39E-09	4.52E-08	1.52208528
PD1neg_CD8_TILs_vs_EM_blood_up_Thommen2018_human	410	Up	6.87E-09	4.52E-08	0.96909198
PD1high_CD8_TILs_vs_EM_blood_down_Thommen2018_human	363	Down	9.34E-08	5.68E-07	-0.4487293
exhaustion_Mel75_up_Tirosh2016_human	126	Up	5.82E-07	3.28E-06	0.6260102
exhausted_CD8_TILs_d8_up_Schietinger2016_murine	184	Up	7.78E-07	4.10E-06	0.82008034
CD8_2_ExhaustionHeatshock_Sade_Feldman2018_human	255	Up	9.16E-07	4.52E-06	0.60029041
CD8_exhaustion_conserved_epigeneticORR_Up_Bengsch2018_human	222	Up	2.95E-06	1.37E-05	0.63419334
LCMV_exhaustion_d30_differentially_sector4_Doering2012_mouse	274	Up	4.33E-06	1.90E-05	0.75744176
TOX_overexpression_in_vitro_up_Scott2019_murine	360	Up	1.21E-05	5.04E-05	0.67109635
CD8_TILs_DP_Tim3pos_CD39pos_OCRs_up_Sade_Feldman2018_human	644	Up	5.35E-05	0.00021115	0.53183365
tumor_CD8_activation_dysfunction_module100_Singer2016_murine	90	Up	6.07E-05	0.00022839	0.71976424
exhausted_CD8_TILs_d34_up_Schietinger2016_murine	175	Up	7.66E-05	0.00027517	0.44227817
PD1high_CD8_TILs_vs_PD1int_low_TILS_down_Thommen2018_human	420	Down	0.00010352	0.00035557	-0.3652676
tumor_specific_TILs_vs_tumor_specific_blood_up_Baitsch2011_human	133	Up	0.00014323	0.00047146	0.55423458
CD8_6_MemoryEffector_Sade_Feldman2018_human	23	Down	0.00023058	0.00072865	-0.5963699
CD8_3_Exhaustion_Sade_Feldman2018_human	185	Up	0.00035556	0.00108035	0.3552836
CD8_blood_PDL1Treatment_correlationMKi67_positive_Huang2017_human	25	Up	0.00040979	0.001199	1.15663988
HIVgag_specific_CD8_progressors_top100_up_Quigley2010_human	83	Up	0.00047671	0.00134501	0.56128709
PBMCs_CD8_EM_EMRA_signature_up_Willinger2005_human	605	Up	0.00064524	0.00169913	0.28603696
PBMCs_CD8_naive_signature_up_Willinger2005_human	605	Up	0.00064524	0.00169913	0.28603696
exhaustion_consistent_core_up_Tirosh2016_human	28	Up	0.00185278	0.0047216	0.81231684
CD8_B_exhaustion_Sade_Feldman2018_human	1083	Up	0.00398642	0.00984148	0.20787906
PD1int_CD8_TILs_vs_EM_blood_down_Thommen2018_human	127	Down	0.00446077	0.01067881	-0.2486609
PD1neg_CD8_TILs_vs_EM_blood_down_Thommen2018_human	68	Down	0.00553709	0.01286559	-0.2724083

tumor_specific_vs_bystander_tumor_up_Scott2019_murine	954	Up	0.00732807	0.0165405	0.32086436
CD8_C4_GZMK_NSCLC_up_Guo2018_human	27	Down	0.00841134	0.01845822	-0.6135566
TOX_overexpression_in_vitro_down_Scott2019_murine	97	Down	0.00945123	0.02017966	-0.1156943
exhaustion_associated_variable_Tirosh2016_human	259	Up	0.02595562	0.05352926	0.32451662
FGFBP2_centered_CD8_cytotoxicity_score_extended_Melanoma_Li2019_human	54	Down	0.02642584	0.05352926	-0.3893151
tumor_specific_blood_vs_EBV_blood_up_Baitsch2011_human	161	Down	0.03229991	0.06379231	0.33410572
TOX_KO_8dpi_Cl13_up_Khan2019_murine	940	Up	0.03777636	0.0727886	0.2703996
PD1hi_vs_HCM_OCRs_down_Philip2017_human	64	Up	0.04339103	0.08161647	0.46652854
PBMCs_CD8_memory_signature_up_Willinger2005_human	55	Up	0.04761192	0.08747306	0.48283466
tumor_specific_blood_vs_CMV_blood_down_Baitsch2011_human	70	Down	0.05829379	0.10466385	-0.153451
HIVgag_specific_CD8_controller_top100_up_Quigley2010_human	81	Up	0.07805508	0.13191115	-0.1380074
tumor_CD8_naive_memory_module100_Singer2016_murine	70	Down	0.07845751	0.13191115	-0.0335859
CX3CR1_centered_CD8_cytotoxicity_score_Melanoma_Li2019_human	28	Down	0.07847879	0.13191115	-0.5333916
FGFBP2_centered_CD8_cytotoxicity_score_Melanoma_Li2019_human	28	Down	0.08369951	0.13556867	-0.5069024
CD8_C3_CX3CR1_NSCLC_up_Guo2018_human	98	Up	0.08424058	0.13556867	0.22077772
CD8_4_MemoryEffector_Sade_Feldman2018_human	145	Down	0.08654875	0.13556867	-0.0769005
PD1hi_vs_HN_OCRs_up_Philip2017_human	234	Up	0.08885467	0.13556867	0.3610031
CD8_exhaustion_conserved_epigeneticORR_Down_Bengsch2018_human	160	Down	0.08923507	0.13556867	-0.0471219
CD8_C5_ZNF683_NSCLC_up_Guo2018_human	34	Up	0.10323192	0.153874	0.26557443
exhausted_CD8_TILs_d34_down_Schietinger2016_murine	179	Down	0.10729074	0.15696239	0.00403343
tumor_specific_blood_vs_CMV_blood_up_Baitsch2011_human	47	Down	0.12255687	0.17603623	0.24455134
CD8_1_ExhaustionCellCycle_Sade_Feldman2018_human	2416	Up	0.14854154	0.20954967	0.16065547
LCMV_exhaustion_d30_differentially_sector5_Doering2012_mouse	27	Up	0.16107184	0.22323992	0.54317777
exhausted_CD8_TILs_d8_down_Schietinger2016_murine	182	Down	0.16454911	0.22412723	-0.0659593
CD8_blood_PDL1Treatment_correlationMKi67_negative_Huang2017_human	12	Down	0.20446971	0.27378148	-0.3528892
CD8_G_MemoryActivationSurvival_Sade_Feldman2018_human	32	Down	0.21764185	0.28656177	-0.0596448
CD8_C2_CD28_NSCLC_up_Guo2018_human	21	Down	0.23011974	0.29802393	-0.3123588
progenitor_like_cluster_LCMV_Yao2019_murine	124	Up	0.26793245	0.3413978	0.30976862
PD1hi_vs_HN_OCRs_down_Philip2017_human	254	Up	0.28346311	0.35545374	0.24366421
CD8_5_EarlyActivated_Sade_Feldman2018_human	34	Up	0.37329854	0.46079039	0.36692257
CD8_TILs_DN_Tim3neg_CD39neg_OCRs_up_Sade_Feldman2018_human	300	Down	0.39943742	0.48547009	-0.0208982
LCMV_exhaustion_coremodule_CM4_Doering2012_mouse	11	Down	0.4177026	0.49997735	0.05751999
tumor_specific_vs_bystander_tumor_down_Scott2019_murine	70	Down	0.4719966	0.55653331	-0.0218863
tumor_specific_blood_vs_EBV_blood_down_Baitsch2011_human	69	Down	0.65971298	0.76425522	0.05854389
tumor_specific_TILs_vs_tumor_specific_blood_down_Baitsch2011_human	72	Down	0.67662586	0.76425522	0.00638388
memory_precursor_cluster_LCMV_Yao2019_murine	104	Up	0.67718817	0.76425522	0.15001344
PD1hi_vs_HEM_OCRs_up_Philip2017_human	13	Up	0.69353285	0.77167739	-0.0052572
TOX_overexpression_invitro_down_Khan2019_murine	910	Down	0.72950628	0.80043051	0.1053172
PD1hi_vs_HEM_OCRs_down_Philip2017_human	23	Up	0.7458899	0.80719592	0.16606236
CD8_C7_SLC4A10_NSCLC_up_Guo2018_human	107	Down	0.79223192	0.8457611	-0.0111112
TOX_overexpression_invitro_up_Khan2019_murine	1340	Up	0.81505273	0.8585222	0.11566879
TOX_KO_8dpi_Cl13_down_Khan2019_murine	1458	Up	0.82714994	0.8598006	0.18661519
tumor_CD8_activation_module100_Singer2016_murine	91	Down	0.83830483	0.86007898	0.04186971
PD1hi_vs_HCM_OCRs_up_Philip2017_human	29	Up	0.87664754	0.88788661	0.05397248
tumor_CD8_dysfunction_module100_Singer2016_murine	90	Up	0.99736358	0.99736358	0.13139751

Supplementary Table 15 Gene Overlap Analysis between Guo et al and Sade-Feldman et al

Adjusted p-value is shown for pairwise comparisons done using GeneOverlap in R studio. Columns show gene sets of Guo et al. and rows gene sets of Sade-Feldmann et al.

	CD8_C1_LEF1	CD8_C2_CD28	CD8_C3_CX3CR1	CD8_C4_GZMK	CD8_C5_ZNF683	CD8_C6_LAYN	CD8_C7_SLC4A10	exhausted_signature_CD8
CD8_1_ExhaustionCellCycle	0.00489578	0.41215323	0.64067939	0.3394551	0.02616349	6.80E-108	0.10660236	2.92E-37
CD8_2_ExhaustionHeatshock	0.12630115	1	0.00569958	0.26917752	0.32432354	2.49E-65	0.70562752	1.45E-58
CD8_3_Exhaustion	0.10050554	1	9.98E-09	2.70E-06	0.24638227	2.78E-80	0.21871883	1.06E-33
CD8_4_MemoryEffector	0.00015687	2.40E-07	0.13862355	1	8.57E-08	0.4706391	6.53E-06	1
CD8_5_EarlyActivated	0.36505306	0.03203629	1	0.04059913	0.0504962	9.36E-08	0.14924383	0.00031755
CD8_6_MemoryEffector	1.24E-11	1.52E-06	8.27E-10	0.02882619	1	1	0.0057379	1
CD8_B_Exhaustion	0.13235368	1	2.21E-05	0.00166705	0.02310747	3.36E-170	0.0720678	3.41E-66
CD8_G_MemoryActivationSurvival	0.0008135	3.70E-06	1	0.0382556	0.00108427	1	0.14111088	1

Supplementary Table 16 Top 14 Entries of Overlap Analysis with TIL Datasets
(full list will be deposited)

SYMBOL	logfc_repetitive-NY-ESO-9V_vs_rested	logcpm_repetitive-NY-ESO-9V	nr_overlaps_ThommenPD1high_up	nr_overlaps_ThommenPD1high_down	nr_overlaps_other_humanTILs	nr_overlaps_total
CTLA4	2.93793286	5.43609358	2	0	6	25
HAVCR2	2.3860671	5.68101255	2	0	5	25
LAG3	2.74584633	6.39138336	2	0	5	22
SNX9	1.83283027	5.44743041	2	0	5	12
RGS1	0.71386542	4.31098979	2	0	4	17
DUSP4	3.64954697	5.60810839	2	0	4	17
NDFIP2	2.43354431	4.5565043	2	0	4	16
ENTPD1	3.13304458	5.7541341	2	0	4	15
PHLDA1	2.77943923	4.29393392	2	0	4	15
GZMB	3.45937571	6.92406011	2	0	3	18
RBPJ	1.87813455	5.93848249	2	0	3	14
LAYN	2.7961173	5.38769842	2	0	3	9
MYO1E	5.28234779	4.2112125	2	0	2	13
FAM3C	3.02584843	5.97824668	2	0	2	11

Supplementary Table 17 Gene Enrichment of CRISPR-Cas9 KO Screen for CD107a+ vs CD107a- Cells after Repetitive Stimulation

NGuides	Direction	PValue	FDR	meanlogfc	ranking	gene
5	Down	9.37E-11	3.09E-09	-1.5362449	1	LAT
5	Down	2.41E-10	3.97E-09	-1.2752135	2	LAMP1
5	Down	0.01068057	0.11748631	-0.5898398	3	ZAP70
5	Up	0.06192237	0.49921481	0.34565201	4	SLC29A1
5	Up	0.08511183	0.49921481	0.32601105	5	DUSP4
5	Up	0.09076633	0.49921481	0.3086746	6	SERPINE1
5	Up	0.1707989	0.69946545	0.25193874	7	GEM
5	Up	0.17091159	0.69946545	0.32191079	8	SNX9
5	Up	0.21084888	0.69946545	0.2244767	9	SPRY1
5	Up	0.21244652	0.69946545	0.22156911	10	PHEX
5	Up	0.2506072	0.69946545	0.20496975	11	SRGAP3
5	Up	0.25435107	0.69946545	0.2340108	12	FAM3C
5	Up	0.36450027	0.84099765	0.17616043	13	NTRK1
5	Down	0.40519758	0.84099765	-0.1727456	14	MYO1E
5	Up	0.40533083	0.84099765	0.14360262	15	SHC4
5	Up	0.41712447	0.84099765	0.16351949	16	PTMS
5	Down	0.43324121	0.84099765	-0.1604188	17	XCL2
5	Up	0.50360125	0.92236591	0.13088173	18	P2RY1
20	Up	0.67411032	0.92236591	0.03021915	19	Intergenic
5	Down	0.68054624	0.92236591	-0.0655856	20	PLS3
5	Down	0.70111252	0.92236591	-0.1169034	21	PTPN22
5	Up	0.72784342	0.92236591	0.07120258	22	ATP9A
5	Down	0.76135767	0.92236591	-0.0953093	23	AKAP5
5	Down	0.78382514	0.92236591	-0.0829796	24	PHLDA1
5	Down	0.80000225	0.92236591	-0.0627175	25	ENTPD1
5	Up	0.81201314	0.92236591	0.0459678	26	NDFIP2
5	Up	0.82843632	0.92236591	0.0360518	27	OAS1
5	Down	0.84134901	0.92236591	-0.0481542	28	RYR1
5	Up	0.86294711	0.92236591	0.00217844	29	SH3BGRL2
5	Up	0.90445012	0.92236591	0.01281605	30	CLNK
5	Up	0.91807477	0.92236591	0.00209548	31	CAMK1
5	Down	0.91845862	0.92236591	-0.0344033	32	MS4A6A
5	Up	0.92236591	0.92236591	-0.0001376	33	PDE7B

3. Summary of the Presented Work

In this thesis, I presented my work on resistance to cancer immunotherapy with a focus on NK and T cells. The first project led to the discovery of a new polymorphism with potential implications in resistance to checkpoint blockade. The results from this work pointed us towards a role for NK cells in PD-1 blockade. This encouraged us to perform a more in-depth characterization of the NK cell compartment in lung cancer and the role of PD-1 expression on NK cells. This exemplifies that more unbiased approaches, such as the RNAseq of responding and non-responding patients, can uncover new aspects of the investigated topic. We are keen to further investigate the role of NK cells and KIRs in cancer immunotherapy. I believe that new technologies with single-cell, temporal and spatial resolution will accelerate the preclinical research in this area. In addition, our work hopefully helps to fuel more research into NK cells and KIRs in cancer immunotherapy.

In the third part, I discussed my ongoing work on T cell dysfunction. The aim of the project was to develop a new tool that enables more detailed investigations into the mechanisms behind T cell dysfunction in human cells. The model mimics the phenotype of dysfunctional T cells in human tumors and allowed us to uncover a potential target in a less studied pathway in T cell dysfunction. We will now confirm these results in other models and investigate the mechanism of this protein in cancer immunotherapy.

As many aspects of T cell dysfunction remain elusive, we feel that the *ex vivo* model could also help other researchers to perform more detailed mechanistic investigations. An important future perspective could be to incorporate other aspects such as a 3D environment and the interaction with other cell types into the model. As T cell reinvigoration is at the heart of many new therapeutic strategies, the model has potential applications in drug identification and validation. It could represent an innovative tool to validate drug targets and compounds in a more physiological way directly with human cells.

4. Acknowledgements

5. References

Abbas, A. K., Lichtman, A. H., Pillai, S., & Preceded by: Abbas, A. K. (n.d.). *Cellular and molecular immunology*.

Abdel-Malek, Z. a, & Swope, V. B. (2011). Melanoma Development. In A. Bosserhoff (Ed.), *Springer-Verlag* (pp. 7–34). Vienna: Springer Vienna. https://doi.org/10.1007/978-3-7091-0371-5

Adusumilli, P. S., Cherkassky, L., Villena-Vargas, J., Colovos, C., Servais, E., Plotkin, J., … Sadelain, M. (2014). Regional delivery of mesothelin-targeted CAR T cell therapy generates potent and long-lasting CD4-dependent tumor immunity. *Science Translational Medicine*, *6*(261), 261ra151. https://doi.org/10.1126/scitranslmed.3010162

Al-Khami, A. A., Hossain, F., Wyczechowska, D., Hernandez, C., Zheng, L., Reiss, K., … Ochoa, A. C. (2015). Inhibition of fatty acid oxidation modulates immunosuppressive functions of myeloid-derived suppressor cells and enhances cancer therapies. *Journal for ImmunoTherapy of Cancer*, *3*(11), 1236–1247. https://doi.org/10.1186/2051-1426-3-S2-O18

Alfei, F., Kanev, K., Hofmann, M., Wu, M., Ghoneim, H. E., Roelli, P., … Zehn, D. (2019). TOX reinforces the phenotype and longevity of exhausted T cells in chronic viral infection. *Nature*, *571*(7764), 265–269. https://doi.org/10.1038/s41586-019-1326-9

Ali, O. A., Lewin, S. A., Dranoff, G., & Mooney, D. J. (2016). Vaccines Combined with Immune Checkpoint Antibodies Promote Cytotoxic T-cell Activity and Tumor Eradication. *Cancer Immunology Research*, *4*(2), 95–100. https://doi.org/10.1158/2326-6066.CIR-14-0126

Allard, B., Longhi, M. S., Robson, S. C., & Stagg, J. (2017). The ectonucleotidases CD39 and CD73: Novel checkpoint inhibitor targets. *Immunological Reviews*. NIH Public Access. https://doi.org/10.1111/imr.12528

Allard, B., Pommey, S., Smyth, M. J., & Stagg, J. (2013). Targeting CD73 enhances the antitumor activity of anti-PD-1 and anti-CTLA-4 mAbs. *Clinical Cancer Research*, *19*(20), 5626–5635. https://doi.org/10.1158/1078-0432.CCR-13-0545

Anfossi, N., André, P., Guia, S., Falk, C. S., Roetynck, S., Stewart, C. A., … Vivier, E. (2006). Human NK Cell Education by Inhibitory Receptors for MHC Class I. *Immunity*, *25*(2), 331–342. https://doi.org/10.1016/j.immuni.2006.06.013

Angelosanto, J. M., Blackburn, S. D., Crawford, A., & Wherry, E. J. (2012). Progressive Loss of Memory T Cell Potential and Commitment to Exhaustion during Chronic Viral Infection. *Journal of Virology*, *86*(15), 8161–8170. https://doi.org/10.1128/JVI.00889-12

Angelova, M., Mlecnik, B., Vasaturo, A., Bindea, G., Fredriksen, T., Lafontaine, L., … Galon, J. (2018). Evolution of Metastases in Space and Time under Immune Selection. *Cell*, *175*(3), 751-765.e16. https://doi.org/10.1016/j.cell.2018.09.018

Ansell, S. M. (2017). Nivolumab in the Treatment of Hodgkin Lymphoma. *Clinical Cancer Research*, *23*(7), 1623–1626. https://doi.org/10.1158/1078-0432.CCR-16-1387

Antonia, S. J., Villegas, A., Daniel, D., Vicente, D., Murakami, S., Hui, R., … Özgüroğlu, M. (2018). Overall Survival with Durvalumab after Chemoradiotherapy in Stage III NSCLC. *New England Journal of Medicine*, *379*(24), 2342–2350. https://doi.org/10.1056/NEJMoa1809697

Arlauckas, S. P., Garris, C. S., Kohler, R. H., Kitaoka, M., Cuccarese, M. F., Yang, K. S., … Pittet, M. J. (2017). In vivo imaging reveals a tumor-associated macrophage-mediated resistance pathway in anti-PD-1 therapy. *Science Translational Medicine*, *9*(389). https://doi.org/10.1126/scitranslmed.aal3604

Aswad, F., Kawamura, H., & Dennert, G. (2005). High Sensitivity of CD4 + CD25 + Regulatory T Cells to Extracellular Metabolites Nicotinamide Adenine Dinucleotide and ATP: A Role for P2X 7 Receptors. *The Journal of Immunology*, *175*(5), 3075–3083. https://doi.org/10.4049/jimmunol.175.5.3075

Azizi, E., Carr, A. J., Plitas, G., Cornish, A. E., Konopacki, C., Prabhakaran, S., … Pe'er, D. (2018). Single-Cell Map of Diverse Immune Phenotypes in the Breast Tumor Microenvironment. *Cell*, *174*(5), 1293-1308.e36. https://doi.org/10.1016/j.cell.2018.05.060

Bacac, M., Klein, C., & Umana, P. (2016). CEA TCB: A novel head-to-tail 2:1 T cell bispecific antibody for treatment of CEA-positive solid tumors. *OncoImmunology*, *5*(8), e1203498. https://doi.org/10.1080/2162402X.2016.1203498

Badour, K., McGavin, M. K. H., Zhang, J., Freeman, S., Vieira, C., Filipp, D., … Siminovitch, K. A. (2007). Interaction of the Wiskott-Aldrich syndrome protein with sorting nexin 9 is required for CD28 endocytosis and cosignalling in T cells. *Proceedings of the National Academy of Sciences of the United States of America*, *104*(5), 1593–1598. https://doi.org/10.1073/pnas.0610543104

Baeuerle, P. A., Ding, J., Patel, E., Thorausch, N., Horton, H., Gierut, J., … Hofmeister, R. (2019). Synthetic TRuC receptors engaging the complete T cell receptor for potent anti-tumor response. *Nature Communications*, *10*(1), 2087. https://doi.org/10.1038/s41467-019-10097-0

Baitsch, L., Baumgaertner, P., Devêvre, E., Raghav, S. K., Legat, A., Barba, L., … Speiser, D. E. (2011). Exhaustion of tumor-specific CD8+ T cells in metastases from melanoma patients. *Journal of Clinical Investigation*, *121*(6), 2350–2360. https://doi.org/10.1172/JCI46102

Balar, A. V, Galsky, M. D., Rosenberg, J. E., Powles, T., Petrylak, D. P., Bellmunt, J., … Bajorin, D. F. (2017). Atezolizumab as first-line treatment in cisplatin-ineligible patients with locally advanced and metastatic urothelial carcinoma: a single-arm, multicentre, phase 2 trial. *The Lancet*, *389*(10064), 67–76. https://doi.org/10.1016/S0140-6736(16)32455-2

Balkhi, M. Y., Ma, Q., Ahmad, S., & Junghans, R. P. (2015). T cell exhaustion and Interleukin 2 downregulation. *Cytokine*, *71*(2), 339–347. https://doi.org/10.1016/j.cyto.2014.11.024

Balwierz, P. J., Pachkov, M., Arnold, P., Gruber, A. J., Zavolan, M., & Van Nimwegen, E. (2014). ISMARA: automated modeling of genomic signals as a democracy of regulatory motifs. *Genome Research*, *24*(5), 869–884. https://doi.org/10.1101/gr.169508.113

Bantug, G. R., Galluzzi, L., Kroemer, G., & Hess, C. (2018). The spectrum of T cell metabolism in health and disease. *Nature Reviews Immunology*, *18*(1), 19–34. https://doi.org/10.1038/nri.2017.99

Barry, K. C., Hsu, J., Broz, M. L., Cueto, F. J., Binnewies, M., Combes, A. J., … Krummel, M. F. (2018). A natural killer–dendritic cell axis defines checkpoint therapy–responsive tumor microenvironments. *Nature Medicine*, *24*(8), 1178–1191. https://doi.org/10.1038/s41591-018-0085-8

Baumgaertner, P., Jandus, C., Rivals, J. P., Derré, L., Lövgren, T., Baitsch, L., … Speiser, D. E. (2012). Vaccination-induced functional competence of circulating human tumor-specific CD8 T-cells. *International Journal of Cancer*, *130*(11), 2607–2617. https://doi.org/10.1002/ijc.26297

Beck, A., Goetsch, L., Dumontet, C., & Corvaïa, N. (2017). Strategies and challenges for the next generation of antibody–drug conjugates. *Nature Reviews Drug Discovery*, *16*(5), 315–337. https://doi.org/10.1038/nrd.2016.268

Beldi-Ferchiou, A., Lambert, M., Dogniaux, S., Vély, F., Vivier, E., Olive, D., … Caillat-Zucman, S. (2016). PD-1 mediates functional exhaustion of activated NK cells in patients with Kaposi sarcoma. *Oncotarget*, *7*(45). https://doi.org/10.18632/oncotarget.12150

Benci, J. L., Xu, B., Qiu, Y., Wu, T. J., Dada, H., Twyman-Saint Victor, C., … Minn, A. J. (2016). Tumor Interferon Signaling

Regulates a Multigenic Resistance Program to Immune Checkpoint Blockade. *Cell*, *167*(6), 1540-1554.e12. https://doi.org/10.1016/j.cell.2016.11.022

Bendris, N., & Schmid, S. L. (2017, March 1). Endocytosis, Metastasis and Beyond: Multiple Facets of SNX9. *Trends in Cell Biology*. Elsevier Current Trends. https://doi.org/10.1016/j.tcb.2016.11.001

Bengsch, B., Johnson, A. L., Kurachi, M., Odorizzi, P. M., Pauken, K. E., Attanasio, J., … Wherry, E. J. (2016). Bioenergetic Insufficiencies Due to Metabolic Alterations Regulated by the Inhibitory Receptor PD-1 Are an Early Driver of CD8+T Cell Exhaustion. *Immunity*, *45*(2), 358–373. https://doi.org/10.1016/j.immuni.2016.07.008

Benson, D. M., Bakan, C. E., Mishra, A., Hofmeister, C. C., Efebera, Y., Becknell, B., … Caligiuri, M. a. (2010). The PD-1/PD-L1 axis modulates the natural killer cell versus multiple myeloma effect: a therapeutic target for CT-011, a novel monoclonal anti-PD-1 antibody. *Blood*, *116*(13), 2286–2294. https://doi.org/10.1182/blood-2010-02-271874

Bentzen, A. K., Marquard, A. M., Lyngaa, R., Saini, S. K., Ramskov, S., Donia, M., … Hadrup, S. R. (2016). Large-scale detection of antigen-specific T cells using peptide-MHC-I multimers labeled with DNA barcodes. *Nature Biotechnology*, *34*(10), 1037–1045. https://doi.org/10.1038/nbt.3662

Binnewies, M., Roberts, E. W., Kersten, K., Chan, V., Fearon, D. F., Merad, M., … Krummel, M. F. (2018). Understanding the tumor immune microenvironment (TIME) for effective therapy. *Nature Medicine*, *24*(5), 541–550. https://doi.org/10.1038/s41591-018-0014-x

Blank, C. U., Haining, W. N., Held, W., Hogan, P. G., Kallies, A., Lugli, E., … Zehn, D. (2019). Defining 'T cell exhaustion.' *Nature Reviews Immunology*, *19*(11), 665–674. https://doi.org/10.1038/s41577-019-0221-9

Blank, C. U., Rozeman, E. A., Fanchi, L. F., Sikorska, K., van de Wiel, B., Kvistborg, P., … Schumacher, T. N. (2018). Neoadjuvant versus adjuvant ipilimumab plus nivolumab in macroscopic stage III melanoma. *Nature Medicine*, *24*(11), 1655–1661. https://doi.org/10.1038/s41591-018-0198-0

Bommareddy, P. K., Shettigar, M., & Kaufman, H. L. (2018). Integrating oncolytic viruses in combination cancer immunotherapy. *Nature Reviews Immunology*, *18*(8), 498–513. https://doi.org/10.1038/s41577-018-0014-6

Bommareddy, P. K., Zloza, A., Rabkin, S. D., & Kaufman, H. L. (2019). Oncolytic virus immunotherapy induces immunogenic cell death and overcomes STING deficiency in melanoma. *OncoImmunology*, *8*(7), e1591875. https://doi.org/10.1080/2162402X.2019.1591875

Borghaei, H., Paz-Ares, L., Horn, L., Spigel, D. R., Steins, M., Ready, N. E., … Brahmer, J. R. (2015a). Nivolumab versus Docetaxel in Advanced Nonsquamous Non-Small-Cell Lung Cancer. *The New England Journal of Medicine*, *373*(17), 1627–1639. https://doi.org/10.1056/NEJMoa1507643

Borghaei, H., Paz-Ares, L., Horn, L., Spigel, D. R., Steins, M., Ready, N. E., … Brahmer, J. R. (2015b). Nivolumab versus Docetaxel in Advanced Nonsquamous Non–Small-Cell Lung Cancer. *New England Journal of Medicine*, *373*(17), 1627–1639. https://doi.org/10.1056/NEJMoa1507643

Böttcher, J. P., Bonavita, E., Chakravarty, P., Blees, H., Cabeza-Cabrerizo, M., Sammicheli, S., … Reis e Sousa, C. (2018). NK Cells Stimulate Recruitment of cDC1 into the Tumor Microenvironment Promoting Cancer Immune Control. *Cell*, *172*(5), 1022-1037.e14. https://doi.org/10.1016/j.cell.2018.01.004

Boudreau, J. E., Giglio, F., Gooley, T. A., Stevenson, P. A., Le Luduec, J.-B., Shaffer, B. C., … Hsu, K. C. (2017). *KIR3DL1 / HL A-B* Subtypes Govern Acute Myelogenous Leukemia Relapse After Hematopoietic Cell Transplantation. *Journal of Clinical Oncology*, *35*(20), 2268–2278. https://doi.org/10.1200/JCO.2016.70.7059

Boudreau, J. E., Liu, X.-R., Zhao, Z., Zhang, A., Shultz, L. D., Greiner, D. L., … Hsu, K. C. (2016). Cell-Extrinsic MHC Class I Molecule Engagement Augments Human NK Cell Education Programmed by Cell-Intrinsic MHC Class I. *Immunity*, *45*(2), 280–291. https://doi.org/10.1016/j.immuni.2016.07.005

Brahmer, J., Reckamp, K. L., Baas, P., Crinò, L., Eberhardt, W. E. E., Poddubskaya, E., … Spigel, D. R. (2015). Nivolumab versus Docetaxel in Advanced Squamous-Cell Non–Small-Cell Lung Cancer. *New England Journal of Medicine*, *373*(2), 123–135. https://doi.org/10.1056/NEJMoa1504627

Brenchley, J. M., Karandikar, N. J., Betts, M. R., Ambrozak, D. R., Hill, B. J., Crotty, L. E., … Koup, R. A. (2003). Expression of CD57 defines replicative senescence and antigen-induced apoptotic death of CD8+ T cells. *Blood*, *101*(7), 2711–2720. https://doi.org/10.1182/blood-2002-07-2103

Brocker, T. (2000). Chimeric Fv-ζ or Fv-ε receptors are not sufficient to induce activation or cytokine production in peripheral T cells. *Blood*, *96*(5), 1999–2001. https://doi.org/10.1182/blood.V96.5.1999.h8001999_1999_2001

Bronte, V., Chappell, D. B., Apolloni, E., Cabrelle, A., Wang, M., Hwu, P., & Restifo, N. P. (1999). Unopposed production of granulocyte-macrophage colony-stimulating factor by tumors inhibits CD8+ T cell responses by dysregulating antigen-presenting cell maturation. *Journal of Immunology*, *162*(10), 5728–5737. Retrieved from http://www.ncbi.nlm.nih.gov/pubmed/10229805

Broz, M. L., Binnewies, M., Boldajipour, B., Nelson, A. E., Pollack, J. L., Erle, D. J., … Krummel, M. F. (2014). Dissecting the Tumor Myeloid Compartment Reveals Rare Activating Antigen-Presenting Cells Critical for T Cell Immunity. *Cancer Cell*, *26*(5), 638–652. https://doi.org/10.1016/J.CCELL.2014.09.007

Brunner-Weinzierl, M. C., & Rudd, C. E. (2018). CTLA-4 and PD-1 Control of T-Cell Motility and Migration: Implications for Tumor Immunotherapy. *Frontiers in Immunology*, *9*, 2737. https://doi.org/10.3389/fimmu.2018.02737

Bucks, C. M., Norton, J. A., Boesteanu, A. C., Mueller, Y. M., & Katsikis, P. D. (2009). Chronic Antigen Stimulation Alone Is Sufficient to Drive CD8+ T Cell Exhaustion. *The Journal of Immunology*, *182*(11), 6697–6708. https://doi.org/10.4049/JIMMUNOL.0800997

Burr, M. L., Sparbier, C. E., Chan, Y.-C. C., Williamson, J. C., Woods, K., Beavis, P. A., … Dawson, M. A. (2017). CMTM6 maintains the expression of PD-L1 and regulates anti-tumour immunity. *Nature*, *advance on*(7670), 101–105. https://doi.org/10.1038/nature23643

Butte, M. J., Keir, M. E., Phamduy, T. B., Sharpe, A. H., & Freeman, G. J. (2007). Programmed Death-1 Ligand 1 Interacts Specifically with the B7-1 Costimulatory Molecule to Inhibit T Cell Responses. *Immunity*, *27*(1), 111–122. https://doi.org/10.1016/j.immuni.2007.05.016

Cai, X., Chiu, Y.-H., & Chen, Z. J. (2014). The cGAS-cGAMP-STING Pathway of Cytosolic DNA Sensing and Signaling. *Molecular Cell*, *54*(2), 289–296. https://doi.org/10.1016/J.MOLCEL.2014.03.040

Canale, F. P., Ramello, M. C., Nuñez, N., Bossio, S. N., Piaggio, E., Gruppi, A., … Montes, C. L. (2018, August 16). CD39 expression defines cell exhaustion in tumor-infiltrating CD8 T cells—response. *Cancer Research*. American Association for Cancer Research. https://doi.org/10.1158/0008-5472.CAN-18-0950

Carbone, D. P., Reck, M., Paz-Ares, L., Creelan, B., Horn, L., Steins, M., … Socinski, M. A. (2017). First-Line Nivolumab in Stage IV or Recurrent Non–Small-Cell Lung Cancer. *New England Journal of Medicine*, *376*(25), 2415–2426. https://doi.org/10.1056/NEJMoa1613493

Carrega, P., Morandi, B., Costa, R., Frumento, G., Forte, G., Altavilla, G., … Ferlazzo, G. (2008). Natural killer cells infiltrating human nonsmall-cell lung cancer are enriched in CD56 bright CD16 - cells and display an impaired capability to kill tumor

cells. *Cancer*, *112*(4), 863–875. https://doi.org/10.1002/cncr.23239

Caruana, I., Savoldo, B., Hoyos, V., Weber, G., Liu, H., Kim, E. S., … Dotti, G. (2015). Heparanase promotes tumor infiltration and antitumor activity of CAR-redirected T lymphocytes. *Nature Medicine*, *21*(5), 524–529. https://doi.org/10.1038/nm.3833

Casares, N., Pequignot, M. O., Tesniere, A., Ghiringhelli, F., Roux, S., Chaput, N., … Kroemer, G. (2005). Caspase-dependent immunogenicity of doxorubicin-induced tumor cell death. *Journal of Experimental Medicine*, *202*(12), 1691–1701. https://doi.org/10.1084/jem.20050915

Chandran, S. S., Somerville, R. P. T., Yang, J. C., Sherry, R. M., Klebanoff, C. A., Goff, S. L., … Kammula, U. S. (2017). Treatment of metastatic uveal melanoma with adoptive transfer of tumour-infiltrating lymphocytes: a single-centre, two-stage, single-arm, phase 2 study. *The Lancet Oncology*, *18*(6), 792–802. https://doi.org/10.1016/S1470-2045(17)30251-6

Chang, C. H., Qiu, J., O'Sullivan, D., Buck, M. D., Noguchi, T., Curtis, J. D., … Pearce, E. J. E. L. (2015). Metabolic Competition in the Tumor Microenvironment Is a Driver of Cancer Progression. *Cell*, *162*(6), 1229–1241. https://doi.org/10.1016/j.cell.2015.08.016

Chaput, N., Lepage, P., Coutzac, C., Soularue, E., Le Roux, K., Monot, C., … Carbonnel, F. (2017). Baseline gut microbiota predicts clinical response and colitis in metastatic melanoma patients treated with ipilimumab. *Annals of Oncology*, *28*(6), 1368–1379. https://doi.org/10.1093/annonc/mdx108

Cheever, M. A., & Higano, C. S. (2011). PROVENGE (Sipuleucel-T) in Prostate Cancer: The First FDA-Approved Therapeutic Cancer Vaccine. *Clinical Cancer Research*, *17*(11), 3520–3526. https://doi.org/10.1158/1078-0432.CCR-10-3126

Chen, D. S., & Mellman, I. (2013, July 25). Oncology meets immunology: The cancer-immunity cycle. *Immunity*. Cell Press. https://doi.org/10.1016/j.immuni.2013.07.012

Chen, D. S., & Mellman, I. (2017). Elements of cancer immunity and the cancer-immune set point. *Nature*, *541*(7637), 321–330. https://doi.org/10.1038/nature21349

Chen, J., López-Moyado, I. F., Seo, H., Lio, C.-W. J., Hempleman, L. J., Sekiya, T., … Rao, A. (2019). NR4A transcription factors limit CAR T cell function in solid tumours. *Nature*, 1. https://doi.org/10.1038/s41586-019-0985-x

Chinnasamy, D., Tran, E., Yu, Z., Morgan, R. A., Restifo, N. P., & Rosenberg, S. A. (2013). Simultaneous Targeting of Tumor Antigens and the Tumor Vasculature Using T Lymphocyte Transfer Synergize to Induce Regression of Established Tumors in Mice. *Cancer Research*, *73*(11), 3371–3380. https://doi.org/10.1158/0008-5472.CAN-12-3913

Chiossone, L., Vienne, M., Kerdiles, Y. M., & Vivier, E. (2017). Natural killer cell immunotherapies against cancer: checkpoint inhibitors and more. *Seminars in Immunology*, *31*, 55–63. https://doi.org/10.1016/j.smim.2017.08.003

Chiu, Y., Shan, L., Huang, H., Haupt, C., Bessell, C., Canaday, D. H., … Schneck, J. P. (2014). Sprouty-2 regulates HIV-specifc T cell polyfunctionality. *Journal of Clinical Investigation*, *124*(1), 1–11. https://doi.org/10.1172/JCI70510.responses

Choppa, P. C., Vojdani, A., Tagle, C., Andrin, R., & Magtoto, L. (1998). Multiplex PCR for the detection of Mycoplasma fermentans, M. hominis and M. penetrans in cell cultures and blood samples of patients with chronic fatigue syndrome. *Molecular and Cellular Probes*, *12*(5), 301–308. https://doi.org/10.1006/mcpr.1998.0186

Chow, R. D., Guzman, C. D., Wang, G., Schmidt, F., Youngblood, M. W., Ye, L., … Chen, S. (2017). AAV-mediated direct in vivo CRISPR screen identifies functional suppressors in glioblastoma. *Nature Neuroscience*, *20*(10), 1329–1341. https://doi.org/10.1038/nn.4620

Chowell, D., Morris, L. G. T. T., Grigg, C. M., Weber, J. K., Samstein, R. M., Makarov, V., … Chan, T. A. (2018). Patient HLA class I genotype influences cancer response to checkpoint blockade immunotherapy. *Science*, *359*(6375), 582–587. https://doi.org/10.1126/science.aao4572

Claus, C., Ferrara, C., Xu, W., Sam, J., Lang, S., Uhlenbrock, F., … Umaña, P. (2019). Tumor-targeted 4-1BB agonists for combination with T cell bispecific antibodies as off-the-shelf therapy. *Science Translational Medicine*, *11*(496). https://doi.org/10.1126/SCITRANSLMED.AAV5989

Collins, S., Waickman, A., Basson, A., Kupfer, A., Licht, J. D., Horton, M. R., & Powell, J. D. (2012). Regulation of CD4+ and CD8+ Effector Responses by Sprouty-1. *PLoS ONE*, *7*(11), e49801. https://doi.org/10.1371/journal.pone.0049801

Coulie, P. G., Van Den Eynde, B. J., Van Der Bruggen, P., & Boon, T. (2014, February 24). Tumour antigens recognized by T lymphocytes: At the core of cancer immunotherapy. *Nature Reviews Cancer*. Nature Publishing Group. https://doi.org/10.1038/nrc3670

Crespo, J., Sun, H., Welling, T. H., Tian, Z., & Zou, W. (2013). T cell anergy, exhaustion, senescence, and stemness in the tumor microenvironment. *Current Opinion in Immunology*, *25*(2), 214–221. https://doi.org/10.1016/j.coi.2012.12.003

da Silva, I. P., Gallois, A., Jimenez-Baranda, S., Khan, S., Anderson, A. C., Kuchroo, V. K., … Bhardwaj, N. (2014). Reversal of NK-Cell Exhaustion in Advanced Melanoma by Tim-3 Blockade. *Cancer Immunology Research*, *2*(5), 410–422. https://doi.org/10.1158/2326-6066.CIR-13-0171

Dai, P., Wang, W., Yang, N., Serna-Tamayo, C., Ricca, J. M., Zamarin, D., … Deng, L. (2017). Intratumoral delivery of inactivated modified vaccinia virus Ankara (iMVA) induces systemic antitumor immunity via STING and Batf3-dependent dendritic cells. *Science Immunology*, *2*(11). https://doi.org/10.1126/sciimmunol.aal1713

Das, V., Nal, B., Dujeancourt, A., Thoulouze, M.-I., Galli, T., Roux, P., … Alcover, A. (2004). Activation-Induced Polarized Recycling Targets T Cell Antigen Receptors to the Immunological Synapse: Involvement of SNARE Complexes. *Immunity*, *20*(5), 577–588. https://doi.org/10.1016/S1074-7613(04)00106-2

Datlinger, P., Rendeiro, A. F., Schmidl, C., Krausgruber, T., Traxler, P., Klughammer, J., … Bock, C. (2017). Pooled CRISPR screening with single-cell transcriptome readout. *Nature Methods*, *14*(3), 297–301. https://doi.org/10.1038/nmeth.4177

Daud, A. I., Loo, K., Pauli, M. L., Sanchez-Rodriguez, R., Sandoval, P. M., Taravati, K., … Rosenblum, M. D. (2016). Tumor immune profiling predicts response to anti–PD-1 therapy in human melanoma. *The Journal of Clinical Investigation*, *126*(9), 3447–3452. https://doi.org/10.1172/JCI87324

Daud, A. I., Wolchok, J. D., Robert, C., Hwu, W.-J., Weber, J. S., Ribas, A., … Hamid, O. (2016). Programmed Death-Ligand 1 Expression and Response to the Anti-Programmed Death 1 Antibody Pembrolizumab in Melanoma. *Journal of Clinical Oncology : Official Journal of the American Society of Clinical Oncology*, *34*(34), 4102–4109. https://doi.org/10.1200/JCO.2016.67.2477

Davila, M. L., Kloss, C. C., Gunset, G., & Sadelain, M. (2013). CD19 CAR-Targeted T Cells Induce Long-Term Remission and B Cell Aplasia in an Immunocompetent Mouse Model of B Cell Acute Lymphoblastic Leukemia. *PLoS ONE*, *8*(4), e61338. https://doi.org/10.1371/journal.pone.0061338

Davila, M. L., Riviere, I., Wang, X., Bartido, S., Park, J., Curran, K., … Brentjens, R. (2014). Efficacy and toxicity management of 19-28z CAR T cell therapy in B cell acute lymphoblastic leukemia. *Science Translational Medicine*, *6*(224), 224ra25. https://doi.org/10.1126/scitranslmed.3008226

De Simone, M., Arrigoni, A., Rossetti, G., Gruarin, P., Ranzani, V., Politano, C., … Pagani, M. (2016). Transcriptional Landscape of Human Tissue Lymphocytes Unveils Uniqueness of Tumor-Infiltrating T Regulatory Cells. *Immunity*, *45*(5), 1135–1147. https://doi.org/10.1016/j.immuni.2016.10.021

De Sousa Linhares, A., Battin, C., Jutz, S., Leitner, J., Hafner, C., Tobias, J., … Steinberger, P. (2019). Therapeutic PD-L1

antibodies are more effective than PD-1 antibodies in blocking PD-1/PD-L1 signaling. *Scientific Reports*, *9*(1), 11472. https://doi.org/10.1038/s41598-019-47910-1

Decker, W. K., da Silva, R. F., Sanabria, M. H., Angelo, L. S., Guimarães, F., Burt, B. M., … Paust, S. (2017). Cancer immunotherapy: Historical perspective of a clinical revolution and emerging preclinical animal models. *Frontiers in Immunology*. Frontiers Media SA. https://doi.org/10.3389/fimmu.2017.00829

Delahaye, N. F., Rusakiewicz, S., Martins, I., Ménard, C., Roux, S., Lyonnet, L., … Zitvogel, L. (2011). Alternatively spliced NKp30 isoforms affect the prognosis of gastrointestinal stromal tumors. *Nature Medicine*, *17*(6), 700–707. https://doi.org/10.1038/nm.2366

Delgoffe, G. M., & Powell, J. D. (2015). Feeding an army: The metabolism of T cells in activation, anergy, and exhaustion. *Molecular Immunology*, *68*(2), 492–496. https://doi.org/10.1016/j.molimm.2015.07.026

Deng, J., Wang, E. S., Jenkins, R. W., Li, S., Dries, R., Yates, K., … Wong, K.-K. (2018). CDK4/6 Inhibition Augments Antitumor Immunity by Enhancing T-cell Activation. *Cancer Discovery*, *8*(2), 216–233. https://doi.org/10.1158/2159-8290.CD-17-0915

Dick, J., Lang, N., Slynko, A., Kopp-Schneider, A., Schulz, C., Dimitrakopoulou-Strauss, A., … Hassel, J. (2016). Use of LDH and autoimmune side effects to predict response to ipilimumab treatment. *Immunotherapy*, *8*(9), 1033–1044. https://doi.org/10.2217/imt-2016-0083

Dighe, A. S., Richards, E., Old, L. J., & Schreiber, R. D. (1994). Enhanced in vivo growth and resistance to rejection of tumor cells expressing dominant negative IFNγ receptors. *Immunity*, *1*(6), 447–456. https://doi.org/10.1016/1074-7613(94)90087-6

Dijkstra, K. K., Cattaneo, C. M., Weeber, F., Chalabi, M., van de Haar, J., Fanchi, L. F., … Voest, E. E. (2018). Generation of Tumor-Reactive T Cells by Co-culture of Peripheral Blood Lymphocytes and Tumor Organoids. *Cell*, *174*(6), 1586-1598.e12. https://doi.org/10.1016/j.cell.2018.07.009

Doering, T. A., Crawford, A., Angelosanto, J. M., Paley, M. A., Ziegler, C. G., & Wherry, E. J. (2012). Network Analysis Reveals Centrally Connected Genes and Pathways Involved in CD8+ T Cell Exhaustion versus Memory. *Immunity*, *37*(6), 1130–1144. https://doi.org/10.1016/j.immuni.2012.08.021

Dong, M. B., Wang, G., Chow, R. D., Ye, L., Zhu, L., Dai, X., … Chen, S. (2019). Systematic Immunotherapy Target Discovery Using Genome-Scale In Vivo CRISPR Screens in CD8 T Cells. *Cell*, *178*(5), 1189-1204.e23. https://doi.org/10.1016/j.cell.2019.07.044

Dudek, A. M., Garg, A. D., Krysko, D. V., De Ruysscher, D., & Agostinis, P. (2013). Inducers of immunogenic cancer cell death. *Cytokine & Growth Factor Reviews*, *24*(4), 319–333. https://doi.org/10.1016/J.CYTOGFR.2013.01.005

Dudley, M. E., Wunderlich, J. R., Robbins, P. F., Yang, J. C., Hwu, P., Schwartzentruber, D. J., … Rosenberg, S. A. (2002). Cancer regression and autoimmunity in patients after clonal repopulation with antitumor lymphocytes. *Science*, *298*(5594), 850–854. https://doi.org/10.1126/science.1076514

Dudley, M. E., Wunderlich, J. R., Shelton, T. E., Even, J., & Rosenberg, S. A. (2003). Generation of Tumor-Infiltrating Lymphocyte Cultures for Use in Adoptive Transfer Therapy for Melanoma Patients. *Journal of Immunotherapy*, *26*(4), 332–342. https://doi.org/10.1097/00002371-200307000-00005

Dudley, M. E., Wunderlich, J. R., Yang, J. C., Sherry, R. M., Topalian, S. L., Restifo, N. P., … Gracia, G. J. (2005). Adoptive Cell Transfer Therapy Following Non-Myeloablative but Lymphodepleting Chemotherapy for the Treatment of Patients With Refractory Metastatic Melanoma. *Journal of Clinical Oncology*, *23*(10), 2346–2357. https://doi.org/10.1200/JCO.2005.00.240

Dudley, M. E., Yang, J. C., Sherry, R., Hughes, M. S., Royal, R., Kammula, U., … Rosenberg, S. A. (2008). Adoptive Cell Therapy for Patients With Metastatic Melanoma: Evaluation of Intensive Myeloablative Chemoradiation Preparative Regimens. *Journal of Clinical Oncology*, *26*(32), 5233–5239. https://doi.org/10.1200/JCO.2008.16.5449

Egen, J. G., & Allison, J. P. (2002). Cytotoxic T Lymphocyte Antigen-4 Accumulation in the Immunological Synapse Is Regulated by TCR Signal Strength. *Immunity*, *16*(1), 23–35. https://doi.org/10.1016/S1074-7613(01)00259-X

Elliott, J. M., & Yokoyama, W. M. (2011). Unifying concepts of MHC-dependent natural killer cell education. *Trends in Immunology*, *32*(8), 364–372. https://doi.org/10.1016/j.it.2011.06.001

ENCODE Project Consortium. (2012). An integrated encyclopedia of DNA elements in the human genome. *Nature*, *489*(7414), 57–74. https://doi.org/10.1038/nature11247

Esteva, F. J., Hubbard-Lucey, V. M., Tang, J., & Pusztai, L. (2019). Immunotherapy and targeted therapy combinations in metastatic breast cancer. *The Lancet Oncology*, *20*(3), e175–e186. https://doi.org/10.1016/S1470-2045(19)30026-9

Evers, B., Jastrzebski, K., Heijmans, J. P. M., Grernrum, W., Beijersbergen, R. L., & Bernards, R. (2016). CRISPR knockout screening outperforms shRNA and CRISPRi in identifying essential genes. *Nature Biotechnology*, *34*(6), 631–633. https://doi.org/10.1038/nbt.3536

Fauriat, C., Long, E. O., Ljunggren, H.-G., & Bryceson, Y. T. (2010). Regulation of human NK-cell cytokine and chemokine production by target cell recognition. *Blood*, *115*(11), 2167–2176. https://doi.org/10.1182/blood-2009-08-238469

Federal Drug Administration. (2017). FDA grants accelerated approval to pembrolizumab for first tissue/site agnostic indication. *Case Medical Research*. https://doi.org/10.31525/fda1-ucm560040.htm

Fehrenbacher, L., Spira, A., Ballinger, M., Kowanetz, M., Vansteenkiste, J., Mazieres, J., … POPLAR Study Group. (2016). Atezolizumab versus docetaxel for patients with previously treated non-small-cell lung cancer (POPLAR): a multicentre, open-label, phase 2 randomised controlled trial. *The Lancet*, *387*(10030), 1837–1846. https://doi.org/10.1016/S0140-6736(16)00587-0

Ferguson, T. A., Choi, J., & Green, D. R. (2011, May 1). Armed response: How dying cells influence T-cell functions. *Immunological Reviews*. John Wiley & Sons, Ltd (10.1111). https://doi.org/10.1111/j.1600-065X.2011.01006.x

Fletcher, M., Ramirez, M. E., Sierra, R. A., Raber, P., Thevenot, P., Al-Khami, A. A., … Rodriguez, P. C. (2015). l-Arginine Depletion Blunts Antitumor T-cell Responses by Inducing Myeloid-Derived Suppressor Cells. *Cancer Research*, *75*(2), 275–283. https://doi.org/10.1158/0008-5472.CAN-14-1491

Forlenza, C. J., Boudreau, J. E., Zheng, J., Le Luduec, J.-B., Chamberlain, E., Heller, G., … Hsu, K. C. (2016). *KIR3DL1* Allelic Polymorphism and HLA-B Epitopes Modulate Response to Anti-GD2 Monoclonal Antibody in Patients With Neuroblastoma. *Journal of Clinical Oncology*, *34*(21), 2443–2451. https://doi.org/10.1200/JCO.2015.64.9558

Freeman, G. J., Long, A. J., Iwai, Y., Bourque, K., Chernova, T., Nishimura, H., … Honjo, T. (2000). Engagement of the PD-1 immunoinhibitory receptor by a novel B7 family member leads to negative regulation of lymphocyte activation. *The Journal of Experimental Medicine*, *192*(7), 1027–1034. https://doi.org/10.1084/jem.192.7.1027

Friberg, M., Jennings, R., Alsarraj, M., Dessureault, S., Cantor, A., Extermann, M., … Antonia, S. J. (2002). Indoleamine 2,3-dioxygenase contributes to tumor cell evasion of T cell-mediated rejection. *International Journal of Cancer*, *101*(2), 151–155. https://doi.org/10.1002/ijc.10645

Fridman, W. H., Zitvogel, L., Sautès–Fridman, C., Kroemer, G., Sautès-Fridman, C., & Kroemer, G. (2017). The immune contexture in cancer prognosis and treatment. *Nature Reviews Clinical Oncology*, *14*(12), 717–734. https://doi.org/10.1038/nrclinonc.2017.101

Fu, J., Kanne, D. B., Leong, M., Glickman, L. H., McWhirter, S. M., Lemmens, E., … Kim, Y. (2015). STING agonist formulated cancer vaccines can cure established tumors resistant to PD-1 blockade. *Science Translational Medicine*, 7(283), 283ra52. https://doi.org/10.1126/scitranslmed.aaa4306

Fu, M., He, Q., Guo, Z., Zhou, X., Li, H., Zhao, L., … Lei, P. (2019). Therapeutic Bispecific T-Cell Engager Antibody Targeting the Transferrin Receptor. *Frontiers in Immunology*, 10, 1396. https://doi.org/10.3389/fimmu.2019.01396

Gabriel, I. H., Sergeant, R., Szydlo, R., Apperley, J. F., deLavallade, H., Alsuliman, A., … Rezvani, K. (2010). Interaction between KIR3DS1 and HLA-Bw4 predicts for progression-free survival after autologous stem cell transplantation in patients with multiple myeloma. *Blood*, 116(12), 2033–2039. https://doi.org/10.1182/blood-2010-03-273706

Galluzzi, L., Buqué, A., Kepp, O., Zitvogel, L., & Kroemer, G. (2017). Immunogenic cell death in cancer and infectious disease. *Nature Reviews Immunology*, 17(2), 97–111. https://doi.org/10.1038/nri.2016.107

Gandhi, L., Rodríguez-Abreu, D., Gadgeel, S., Esteban, E., Felip, E., De Angelis, F., … Garassino, M. C. (2018). Pembrolizumab plus chemotherapy in metastatic non-small-cell lung cancer. *New England Journal of Medicine*, 378(22), 2078–2092. https://doi.org/10.1056/NEJMoa1801005

Garcia-Beltran, W. F., Hölzemer, A., Martrus, G., Chung, A. W., Pacheco, Y., Simoneau, C. R., … Altfeld, M. (2016). Open conformers of HLA-F are high-affinity ligands of the activating NK-cell receptor KIR3DS1. *Nature Immunology*, 17(9), 1067. https://doi.org/10.1038/NI.3513

Garon, E. B., Hellmann, M. D., Rizvi, N. A., Carcereny, E., Leighl, N. B., Ahn, M.-J., … Hui, R. (2019). Five-Year Overall Survival for Patients With Advanced Non–Small-Cell Lung Cancer Treated With Pembrolizumab: Results From the Phase I KEYNOTE-001 Study. *Journal of Clinical Oncology*, JCO.19.00934. https://doi.org/10.1200/jco.19.00934

Garris, C. S., Arlauckas, S. P., Kohler, R. H., Trefny, M. P., Garren, S., Piot, C., … Pittet, M. J. (2018). Successful Anti-PD-1 Cancer Immunotherapy Requires T Cell-Dendritic Cell Crosstalk Involving the Cytokines IFN-γ and IL-12. *Immunity*, 49(6), 1148-1161.e7. https://doi.org/10.1016/j.immuni.2018.09.024

Gauthier, L., Morel, A., Anceriz, N., Rossi, B., Blanchard-Alvarez, A., Grondin, G., … Vivier, E. (2019). Multifunctional Natural Killer Cell Engagers Targeting NKp46 Trigger Protective Tumor Immunity. *Cell*, 177(7), 1701-1713.e16. https://doi.org/10.1016/J.CELL.2019.04.041

Gawden-Bone, C. M., Frazer, G. L., Richard, A. C., Ma, C. Y., Strege, K., & Griffiths, G. M. (2018). PIP5 Kinases Regulate Membrane Phosphoinositide and Actin Composition for Targeted Granule Secretion by Cytotoxic Lymphocytes. *Immunity*, 49(3), 427-437.e4. https://doi.org/10.1016/j.immuni.2018.08.017

Gejman, R. S., Chang, A. Y., Jones, H. F., Dikun, K., Hakimi, A. A., Schietinger, A., & Scheinberg, D. A. (2018). Rejection of immunogenic tumor clones is limited by clonal fraction. *ELife*, 7, 1–22. https://doi.org/10.7554/eLife.41090

Gerriets, V. A., Kishton, R. J., Johnson, M. O., Cohen, S., Siska, P. J., Nichols, A. G., … Rathmell, J. C. (2016). Foxp3 and Toll-like receptor signaling balance Treg cell anabolic metabolism for suppression. *Nature Immunology*, 17(12), 1459–1466. https://doi.org/10.1038/ni.3577

Ghoneim, H. E., Fan, Y., Moustaki, A., Abdelsamed, H. A., Dash, P., Dogra, P., … Youngblood, B. (2017). De Novo Epigenetic Programs Inhibit PD-1 Blockade-Mediated T Cell Rejuvenation. *Cell*, 170(1), 142-157.e19. https://doi.org/10.1016/j.cell.2017.06.007

Gill, S., Vasey, A. E., De Souza, A., Baker, J., Smith, A. T., Kohrt, H. E., … Negrin, R. S. (2012). Rapid development of exhaustion and down-regulation of eomesodermin limit the antitumor activity of adoptively transferred murine natural killer cells. *Blood*, 119(24), 5758–5768. https://doi.org/10.1182/blood-2012-03-415364

Goel, S., DeCristo, M. J., McAllister, S. S., & Zhao, J. J. (2018). CDK4/6 Inhibition in Cancer: Beyond Cell Cycle Arrest. *Trends in Cell Biology*, 28(11), 911–925. https://doi.org/10.1016/J.TCB.2018.07.002

Goel, S., DeCristo, M. J., Watt, A. C., BrinJones, H., Sceneay, J., Li, B. B., … Zhao, J. J. (2017). CDK4/6 inhibition triggers anti-tumour immunity. *Nature*, 548(7668), 471–475. https://doi.org/10.1038/nature23465

Golstein, P., & Griffiths, G. M. (2018). An early history of T cell-mediated cytotoxicity. *Nature Reviews Immunology*, 18(8), 527–535. https://doi.org/10.1038/s41577-018-0009-3

Gopalakrishnan, V, Spencer, C. N., Nezi, L., Reuben, A., Andrews, M. C., Karpinets, T. V, … Wargo, J. A. (2018). Gut microbiome modulates response to anti-PD-1 immunotherapy in melanoma patients. *Science*, 359(6371), 97–103. https://doi.org/10.1126/science.aan4236

Gopalakrishnan, Vancheswaran, Helmink, B. A., Spencer, C. N., Reuben, A., & Wargo, J. A. (2018). The Influence of the Gut Microbiome on Cancer, Immunity, and Cancer Immunotherapy. *Cancer Cell*, 33(4), 570–580. https://doi.org/10.1016/J.CCELL.2018.03.015

Gordon, S. R., Maute, R. L., Dulken, B. W., Hutter, G., George, B. M., McCracken, M. N., … Weissman, I. L. (2017). PD-1 expression by tumour-associated macrophages inhibits phagocytosis and tumour immunity. *Nature*, 545(7655), 495–499. https://doi.org/10.1038/nature22396

Grosser, R., Cherkassky, L., Chintala, N., & Adusumilli, P. S. (2019, November 11). Combination Immunotherapy with CAR T Cells and Checkpoint Blockade for the Treatment of Solid Tumors. *Cancer Cell*. Elsevier. https://doi.org/10.1016/j.ccell.2019.09.006

Grupp, S. A., Kalos, M., Barrett, D., Aplenc, R., Porter, D. L., Rheingold, S. R., … June, C. H. (2013). Chimeric antigen receptor-modified T cells for acute lymphoid leukemia. *New England Journal of Medicine*, 368(16), 1509–1518. https://doi.org/10.1056/NEJMoa1215134

Gubin, M. M., Esaulova, E., Ward, J. P., Malkova, O. N., Runci, D., Wong, P., … Artyomov, M. N. (2018). High-Dimensional Analysis Delineates Myeloid and Lymphoid Compartment Remodeling during Successful Immune-Checkpoint Cancer Therapy. *Cell*, 175(4), 1014-1030.e19. https://doi.org/10.1016/j.cell.2018.09.030

Gubin, M. M., Zhang, X., Schuster, H., Caron, E., Ward, J. P., Noguchi, T., … Schreiber, R. D. (2014). Checkpoint blockade cancer immunotherapy targets tumour-specific mutant antigens. *Nature*, 515(7528), 577–581. https://doi.org/10.1038/nature13988

Guedan, S., Ruella, M., & June, C. H. (2019). Emerging Cellular Therapies for Cancer. *Annual Review of Immunology*, 37(1), annurev-immunol-042718-041407. https://doi.org/10.1146/annurev-immunol-042718-041407

Guillerey, C., Huntington, N. D., & Smyth, M. J. (2016). Targeting natural killer cells in cancer immunotherapy. *Nature Immunology*, 17(9), 1025–1036. https://doi.org/10.1038/ni.3518

Guillerey, C., & Smyth, M. J. (2016). NK Cells and Cancer Immunoediting. *Current Topics in Microbiology and Immunology*, 395, 115–145. https://doi.org/10.1007/82_2015_446

Gulley, J. L., Madan, R. A., Pachynski, R., Mulders, P., Sheikh, N. A., Trager, J., & Drake, C. G. (2017). Role of Antigen Spread and Distinctive Characteristics of Immunotherapy in Cancer Treatment. *Journal of the National Cancer Institute*, 109(4). https://doi.org/10.1093/jnci/djw261

Guo, X., Zhang, Y., Zheng, L., Zheng, C., Song, J., Zhang, Q., … Zhang, Z. (2018). Global characterization of T cells in non-small-cell lung cancer by single-cell sequencing. *Nature Medicine*, 24(7), 978–985. https://doi.org/10.1038/s41591-018-0045-3

Havel, J. J., Chowell, D., & Chan, T. A. (2019). The evolving landscape of biomarkers for checkpoint inhibitor immunotherapy. *Nature Reviews Cancer*, *19*(3), 133–150. https://doi.org/10.1038/s41568-019-0116-x

Hebeisen, M., Oberle, S. G., Presotto, D., Speiser, D. E., Zehn, D., & Rufer, N. (2013). Molecular insights for optimizing T cell receptor specificity against cancer. *Frontiers in Immunology*, *4*(JUN), 1–10. https://doi.org/10.3389/fimmu.2013.00154

Hellmann, M. D., Ciuleanu, T.-E., Pluzanski, A., Lee, J. S., Otterson, G. A., Audigier-Valette, C., … Paz-Ares, L. (2018). Nivolumab plus Ipilimumab in Lung Cancer with a High Tumor Mutational Burden. *New England Journal of Medicine*, *378*(22), 2093–2104. https://doi.org/10.1056/NEJMoa1801946

Henning, A. N., Roychoudhuri, R., & Restifo, N. P. (2018). Epigenetic control of CD8+ T cell differentiation. *Nature Reviews Immunology*. https://doi.org/10.1038/nri.2017.146

Herbst, R. S., Baas, P., Kim, D.-W., Felip, E., Pérez-Gracia, J. L., Han, J.-Y., … Garon, E. B. (2016). Pembrolizumab versus docetaxel for previously treated, PD-L1-positive, advanced non-small-cell lung cancer (KEYNOTE-010): a randomised controlled trial. *The Lancet*, *387*(10027), 1540–1550. https://doi.org/10.1016/S0140-6736(15)01281-7

Hill, A. J., McFaline-Figueroa, J. L., Starita, L. M., Gasperini, M. J., Matreyek, K. A., Packer, J., … Trapnell, C. (2018). On the design of CRISPR-based single-cell molecular screens. *Nature Methods*, *15*(4), 271–274. https://doi.org/10.1038/nmeth.4604

Hirst, J., Motley, A., Harasaki, K., Peak Chew, S. Y., & Robinson, M. S. (2003). EpsinR: an ENTH Domain-containing Protein that Interacts with AP-1. *Molecular Biology of the Cell*, *14*(2), 625–641. https://doi.org/10.1091/mbc.e02-09-0552

Ho, P. C., Bihuniak, J. D., MacIntyre, A. N., Staron, M., Liu, X., Amezquita, R., … Kaech, S. M. (2015). Phosphoenolpyruvate Is a Metabolic Checkpoint of Anti-tumor T Cell Responses. *Cell*, *162*(6), 1217–1228. https://doi.org/10.1016/j.cell.2015.08.012

Hollern, D. P., Xu, N., Thennavan, A., Glodowski, C., Garcia-Recio, S., Mott, K. R., … Perou, C. M. (2019). B Cells and T Follicular Helper Cells Mediate Response to Checkpoint Inhibitors in High Mutation Burden Mouse Models of Breast Cancer. *Cell*, *179*(5), 1191-1206.e21. https://doi.org/10.1016/j.cell.2019.10.028

Hsu, J., Hodgins, J. J., Marathe, M., Nicolai, C. J., Bourgeois-Daigneault, M.-C., Trevino, T. N., … Ardolino, M. (2018). Contribution of NK cells to immunotherapy mediated by PD-1/PD-L1 blockade. *Journal of Clinical Investigation*. https://doi.org/10.1172/JCI99317

Hsu, K. C., Chida, S., Geraghty, D. E., & Dupont, B. (2002). The killer cell immunoglobulin-like receptor (KIR) genomic region: gene-order, haplotypes and allelic polymorphism. *Immunological Reviews*, *190*(1), 40–52. https://doi.org/10.1034/j.1600-065X.2002.19004.x

Huang, A. C., Postow, M. A., Orlowski, R. J., Mick, R., Bengsch, B., Manne, S., … Wherry, E. J. (2017). T-cell invigoration to tumour burden ratio associated with anti-PD-1 response. *Nature*, *545*(7652), 60–65. https://doi.org/10.1038/nature22079

Huang, C.-Y., Lin, Y.-C., Hsiao, W.-Y., Liao, F.-H., Huang, P.-Y., & Tan, T.-H. (2012). DUSP4 deficiency enhances CD25 expression and CD4 + T-cell proliferation without impeding T-cell development. *European Journal of Immunology*, *42*(2), 476–488. https://doi.org/10.1002/eji.201041295

Huang, Y., Yuan, J., Righi, E., Kamoun, W. S., Ancukiewicz, M., Nezivar, J., … Poznansky, M. C. (2012). Vascular normalizing doses of antiangiogenic treatment reprogram the immunosuppressive tumor microenvironment and enhance immunotherapy. *Proceedings of the National Academy of Sciences of the United States of America*, *109*(43), 17561–17566. https://doi.org/10.1073/pnas.1215397109

Hudak, J. E., Canham, S. M., & Bertozzi, C. R. (2014). Glycocalyx engineering reveals a Siglec-based mechanism for NK cell immunoevasion. *Nature Chemical Biology*, *10*(1), 69–75. https://doi.org/10.1038/nchembio.1388

Hugo, W., Zaretsky, J. M., Sun, L., Song, C., Moreno, B. H., Hu-Lieskovan, S., … Lo, R. S. (2016). Genomic and Transcriptomic Features of Response to Anti-PD-1 Therapy in Metastatic Melanoma. *Cell*, *165*(1), 35–44. https://doi.org/10.1016/J.CELL.2016.02.065

Hui, E., Cheung, J., Zhu, J., Su, X., Taylor, M. J., Wallweber, H. A., … Vale, R. D. (2017). T cell costimulatory receptor CD28 is a primary target for PD-1-mediated inhibition. *Science*, *355*(6332), 1428–1433. https://doi.org/10.1126/science.aaf1292

Im, S. J., Hashimoto, M., Gerner, M. Y., Lee, J., Kissick, H. T., Burger, M. C., … Ahmed, R. (2016). Defining CD8+T cells that provide the proliferative burst after PD-1 therapy. *Nature*, *537*(7620), 417–421. https://doi.org/10.1038/nature19330

Irving, M., Zoete, V., Hebeisen, M., Schmid, D., Baumgartner, P., Guillaume, P., … Michielin, O. (2012). Interplay between T cell receptor binding kinetics and the level of cognate peptide presented by major histocompatibility complexes governs CD8+ T cell responsiveness. *The Journal of Biological Chemistry*, *287*(27), 23068–23078. https://doi.org/10.1074/jbc.M112.357673

Ish-Shalom, E., Meirow, Y., Sade-Feldman, M., Kanterman, J., Wang, L., Mizrahi, O., … Baniyash, M. (2016). Impaired SNX9 Expression in Immune Cells during Chronic Inflammation: Prognostic and Diagnostic Implications. *Journal of Immunology (Baltimore, Md. : 1950)*, *196*(1), 156–167. https://doi.org/10.4049/jimmunol.1402877

Jaitin, D. A., Weiner, A., Yofe, I., Lara-Astiaso, D., Keren-Shaul, H., David, E., … Amit, I. (2016). Dissecting Immune Circuits by Linking CRISPR-Pooled Screens with Single-Cell RNA-Seq. *Cell*, *167*(7), 1883-1896.e15. Retrieved from https://www.sciencedirect.com/science/article/pii/S0092867416316117

Jamal-Hanjani, M., Wilson, G. A., McGranahan, N., Birkbak, N. J., Watkins, T. B. K., Veeriah, S., … TRACERx Consortium. (2017). Tracking the Evolution of Non–Small-Cell Lung Cancer. *New England Journal of Medicine*, *376*(22), 2109–2121. https://doi.org/10.1056/NEJMoa1616288

Jandus, C., Boligan, K. F., Chijioke, O., Liu, H., Dahlhaus, M., Démoulins, T., … Von Gunten, S. (2014). Interactions between Siglec-7/9 receptors and ligands influence NK cell-dependent tumor immunosurveillance. *Journal of Clinical Investigation*, *124*(4), 1810–1820. https://doi.org/10.1172/JCI65899

Jenkins, R. W., Aref, A. R., Lizotte, P. H., Ivanova, E., Stinson, S., Zhou, C. W., … Barbie, D. A. (2018). Ex Vivo Profiling of PD-1 Blockade Using Organotypic Tumor Spheroids. *Cancer Discovery*, *8*(2), 196–215. https://doi.org/10.1158/2159-8290.CD-17-0833

Jenkins, R. W., Barbie, D. A., & Flaherty, K. T. (2018). Mechanisms of resistance to immune checkpoint inhibitors. *British Journal of Cancer*, *118*(1), 9–16. https://doi.org/10.1038/bjc.2017.434

Jiang, P., Gu, S., Pan, D., Fu, J., Sahu, A., Hu, X., … Liu, X. S. (2018). Signatures of T cell dysfunction and exclusion predict cancer immunotherapy response. *Nature Medicine*, *24*(10), 1550–1558. https://doi.org/10.1038/s41591-018-0136-1

Jiao, S., Subudhi, S. K., Aparicio, A., Ge, Z., Guan, B., Miura, Y., & Sharma, P. (2019). Differences in Tumor Microenvironment Dictate T Helper Lineage Polarization and Response to Immune Checkpoint Therapy. *Cell*, *179*(5), 1177-1190.e13. https://doi.org/10.1016/j.cell.2019.10.029

Jocham, D., Richter, A., Hoffmann, L., Iwig, K., Fahlenkamp, D., Zakrzewski, G., … Doehn, C. (2004). Adjuvant autologous renal tumour cell vaccine and risk of tumour progression in patients with renal-cell carcinoma after radical nephrectomy: Phase III, randomised controlled trial. *Lancet*, *363*(9409), 594–599. https://doi.org/10.1016/S0140-6736(04)15590-6

Johnston, R. J., Comps-Agrar, L., Hackney, J., Yu, X., Huseni, M., Yang, Y., … Grogan, J. L. (2014). The Immunoreceptor TIGIT

Regulates Antitumor and Antiviral CD8+T Cell Effector Function. *Cancer Cell*, *26*(6), 923–937. https://doi.org/10.1016/j.ccell.2014.10.018

Jonna, S., Vanderwalde, A. M., Nieva, J. J., Poorman, K. A., Saul, M., von Buttlar, X., … Liu, S. V. (2019). Impact of prior chemotherapy or radiation therapy on tumor mutation burden in NSCLC. *Journal of Clinical Oncology*, *37*(15_suppl), 2627–2627. https://doi.org/10.1200/JCO.2019.37.15_suppl.2627

June, C. H., O'Connor, R. S., Kawalekar, O. U., Ghassemi, S., Milone, M. C., O'Connor, R. S., … Milone, M. C. (2018). CAR T cell immunotherapy for human cancer. *Science*, *359*(6382), 1361–1365. https://doi.org/10.1126/science.aar6711

June, C. H., & Sadelain, M. (2018). Chimeric antigen receptor therapy. *New England Journal of Medicine*, *379*(1), 64–73. https://doi.org/10.1056/NEJMra1706169

Kalos, M., Levine, B. L., Porter, D. L., Katz, S., Grupp, S. A., Bagg, A., & June, C. H. (2011). T Cells with Chimeric Antigen Receptors Have Potent Antitumor Effects and Can Establish Memory in Patients with Advanced Leukemia. *Science Translational Medicine*, *3*(95), 95ra73-95ra73. https://doi.org/10.1126/scitranslmed.3002842

Kammertoens, T., Schüler, T., & Blankenstein, T. (2005). Immunotherapy: target the stroma to hit the tumor. *Trends in Molecular Medicine*, *11*(5), 225–231. https://doi.org/10.1016/J.MOLMED.2005.03.002

Kamphorst, A. O., Wieland, A., Nasti, T., Yang, S., Zhang, R., Barber, D. L., … Ahmed, R. (2017). Rescue of exhausted CD8 T cells by PD-1-targeted therapies is CD28-dependent. *Science*, *355*(6332), 1423–1427. https://doi.org/10.1126/science.aaf0683

Kaneda, M. M., Messer, K. S., Ralainirina, N., Li, H., Leem, C. J., Gorjestani, S., … Varner, J. A. (2016). PI3Kγ 3 is a molecular switch that controls immune suppression. *Nature*, *539*(7629), 437–442. https://doi.org/10.1038/nature19834

Kashyap, A. S., Fernandez-Rodriguez, L., Zhao, Y., Monaco, G., Trefny, M. P., Yoshida, N., … Zippelius, A. (2019). GEF-H1 Signaling upon Microtubule Destabilization Is Required for Dendritic Cell Activation and Specific Anti-tumor Responses. *Cell Reports*, *28*(13), 3367-3380.e8. https://doi.org/10.1016/j.celrep.2019.08.057

Kashyap, A. S., Thelemann, T., Klar, R., Kallert, S. M., Festag, J., Buchi, M., … Zippelius, A. (2019). Antisense oligonucleotide targeting CD39 improves anti-tumor T cell immunity. *Journal for ImmunoTherapy of Cancer*, *7*(1), 67. https://doi.org/10.1186/s40425-019-0545-9

Kawalekar, O. U., O'Connor, R. S., Fraietta, J. A., Guo, L., McGettigan, S. E., Posey, A. D., … June, C. H. (2016). Distinct Signaling of Coreceptors Regulates Specific Metabolism Pathways and Impacts Memory Development in CAR T Cells. *Immunity*, *44*(2), 380–390. https://doi.org/10.1016/j.immuni.2016.01.021

Kearney, C. J., Vervoort, S. J., Hogg, S. J., Ramsbottom, K. M., Freeman, A. J., Lalaoui, N., … Oliaro, J. (2018). Tumor immune evasion arises through loss of TNF sensitivity. *Science Immunology*, *3*(23). https://doi.org/10.1126/sciimmunol.aar3451

Keir, M. E., Francisco, L. M., & Sharpe, A. H. (2007). PD-1 and its ligands in T-cell immunity. *Current Opinion in Immunology*, *19*(3), 309–314. https://doi.org/10.1016/J.COI.2007.04.012

Kelderman, S., Heemskerk, B., van Tinteren, H., van den Brom, R. R. H., Hospers, G. A. P., van den Eertwegh, A. J. M., … Blank, C. U. (2014). Lactate dehydrogenase as a selection criterion for ipilimumab treatment in metastatic melanoma. *Cancer Immunology, Immunotherapy*, *63*(5), 449–458. https://doi.org/10.1007/s00262-014-1528-9

Kenter, G. G., Welters, M. J. P., Valentijn, A. R. P. M., Lowik, M. J. G., Berends-van der Meer, D. M. A., Vloon, A. P. G., … Melief, C. J. M. (2009). Vaccination against HPV-16 Oncoproteins for Vulvar Intraepithelial Neoplasia. *New England Journal of Medicine*, *361*(19), 1838–1847. https://doi.org/10.1056/NEJMoa0810097

Kepp, O., Zitvogel, L., & Kroemer, G. (2019). Clinical evidence that immunogenic cell death sensitizes to PD-1/PD-L1 blockade. *OncoImmunology*, *8*(10), e1637188. https://doi.org/10.1080/2162402X.2019.1637188

Kershaw, M. H., Westwood, J. A., Parker, L. L., Wang, G., Eshhar, Z., Mavroukakis, S. A., … Hwu, P. (2006). A phase I study on adoptive immunotherapy using gene-modified T cells for ovarian cancer. *Clinical Cancer Research*, *12*(20 PART 1), 6106–6115. https://doi.org/10.1158/1078-0432.CCR-06-1183

Khan, O., Giles, J. R., McDonald, S., Manne, S., Ngiow, S. F., Patel, K. P., … Wherry, E. J. (2019). TOX transcriptionally and epigenetically programs CD8+ T cell exhaustion. *Nature*, *571*(7764), 211–218. https://doi.org/10.1038/s41586-019-1325-x

Kim, P. S., & Ahmed, R. (2010). Features of responding T cells in cancer and chronic infection. *Current Opinion in Immunology*, *22*(2), 223–230. https://doi.org/10.1016/J.COI.2010.02.005

Klein, C., Codarri-Deak, L., Nicolini, V., Seeber, S., Lauener, L., Richard, M., … Umana, P. (2019). Abstract 1552: A novel PD1-IL2v immunocytokine for preferential cis -activation of IL-2R signaling on PD-1 expressing T cell subsets strongly potentiates anti-tumor T cell activity of PD-1 checkpoint inhibition and IL2R-beta-gamma agonism. In *Immunology* (Vol. 79, pp. 1552–1552). American Association for Cancer Research. https://doi.org/10.1158/1538-7445.sabcs18-1552

Kochenderfer, J. N., Wilson, W. H., Janik, J. E., Dudley, M. E., Stetler-Stevenson, M., Feldman, S. A., … Rosenberg, S. A. (2010). Eradication of B-lineage cells and regression of lymphoma in a patient treated with autologous T cells genetically engineered to recognize CD19. *Blood*, *116*(20), 4099–4102. https://doi.org/10.1182/blood-2010-04-281931

Komiya, T., & Huang, C. H. (2018). Updates in the Clinical Development of Epacadostat and Other Indoleamine 2,3-Dioxygenase 1 Inhibitors (IDO1) for Human Cancers. *Frontiers in Oncology*, *8*. https://doi.org/10.3389/FONC.2018.00423

Kowolik, C. M., Topp, M. S., Gonzalez, S., Pfeiffer, T., Olivares, S., Gonzalez, N., … Cooper, L. J. N. (2006). CD28 Costimulation Provided through a CD19-Specific Chimeric Antigen Receptor Enhances In vivo Persistence and Antitumor Efficacy of Adoptively Transferred T Cells. *Cancer Research*, *66*(22), 10995–11004. https://doi.org/10.1158/0008-5472.CAN-06-0160

Koyama, S., Akbay, E. A., Li, Y. Y., Herter-Sprie, G. S., Buczkowski, K. A., Richards, W. G., … Hammerman, P. S. (2016). Adaptive resistance to therapeutic PD-1 blockade is associated with upregulation of alternative immune checkpoints. *Nature Communications*, *7*(1), 1–9. https://doi.org/10.1038/ncomms10501

Kreiter, S., Vormehr, M., van de Roemer, N., Diken, M., Löwer, M., Diekmann, J., … Sahin, U. (2015). Mutant MHC class II epitopes drive therapeutic immune responses to cancer. *Nature*, *520*(7549), 692–696. https://doi.org/10.1038/nature14426

Kurtulus, S., Madi, A., Kuchroo, V. K., Regev, A., & Anderson, A. C. (2018). Checkpoint Blockade Immunotherapy Induces Dynamic Changes in PD-1-CD8 + Tumor-Infiltrating T Cells. *Immunity*, *50*(1), 181-194.e6. https://doi.org/10.1016/j.immuni.2018.11.014

Larkin, J., Chiarion-Sileni, V., Gonzalez, R., Grob, J. J., Cowey, C. L., Lao, C. D., … Wolchok, J. D. (2015). Combined Nivolumab and Ipilimumab or Monotherapy in Untreated Melanoma. *New England Journal of Medicine*, *373*(1), 23–34. https://doi.org/10.1056/NEJMoa1504030

Läubli, H., Müller, P., D'Amico, L., Buchi, M., Kashyap, A. S., & Zippelius, A. (2018). The multi-receptor inhibitor axitinib reverses tumor-induced immunosuppression and potentiates treatment with immune-modulatory antibodies in preclinical murine models. *Cancer Immunology, Immunotherapy : CII*, *67*(5), 815–824. https://doi.org/10.1007/s00262-018-2136-x

Läubli, H., Pearce, O. M. T., Schwarz, F., Siddiqui, S. S., Deng, L., Stanczak, M. A., … Varki, A. (2014). Engagement of myelomonocytic Siglecs by tumor-associated ligands modulates the innate immune response to cancer. *Proceedings of the National Academy of Sciences of the United States of America*, *111*(39), 14211–14216. https://doi.org/10.1073/pnas.1409580111

Lawrence, M. S., Stojanov, P., Polak, P., Kryukov, G. V., Cibulskis, K., Sivachenko, A., … Getz, G. (2013). Mutational heterogeneity in cancer and the search for new cancer-associated genes. *Nature*, *499*(7457), 214–218. https://doi.org/10.1038/nature12213

Le, D. T., Durham, J. N., Smith, K. N., Wang, H., Bartlett, B. R., Aulakh, L. K., … Diaz, L. A. (2017). Mismatch repair deficiency predicts response of solid tumors to PD-1 blockade. *Science*, *357*(6349), 409–413. https://doi.org/10.1126/science.aan6733

Lhuillier, C., Rudqvist, N.-P., Elemento, O., Formenti, S. C., & Demaria, S. (2019). Radiation therapy and anti-tumor immunity: exposing immunogenic mutations to the immune system. *Genome Medicine*, *11*(1), 40. https://doi.org/10.1186/s13073-019-0653-7

Li, H., Handsaker, B., Wysoker, A., Fennell, T., Ruan, J., Homer, N., … 1000 Genome Project Data Processing Subgroup. (2009). The Sequence Alignment/Map format and SAMtools. *Bioinformatics*, *25*(16), 2078–2079. https://doi.org/10.1093/bioinformatics/btp352

Li, Hanjie, van der Leun, A. M., Yofe, I., Lubling, Y., Gelbard-Solodkin, D., van Akkooi, A. C. J., … Amit, I. (2018). Dysfunctional CD8 T Cells Form a Proliferative, Dynamically Regulated Compartment within Human Melanoma. *Cell*, 1–15. https://doi.org/10.1016/j.cell.2018.11.043

Li, J., Byrne, K. T., Yan, F., Yamazoe, T., Chen, Z., Baslan, T., … Stanger, B. Z. (2018). Tumor Cell-Intrinsic Factors Underlie Heterogeneity of Immune Cell Infiltration and Response to Immunotherapy. *Immunity*, *49*(1), 178-193.e7. https://doi.org/10.1016/J.IMMUNI.2018.06.006

Liao, Y., Smyth, G. K., & Shi, W. (2014). featureCounts: an efficient general purpose program for assigning sequence reads to genomic features. *Bioinformatics*, *30*(7), 923–930. https://doi.org/10.1093/bioinformatics/btt656

Lim, W. A., & June, C. H. (2017). The Principles of Engineering Immune Cells to Treat Cancer. *Cell*, *168*(4), 724–740. https://doi.org/10.1016/j.cell.2017.01.016

Lin, A., Zhang, X., Ruan, Y.-Y., Wang, Q., Zhou, W.-J., & Yan, W.-H. (2011). HLA-F expression is a prognostic factor in patients with non-small-cell lung cancer. *Lung Cancer*, *74*(3), 504–509. https://doi.org/10.1016/j.lungcan.2011.04.006

Linsley, P. S., & Golstein, P. (1996). Lymphocyte activation: T-cell regulation by CTLA-4. *Current Biology*, *6*(4), 398–400. https://doi.org/10.1016/S0960-9822(02)00506-7

Liu, Xiangdong, Shin, N., Koblish, H. K., Yang, G., Wang, Q., Wang, K., … Scherle, P. A. (2010). Selective inhibition of IDO1 effectively regulates mediators of antitumor immunity. *Blood*, *115*(17), 3520–3530. https://doi.org/10.1182/blood-2009-09-246124

Liu, Xin-guang, Hou, M., & Liu, Y. (2017). TIGIT, A Novel Therapeutic Target for Tumor Immunotherapy. *Immunological Investigations*, *46*(2), 172–182. https://doi.org/10.1080/08820139.2016.1237524

Liu, Xindong, Wang, Y., Lu, H., Li, J., Yan, X., Xiao, M., … Dong, C. (2019). Genome-wide analysis identifies NR4A1 as a key mediator of T cell dysfunction. *Nature*, 1. https://doi.org/10.1038/s41586-019-0979-8

Liu, Y., Cheng, Y., Xu, Y., Wang, Z., Du, X., Li, C., … Ma, C. (2017). Increased expression of programmed cell death protein 1 on NK cells inhibits NK-cell-mediated anti-tumor function and indicates poor prognosis in digestive cancers. *Oncogene*, *36*(44), 6143–6153. https://doi.org/10.1038/onc.2017.209

Ljunggren, H.-G., & Malmberg, K.-J. (2007). Prospects for the use of NK cells in immunotherapy of human cancer. *Nature Reviews Immunology*, *7*(5), 329–339. https://doi.org/10.1038/nri2073

Long, A. H., Haso, W. M., Shern, J. F., Wanhainen, K. M., Murgai, M., Ingaramo, M., … Mackall, C. L. (2015). 4-1BB costimulation ameliorates T cell exhaustion induced by tonic signaling of chimeric antigen receptors. *Nature Medicine*, *21*(6), 581–590. https://doi.org/10.1038/nm.3838

López-Soto, A., Gonzalez, S., Smyth, M. J., & Galluzzi, L. (2017). Control of Metastasis by NK Cells. *Cancer Cell*, *32*(2), 135–154. https://doi.org/10.1016/j.ccell.2017.06.009

Lundmark, R., & Carlsson, S. R. (2009). SNX9 - a prelude to vesicle release. *Journal of Cell Science*, *122*(Pt 1), 5–11. https://doi.org/10.1242/jcs.037135

Ma, C., Cheung, A. F., Chodon, T., Koya, R. C., Wu, Z., Ng, C., … Heath, J. R. (2013). Multifunctional T-cell analyses to study response and progression in adoptive cell transfer immunotherapy. *Cancer Discovery*, *3*(4), 418–429. https://doi.org/10.1158/2159-8290.CD-12-0383

MacFarlane, A. W., Jillab, M., Plimack, E. R., Hudes, G. R., Uzzo, R. G., Litwin, S., … Campbell, K. S. (2014). PD-1 Expression on Peripheral Blood Cells Increases with Stage in Renal Cell Carcinoma Patients and Is Rapidly Reduced after Surgical Tumor Resection. *Cancer Immunology Research*, *2*(4), 320–331. https://doi.org/10.3892/etm.2018.5788

Maine, C. J., Teijaro, J. R., Marquardt, K., & Sherman, L. A. (2016). PTPN22 contributes to exhaustion of T lymphocytes during chronic viral infection. *Proceedings of the National Academy of Sciences*, *113*(46), E7231–E7239. https://doi.org/10.1073/pnas.1603738113

Malmberg, K.-J., Sohlberg, E., Goodridge, J. P., & Ljunggren, H.-G. (2017). Immune selection during tumor checkpoint inhibition therapy paves way for NK-cell "missing self" recognition. *Immunogenetics*, *69*(8–9), 547–556. https://doi.org/10.1007/s00251-017-1011-9

Mamessier, E., Sylvain, A., Thibult, M. L., Houvenaeghel, G., Jacquemier, J., Castellano, R., … Olive, D. (2011). Human breast cancer cells enhance self tolerance by promoting evasion from NK cell antitumor immunity. *Journal of Clinical Investigation*, *121*(9), 3609–3622. https://doi.org/10.1172/jci45816

Man, K., Gabriel, S. S., Liao, Y., Gloury, R., Preston, S., Henstridge, D. C., … Kallies, A. (2017). Transcription Factor IRF4 Promotes CD8+T Cell Exhaustion and Limits the Development of Memory-like T Cells during Chronic Infection. *Immunity*, *47*(6), 1129-1141.e5. https://doi.org/10.1016/j.immuni.2017.11.021

Manguso, R. T., Pope, H. W., Zimmer, M. D., Brown, F. D., Yates, K. B., Miller, B. C., … Haining, W. N. (2017). In vivo CRISPR screening identifies Ptpn2 as a cancer immunotherapy target. *Nature*, *547*(7664), 413–418. https://doi.org/10.1038/nature23270

Mantovani, A., Sozzani, S., Locati, M., Allavena, P., & Sica, A. (2002). Macrophage polarization: tumor-associated macrophages as a paradigm for polarized M2 mononuclear phagocytes. *Trends in Immunology*, *23*(11), 549–555. https://doi.org/10.1016/s1471-4906(02)02302-5

Mariathasan, S., Turley, S. J., Nickles, D., Castiglioni, A., Yuen, K., Wang, Y., … Powles, T. (2018). TGFβ attenuates tumour response to PD-L1 blockade by contributing to exclusion of T cells. *Nature*, *554*(7693), 544–548. https://doi.org/10.1038/nature25501

Martin, K., Müller, P., Schreiner, J., Prince, S. S., Lardinois, D., Heinzelmann-Schwarz, V. A., … Zippelius, A. (2014). The microtubule-depolymerizing agent ansamitocin P3 programs dendritic cells toward enhanced anti-tumor immunity. *Cancer Immunology, Immunotherapy*, *63*(9), 925–938. https://doi.org/10.1007/s00262-014-1565-4

Martínez-Usatorre, A., Donda, A., Zehn, D., & Romero, P. (2018). PD-1 Blockade Unleashes Effector Potential of Both High- and Low-Affinity Tumor-Infiltrating T Cells. *The Journal of Immunology*, *201*(2), 792–803.

https://doi.org/10.4049/jimmunol.1701644

Martinez, G. J., Pereira, R. M., Äijö, T., Kim, E. Y., Marangoni, F., Pipkin, M. E., … Rao, A. (2015). The Transcription Factor NFAT Promotes Exhaustion of Activated CD8+ T Cells. *Immunity*, *42*(2), 265–278. https://doi.org/10.1016/J.IMMUNI.2015.01.006

Masoud, G. N., & Li, W. (2015). HIF-1α pathway: role, regulation and intervention for cancer therapy. *Acta Pharmaceutica Sinica B*, *5*(5), 378–389. https://doi.org/10.1016/j.apsb.2015.05.007

Massarelli, E., William, W., Johnson, F., Kies, M., Ferrarotto, R., Guo, M., … Glisson, B. (2019). Combining Immune Checkpoint Blockade and Tumor-Specific Vaccine for Patients With Incurable Human Papillomavirus 16–Related Cancer. *JAMA Oncology*, *5*(1), 67. https://doi.org/10.1001/jamaoncol.2018.4051

Matson, V., Fessler, J., Bao, R., Chongsuwat, T., Zha, Y., Alegre, M.-L., … Gajewski, T. F. (2018). The commensal microbiome is associated with anti-PD-1 efficacy in metastatic melanoma patients. *Science (New York, N.Y.)*, *359*(6371), 104–108. https://doi.org/10.1126/science.aao3290

Matsushita, H., Vesely, M. D., Koboldt, D. C., Rickert, C. G., Uppaluri, R., Magrini, V. J., … Schreiber, R. D. (2012). Cancer exome analysis reveals a T-cell-dependent mechanism of cancer immunoediting. *Nature*, *482*(7385), 400–404. https://doi.org/10.1038/nature10755

Matzinger, P. (1994). Tolerance, Danger, and the Extended Family. *Annual Review of Immunology*, *12*(1), 991–1045. https://doi.org/10.1146/annurev.iy.12.040194.005015

McDermott, D., Lebbé, C., Hodi, F. S., Maio, M., Weber, J. S., Wolchok, J. D., … Balch, C. M. (2014). Durable benefit and the potential for long-term survival with immunotherapy in advanced melanoma. *Cancer Treatment Reviews*, *40*(9), 1056–1064. https://doi.org/10.1016/J.CTRV.2014.06.012

McGranahan, N., Furness, A. J. S., Rosenthal, R., Ramskov, S., Lyngaa, R., Saini, S. K., … Swanton, C. (2016). Clonal neoantigens elicit T cell immunoreactivity and sensitivity to immune checkpoint blockade. *Science*, *351*(6280), 1463–1469. https://doi.org/10.1126/science.aaf1490

McKinney, E. F., Lee, J. C., Jayne, D. R. W., Lyons, P. A., & Smith, K. G. C. (2015). T-cell exhaustion, co-stimulation and clinical outcome in autoimmunity and infection. *Nature*, *523*(7562), 612–616. https://doi.org/10.1038/nature14468

Melero, I., Berman, D. M., Aznar, M. A., Korman, A. J., Gracia, J. L. P., & Haanen, J. (2015, August 1). Evolving synergistic combinations of targeted immunotherapies to combat cancer. *Nature Reviews Cancer*. Nature Publishing Group. https://doi.org/10.1038/nrc3973

Memarnejadian, A., Meilleur, C. E., Shaler, C. R., Khazaie, K., Bennink, J. R., Schell, T. D., & Haeryfar, S. M. M. (2017). PD-1 Blockade Promotes Epitope Spreading in Anticancer CD8+ T Cell Responses by Preventing Fratricidal Death of Subdominant Clones To Relieve Immunodomination. *Journal of Immunology (Baltimore, Md. : 1950)*, *199*(9), 3348–3359. https://doi.org/10.4049/jimmunol.1700643

Meng, X., Liu, X., Guo, X., Jiang, S., Chen, T., Hu, Z., … Xu, C. (2018, December 28). FBXO38 mediates PD-1 ubiquitination and regulates anti-tumour immunity of T cells. *Nature*. Nature Publishing Group. https://doi.org/10.1038/s41586-018-0756-0

Mestas, J., & Hughes, C. C. W. (2004). Of mice and not men: differences between mouse and human immunology. *Journal of Immunology (Baltimore, Md. : 1950)*, *172*(5), 2731–2738. https://doi.org/10.4049/jimmunol.172.5.2731

Migden, M. R., Rischin, D., Schmults, C. D., Guminski, A., Hauschild, A., Lewis, K. D., … Fury, M. G. (2018). PD-1 Blockade with Cemiplimab in Advanced Cutaneous Squamous-Cell Carcinoma. *New England Journal of Medicine*, *379*(4), 341–351. https://doi.org/10.1056/NEJMoa1805131

Miller, B. C., Sen, D. R., Al Abosy, R., Bi, K., Virkud, Y. V., LaFleur, M. W., … Haining, W. N. (2019). Subsets of exhausted CD8+ T cells differentially mediate tumor control and respond to checkpoint blockade. *Nature Immunology*, *20*(3), 326–336. https://doi.org/10.1038/s41590-019-0312-6

Miller, J. F. A. P., Mitchell, G. F., & Weiss, N. S. (1967). Cellular basis of the immunological defects in thymectomized mice. *Nature*, *214*(5092), 992–997. https://doi.org/10.1038/214992a0

Milone, M. C., Fish, J. D., Carpenito, C., Carroll, R. G., Binder, G. K., Teachey, D., … June, C. H. (2009). Chimeric Receptors Containing CD137 Signal Transduction Domains Mediate Enhanced Survival of T Cells and Increased Antileukemic Efficacy In Vivo. *Molecular Therapy*, *17*(8), 1453–1464. https://doi.org/10.1038/MT.2009.83

Molon, B., Ugel, S., Pozzo, F. Del, Soldani, C., Zilio, S., Avella, D., … Viola, A. (2011). Chemokine nitration prevents intratumoral infiltration of antigen-specific T cells. *Journal of Experimental Medicine*, *208*(10), 1949–1962. https://doi.org/10.1084/JEM.20101956

Moretta, A., Bottino, C., Vitale, M., Pende, D., Cantoni, C., Mingari, M. C., … Moretta, L. (2001). Activating receptors and coreceptors involved in human natural killer cell-mediated cytolysis. *Annu Rev Immunol*, *19*, 197–223. https://doi.org/10.1146/annurev.immunol.19.1.197

Morgan, R. A., Dudley, M. E., Wunderlich, J. R., Hughes, M. S., Yang, J. C., Sherry, R. M., … Rosenberg, S. A. (2006). Cancer Regression in Patients After Transfer of Genetically Engineered Lymphocytes. *Science*, *314*(5796), 126–129. https://doi.org/10.1126/science.1129003

Morgan, R. A., Yang, J. C., Kitano, M., Dudley, M. E., Laurencot, C. M., & Rosenberg, S. A. (2010). Case Report of a Serious Adverse Event Following the Administration of T Cells Transduced With a Chimeric Antigen Receptor Recognizing ERBB2. *Molecular Therapy*, *18*(4), 843–851. https://doi.org/10.1038/MT.2010.24

Morgens, D. W., Deans, R. M., Li, A., & Bassik, M. C. (2016). Systematic comparison of CRISPR/Cas9 and RNAi screens for essential genes. *Nature Biotechnology*, *34*(6), 634–636. https://doi.org/10.1038/nbt.3567

Morton, D. L., Mozzillo, N., Thompson, J. F., Kelley, M. C., Faries, M., Wagner, J., … Elashoff, R. (2007). An international, randomized, phase III trial of bacillus Calmette-Guerin (BCG) plus allogeneic melanoma vaccine (MCV) or placebo after complete resection of melanoma metastatic to regional or distant sites. *Journal of Clinical Oncology*, *25*(18_suppl), 8508. https://doi.org/10.1200/jco.2007.25.18_suppl.8508

Morvan, M. G., & Lanier, L. L. (2016). NK cells and cancer: You can teach innate cells new tricks. *Nature Reviews Cancer*, *16*(1), 7–19. https://doi.org/10.1038/nrc.2015.5

Motzer, R. J., Escudier, B., McDermott, D. F., George, S., Hammers, H. J., Srinivas, S., … Sharma, P. (2015). Nivolumab versus Everolimus in Advanced Renal-Cell Carcinoma. *New England Journal of Medicine*, *373*(19), 1803–1813. https://doi.org/10.1056/NEJMoa1510665

Motzer, R. J., Penkov, K., Haanen, J., Rini, B., Albiges, L., Campbell, M. T., … Choueiri, T. K. (2019). Avelumab plus Axitinib versus Sunitinib for Advanced Renal-Cell Carcinoma. *New England Journal of Medicine*, NEJMoa1816047. https://doi.org/10.1056/NEJMoa1816047

Motzer, R. J., Tannir, N. M., McDermott, D. F., Arén Frontera, O., Melichar, B., Choueiri, T. K., … Escudier, B. (2018). Nivolumab plus Ipilimumab versus Sunitinib in Advanced Renal-Cell Carcinoma. *New England Journal of Medicine*, *378*(14), 1277–1290. https://doi.org/10.1056/NEJMoa1712126

Mueller, S. N., & Ahmed, R. (2009). High antigen levels are the cause of T cell exhaustion during chronic viral infection. *Proceedings of the National Academy of Sciences of the United States of America*, *106*(21), 8623–8628.

https://doi.org/10.1073/pnas.0809818106

Müller, P., Kreuzaler, M., Khan, T., Thommen, D. S., Martin, K., Glatz, K., … Zippelius, A. (2015). Trastuzumab emtansine (T-DM1) renders HER2+breast cancer highly susceptible to CTLA-4/PD-1 blockade. *Science Translational Medicine*, *7*(315), 315ra188-315ra188. https://doi.org/10.1126/scitranslmed.aac4925

Nagarsheth, N., Wicha, M. S., & Zou, W. (2017). Chemokines in the cancer microenvironment and their relevance in cancer immunotherapy. *Nature Reviews Immunology*, *17*(9), 559–572. https://doi.org/10.1038/nri.2017.49

Nagorsen, D., & Baeuerle, P. A. (2011). Immunomodulatory therapy of cancer with T cell-engaging BiTE antibody blinatumomab. *Experimental Cell Research*, *317*(9), 1255–1260. https://doi.org/10.1016/J.YEXCR.2011.03.010

Nair, S., Boczkowski, D., Moeller, B., Dewhirst, M., Vieweg, J., & Gilboa, E. (2003). Synergy between tumor immunotherapy and antiangiogenic therapy. *Blood*, *102*(3), 964–971. https://doi.org/10.1182/blood-2002-12-3738

Neal, J. T., Li, X., Zhu, J., Giangarra, V., Grzeskowiak, C. L., Ju, J., … Kuo, C. J. (2018). Organoid Modeling of the Tumor Immune Microenvironment. *Cell*, *175*(7), 1972-1988.e16. https://doi.org/10.1016/j.cell.2018.11.021

Neri, D., & Sondel, P. M. (2016). Immunocytokines for cancer treatment: past, present and future. *Current Opinion in Immunology*, *40*, 96–102. https://doi.org/10.1016/J.COI.2016.03.006

Neubert, N. J., Schmittnaegel, M., Bordry, N., Nassiri, S., Wald, N., Martignier, C., … Speiser, D. E. (2018). T cell-induced CSF1 promotes melanoma resistance to PD1 blockade. *Science Translational Medicine*, *10*(436). https://doi.org/10.1126/scitranslmed.aan3311

Norman, P. J., Hollenbach, J. A., Nemat-Gorgani, N., Marin, W. M., Norberg, S. J., Ashouri, E., … Parham, P. (2016). Defining KIR and HLA Class I Genotypes at Highest Resolution via High-Throughput Sequencing. *The American Journal of Human Genetics*, *99*(2), 375–391. https://doi.org/10.1016/j.ajhg.2016.06.023

O'Donnell, J. S., Teng, M. W. L., & Smyth, M. J. (2019). Cancer immunoediting and resistance to T cell-based immunotherapy. *Nature Reviews Clinical Oncology*, *16*(3), 151–167. https://doi.org/10.1038/s41571-018-0142-8

Odorizzi, P. M., Pauken, K. E., Paley, M. A., Sharpe, A., & Wherry, E. J. (2015). Genetic absence of PD-1 promotes accumulation of terminally differentiated exhausted CD8 $^+$ T cells. *The Journal of Experimental Medicine*, *212*(7), 1125–1137. https://doi.org/10.1084/jem.20142237

Ohashi, T., Akazawa, T., Aoki, M., Kuze, B., Mizuta, K., Ito, Y., & Inoue, N. (2013). Dichloroacetate improves immune dysfunction caused by tumor-secreted lactic acid and increases antitumor immunoreactivity. *International Journal of Cancer*, *133*(5), 1107–1118. https://doi.org/10.1002/ijc.28114

Okazaki, T., & Honjo, T. (2007). PD-1 and PD-1 ligands: from discovery to clinical application. *International Immunology*, *19*(7), 813–824. https://doi.org/10.1093/intimm/dxm057

Okazaki, Taku, & Wang, J. (2005). PD-1/PD-L pathway and autoimmunity. *Autoimmunity*, *38*(5), 353–357. https://doi.org/10.1080/08916930500124072

Östman, A., & Augsten, M. (2009). Cancer-associated fibroblasts and tumor growth – bystanders turning into key players. *Current Opinion in Genetics & Development*, *19*(1), 67–73. https://doi.org/10.1016/J.GDE.2009.01.003

Ott, P. A., Hu, Z., Keskin, D. B., Shukla, S. A., Sun, J., Bozym, D. J., … Wu, C. J. (2017). An immunogenic personal neoantigen vaccine for patients with melanoma. *Nature*, *547*(7662), 217–221. https://doi.org/10.1038/nature22991

Pagès, F., Mlecnik, B., Marliot, F., Bindea, G., Ou, F. S., Bifulco, C., … Galon, J. (2018). International validation of the consensus Immunoscore for the classification of colon cancer: a prognostic and accuracy study. *The Lancet*, *391*(10135), 2128–2139. https://doi.org/10.1016/S0140-6736(18)30789-X

Palucka, A. K., & Coussens, L. M. (2016). The Basis of Oncoimmunology. *Cell*, *164*(6), 1233–1247. https://doi.org/10.1016/j.cell.2016.01.049

Pan, D., Pan, D., Kobayashi, A., Jiang, P., Andrade, L. F. De, Tay, R. E., … Wucherpfennig, K. W. (2018). A major chromatin regulator determines resistance of tumor cells to T cell – mediated killing, *1710*(January), 1–12. https://doi.org/10.1126/science.aao1710

Parham, P., Norman, P. J., Abi-Rached, L., & Guethlein, L. A. (2011). Variable NK Cell Receptors Exemplified by Human KIR3DL1/S1. *The Journal of Immunology*, *187*(1), 11–19. https://doi.org/10.4049/jimmunol.0902332

Park, J. H., Rivière, I., Gonen, M., Wang, X., Sénéchal, B., Curran, K. J., … Sadelain, M. (2018). Long-term follow-up of CD19 CAR therapy in acute lymphoblastic leukemia. *New England Journal of Medicine*, *378*(5), 449–459. https://doi.org/10.1056/NEJMoa1709919

Patel, S. J., Sanjana, N. E., Kishton, R. J., Eidizadeh, A., Vodnala, S. K., Cam, M., … Restifo, N. P. (2017). Identification of essential genes for cancer immunotherapy. *Nature*, *548*(7669), 537–542. https://doi.org/10.1038/nature23477

Patel, S. P., & Kurzrock, R. (2015). PD-L1 Expression as a Predictive Biomarker in Cancer Immunotherapy. *Molecular Cancer Therapeutics*, *14*(4), 847–856. https://doi.org/10.1158/1535-7163.MCT-14-0983

Patsoukis, N., Bardhan, K., Chatterjee, P., Sari, D., Liu, B., Bell, L. N., … Boussiotis, V. A. (2015). PD-1 alters T-cell metabolic reprogramming by inhibiting glycolysis and promoting lipolysis and fatty acid oxidation. *Nature Communications*, *6*(1), 6692. https://doi.org/10.1038/ncomms7692

Pauken, K. E., Sammons, M. A., Odorizzi, P. M., Manne, S., Godec, J., Khan, O., … Wherry, E. J. (2016). Epigenetic stability of exhausted T cells limits durability of reinvigoration by PD-1 blockade. *Science*, *354*(6316), 1160–1165. https://doi.org/10.1126/science.aaf2807

Paz-Ares, L., Luft, A., Vicente, D., Tafreshi, A., Gümüş, M., Mazières, J., … Kowalski, D. M. (2018). Pembrolizumab plus chemotherapy for squamous non-small-cell lung cancer. *New England Journal of Medicine*, *379*(21), 2040–2051. https://doi.org/10.1056/NEJMoa1810865

Pedersen, S. R., Sørensen, M. R., Buus, S., Christensen, J. P., & Thomsen, A. R. (2013). Comparison of Vaccine-Induced Effector CD8 T Cell Responses Directed against Self- and Non–Self-Tumor Antigens: Implications for Cancer Immunotherapy. *The Journal of Immunology*, *191*(7), 3955–3967. https://doi.org/10.4049/jimmunol.1300555

Peng, D., Kryczek, I., Nagarsheth, N., Zhao, L., Wei, S., Wang, W., … Zou, W. (2015). Epigenetic silencing of TH1-type chemokines shapes tumour immunity and immunotherapy. *Nature*, *527*(7577), 249–253. https://doi.org/10.1038/nature15520

Pereira, C., Gimenez-Xavier, P., Pros, E., Pajares, M. J., Moro, M., Gomez, A., … Sanchez-Cespedes, M. (2017). Genomic Profiling of Patient-Derived Xenografts for Lung Cancer Identifies B2M Inactivation Impairing Immunorecognition. *Clinical Cancer Research : An Official Journal of the American Association for Cancer Research*, *23*(12), 3203–3213. https://doi.org/10.1158/1078-0432.CCR-16-1946

Perrot, I., Michaud, H. A., Giraudon-Paoli, M., Augier, S., Docquier, A., Gros, L., … Bonnefoy, N. (2019). Blocking Antibodies Targeting the CD39/CD73 Immunosuppressive Pathway Unleash Immune Responses in Combination Cancer Therapies. *Cell Reports*, *27*(8), 2411-2425.e9. https://doi.org/10.1016/j.celrep.2019.04.091

Pesce, S., Greppi, M., Tabellini, G., Rampinelli, F., Parolini, S., Olive, D., … Marcenaro, E. (2017). Identification of a subset of human natural killer cells expressing high levels of programmed death 1: A phenotypic and functional characterization.

Journal of Allergy and Clinical Immunology, *139*(1), 335-346.e3. https://doi.org/10.1016/j.jaci.2016.04.025

Pfirschke, C., Engblom, C., Rickelt, S., Cortez-Retamozo, V., Garris, C., Pucci, F., … Pittet, M. J. (2016). Immunogenic Chemotherapy Sensitizes Tumors to Checkpoint Blockade Therapy. *Immunity*, *44*(2), 343–354. https://doi.org/10.1016/J.IMMUNI.2015.11.024

Philip, M., Fairchild, L., Sun, L., Horste, E. L., Camara, S., Shakiba, M., … Schietinger, A. (2017). Chromatin states define tumour-specific T cell dysfunction and reprogramming. *Nature*, *545*(7655), 452–456. https://doi.org/10.1038/nature22367

Pitt, J. M., Kroemer, G., & Zitvogel, L. (2017). Immunogenic and non-immunogenic cell death in the tumor microenvironment. In *Advances in Experimental Medicine and Biology* (Vol. 1036, pp. 65–79). Springer, Cham. https://doi.org/10.1007/978-3-319-67577-0_5

Place, T. L., Domann, F. E., & Case, A. J. (2017). Limitations of oxygen delivery to cells in culture: An underappreciated problem in basic and translational research. *Free Radical Biology and Medicine*, *113*, 311–322. https://doi.org/10.1016/j.freeradbiomed.2017.10.003

Platonova, S., Cherfils-Vicini, J., Damotte, D., Crozet, L., Vieillard, V., Validire, P., … Cremer, I. (2011). Profound coordinated alterations of intratumoral NK cell phenotype and function in lung carcinoma. *Cancer Research*, *71*(16), 5412–5422. https://doi.org/10.1158/0008-5472.CAN-10-4179

Pol, J., Kroemer, G., & Galluzzi, L. (2016). First oncolytic virus approved for melanoma immunotherapy. *OncoImmunology*, *5*(1), e1115641. https://doi.org/10.1080/2162402X.2015.1115641

Porter, D. L., Levine, B. L., Kalos, M., Bagg, A., & June, C. H. (2011). Chimeric antigen receptor-modified T cells in chronic lymphoid leukemia. *New England Journal of Medicine*, *365*(8), 725–733. https://doi.org/10.1056/NEJMoa1103849

Postow, M. A., Chesney, J., Pavlick, A. C., Robert, C., Grossmann, K., McDermott, D., … Hodi, F. S. (2015). Nivolumab and Ipilimumab versus Ipilimumab in Untreated Melanoma. *New England Journal of Medicine*, *372*(21), 2006–2017. https://doi.org/10.1056/NEJMoa1414428

Przepiorka, D., Ko, C.-W., Deisseroth, A., Yancey, C. L., Candau-Chacon, R., Chiu, H.-J., … Pazdur, R. (2015). FDA Approval: Blinatumomab. *Clinical Cancer Research*, *21*(18), 4035–4039. https://doi.org/10.1158/1078-0432.CCR-15-0612

Qin, Z., Schwartzkopff, J., Pradera, F., Kammertoens, T., Seliger, B., Pircher, H., & Blankenstein, T. (2003). A critical requirement of interferon gamma-mediated angiostasis for tumor rejection by CD8+ T cells. *Cancer Research*, *63*(14), 4095–4100. Retrieved from http://www.ncbi.nlm.nih.gov/pubmed/12874012

Quatrini, L., Wieduwild, E., Escaliere, B., Filtjens, J., Chasson, L., Laprie, C., … Ugolini, S. (2018). Endogenous glucocorticoids control host resistance to viral infection through the tissue-specific regulation of PD-1 expression on NK cells. *Nature Immunology*, *19*(9), 954–962. https://doi.org/10.1038/s41590-018-0185-0

Radoja, S., Saio, M., Schaer, D., Koneru, M., Vukmanovic, S., & Frey, A. B. (2001). CD8 + Tumor-Infiltrating T Cells Are Deficient in Perforin-Mediated Cytolytic Activity Due to Defective Microtubule-Organizing Center Mobilization and Lytic Granule Exocytosis. *The Journal of Immunology*, *167*(9), 5042–5051. https://doi.org/10.4049/jimmunol.167.9.5042

Rangarajan, A., & Weinberg, R. A. (2003). Comparative biology of mouse versus human cells: modelling human cancer in mice. *Nature Reviews Cancer*, *3*(12), 952–959. https://doi.org/10.1038/nrc1235

Rapoport, A. P., Stadtmauer, E. A., Binder-Scholl, G. K., Goloubeva, O., Vogl, D. T., Lacey, S. F., … June, C. H. (2015). NY-ESO-1–specific TCR–engineered T cells mediate sustained antigen-specific antitumor effects in myeloma. *Nature Medicine*, *21*(8), 914–921. https://doi.org/10.1038/nm.3910

Raulet, D. H., & Vance, R. E. (2006). Self-tolerance of natural killer cells. *Nature Reviews Immunology*, *6*(7), 520–531. https://doi.org/10.1038/nri1863

Reck, M., Rodriguez-Abreu, D., Robinson, A. G., Hui, R., Csöszi, T., Fülöp, A., … Brahmer, J. R. (2016). Pembrolizumab versus Chemotherapy for PD-L1-Positive Non-Small-Cell Lung Cancer. *New England Journal of Medicine*, *375*(19), 1823–1833. https://doi.org/10.1056/NEJMoa1606774

Reck, M., Rodríguez-Abreu, D., Robinson, A. G., Hui, R., Csőszi, T., Fülöp, A., … Brahmer, J. R. (2016). Pembrolizumab versus Chemotherapy for PD-L1–Positive Non–Small-Cell Lung Cancer. *New England Journal of Medicine*, *375*(19), 1823–1833. https://doi.org/10.1056/NEJMoa1606774

Remark, R., Alifano, M., Cremer, I., Lupo, A., Dieu-Nosjean, M.-C., Riquet, M., … Damotte, D. (2013). Characteristics and clinical impacts of the immune environments in colorectal and renal cell carcinoma lung metastases: influence of tumor origin. *Clinical Cancer Research : An Official Journal of the American Association for Cancer Research*, *19*(15), 4079–4091. https://doi.org/10.1158/1078-0432.CCR-12-3847

Ren, J., Liu, X., Fang, C., Jiang, S., June, C. H., & Zhao, Y. (2017). Multiplex Genome Editing to Generate Universal CAR T Cells Resistant to PD1 Inhibition. *Clinical Cancer Research*, *23*(9), 2255–2266. https://doi.org/10.1158/1078-0432.CCR-16-1300

Ribas, A., Hamid, O., Daud, A., Hodi, F. S., Wolchok, J. D., Kefford, R., … Robert, C. (2016). Association of Pembrolizumab With Tumor Response and Survival Among Patients With Advanced Melanoma. *JAMA*, *315*(15), 1600. https://doi.org/10.1001/jama.2016.4059

Ribas, A., & Wolchok, J. D. (2018, March 23). Cancer immunotherapy using checkpoint blockade. *Science*. American Association for the Advancement of Science. https://doi.org/10.1126/science.aar4060

Ritter, A. T., Asano, Y., Stinchcombe, J. C., Dieckmann, N. M. G., Chen, B.-C., Gawden-Bone, C., … Griffiths, G. M. (2015). Actin Depletion Initiates Events Leading to Granule Secretion at the Immunological Synapse. *Immunity*, *42*(5), 864–876. https://doi.org/10.1016/J.IMMUNI.2015.04.013

Ritter, A. T., Kapnick, S. M., Murugesan, S., Schwartzberg, P. L., Griffiths, G. M., & Lippincott-Schwartz, J. (2017). Cortical actin recovery at the immunological synapse leads to termination of lytic granule secretion in cytotoxic T lymphocytes. *Proceedings of the National Academy of Sciences*, *114*(32), E6585–E6594. https://doi.org/10.1073/PNAS.1710751114

Rizvi, N. A., Hellmann, M. D., Snyder, A., Kvistborg, P., Makarov, V., Havel, J. J., … Chan, T. A. (2015). Mutational landscape determines sensitivity to PD-1 blockade in non-small cell lung cancer. *Science*, *348*(6230), 124–128. https://doi.org/10.1126/science.aaa1348

Rizzuto, G. A., Merghoub, T., Hirschhorn-Cymerman, D., Liu, C., Lesokhin, A. M., Sahawneh, D., … Houghton, A. N. (2009). Self-antigen-specific CD8+ T cell precursor frequency determines the quality of the antitumor immune response. *The Journal of Experimental Medicine*, *206*(4), 849–866. https://doi.org/10.1084/jem.20081382

Robert, C., Long, G. V., Brady, B., Dutriaux, C., Maio, M., Mortier, L., … Ascierto, P. A. (2015). Nivolumab in Previously Untreated Melanoma without *BRAF* Mutation. *New England Journal of Medicine*, *372*(4), 320–330. https://doi.org/10.1056/NEJMoa1412082

Robert, C., Schachter, J., Long, G. V., Arance, A., Grob, J. J., Mortier, L., … Ribas, A. (2015). Pembrolizumab versus Ipilimumab in Advanced Melanoma. *New England Journal of Medicine*, *372*(26), 2521–2532. https://doi.org/10.1056/NEJMoa1503093

Roden, R. B. S., & Stern, P. L. (2018). Opportunities and challenges for human papillomavirus vaccination in cancer. *Nature Reviews Cancer*, *18*(4), 240–254. https://doi.org/10.1038/nrc.2018.13

Rodig, S. J., Gusenleitner, D., Jackson, D. G., Gjini, E., Giobbie-Hurder, A., Jin, C., … Hodi, F. S. (2018). MHC proteins confer

differential sensitivity to CTLA-4 and PD-1 blockade in untreated metastatic melanoma. *Science Translational Medicine*, *10*(450), eaar3342. https://doi.org/10.1126/scitranslmed.aar3342

Rodríguez, E., Schetters, S. T. T., & Van Kooyk, Y. (2018, March 5). The tumour glyco-code as a novel immune checkpoint for immunotherapy. *Nature Reviews Immunology*. Nature Publishing Group. https://doi.org/10.1038/nri.2018.3

Rodriguez, P. C., Quiceno, D. G., & Ochoa, A. C. (2007). l-arginine availability regulates T-lymphocyte cell-cycle progression. *Blood*, *109*(4), 1568–1573. https://doi.org/10.1182/blood-2006-06-031856

Rohaan, M. W., van den Berg, J. H., Kvistborg, P., & Haanen, J. B. A. G. (2018). Adoptive transfer of tumor-infiltrating lymphocytes in melanoma: a viable treatment option. *Journal for ImmunoTherapy of Cancer*, *6*(1), 102. https://doi.org/10.1186/s40425-018-0391-1

Rohaan, M. W., Wilgenhof, S., & Haanen, J. B. A. G. (2019). Adoptive cellular therapies: the current landscape. *Virchows Archiv*, *474*(4), 449–461. https://doi.org/10.1007/s00428-018-2484-0

Romero, P., Banchereau, J., Bhardwaj, N., Cockett, M., Disis, M. L., Dranoff, G., … Couko, G. (2016, April 13). The human vaccines project: A roadmap for cancer vaccine development. *Science Translational Medicine*. American Association for the Advancement of Science. https://doi.org/10.1126/scitranslmed.aaf0685

Romero, P., Dunbar, P. R., Valmori, D., Pittet, M., Ogg, G. S., Rimoldi, D., … Cerundolo, V. (1998). Ex vivo staining of metastatic lymph nodes by class I major histocompatibility complex tetramers reveals high numbers of antigen-experienced tumor-specific cytolytic T lymphocytes. *The Journal of Experimental Medicine*, *188*(9), 1641–1650. https://doi.org/10.1084/jem.188.9.1641

Romero, P., Dutoit, V., Rubio-Godoy, V., Liénard, D., Speiser, D., Guillaume, P., … Valmori, D. (2001). CD8+ T-cell response to NY-ESO-1: Relative antigenicity and in vitro immunogenicity of natural and analogue sequences. *Clinical Cancer Research*, *7*(11 SUPPL.), 766–772.

Rooney, M. S. S., Shukla, S. A. A., Wu, C. J. J., Getz, G., & Hacohen, N. (2015). Molecular and genetic properties of tumors associated with local immune cytolytic activity. *Cell*, *160*(1–2), 48–61. https://doi.org/10.1016/j.cell.2014.12.033

Rosenberg, S A, Spiess, P., & Lafreniere, R. (1986). A new approach to the adoptive immunotherapy of cancer with tumor-infiltrating lymphocytes. *Science (New York, N.Y.)*, *233*(4770), 1318–1321. Retrieved from http://www.ncbi.nlm.nih.gov/pubmed/3489291

Rosenberg, Steven A. Progress in human tumour immunology and immunotherapy, 411 § (2001). Nature Publishing Group. https://doi.org/10.1038/35077246

Rosenberg, Steven A. (2011). Cell transfer immunotherapy for metastatic solid cancer—what clinicians need to know. *Nature Reviews Clinical Oncology*, *8*(10), 577–585. https://doi.org/10.1038/nrclinonc.2011.116

Rosenberg, Steven A., & Restifo, N. P. (2015, April 3). Adoptive cell transfer as personalized immunotherapy for human cancer. *Science*. https://doi.org/10.1126/science.aaa4967

Rota, G., Niogret, C., Dang, A. T., Barros, C. R., Fonta, N. P., Alfei, F., … Guarda, G. (2018). Shp-2 Is Dispensable for Establishing T Cell Exhaustion and for PD-1 Signaling In Vivo. *Cell Reports*, *23*(1), 39–49. https://doi.org/10.1016/j.celrep.2018.03.026

Rottman, J. B., & Horvath, C. J. (2017). ROR1-Directed Chimeric Antigen Receptor T Cell Recognition of Self-Antigen Is Associated with Acute Toxicity, T Cell Dysfunction, and Poor Tumor Control. In *ASH* (Vol. 130, pp. 4450–4450). American Society of Hematology. https://doi.org/10.1182/BLOOD.V130.SUPPL_1.4450.4450

Routy, B., Le Chatelier, E., Derosa, L., Duong, C. P. M., Alou, M. T., Daillère, R., … Zitvogel, L. (2018). Gut microbiome influences efficacy of PD-1-based immunotherapy against epithelial tumors. *Science (New York, N.Y.)*, *359*(6371), 91–97. https://doi.org/10.1126/science.aan3706

Roy Baynes. (2018). Incyte and Merck Provide Update on Phase 3 Study of Epacadostat in Combination with KEYTRUDA® (pembrolizumab) in Patients with Unresectable or Metastatic Melanoma. Retrieved November 14, 2019, from https://investors.merck.com/news/press-release-details/2018/Incyte-and-Merck-Provide-Update-on-Phase-3-Study-of-Epacadostat-in-Combination-with-KEYTRUDA-pembrolizumab-in-Patients-with-Unresectable-or-Metastatic-Melanoma/default.aspx

Ruella, M., Barrett, D. M., Kenderian, S. S., Shestova, O., Hofmann, T. J., Perazzelli, J., … Gill, S. (2016). Dual CD19 and CD123 targeting prevents antigen-loss relapses after CD19-directed immunotherapies. *Journal of Clinical Investigation*, *126*(10), 3814–3826. https://doi.org/10.1172/JCI87366

Rupp, L. J., Schumann, K., Roybal, K. T., Gate, R. E., Ye, C. J., Lim, W. A., & Marson, A. (2017). CRISPR/Cas9-mediated PD-1 disruption enhances anti-Tumor efficacy of human chimeric antigen receptor T cells. *Scientific Reports*, *7*(1), 737. https://doi.org/10.1038/s41598-017-00462-8

Sade-Feldman, M., Yizhak, K., Bjorgaard, S. L., Ray, J. P., de Boer, C. G., Jenkins, R. W., … Hacohen, N. (2018). Defining T Cell States Associated with Response to Checkpoint Immunotherapy in Melanoma. *Cell*, *175*(4), 998-1013.e20. https://doi.org/10.1016/j.cell.2018.10.038

Sahin, U., Derhovanessian, E., Miller, M., Kloke, B.-P., Simon, P., Löwer, M., … Türeci, Ö. (2017). Personalized RNA mutanome vaccines mobilize poly-specific therapeutic immunity against cancer. *Nature*, *547*(7662), 222–226. https://doi.org/10.1038/nature23003

Sakuishi, K., Apetoh, L., Sullivan, J. M., Blazar, B. R., Kuchroo, V. K., & Anderson, A. C. (2010). Targeting Tim-3 and PD-1 pathways to reverse T cell exhaustion and restore anti-tumor immunity. *Journal of Experimental Medicine*, *207*(10), 2187–2194. https://doi.org/10.1084/jem.20100643

Salter, R. D., & Cresswell, P. (1986). Impaired assembly and transport of HLA-A and -B antigens in a mutant TxB cell hybrid. *The EMBO Journal*, *5*(5), 943–949. Retrieved from http://www.ncbi.nlm.nih.gov/pubmed/3522223

Samaha, H., Pignata, A., Fousek, K., Ren, J., Lam, F. W., Stossi, F., … Ahmed, N. (2018). A homing system targets therapeutic T cells to brain cancer. *Nature*, *561*(7723), 331–337. https://doi.org/10.1038/s41586-018-0499-y

Sánchez-Paulete, A. R., Teijeira, A., Cueto, F. J., Garasa, S., Pérez-Gracia, J. L., Sánchez-Arráez, A., … Melero, I. (2017). Antigen cross-presentation and T-cell cross-priming in cancer immunology and immunotherapy. *Annals of Oncology*, *28*(suppl_12), xii44–xii55. https://doi.org/10.1093/annonc/mdx237

Satpathy, A. T., Granja, J. M., Yost, K. E., Qi, Y., Meschi, F., McDermott, G. P., … Chang, H. Y. (2019). Massively parallel single-cell chromatin landscapes of human immune cell development and intratumoral T cell exhaustion. *Nature Biotechnology*, *37*(8), 925–936. https://doi.org/10.1038/s41587-019-0206-z

Savas, P., Virassamy, B., Ye, C., Salim, A., Mintoff, C. P., Caramia, F., … Loi, S. (2018). Single-cell profiling of breast cancer T cells reveals a tissue-resident memory subset associated with improved prognosis. *Nature Medicine*, *24*(7), 986–993. https://doi.org/10.1038/s41591-018-0078-7

Savic Prince, S., & Bubendorf, L. (2019). Predictive potential and need for standardization of PD-L1 immunohistochemistry. *Virchows Archiv*, *474*(4), 475–484. https://doi.org/10.1007/s00428-018-2445-7

Scharping, N. E. E., Menk, A. V. V., Moreci, R. S. S., Whetstone, R. D. D., Dadey, R. E. E., Watkins, S. C. C., … Delgoffe, G. M. M. (2016). The Tumor Microenvironment Represses T Cell Mitochondrial Biogenesis to Drive Intratumoral T Cell Metabolic

Insufficiency and Dysfunction. *Immunity*, *45*(2), 374–388. https://doi.org/10.1016/j.immuni.2016.07.009

Scharping, N. E., Menk, A. V., Whetstone, R. D., Zeng, X., & Delgoffe, G. M. (2017). Efficacy of PD-1 blockade is potentiated by metformin-induced reduction of tumor hypoxia. *Cancer Immunology Research*, *5*(1), 9–16. https://doi.org/10.1158/2326-6066.CIR-16-0103

Schietinger, A., & Greenberg, P. D. (2014). Tolerance and exhaustion: Defining mechanisms of T cell dysfunction. *Trends in Immunology*, *35*(2), 51–60. https://doi.org/10.1016/j.it.2013.10.001

Schietinger, A., Philip, M., Krisnawan, V. E., Chiu, E. Y., Delrow, J. J., Basom, R. S., … Greenberg, P. D. (2016). Tumor-Specific T Cell Dysfunction Is a Dynamic Antigen-Driven Differentiation Program Initiated Early during Tumorigenesis. *Immunity*, *45*(2), 389–401. https://doi.org/10.1016/j.immuni.2016.07.011

Schmid, D. A., Irving, M. B., Posevitz, V., Hebeisen, M., Posevitz-Fejfar, A., Sarria, J. C. F., … Rufer, N. (2010). Evidence for a TCR Affinity Threshold Delimiting Maximal CD8 T Cell Function. *The Journal of Immunology*, *184*(9), 4936–4946. https://doi.org/10.4049/jimmunol.1000173

Schneider, L. (2019). Texas Photoshop Massacre (in Nature). Retrieved November 14, 2019, from https://forbetterscience.com/2019/01/14/texas-photoshop-massacre-in-nature/

Schreiber, R. D., Old, L. J., & Smyth, M. J. (2011). Cancer Immunoediting: Integrating Immunity's Roles in Cancer Suppression and Promotion. *Science*, *331*(6024), 1565–1570. https://doi.org/10.1126/science.1203486

Schumacher, T. N., & Schreiber, R. D. (2015). Neoantigens in cancer immunotherapy. *Science*, *348*(6230), 69–74. https://doi.org/10.1126/science.aaa4971

Schwartz, R. H. (2003). T Cell Anergy. *Annual Review of Immunology*, *21*(1), 305–334. https://doi.org/10.1146/annurev.immunol.21.120601.141110

Sconocchia, G., Arriga, R., Tornillo, L., Terracciano, L., Ferrone, S., & Spagnoli, G. C. (2012). Melanoma Cells Inhibit NK Cell Functions--Letter. *Cancer Research*, *72*(20), 5428–5429. https://doi.org/10.1158/0008-5472.CAN-12-1181

Scott, A. C., Dündar, F., Zumbo, P., Chandran, S. S., Klebanoff, C. A., Shakiba, M., … Schietinger, A. (2019). TOX is a critical regulator of tumour-specific T cell differentiation. *Nature*, *571*(7764), 270–274. https://doi.org/10.1038/s41586-019-1324-y

Screpanti, V., Wallin, R. P. A., Grandien, A., & Ljunggren, H.-G. (2005). Impact of FASL-induced apoptosis in the elimination of tumor cells by NK cells. *Molecular Immunology*, *42*(4), 495–499. https://doi.org/10.1016/j.molimm.2004.07.033

Seidel, U. J. E., Schlegel, P., & Lang, P. (2013). Natural killer cell mediated antibody-dependent cellular cytotoxicity in tumor immunotherapy with therapeutic antibodies. *Frontiers in Immunology*, *4*(MAR), 1–8. https://doi.org/10.3389/fimmu.2013.00076

Sen, D. R., Kaminski, J., Barnitz, R. A., Kurachi, M., Gerdemann, U., Yates, K. B., … Haining, W. N. (2016). The epigenetic landscape of T cell exhaustion. *Science*, *354*(6316), 1165–1169. https://doi.org/10.1126/science.aae0491

Shankaran, V., Ikeda, H., Bruce, A. T., White, J. M., Swanson, P. E., Old, L. J., & Schreiber, R. D. (2001). IFNγ and lymphocytes prevent primary tumour development and shape tumour immunogenicity. *Nature*, *410*(6832), 1107–1111. https://doi.org/10.1038/35074122

Sharma, A., Subudhi, S. K., Blando, J., Scutti, J., Vence, L., Wargo, J., … Sharma, P. (2019). Anti-CTLA-4 Immunotherapy Does Not Deplete FOXP3 + Regulatory T Cells (Tregs) in Human Cancers. *Clinical Cancer Research*, *25*(4), 1233–1238. https://doi.org/10.1158/1078-0432.CCR-18-0762

Sharma, P., Hu-Lieskovan, S., Wargo, J. A., & Ribas, A. (2017). Primary, Adaptive, and Acquired Resistance to Cancer Immunotherapy. *Cell*, *168*(4), 707–723. https://doi.org/10.1016/j.cell.2017.01.017

Shay, T., Jojic, V., Zuk, O., Rothamel, K., Puyraimond-Zemmour, D., Feng, T., … ImmGen Consortium, the I. (2013). Conservation and divergence in the transcriptional programs of the human and mouse immune systems. *Proceedings of the National Academy of Sciences of the United States of America*, *110*(8), 2946–2951. https://doi.org/10.1073/pnas.1222738110

Shifrin, N., Raulet, D. H., & Ardolino, M. (2014). NK cell self tolerance, responsiveness and missing self recognition. *Seminars in Immunology*, *26*(2), 138–144. https://doi.org/10.1016/j.smim.2014.02.007

Shifrut, E., Carnevale, J., Tobin, V., Roth, T. L., Woo, J. M., Bui, C. T., … Marson, A. (2018). Genome-wide CRISPR Screens in Primary Human T Cells Reveal Key Regulators of Immune Function. *Cell*, 384776. https://doi.org/10.1016/j.cell.2018.10.024

Shin, D. S., Zaretsky, J. M., Escuin-Ordinas, H., Garcia-Diaz, A., Hu-Lieskovan, S., Kalbasi, A., … Ribas, A. (2017). Primary resistance to PD-1 blockade mediated by JAK1/2 mutations. *Cancer Discovery*, *7*(2), 188–201. https://doi.org/10.1158/2159-8290.CD-16-1223

Shin, N., Lee, S., Ahn, N., Kim, S. A., Ahn, S. G., YongPark, Z., & Chang, S. (2007). Sorting nexin 9 interacts with dynamin 1 and N-WASP and coordinates synaptic vesicle endocytosis. *Journal of Biological Chemistry*, *282*(39), 28939–28950. https://doi.org/10.1074/jbc.M700283200

Sica, G. L., Choi, I. H., Zhu, G., Tamada, K., Wang, S. D., Tamura, H., … Chen, L. (2003). B7-H4, a Molecule of the B7 Family, Negatively Regulates T Cell Immunity. *Immunity*, *18*(6), 849–861. https://doi.org/10.1016/S1074-7613(03)00152-3

Siddiqui, I., Schaeuble, K., Chennupati, V., Marraco, S. A. F., Calderon-copete, S., Ferreira, D. P., … Held, W. (2019). Intratumoral Tcf1+PD-1+CD8+ T Cells with Stem-like Properties Promote Tumor Control in Response to Vaccination and Checkpoint Blockade Immunotherapy. *Immunity*, *50*(1), 1–17. https://doi.org/10.1016/j.immuni.2018.12.021

Silva-Vilches, C., Ring, S., & Mahnke, K. (2018, November 9). ATP and its metabolite adenosine as regulators of dendritic cell activity. *Frontiers in Immunology*. Frontiers. https://doi.org/10.3389/fimmu.2018.02581

Simon, S., Vignard, V., Florenceau, L., Dreno, B., Khammari, A., Lang, F., & Labarriere, N. (2016). PD-1 expression conditions T cell avidity within an antigen-specific repertoire. *OncoImmunology*, *5*(1), e1104448. https://doi.org/10.1080/2162402x.2015.1104448

Simpson, T. R., Li, F., Montalvo-Ortiz, W., Sepulveda, M. A., Bergerhoff, K., Arce, F., … Quezada, S. A. (2013). Fc-dependent depletion of tumor-infiltrating regulatory T cells co-defines the efficacy of anti-CTLA-4 therapy against melanoma. *The Journal of Experimental Medicine*, *210*(9), 1695–1710. https://doi.org/10.1084/jem.20130579

Singh, S., Ross, S. R., Acena, M., Rowley, D. A., & Schreiber, H. (1992). Stroma is critical for preventing or permitting immunological destruction of antigenic cancer cells. *The Journal of Experimental Medicine*, *175*(1), 139–146. https://doi.org/10.1084/jem.175.1.139

Siska, P. J., Beckermann, K. E., Mason, F. M., Andrejeva, G., Greenplate, A. R., Sendor, A. B., … Rathmell, J. C. (2017). Mitochondrial dysregulation and glycolytic insufficiency functionally impair CD8 T cells infiltrating human renal cell carcinoma. *JCI Insight*, *2*(12). https://doi.org/10.1172/jci.insight.93411

Skoulidis, F., Goldberg, M. E., Greenawalt, D. M., Hellmann, M. D., Awad, M. M., Gainor, J. F., … Heymach, J. V. (2018). STK11/LKB1 Mutations and PD-1 Inhibitor Resistance in KRAS -Mutant Lung Adenocarcinoma. *Cancer Discovery*, *8*(7), 822–835. https://doi.org/10.1158/2159-8290.CD-18-0099

Smith, C. C., Beckermann, K. E., Bortone, D. S., Cubas, A. A., Bixby, L. M., Lee, S. J., … Vincent, B. G. (2018). Endogenous retroviral signatures predict immunotherapy response in clear cell renal cell carcinoma. *Journal of Clinical Investigation*,

128(11), 4804–4820. https://doi.org/10.1172/JCI121476

Smith, C. C., Selitsky, S. R., Chai, S., Armistead, P. M., Vincent, B. G., & Serody, J. S. (2019). Alternative tumour-specific antigens. *Nature Reviews Cancer*, *19*(8), 465–478. https://doi.org/10.1038/s41568-019-0162-4

Snyder, A., Makarov, V., Merghoub, T., Yuan, J., Zaretsky, J. M., Desrichard, A., … Chan, T. A. (2014). Genetic Basis for Clinical Response to CTLA-4 Blockade in Melanoma. *New England Journal of Medicine*, *371*(23), 2189–2199. https://doi.org/10.1056/NEJMoa1406498

Socinski, M. A., Jotte, R. M., Cappuzzo, F., Orlandi, F., Stroyakovskiy, D., Nogami, N., … Reck, M. (2018). Atezolizumab for First-Line Treatment of Metastatic Nonsquamous NSCLC. *New England Journal of Medicine*, *378*(24), 2288–2301. https://doi.org/10.1056/NEJMoa1716948

Sotillo, E., Barrett, D. M., Black, K. L., Bagashev, A., Oldridge, D., Wu, G., … Thomas-Tikhonenko, A. (2015). Convergence of acquired mutations and alternative splicing of CD19 enables resistance to CART-19 immunotherapy. *Cancer Discovery*, *5*(12), 1282–1295. https://doi.org/10.1158/2159-8290.CD-15-1020

Sotomayor, E. M., Borrello, I., Tubb, E., Allison, J. P., & Levitsky, H. I. (1999). In vivo blockade of CTLA-4 enhances the priming of responsive T cells but fails to prevent the induction of tumor antigen-specific tolerance. *Proceedings of the National Academy of Sciences*, *96*(20), 11476–11481. https://doi.org/10.1073/pnas.96.20.11476

Spahn, P. N., Bath, T., Weiss, R. J., Kim, J., Esko, J. D., Lewis, N. E., & Harismendy, O. (2017). PinAPL-Py: A comprehensive web-application for the analysis of CRISPR/Cas9 screens. *Scientific Reports*, *7*(1), 15854. https://doi.org/10.1038/s41598-017-16193-9

Speiser, D. E., Liénard, D., Rufer, N., Rubio-Godoy, V., Rimoldi, D., Lejeune, F., … Romero, P. (2005). Rapid and strong human CD8+ T cell responses to vaccination with peptide, IFA, and CpG oligodeoxynucleotide 7909. *The Journal of Clinical Investigation*, *115*(3), 739–746. https://doi.org/10.1172/JCI23373

Speiser, D. E., Utzschneider, D. T., Oberle, S. G., Münz, C., Romero, P., & Zehn, D. (2014). T cell differentiation in chronic infection and cancer: Functional adaptation or exhaustion? *Nature Reviews Immunology*, *14*(11), 768–774. https://doi.org/10.1038/nri3740

Spranger, S., Bao, R., & Gajewski, T. F. (2015). Melanoma-intrinsic β-catenin signalling prevents anti-tumour immunity. *Nature*, *523*(7559), 231–235. https://doi.org/10.1038/nature14404

Spranger, S., Dai, D., Horton, B., & Gajewski, T. F. (2017). Tumor-Residing Batf3 Dendritic Cells Are Required for Effector T Cell Trafficking and Adoptive T Cell Therapy. *Cancer Cell*, *31*(5), 711-723.e4. https://doi.org/10.1016/j.ccell.2017.04.003

Spranger, S., & Gajewski, T. F. (2018, January 12). Impact of oncogenic pathways on evasion of antitumour immune responses. *Nature Reviews Cancer*. Nature Publishing Group. https://doi.org/10.1038/nrc.2017.117

Stanczak, M. A., Siddiqui, S. S., Trefny, M. P., Thommen, D. S., Boligan, K. F., von Gunten, S., … Läubli, H. (2018). Self-associated molecular patterns mediate cancer immune evasion by engaging Siglecs on T cells. *The Journal of Clinical Investigation*, *128*(11), 4912–4923. https://doi.org/10.1172/JCI120612

Steinman, R. M., & Cohn, Z. A. (1973). Identification of a novel cell type in peripheral lymphoid organs of mice: I. Morphology, quantitation, tissue distribution. *Journal of Experimental Medicine*, *137*(5), 1142–1162. https://doi.org/10.1084/jem.137.5.1142

Stowell, S. R., Ju, T., & Cummings, R. D. (2015). Protein glycosylation in cancer. *Annual Review of Pathology*, *10*, 473–510. https://doi.org/10.1146/annurev-pathol-012414-040438

Streeck, H., Brumme, Z. L., Anastario, M., Cohen, K. W., Jolin, J. S., Meier, A., … Altfeld, M. (2008). Antigen Load and Viral Sequence Diversification Determine the Functional Profile of HIV-1–Specific CD8+ T Cells. *PLoS Medicine*, *5*(5), e100. https://doi.org/10.1371/journal.pmed.0050100

Sun, X., Wu, Y., Gao, W., Enjyoji, K., Csizmadia, E., Müller, C. E., … Robson, S. C. (2010). CD39/ENTPD1 expression by CD4+Foxp3+ regulatory T cells promotes hepatic metastatic tumor growth in mice. *Gastroenterology*, *139*(3), 1030–1040. https://doi.org/10.1053/j.gastro.2010.05.007

Syn, N. L., Teng, M. W. L., Mok, T. S. K., & Soo, R. A. (2017). *De-novo and acquired resistance to immune checkpoint targeting. The Lancet Oncology* (Vol. 18). https://doi.org/10.1016/S1470-2045(17)30607-1

Takenaka, M. C., Robson, S., & Quintana, F. J. (2016). Regulation of the T Cell Response by CD39. *Trends in Immunology*, *37*(7), 427–439. https://doi.org/10.1016/J.IT.2016.04.009

Tang, J., Yu, J. X., Hubbard-Lucey, V. M., Neftelinov, S. T., Hodge, J. P., & Lin, Y. (2018). The clinical trial landscape for PD1/PDL1 immune checkpoint inhibitors. *Nature Reviews Drug Discovery*, *17*(12), 854–855. https://doi.org/10.1038/nrd.2018.210

Tauriello, D. V. F., Palomo-Ponce, S., Stork, D., Berenguer-Llergo, A., Badia-Ramentol, J., Iglesias, M., … Batlle, E. (2018). TGFβ drives immune evasion in genetically reconstituted colon cancer metastasis. *Nature*, *554*(7693), 538–543. https://doi.org/10.1038/nature25492

Taylor, P. A., Lees, C. J., Fournier, S., Allison, J. P., Sharpe, A. H., & Blazar, B. R. (2004). B7 Expression on T Cells Down-Regulates Immune Responses through CTLA-4 Ligation via R-T Interactions. *The Journal of Immunology*, *173*(3), 2199.2-2199. https://doi.org/10.4049/jimmunol.173.3.2199-a

Thelen, M., Lechner, A., Wennhold, K., von Bergwelt-Baildon, M., & Schlößer, H. A. (2018). CD39 Expression Defines Cell Exhaustion in Tumor-Infiltrating CD8 + T Cells—Letter. *Cancer Research*, *78*(17), 5173–5174. https://doi.org/10.1158/0008-5472.CAN-18-0873

Thommen, D., Koelzer, V., Herzig, P., Roller, A., Trefny, M., Dimeloe, S., … Zippelius, A. (2018). A transcriptionally and functionally distinct CD8+ T cell pool with predictive potential in non-small cell lung cancer. *Nature Medicine*, *in press*.

Thommen, D. S., Koelzer, V. H., Herzig, P., Roller, A., Trefny, M., Dimeloe, S., … Zippelius, A. (2018). A transcriptionally and functionally distinct PD-1+ CD8+ T cell pool with predictive potential in non-small-cell lung cancer treated with PD-1 blockade. *Nature Medicine*, *24*(7), 994–1004. https://doi.org/10.1038/s41591-018-0057-z

Thommen, D. S., Schreiner, J., Muller, P., Herzig, P., Roller, A., Belousov, A., … Zippelius, A. (2015). Progression of Lung Cancer Is Associated with Increased Dysfunction of T Cells Defined by Coexpression of Multiple Inhibitory Receptors. *Cancer Immunology Research*, *3*(12), 1344–1355. https://doi.org/10.1158/2326-6066.CIR-15-0097

Thommen, D. S., & Schumacher, T. N. (2018). T Cell Dysfunction in Cancer. *Cancer Cell*, *33*(4), 547–562. https://doi.org/10.1016/j.ccell.2018.03.012

Tirosh, I., Izar, B., Prakadan, S. M., Ii, M. H. W., Treacy, D., Trombetta, J. J., … Kolb, K. E. (2016). Dissecting the multicellular exosystem of metastatic melanoma by single-cell RNA-seq. *Science*, *352*(6282), 189–196. https://doi.org/10.1126/science.aad0501.Dissecting

Topalian, S. L., Drake, C. G., & Pardoll, D. M. (2015). Immune Checkpoint Blockade: A Common Denominator Approach to Cancer Therapy. *Cancer Cell*, *27*(4), 450–461. https://doi.org/10.1016/j.ccell.2015.03.001

Topalian, S. L., Hodi, F. S., Brahmer, J. R., Gettinger, S. N., Smith, D. C., McDermott, D. F., … Sznol, M. (2019). Five-Year Survival and Correlates Among Patients With Advanced Melanoma, Renal Cell Carcinoma, or Non–Small Cell Lung Cancer Treated With Nivolumab. *JAMA Oncology*, *5*(10), 1411. https://doi.org/10.1001/jamaoncol.2019.2187

Trefny, M. P., Rothschild, S. I., Uhlenbrock, F., Rieder, D., Kasenda, B., Stanczak, M. A., … Laubli, H. (2019). A variant of a killer cell immunoglobulin-like receptor is associated with resistance to PD-1 blockade in lung cancer. *Clinical Cancer Research*, *25*(10), 3026–3034. https://doi.org/10.1158/1078-0432.CCR-18-3041

Tumeh, P. C., Harview, C. L., Yearley, J. H., Shintaku, I. P., Taylor, E. J. M., Robert, L., … Ribas, A. (2014). PD-1 blockade induces responses by inhibiting adaptive immune resistance. *Nature*, *515*(7528), 568–571. https://doi.org/10.1038/nature13954

Uhrberg, M., Valiante, N. M., Shum, B. P., Shilling, H. G., Lienert-Weidenbach, K., Corliss, B., … Parham, P. (1997). Human diversity in killer cell inhibitory receptor genes. *Immunity*, *7*(6), 753–763. https://doi.org/10.1016/S1074-7613(00)80394-5

Umansky, V., & Sevko, A. (2013). Tumor microenvironment and myeloid-derived suppressor cells. *Cancer Microenvironment*, *6*(2), 169–177. https://doi.org/10.1007/s12307-012-0126-7

Utzschneider, D. T., Alfei, F., Roelli, P., Barras, D., Chennupati, V., Darbre, S., … Zehn, D. (2016). High antigen levels induce an exhausted phenotype in a chronic infection without impairing T cell expansion and survival. *Journal of Experimental Medicine*, *213*(9), 1819–1834. https://doi.org/10.1084/jem.20150598

Uyttenhove, C., Pilotte, L., Théate, I., Stroobant, V., Colau, D., Parmentier, N., … Van den Eynde, B. J. (2003). Evidence for a tumoral immune resistance mechanism based on tryptophan degradation by indoleamine 2,3-dioxygenase. *Nature Medicine*, *9*(10), 1269–1274. https://doi.org/10.1038/nm934

Van Allen, E. M., Miao, D., Schilling, B., Shukla, S. A., Blank, C., Zimmer, L., … Garraway, L. A. (2015). Genomic correlates of response to CTLA-4 blockade in metastatic melanoma. *Science*, *350*(6257), 207–211. https://doi.org/10.1126/science.aad0095

van der Bruggen, P., Traversari, C., Chomez, P., Lurquin, C., De Plaen, E., Van den Eynde, B., … Boon, T. (1991). A gene encoding an antigen recognized by cytolytic T lymphocytes on a human melanoma. *Science*, *254*(5038), 1643–1647. https://doi.org/10.1126/science.1840703

Vanpouille-Box, C., Alard, A., Aryankalayil, M. J., Sarfraz, Y., Diamond, J. M., Schneider, R. J., … Demaria, S. (2017). DNA exonuclease Trex1 regulates radiotherapy-induced tumour immunogenicity. *Nature Communications*, *8*(1), 15618. https://doi.org/10.1038/ncomms15618

Venstrom, J. M., Pittari, G., Gooley, T. A., Chewning, J. H., Spellman, S., Haagenson, M., … Hsu, K. C. (2012). *HLA-C* –Dependent Prevention of Leukemia Relapse by Donor Activating *KIR2DS1*. *New England Journal of Medicine*, *367*(9), 805–816. https://doi.org/10.1056/NEJMoa1200503

Vétizou, M., Pitt, J. M., Daillère, R., Lepage, P., Waldschmitt, N., Flament, C., … Zitvogel, L. (2015). Anticancer immunotherapy by CTLA-4 blockade relies on the gut microbiota. *Science*, *350*(6264), 1079–1084. https://doi.org/10.1126/science.aad1329

Viaud, S., Saccheri, F., Mignot, G., Yamazaki, T., Daillère, R., Hannani, D., … Zitvogel, L. (2013). The intestinal microbiota modulates the anticancer immune effects of cyclophosphamide. *Science (New York, N.Y.)*, *342*(6161), 971–976. https://doi.org/10.1126/science.1240537

Vitale, M., Cantoni, C., Pietra, G., Mingari, M. C., & Moretta, L. (2014). Effect of tumor cells and tumor microenvironment on NK-cell function. *European Journal of Immunology*, *44*(6), 1582–1592. https://doi.org/10.1002/eji.201344272

Vivier, E., Raulet, D. H., Moretta, A., Caligiuri, M. A., Zitvogel, L., Lanier, L. L., … Ugolini, S. (2011, January 7). Innate or adaptive immunity? The example of natural killer cells. *Science*. American Association for the Advancement of Science. https://doi.org/10.1126/science.1198687

Voskoboinik, I., Smyth, M. J., & Trapani, J. A. (2006). Perforin-mediated target-cell death and immune homeostasis. *Nature Reviews. Immunology*, *6*(12), 940–952. https://doi.org/10.1038/nri1983

Waggoner, S. N., Cornberg, M., Selin, L. K., & Welsh, R. M. (2012). Natural killer cells act as rheostats modulating antiviral T cells. *Nature*, *481*(7381), 394–398. https://doi.org/10.1038/nature10624

Waickman, A. T., Alme, A., Senaldi, L., Zarek, P. E., Horton, M., & Powell, J. D. (2012). Enhancement of tumor immunotherapy by deletion of the A2A adenosine receptor. *Cancer Immunology, Immunotherapy*, *61*(6), 917–926. https://doi.org/10.1007/s00262-011-1155-7

Wang, C., Singer, M., & Anderson, A. C. (2017). Molecular Dissection of CD8+T-Cell Dysfunction. *Trends in Immunology*, *38*(8), 567–576. https://doi.org/10.1016/j.it.2017.05.008

Wang, G., Chow, R. D., Bai, Z., Zhu, L., Errami, Y., Dai, X., … Chen, S. (2019). Multiplexed activation of endogenous genes by CRISPRa elicits potent antitumor immunity. *Nature Immunology*, *20*(11), 1494–1505. https://doi.org/10.1038/s41590-019-0500-4

Wang, R., & Green, D. R. (2012). Metabolic reprogramming and metabolic dependency in T cells. *Immunological Reviews*, *249*(1), 14–26. https://doi.org/10.1111/j.1600-065X.2012.01155.x

Wang, T., Birsoy, K., Hughes, N. W., Krupczak, K. M., Post, Y., Wei, J. J., … Sabatini, D. M. (2015). Identification and characterization of essential genes in the human genome. *Science*, *350*(6264), 1096–1101. https://doi.org/10.1126/science.aac7041

Wang, T., Lander, E. S., & Sabatini, D. M. (2016). Single Guide RNA Library Design and Construction. *Cold Spring Harbor Protocols*, *2016*(3), pdb.prot090803. https://doi.org/10.1101/pdb.prot090803

Wang, T., Wei, J. J., Sabatini, D. M., & Lander, E. S. (2014). Genetic Screens in Human Cells Using the CRISPR-Cas9 System. *Science*, *343*(6166), 80–84. https://doi.org/10.1126/science.1246981

Wang, T., Yu, H., Hughes, N. W., Liu, B., Kendirli, A., Klein, K., … Sabatini, D. M. (2017). Gene Essentiality Profiling Reveals Gene Networks and Synthetic Lethal Interactions with Oncogenic Ras. *Cell*, *168*(5), 890-903.e15. https://doi.org/10.1016/j.cell.2017.01.013

Wei, S. C., Anang, N.-A. A. S., Sharma, R., Andrews, M. C., Reuben, A., Levine, J. H., … Allison, J. P. (2019). Combination anti–CTLA-4 plus anti–PD-1 checkpoint blockade utilizes cellular mechanisms partially distinct from monotherapies. *Proceedings of the National Academy of Sciences*, *116*(45), 22699–22709. https://doi.org/10.1073/PNAS.1821218116

Wei, S. C., Duffy, C. R., & Allison, J. P. (2018). Fundamental Mechanisms of Immune Checkpoint Blockade Therapy. *Cancer Discovery*, *8*(9), 1069–1086. https://doi.org/10.1158/2159-8290.CD-18-0367

Wei, S. C., Levine, J. H., Cogdill, A. P., Zhao, Y., Anang, N. A. A. S., Andrews, M. C., … Allison, J. P. (2017). Distinct Cellular Mechanisms Underlie Anti-CTLA-4 and Anti-PD-1 Checkpoint Blockade. *Cell*, *170*(6), 1120-1133.e17. https://doi.org/10.1016/j.cell.2017.07.024

Weigelin, B., Melero, I., Chen, L., Wagena, E., Morales-Kastresana, A., Quetglas, J. I., … Bolaños, E. (2015). Focusing and sustaining the antitumor CTL effector killer response by agonist anti-CD137 mAb. *Proceedings of the National Academy of Sciences*, *112*(24), 7551–7556. https://doi.org/10.1073/pnas.1506357112

Weigert, A., Tzieply, N., von Knethen, A., Johann, A. M., Schmidt, H., Geisslinger, G., & Brüne, B. (2007). Tumor Cell Apoptosis Polarizes Macrophages—Role of Sphingosine-1-Phosphate. *Molecular Biology of the Cell*, *18*(10), 3810–3819. https://doi.org/10.1091/mbc.e06-12-1096

142

Weinkove, R., George, P., Dasyam, N., & McLellan, A. D. (2019). Selecting costimulatory domains for chimeric antigen receptors: functional and clinical considerations. *Clinical and Translational Immunology*, 8(5), e1049. https://doi.org/10.1002/cti2.1049

Wherry, E. J. (2011). T cell exhaustion. *Nature Immunology*, 12(6), 492–499. https://doi.org/10.1038/ni.2035

Wherry, E. J., Ha, S.-J., Kaech, S. M., Haining, W. N., Sarkar, S., Kalia, V., … Ahmed, R. (2007). Molecular Signature of CD8+ T Cell Exhaustion during Chronic Viral Infection. *Immunity*, 27(4), 670–684. https://doi.org/10.1016/j.immuni.2007.09.006

Wherry, E. J., & Kurachi, M. (2015). Molecular and cellular insights into T cell exhaustion. *Nature Reviews Immunology*, 15(8), 486–499. https://doi.org/10.1038/nri3862

Wiesmayr, S., Webber, S. A., Macedo, C., Popescu, I., Smith, L., Luce, J., & Metes, D. (2012). Decreased NKp46 and NKG2D and elevated PD-1 are associated with altered NK-cell function in pediatric transplant patients with PTLD. *European Journal of Immunology*, 42(2), 541–550. https://doi.org/10.1002/eji.201141832

Wolf, Y., Bartok, O., Patkar, S., Eli, G. B., Cohen, S., Litchfield, K., … Samuels, Y. (2019). UVB-Induced Tumor Heterogeneity Diminishes Immune Response in Melanoma. *Cell*, 179(1), 219-235.e21. https://doi.org/10.1016/j.cell.2019.08.032

Woo, S.-R., Turnis, M. E., Goldberg, M. V., Bankoti, J., Selby, M., Nirschl, C. J., … Vignali, D. A. A. (2012). Immune Inhibitory Molecules LAG-3 and PD-1 Synergistically Regulate T-cell Function to Promote Tumoral Immune Escape. *Cancer Research*, 72(4), 917–927. https://doi.org/10.1158/0008-5472.CAN-11-1620

Woo, Seng-Ryong, Fuertes, M. B., Corrales, L., Spranger, S., Furdyna, M. J., Leung, M. Y. K., … Gajewski, T. F. (2014). STING-Dependent Cytosolic DNA Sensing Mediates Innate Immune Recognition of Immunogenic Tumors. *Immunity*, 41(5), 830–842. https://doi.org/10.1016/J.IMMUNI.2014.10.017

Workel, H. H., Lubbers, J. M., Arnold, R., Prins, T. M., van der Vlies, P., de Lange, K., … de Bruyn, M. (2019). A Transcriptionally Distinct CXCL13+CD103+CD8+ T-cell Population Is Associated with B-cell Recruitment and Neoantigen Load in Human Cancer. *Cancer Immunology Research*, 7(5), 784–796. https://doi.org/10.1158/2326-6066.CIR-18-0517

Xu, W., Hiểu, T., Malarkannan, S., & Wang, L. (2018). The structure, expression, and multifaceted role of immune-checkpoint protein VISTA as a critical regulator of anti-tumor immunity, autoimmunity, and inflammation. *Cellular & Molecular Immunology*, 15(5), 438–446. https://doi.org/10.1038/cmi.2017.148

Yan, D., Yang, Q., Shi, M., Zhong, L., Wu, C., Meng, T., … Zhou, J. (2013). Polyunsaturated fatty acids promote the expansion of myeloid-derived suppressor cells by activating the JAK/STAT3 pathway. *European Journal of Immunology*, 43(11), 2943–2955. https://doi.org/10.1002/eji.201343472

Yarar, D., Waterman-Storer, C. M., & Schmid, S. L. (2007). SNX9 Couples Actin Assembly to Phosphoinositide Signals and Is Required for Membrane Remodeling during Endocytosis. *Developmental Cell*, 13(1), 43–56. https://doi.org/10.1016/j.devcel.2007.04.014

Ye, L., Park, J. J., Dong, M. B., Yang, Q., Chow, R. D., Peng, L., … Chen, S. (2019). In vivo CRISPR screening in CD8 T cells with AAV–Sleeping Beauty hybrid vectors identifies membrane targets for improving immunotherapy for glioblastoma. *Nature Biotechnology*, 37(11), 1302–1313. https://doi.org/10.1038/s41587-019-0246-4

Yost, K. E., Satpathy, A. T., Wells, D. K., Qi, Y., Wang, C., Kageyama, R., … Chang, H. Y. (2019). Clonal replacement of tumor-specific T cells following PD-1 blockade. *Nature Medicine*, 25(8), 1251–1259. https://doi.org/10.1038/s41591-019-0522-3

Younes, A., Santoro, A., Shipp, M., Zinzani, P. L., Timmerman, J. M., Ansell, S., … Engert, A. (2016). Nivolumab for classical Hodgkin's lymphoma after failure of both autologous stem-cell transplantation and brentuximab vedotin: a multicentre, multicohort, single-arm phase 2 trial. *The Lancet Oncology*, 17(9), 1283–1294. https://doi.org/10.1016/S1470-2045(16)30167-X

Yu, H., Sotillo, E., Harrington, C., Wertheim, G., Paessler, M., Maude, S. L., … Pillai, V. (2017, January 1). Repeated loss of target surface antigen after immunotherapy in primary mediastinal large B cell lymphoma. *American Journal of Hematology*. John Wiley & Sons, Ltd. https://doi.org/10.1002/ajh.24594

Zacharakis, N., Chinnasamy, H., Black, M., Xu, H., Lu, Y.-C., Zheng, Z., … Feldman, S. A. (2018). Immune recognition of somatic mutations leading to complete durable regression in metastatic breast cancer. *Nature Medicine*, 24(6), 724–730. https://doi.org/10.1038/s41591-018-0040-8

Zah, E., Lin, M. Y., Anne, S. B., Jensen, M. C., & Chen, Y. Y. (2016). T cells expressing CD19/CD20 bispecific chimeric antigen receptors prevent antigen escape by malignant B cells. *Cancer Immunology Research*, 4(6), 498–508. https://doi.org/10.1158/2326-6066.CIR-15-0231

Zaretsky, J. M., Garcia-Diaz, A., Shin, D. S., Escuin-Ordinas, H., Hugo, W., Hu-Lieskovan, S., … Ribas, A. (2016). Mutations Associated with Acquired Resistance to PD-1 Blockade in Melanoma. *New England Journal of Medicine*, 375(9), 819–829. https://doi.org/10.1056/NEJMoa1604958

Zehn, D., Lee, S. Y., & Bevan, M. J. (2009). Complete but curtailed T-cell response to very low-affinity antigen. *Nature*, 458(7235), 211–214. https://doi.org/10.1038/nature07657

Zhang, B., Zhang, Y., Bowerman, N. A., Schietinger, A., Fu, Y.-X., Kranz, D. M., … Schreiber, H. (2008). Equilibrium between Host and Cancer Caused by Effector T Cells Killing Tumor Stroma. *Cancer Research*, 68(5), 1563–1571. https://doi.org/10.1158/0008-5472.CAN-07-5324

Zhao, F., Sucker, A., Horn, S., Heeke, C., Bielefeld, N., Schro rs, B., … Paschen, A. (2016). Melanoma Lesions Independently Acquire T-cell Resistance during Metastatic Latency. *Cancer Research*, 76(15), 4347–4358. https://doi.org/10.1158/0008-5472.CAN-16-0008

Zheng, C., Zheng, L., Yoo, J.-K. K., Guo, H., Zhang, Y., Guo, X., … Zhang, Z. (2017). Landscape of Infiltrating T Cells in Liver Cancer Revealed by Single-Cell Sequencing. *Cell*, 169(7), 1342-1356.e16. https://doi.org/10.1016/j.cell.2017.05.035

Zhou, P., Shaffer, D. R., Alvarez Arias, D. A., Nakazaki, Y., Pos, W., Torres, A. J., … Wucherpfennig, K. W. (2014). In vivo discovery of immunotherapy targets in the tumour microenvironment. *Nature*, 506(7486), 52–57. https://doi.org/10.1038/nature12988

Zimmer, J., Donato, L., Hanau, D., Cazenave, J., Tongio, M., Moretta, A., & de la Salle, H. (1998). Activity and Phenotype of Natural Killer Cells in Peptide Transporter (TAP)-deficient Patients (Type I Bare Lymphocyte Syndrome). *Journal of Experimental Medicine*, 187(1), 117–122. https://doi.org/10.1084/JEM.187.1.117

Zinkernagel, R., & Doherty, P. C. (1974). Restriction of in vitro T cell-mediated cytotoxicity in lymphocytic choriomeningitis within a syngeneic or semiallogeneic system. *Nature*, 248(5450), 701–702. https://doi.org/10.1038/248701a0

Zippelius, A., Batard, P., Rubio-Godoy, V., Bioley, G., Liénard, D., Lejeune, F., … Pittet, M. J. (2004). Effector Function of Human Tumor-Specific CD8 T Cells in Melanoma Lesions: A State of Local Functional Tolerance. *Cancer Research*, 64(8), 2865–2873. https://doi.org/10.1158/0008-5472.CAN-03-3066

Zippelius, A., Schreiner, J., Herzig, P., & Muller, P. (2015). Induced PD-L1 Expression Mediates Acquired Resistance to Agonistic Anti-CD40 Treatment. *Cancer Immunology Research*, 3(3), 236–244. https://doi.org/10.1158/2326-6066.CIR-14-0226

Zychlinski, D., Schambach, A., Modlich, U., Maetzig, T., Meyer, J., Grassman, E., … Baum, C. (2008). Physiological Promoters Reduce the Genotoxic Risk of Integrating Gene Vectors. *Molecular Therapy*, 16(4), 718–725. https://doi.org/10.1038/MT.2008.5